A MATERIAL-EMISSIONS-UPTAKE-NEXUS DRIVEN FRAMEWORK FOR DECARBONIZING CEMENT SECTOR IN CHINA

TONGYUAN WU (吴统元)

B.Eng., SHENZHEN UNIVERSITY, CHINA

M.Eng., SOUTH CHINA UNIVERSITY OF TECHNOLOGY, CHINA

A thesis submitted in partial fulfillment of the requirements for the Degree of Doctor of Philosophy at The University of Hong Kong

JULY 2024

[This page is intended to be blank.]

Abstract of thesis entitled

"A material-emissions-uptake-nexus driven framework for decarbonizing cement sector in China"

Submitted by

Tongyuan Wu

for the degree of Doctor of Philosophy

at The University of Hong Kong

in July 2024

Over four gigatons of cement are produced annually worldwide, contributing approximately 7.5% of total anthropogenic CO_2 emissions. Decarbonizing the cement sector is both arduous and urgent, given the imperative to achieve net-zero CO_2 emissions by 2050 to limit global warming to 1.5°C above pre-industrial levels. The process of cement production, particularly clinker production, is one of the most challenging to decarbonize. Approximately two-thirds of the emissions from clinker production stem from limestone decomposition, which cannot be mitigated by decarbonizing energy alone. Alternative cements and clinkers are not yet ready for large-scale deployment. Traditional supply-side strategies, such as energy efficiency improvements and fuel switching, leave limited room for further significant reductions. Consequently, carbon capture and storage (CCS) technologies must play a crucial role on the supply-side decarbonization. Furthermore, previous decarbonization roadmaps often lack spatially explicit guidance for practical implementation, particularly for CCS. On the demand side, future cement consumption is rarely projected systematically, and mitigation potentials from the demand side are seldom investigated. Moreover, the potential role of atmospheric CO_2 absorption through carbonation reactions in cement materials, which could serve as a significant carbon sink, has not been fully integrated into existing decarbonization strategies.

In response, this research develops a comprehensive framework to decarbonize the cement sector within a material-emissions-uptake (MEU) nexus, effectively integrating both demand- and supply-side dynamics. The world's largest cement producer, China's cement sector, is selected as a detailed case study throughout this thesis. Through the MEU framework, historical in-use cement stocks and the associated carbon fluxes (both emissions and uptake), are explicitly analyzed. Then, future in-use cement stock and demand, as well as mitigation potentials, are thoroughly explored and projected through demand-side scenario analysis, with their impacts on emissions and uptake being quantitatively assessed. Following this, the study integrates these demand-side insights with traditional supply-side measures and CCS technologies to develop decarbonization pathways aligned with 1.5°C, 1.7°C, and 2.0°C climate targets. Additionally, a spatial supply-demand and emissions-storage matching analysis is conducted to identify strategic locations for large-scale CCS deployments across China. This comprehensive approach not only provides a robust and feasible pathway for achieving net-zero emissions in the cement industry but also balances supply- and demand-side efforts while leveraging spatial analysis for optimized CCS implementation.

The contributions of this thesis are multifaceted. Theoretically, it advances the understanding of the material-emissions-uptake nexus for the cement sector, enabling a more comprehensive analysis by integrating supply- and demand-side dynamics. Methodologically, it introduces a simplified supply-demand matching model that reduces computation time while maintaining empirical accuracy. Practically, it provides valuable spatial-temporal insights for policymakers and industry investors, identifying priority regions for CCS deployment to enhance efficiency and reduce pipeline construction and transportation costs as well failure risks of CCS projects.

(449 words)

Declaration

I declare that this thesis represents my own work, except where due acknowledgement is made, and that it has not been previously included in a thesis, dissertation or report submitted to this University or to any other institution for a degree, diploma or other qualifications.

Signed: ________________

WU, Tongyuan

August, 2024

Acknowledgement

First and foremost, I would like to express my heartfelt gratitude to my supervisors, Prof. Thomas Ng and Prof. Ji Chen, for their unwavering support both in my research and in my daily life over the past four years. Their kindness and encouragement allowed me to pursue my research with both flexibility and independence. I am deeply appreciative of the insightful discussions we shared, which provided me with valuable guidance and helped shape the direction of my research. Working with Prof. Ng and Prof. Chen has been a truly meaningful, productive, and memorable journey, and I have greatly enjoyed every moment of it during my PhD studies.

Special thanks to my research collaborator Prof. Zhi Cao in Nankai university, who helped me during my research on material flow analysis and inspired me during the discussions.

Many thanks to the members of our research group in HKU, Dr Jicao Dao, Dr Prince Antwi-afari, Dr Shushu Fan, Dr Yuyang Shao and Miss Dewagoda Kaveesha Gihani, and the former group members, Dr Shenghua Zhou and Dr Yifan Yang, for selfless help and valuable suggestions. Also, I would express my sincere thanks to my friends in HKU, Mr. Li Zhang and Dr Yihan Wang, for the valuable conversations and discussions with them.

Finally, I am truly grateful to my father and mother, my grandpa and grandma, my elder sister and brother, and my girlfriend, for their unconditional love, endless support, and encouragement during my PhD journey.

Table of contents

Abstract of thesis entitled .... **I**

Declaration .... **I**

Acknowledgement .... **II**

Table of contents .... **III**

Table of Figures .... **VIII**

List of Tables .... **XIII**

List of Abbreviations .... **XIV**

List of Publications .... **XVI**

Chapter 1. Introduction **1**

1.1 Research background 1

1.1.1 Climate crisis calls for net-zero transition 1

1.1.2 Substantial carbon emissions from cement production 2

1.1.3 Challenges in decarbonization for the cement sector 3

1.2 Research questions statement 3

1.3 Research aim and objectives 5

1.4 Research scope 7

1.5 Research significance and contribution 7

1.6 Structure of this thesis 8

1.7 Chapter summary 10

Chapter 2. Literature review **11**

2.1 Introduction 11

2.2 CO_2 emissions and drivers of cement sector 11

2.2.1 Portland cement production 11

2.2.2 CO_2 emissions accounting 13

2.2.3 Emissions drivers 14
2.3 CO_2 uptake by carbonation and quantification 18
2.3.1 Principle of carbonation reaction 18
2.3.2 Quantification on carbon uptake at global and regional scale 19
2.4 Cement stock dynamics 20
2.5 Decarbonization pathways for cement sector 22
2.5.1 Supply-side pathways 22
2.5.2 Demand-side potentials 27
2.6 Research gaps 31
2.7 Chapter summary 32
Chapter 3. Research methodology 33
3.1 Introduction 33
3.2 Research design 33
3.3 Research methods 35
3.3.1 Literature review 35
3.3.2 Scientific modeling 35
3.3.3 Scenario approach 36
3.4 Modeling techniques 37
3.4.1 IPCC emissions estimation method 37
3.4.2 Index decomposition analysis 38
3.4.3 Material flows analysis 39
3.4.4 Optimization model 40
3.5 Chapter summary 41
Chapter 4. Developing an integrated modeling framework to decipher material-emissions-uptake (MEU) nexus of cement sector 42
4.1 Introduction 42
4.2 An integrated modeling framework for material-emissions-uptake nexus of cement sector 43

4.3 Module 1: Dynamic material flow analysis 44
4.3.1 Inflow-driven model 45
4.3.2 Stock-driven model 47
4.3.3 Data source for case study 48
4.4 Module 2: CO_2 emissions accounting 48
4.4.1 Total emissions accounting 48
4.4.2 Decomposition on emissions drivers 50
4.4.3 Uncertainty analysis 54
4.4.4 Data source for case study 54
4.5 Module 3: CO_2 uptake quantification 54
4.6 A demonstrative case: China's cement sector 57
4.6.1 China's in-use cement stock 57
4.6.2 Historical CO_2 emissions and drivers 58
4.6.3 CO_2 uptake by China's cement stock 63
4.6.4 Net carbon emissions pathways 65
4.7 Chapter summary 66
Chapter 5. Future cement demand, mitigation potentials and implications for carbon emissions and uptake 67
5.1 Introduction 67
5.2 Developing scenarios for future cement stock 68
5.2.1 Scenarios for future per-capita stock 68
5.2.2 Robustness of stock saturation assumption 75
5.2.3 Lifetime extension 76
5.2.4 The scenario matrix 77
5.3 Results 77
5.3.1 Future cement stocks, outflows, and inflows 77
5.3.2 CO_2 uptake 81

5.3.3 Net CO_2 emissions 83
5.4 Chapter summary 85
Chapter 6. Developing decarbonization roadmaps for cement sector within the MEU nexus 87
6.1 Introduction 87
6.2 Methods 88
6.2.1 Supply-side scenarios 89
6.2.2 Plant turnover simulation 90
6.2.3 Determining CCS deployments 93
6.2.4 Emissions budget 94
6.3 Results 97
6.3.1 Emission intensity of clinker and cement production 97
6.3.2 Emission pathways consistent with climate targets 99
6.3.3 Production capacity and CCS deployment 103
6.4 Chapter summary 106
Chapter 7. Advancing decarbonization roadmaps within a geographical context: A case of future CCS deployment across China's cities 107
7.1 Introduction 107
7.2 Method 108
7.2.1 Downscaling national demand to city level 109
7.2.2 City-level supply-demand matching 110
7.2.3 Carbon storage potentials 112
7.2.4 City-level carbon emissions-storage matching 114
7.2.5 Data source 114
7.3 Results and discussion 115
7.3.1 Cement plants in China 115
7.3.2 Future clinker production and capacity at city level 118
7.3.3 Carbon storage potentials across China's cities 121

7.3.4 Prioritized cities for CCS deployment 123
7.3.5 Discussion 125
7.4 Chapter summary 126
Chapter 8. Discussion 128
8.1 Introduction 128
8.2 Advancement of MEU framework 128
8.3 Implications from the case of China 130
8.3.1 Implications of a lower per-capita cement stock 131
8.3.2 Opportunities and challenges of service-life extension 133
8.3.3 Speeding up CCS deployments like historical NSP kilns 136
8.3.4 Policy recommendations 138
8.4 Validation on the case results 139
8.5 Chapter summary 142
Chapter 9. Conclusions 143
9.1 Introduction 143
9.2 Achievements of the objectives 143
9.3 Summary of Research Findings 145
9.4 Contributions of the Research 148
9.4.1 Theoretical contributions to the knowledge 148
9.4.2 Methodological improvements 148
9.4.3 Practical implications 149
9.5 Limitations and future research 149
References 152

Table of Figures

Figure 1-1 | Global cement production in 1930-2022. Data source: Robbie Andrew (2023). 2
Figure 2-1 | Cement production processes (adapted from Habert et al. (2020)).... 12
Figure 2-2 | Comparison of process emission factors of clinker production (Wu et al., 2022). 14
Figure 2-3 | Energy efficiency, fuel structure, and clinker-to-cement ratio of global cement sector. (Data source: "*Getting the Numbers Right (GNR)*" database 2.0 (GCCA, 2024).) 24
Figure 2-4 | Cementitious material use hierarchy (adapted from Miller et al. (2021)). 30
Figure 3-1 | Research roadmap of this thesis. 34
Figure 3-2 | Different approaches to assess the future in relation to uncertainty and system complexity (Zurek & Henrichs, 2007). 37
Figure 4-1 | Integrated modeling framework of the material-emission-uptake (MEU) nexus of cement sector. 43
Figure 4-2 | System boundary definition (a) and the calculation process based on stock matrix in this study (b). 45
Figure 4-3 | System boundary of CO_2 emission accounting (Wu, Ng, Chen, et al., 2023). 49
Figure 4-4 | Decomposition on total emissions and emission intensity (Wu et al., 2022). 50
Figure 4-5 | Two-dimensional schematic representation of simplified geometries (Wu, Ng, Chen, et al., 2023). 55
Figure 4-6 | CO_2 uptake accounting model architecture harmonized with DMFA model. Material types and service stages (a) and calculation procedure in this study (b) (Wu, Ng, Chen, et al., 2023). 56
Figure 4-7 | Historical in-use cement stock in China. 58
Figure 4-8 | CO_2 emissions and emission intensity of cement production in China (Wu et al., 2022). (Notes: The shaded area around the lines represents the 95% uncertainty interval of carbon emissions calculated by this study.) 59

Figure 4-9 | Total emissions change caused by varying production volume and emission intensity (a), and the correlations between emissions change rate and that of production volume and emission intensity (b) (Wu et al., 2022). 60
Figure 4-10 | Decomposition on total emissions (Wu et al., 2022). 61
Figure 4-11 | Decomposition on the aggregate emission intensity of cement production in China (Wu et al., 2022). 63
Figure 4-12 | CO_2 uptake by cement carbonation in China (1949-2022). 64
Figure 4-13 | Unit uptake of cement carbonation (a) and carbonation depth of concrete and mortar over time (b)..65
Figure 4-14 | CO_2 balance of China's cement cycle in 1990-2022........................66
Figure 5-1 | The layer of demand-side scenarios for MEU framework. 68
Figure 5-2 | Current and future scenarios for service levels of road and railway infrastructure in China. 72
Figure 5-3 | Current and future scenarios for road type propositions in China. 73
Figure 5-4 | ARIMA forecast on the (a) level, (b) NAS, and (c) acceleration based on the historical trend of China's cement stock in 1949-2060, as well as (d) the trajectory of stock to NAS ratio (Wu, Ng, Chen, et al., 2023). 76
Figure 5-5 | Service-life matrix for Short Lifetime (a), Moderate Lifetime Extension (b), and Substantial Lifetime Extension (c) scenarios in this study (Wu, Ng, Chen, et al., 2023). 77
Figure 5-6 | Scenario matrix and each scenario dimension with key assumptions. 77
Figure 5-7 | Future dynamics of China's in-use cement stock, inflow, and outflow of all scenarios during 2000-2060 (adapted from Wu et al. (2023))......................79
Figure 5-8 | Cumulative cement consumption and outflows in China during 2023-2060. 80
Figure 5-9 | CO_2 uptake by carbonation of cement-related materials during 2023-2060 (Wu, Ng, Chen, et al., 2023). 81
Figure 5-10 | Impacts of parameter changes on total CO_2 uptake by cement carbonation during 2023-2060 (Wu, Ng, Chen, et al., 2023). 83
Figure 5-11 | Carbon balances of China's cement cycle in 2022-2060. 84
Figure 5-12 | Cumulative CO_2 emissions and uptake associated with China's cement cycle during 2023-2060. (a)-(i) cumulative CO_2 emissions reductions, uptake, and CO_2 balance of scenarios S1-S9. 85

Figure 6-1 | Research flowchart and interactions with the MEU framework........88
Figure 6-2 | (a) Thermal energy intensity for clinker production, CO_2 emission factors for (b) fossil fuels and (c) alternative fuels (Wu, Ng, & Chen, 2023).......92
Figure 6-3 | Capped emissions trajectories consistent with remaining carbon budgets. (a) Change in the ratio of capped emissions to current emissions. (b)-(d) capped emissions trajectory and remaining carbon budget (2023-2060) for China's cement sector under 1.5, 1.7, and 2.0 °C, respectively..96
Figure 6-4 | Mitigation in emission intensity of clinker and cement production in 2022-2060 (Notes: This figure is adapted from Wu, Ng, & Chen (2023). And NG refers to natural gas.) 98
Figure 6-5 | Emission pathways of China's cement sector with the implementation of an ambitious portfolio of supply-side strategies (AMB scenario), but without CCS deployment...99
Figure 6-6 | Emissions gap between carbon budgets and remaining CO_2 emissions across scenarios (2023-2060)..100
Figure 6-7 | Emissions pathways of China's cement sector consistent with 1.5 °C budget, without emission offset by carbonation uptake......................................101
Figure 6-8 | Emissions pathways of China's cement sector consistent with 1.7°C and 2.0°C budget, without emission offset by carbonation uptake. 102
Figure 6-9 | Emissions pathways of China's cement sector consistent with 1.5°C and 1.7°C budget, with part of emissions offset by carbonation uptake. 103
Figure 6-10 | Clinker production capacity turnover and CCS deployment in 2022-2060. (Notes: carb. represents emission offset by carbonation reactions.)..........104
Figure 6-11 | Average annual growth rate (AAGR) of CCS deployment in China's cement sector, aiming at 1.5°C, 1.7°C, and 2.0°C. (Notes: carb. denotes for carbonation uptake.)..105
Figure 7-1 | Research flowchart of this chapter and its relationship to MEU framework..109
Figure 7-2 | Schematic diagram of the supply-demand matching module. 110
Figure 7-3 | Carbon storage potentials across China. (a) Deep saline aquifer (DSA) and (b) oil field. 113
Figure 7-4 | Driving distance matrix of China's cities in 2022...........................115
Figure 7-5 | Cement plants and clinker production capacity across the cities of China in 2020...116

Figure 7-6 | Age structure of China's cement plants. 116
Figure 7-7 | Utilization of clinker production capacity (a) and clinker importer and exporter cities in China. (Source: City-level clinker and cement production data in 2019 are from (Y. Wang et al., 2023).) 117
Figure 7-8 | (a) Supply-demand gap versus supply radius and (b) comparison between the predicted clinker production in this study and real production data from Wang et al. (2023). 118
Figure 7-9 | City-level clinker demand (a) and production (b) in 2022. 119
Figure 7-10 | City-level clinker demand and production in 2050 of HS-SL+AMB, MS-ML+AMB, and LS-ML+AMB scenarios. 119
Figure 7-11 | Future clinker demand, production, and capacity of case cities in the HS-SL+AMB, MS-ML+AMB, and LS-ML+AMB scenarios. 120
Figure 7-12 | Carbon storage potentials of deep saline aquifer (DSA) and CO_2-enhanced oil recovery (CO_2-EOR) across cities in China. (Notes: The error bar shows the 95% confidence interval of estimated storage capacity.) 122
Figure 7-13 | Captured emissions and gap vary with maximum transportation distance. 123
Figure 7-14 | Emissions-storage matching results for HS-SL+AMB, MS-ML+AMB, and LS-ML+AMB scenarios. 124
Figure 7-15 | Spatial layout of cumulative carbon emissions (a), stored emissions (b), and remaining emissions (c) for China's cities. 125
Figure 8-1 | Integrated decarbonization roadmaps for China's cement sector, developed by the MEU framework. 131
Figure 8-2 | Comparison of China's future per-capita cement stock scenarios with other countries (a), and the relationship between per-capita stock and Human Development Index (HDI) (b). Adapted from Wu et al. (2023). 133
Figure 8-3 | Current composition of China's building stocks. (a) Residential building stock composition by building floor. (b) Residential building stock composition by building material. (c) Year built of private buildings in Hong Kong Special Administrative Region. (d) Vintage composition of residential buildings by province as well as HKSAR. (e) Building floors versus year built in HKSAR (Wu, Ng, Chen, et al., 2023). 134
Figure 8-4 | Historical development of NSP kilns in China (Wu et al., 2022). ... 137

Figure 8-5 | (a) Diffusion of NSP during 1995 and 2010 and (b) current CCS demonstration projects in cement sector (Wu, Ng, & Chen, 2023). 138
Figure 8-6 | Comparison of total CO_2 emissions (a), process emissions, and fuel emissions (c) of China's cement sector with previous studies and official reports (Wu et al., 2022). 140
Figure 8-7 | Comparison of cement demand projection with previous studies....141

List of Tables

Table 2-1 | The studies decomposing the emissions drivers of cement sector. 17
Table 2-2 | Material efficiency strategies (Hertwich et al., 2019).........................29
Table 5-1 | Calculated cement intensities (Unit: kg/m^2). 69
Table 5-2 | Aggregate cement intensity and related stock composition of three stock scenarios. 71
Table 5-3 | Assumptions on future stock level and related service levels. 74
Table 6-1 | Scenario narratives on supply-side mitigation strategies. 90
Table 7-1 | Parameters and sources for estimating carbon storage potentials......114

List of Abbreviations

AAGR	Average annual growth rate
AD	Activity data
AMB	The scenario of an ambitious portfolio of supply-side mitigation strategies.
ARIMA	Autoregressive Integrated Moving Average model
BAT	The best available technologies
BAU	The business-as-usual supply-side scenario.
CCID	*China Cement Industry Dataset*
CCR	Clinker-to-cement mass ratio
CCS	Carbon capture and storage
CKD	Cement kiln dust
CO_2	Carbon dioxide
CV	Coefficient of variation
DMFA	Dynamic material flow analysis
DSA	Deep saline aquifers
EF	Emissions factor
EI	Emissions intensity
EOR	Enhanced oil recovery
GCCA	Global Cement and Concrete Association
GDP	Gross domestic product
GHG	Greenhouse gas emissions
GNR	*Getting the Numbers Right* database
HDI	Human development index
HS	*High Stock* scenario
IDA	Index decomposition analysis
IEA	International Energy Agency
INFRA	Infrastructure sector
IOT	Input-output table
IPCC	Intergovernmental Panel on Climate Change
LC^3	Calcined clay limestone cements
LL	*Substantial Lifetime Extension* scenario
LMDI	Logarithmic mean Divisia index
LS	*Low Stock* scenario
ME	Material efficiency
MEU	The material-emissions-uptake nexus
MFA	Material flow analysis
ML	*Moderate Lifetime Extension* scenario
MS	*Medium Stock* scenario
NAS	Net addition to stock
NC	New cement kiln capacity
NDRC	National Development and Reform Commission of China
NRES	Non-residential building sector
NSP	Synonym of *Cement kilns with preheaters and pre-calciner* in China
NZE	Net-zero emissions
OOIP	Original oil-in-place
OPC	Ordinary Portland cement
PLT	The expected operational lifetime of cement plants
RAI	Rural access index
RC	Retied cement kiln capacity
RES	Residential building sector
SCM	Supplementary cementitious materials
SDA	Structural decomposition analysis
SL	*Short Lifetime* scenario
TC	Total cement kiln capacity

TEI	Thermal energy intensity
UN	United Nations
UNFCCC	United Nations Framework Conventions on Climate Change

Units

Gt	Gigaton
Mt	Million ton
Kt	Thousand ton
GJ	Gigajoule
MJ	Megajoule
°C	Degree Celsius
CNY	Chinese yuan

List of Publications

Journal papers directly relevant and used in this thesis:

1. **Tongyuan Wu**, S. Thomas Ng, & Ji Chen (2024). City-level carbon capture and storage deployment pathways for net-zero cement sector in China, in preparation.
2. **Tongyuan Wu**, S. Thomas Ng, & Ji Chen (2023). Incorporating carbon capture and storage in decarbonizing China's cement sector for a 1.5 °C future, *Renewable & Sustainable Energy Reviews*, Major revision. (IF[1]: **16.3**, Quartile: Q1)
3. **Tongyuan Wu**, S. Thomas Ng, Ji Chen, & Zhi Cao (2023). More intensive use and lifetime extension can enable net-zero emissions in China's cement cycle. *Resources, Conservation & Recycling*, 198, 107144 (IF: **11.2**, Quartile: Q1).
4. **Tongyuan Wu**, S. Thomas Ng, & Chen Ji (2022). Deciphering the CO2 emissions and emission intensity of cement sector in China through decomposition analysis. *Journal of Cleaner Production*, 352, 131627 (IF: **9.7**, Quantile: Q1, Google Scholar Citations: **59**).

Conference paper:

Tongyuan Wu (2023). Incorporating supply- and demand-side to decarbonize China's cement sector for 1.5 °C future, *The 1st International Conference on Urban Science and Sustainability (USS)*, Xiamen, China (Oral presentation).

[1] IF represents the abbreviation of Impact Factor of the journal in Journal Citation Report 2024.

Chapter 1. Introduction

1.1 Research background

1.1.1 Climate crisis calls for net-zero transition

Substantial greenhouse gas (GHG) emissions released by human activities have unequivocally caused global warming, which is already affecting many weather and climate extremes across our planet. The Intergovernmental Panel on Climate Change (IPCC)'s Sixth Assessment Report highlights that cumulative net carbon dioxide (CO2) emissions from 1850 to 2019 totaled up to 2400 gigatons (Gt), leading to a significant increase in atmospheric GHG concentrations (IPCC, 2023). Atmospheric CO_2 concentration rose from 280 parts per million in 1850 to 410 ppm in 2019, resulting in positive radiative forcing and 1.1 degrees Celsius (°C) rise in global surface temperatures compared to pre-industrial levels. This warming has intensified heatwaves, heavy precipitation, droughts, tropical cyclones, and other extreme weather events globally, alongside rising sea levels by 0.20 meters from 1901 to 2018. Climate change has also inflicted irreversible damage on terrestrial, freshwater, cryosphere, coastal, and ocean ecosystems worldwide. It is a defining crisis of our time, and no corner of the globe is immune from the devastating consequences of climate change.

To stabilize global mean temperature, net CO_2 emissions by human activities, including energy services and industrial production, land use and agriculture, must approach zero (Davis et al., 2018). This urgency prompted 196 countries to sign the Paris Agreement in 2015, aiming to limit global warming to well below 2°C, preferably 1.5°C (UNFCCC, 2015). Recent research underscores the critical need to achieve the 1.5°C target to avoid severe climate impacts. For a >50% chance of limiting warming to 1.5°C with minimal overshoot, global CO_2 emissions must hit net zero by the early 2050s; whereas for a >67% chance of limiting warming to 2°C, this can be postponed to the early 2070s (IPCC, 2023). Countries worldwide are increasingly committing to net-zero emissions by 2050, with China, as the largest global emitter, aiming for carbon peak by 2030 and carbon neutrality by 2060 through significant socio-economic shifts and development in renewable energy, efficiency improvements, and carbon removal technologies (Z. Liu et al., 2021).

1.1.2 Substantial carbon emissions from cement production

Cement is the mineral glue that binds sand and gravel together to form concrete, a fundamental material in modern and industrialized societies. Its production, however, is carbon-intensive, primarily due to the production of clinker, the precursor and active component of Portland cement (Habert et al., 2020). Clinker is produced by heating ground limestone and clay at temperatures of approximately 1400-1500°C. This process involves significant carbon emissions: one-third from fuel combustion required for pyro-processing, and two-thirds from the chemical decomposition of limestone (Voldsund et al., 2019). Consequently, producing one ton of conventional cement clinker releases around 850 kilograms (kg) of CO_2, making the production process highly emission intensive.

Specifically, the large-scale production of cement leads to substantial carbon emissions. As illustrated in Figure 1-1, global cement production has increased more than 30-fold since 1950 and nearly 4-fold since 1990, currently exceeding a rate of 4 gigatons (Gt) per year (Andrew, 2019). This vast production scale results in significant emissions, with up to 1.5 Gt of CO_2 released annually from limestone decomposition alone, equivalent to about 4% of global emissions from fossil fuels (Andrew, 2019). These statistics underscore the urgent need for effective decarbonization strategies within the cement sector.

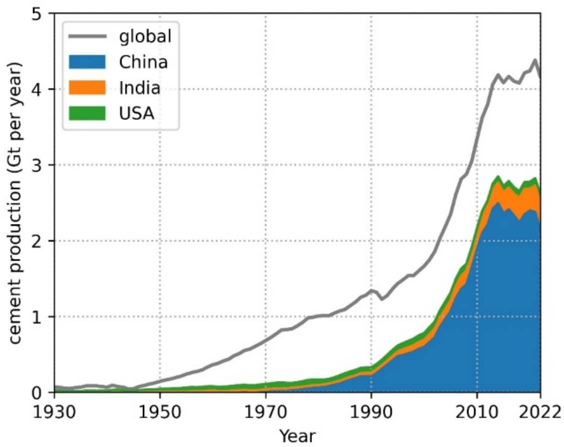

Figure 1-1 | Global cement production in 1930-2022. Data source: Robbie Andrew (2023).

1.1.3 Challenges in decarbonization for the cement sector

Decarbonizing the cement sector presents numerous challenges due to its inherently carbon-intensive production processes and the critical role cement plays in construction and infrastructure (Habert et al., 2020). One significant challenge is the high emission intensity associated with clinker production, which relies heavily on carbon-intensive fuel combustion and the chemical decomposition of limestone (Davis et al., 2018). The reliance on traditional kiln technologies further complicates efforts to reduce emissions, as transitioning to low-carbon alternatives requires substantial investment and technological innovation. Additionally, the durability and performance characteristics of conventional Portland cement, which have been refined over decades, pose challenges for the adoption of alternative materials and methods that may not yet match these standards (Monteiro et al., 2017).

Another major challenge lies in the limited availability and scalability of alternative materials and technologies. While supplementary cementitious materials (SCMs) and alternative binders can reduce clinker content and associated emissions, their supply is often insufficient to meet global demand (Kermeli et al., 2019). Moreover, the deployment of carbon capture and storage (CCS) technologies, which can significantly mitigate emissions, faces economic and logistical barriers. CCS requires significant capital investment, and the infrastructure for capturing, transporting, and storing CO_2 is not yet widely established (Hills, Leeson, et al., 2016). Additionally, regulatory and policy frameworks must evolve to support these technological advancements, ensuring that emission reductions are economically viable and aligned with broader climate targets. Addressing these challenges requires coordinated efforts across industry, government, and research institutions to drive innovation and implement effective decarbonization strategies.

1.2 Research questions statement

Despite previous studies have devoted efforts into developing decarbonization roadmaps for cement sector, the deficiencies remain in the integration of supply-and demand-side dynamics within the emissions-uptake nexus. Four research questions pertinent to these deficiencies are proposed as below.

Before developing future decarbonization pathways, it is crucial to comprehensively understand the historical trends and current status of carbon emissions in the cement sector. Identifying and quantitatively assessing the drivers of emissions growth or mitigation is essential to determine the remaining mitigation potential for achieving a net-zero future by mid-century. Thus, the first research question is proposed as follows:

(1) What are growth and mitigation drivers in historical carbon emissions of cement sector?

Explicit demand projections are necessary to serve as a robust benchmark for emissions mitigation. Previous studies typically predicted cement consumption using socio-economic regressors (Ke et al., 2012; Ren et al., 2023; Van Ruijven et al., 2016; J. Wei & Cen, 2019), but cement consumption may decouple from economic development in the long term, as observed in some industrialized economies (Bleischwitz et al., 2018). This projection approach may obscure the role of historically consumed cement accumulated in society and its linkage to the services provided. Additionally, cement materials can gradually reabsorb atmospheric carbon dioxide through carbonation reactions during their use and end-of-life stages, potentially serving as a carbon sink (Cao et al., 2020; Huang et al., 2023; M. Ma et al., 2024; Watari et al., 2022; Xi et al., 2016). This carbon uptake may significantly offset production emissions and alter the required mitigation efforts. Thus, the second research question is proposed as follows:

(2) How can future cement consumption be systematically projected, how much mitigation potentials, and what are the implications for carbon emissions and uptake?

Demand-side dynamics are seldom systematically integrated into previous roadmaps. For instance, only a single demand scenario was adopted for emission mitigation planning, without investigating potential mitigation from the demand side (Dinga & Wen, 2022; Xu et al., 2016; C.-Y. Zhang et al., 2021). While some material flow analysis-based studies integrate future stock dynamics and carbonation uptake (Cao et al., 2020; Watari et al., 2022), they often subjectively envision a moderate portfolio of supply-side efforts for emissions mitigation, which may not explicitly align with climate targets such as 1.5°C and 2.0°C. Furthermore, there are still obstacles on the supply side. In the absence of large-scale replacement materials for Portland cement, expensive carbon capture and storage (CCS) technologies are indispensable for a net-zero transition in the cement sector. However, the capital-intensive existing production facilities, committed to operate for several decades, may hinder the fast scaling up of CCS, especially in relatively new cement plants in developing economies (C. Chen et al., 2022; Cheng et al., 2023). Therefore, the third research question is proposed as follows:

(3) How to integrate supply- and demand-side dynamics to develop decarbonization pathways for cement sector that consistent with climate targets?

Additionally, previous decarbonization roadmaps lack spatially explicit guidance for practical implementation (Dinga & Wen, 2022; Ren et al., 2023; Tan et al., 2022; C.-Y. Zhang et al., 2021). Especially for CCS deployment, it is essential to consider suitable capacities for retrofitting as well as local or nearby accessible storage sites for captured emissions. Implicit spatial information or overlooking regional discrepancies may hinder the scaling up of CCS in the cement sector. Although some source-sink matching analyses have been conducted for CCS deployment in energy and industrial sectors (H. Tang et al., 2021; Y. Wang et al., 2024; Y.-M. Wei et al., 2021), the impacts of changing emissions layouts are seldom discussed. Accordingly, the final research question is proposed as follows:

(4) How to integrate spatially explicit carbon emissions and storage information into decarbonization pathways for planning CCS deployment in cement sector?

1.3 Research aim and objectives

To address the above research questions, this study aims to develop a framework to decarbonize the cement sector within a material-emissions-uptake nexus. The framework serves as the foundation for both retrospective analysis of historical carbon emissions, material stock, and emissions uptake, and perspective analysis of future dynamics to develop decarbonization pathways. The initial step involves synthesizing knowledge from material flow analysis, carbon emissions accounting, and carbon uptake quantification, and integrating them into the framework to characterize material flows, stocks, and related carbon dioxide fluxes. Once developed, the framework will be tested and demonstrated through a detailed historical case study.

As for future, explicit demand projection is the prerequisite for developing robust decarbonization pathways. Thus, the second objective mainly aims to make robust projections on future cement demand. The systematic projection should be conducted from a material stock perspective as adopted for retrospective analysis. At the same time, mitigation potentials and their implications from demand-side should also be explored and investigated. Furthermore, the impacts of the varying in-use stocks, inflows (or demand), and outflows on future emissions and uptake should be systematically assessed.

The third objective of this research is to develop carbonization pathways from a supply-side perspective, while integrating future demand-side dynamics and emissions offset by carbonation uptake. Besides conventional mitigation measures, the developed roadmaps will emphasize the expected scale, scale-up speed, and potential opportunities and challenges of CCS deployment, which is seen as an indispensable option to realize net-zero.

Nevertheless, how much the emissions reduction potentials of CCS delineated in the national decarbonization roadmaps can be tapped, also hinges on the future emissions distribution and accessible carbon storage sites. Therefore, the last objective of this research is to simulate future spatial distribution of carbon emissions of cement sector, which can provide spatially explicit data basis to prioritize locations for large-scale CCS deployments.

In summary, four specific objectives of this research are listed below.

(1) To develop a framework than can characterize the material-emissions-uptake (MEU) nexus of cement sector.
(2) To project future dynamics of cement materials stock and explore the mitigation potentials of cement demand.

(3) To develop robust and efficient decarbonization pathways for the cement sector to be aligned with climate targets, within the MEU nexus.
(4) To improve practicability of decarbonization pathways by integrating geographical contexts.

1.4 Research scope

This study intends to outline a feasible and pragmatic long-term transition pathway for a material manufacturing sector, cement sector, thus the related research scope can be determined as follows. First, from a technical perspective, cement mainly refers to the Portland cement in most cases in this study. Second, cement sector refers to a specific collection of cement plants (producing clinker), grinding stations, and any other related cement production facilities distributed within a certain spatial range, e.g., a district, city, province, state, and region. Third, greenhouse gas emissions from cement production only refer to carbon dioxide (CO_2). Fourth, the spatial coverage is limited to 31 provinces within the mainland China. As for temporal coverage, the retrospective analysis extends back from 2022 to 1949, and the perspective analysis looks forward to mid-century (2050 or 2060), with the resolution of the period of one year.

1.5 Research significance and contribution

Overall, this study can enhance current decarbonization pathways for the cement sector by integrating both supply- and demand-side dynamics. The contributions of this research can be summarized from theoretical, methodological, and practical perspectives.

Theoretically, this study develops an integrated modeling framework that characterizes the material-emissions-uptake nexus for the cement sector. This framework allows for the synthesis of supply- and demand-side dynamics, providing a comprehensive view of their combined impacts on decarbonization pathways. Previous studies often treated supply and demand separately, but this integrated approach enables a more holistic analysis.

Methodologically, this study introduces a simplified supply-demand matching model to simulate the future geographical distribution of production emissions.

This model can also match carbon emissions with storage sites for CCS deployment planning. By avoiding the use of complex spatial optimization models like mixed-integer programming, this simplified matching model reduces computation time while still delivering empirically accurate results.

Practically, this study offers spatial-temporal insights into CCS deployments in the cement sector for policymakers and industry investors. Cities with large clinker production and nearby carbon storage capacity can be prioritized for retrofitting or developing CCS capacity, thus reducing both pipeline construction and transportation costs. Policymakers are advised to promote capacity deployment in these regions, potentially through city-specific subsidies, while limiting new capacity development in less favorable locations. For investors, these hotspot cities provide valuable references for decision-making, helping to minimize the risk of stranded assets.

1.6 Structure of this thesis

This thesis totally contains nine chapters.

Chapter One establishes the context for this research, covering the background, research questions, aim and objectives, scope, significance and contributions, and thesis structure.

Chapter Two conducts a thorough literature review on carbon emissions drivers of cement sector, carbon dioxide uptake by carbonation of cement materials, cement stock dynamics, and decarbonization pathways for cement sector. Research gaps are identified and summarized.

Chapter Three designs the research roadmap and presents the methodologies of this research. The adopted research methods, i.e., literature review, scientific modeling, and scenario analysis, are introduced, and several modeling techniques involved in the subsequent chapters are also listed and introduced.

Chapter Four develops an integrated modeling framework to characterize the materials-emissions-uptake (MEU) nexus of cement sector. Then, this chapter introduces and justifies each module of the framework, i.e., dynamic material flow analysis, carbon emissions accounting, and carbon uptake quantification models. After that, a retrospective analysis on China's cement sector is adopted as a case study to demonstrate framework's capability to decipher the MEU nexus, of which the results will serve as the basis for perspective analysis.

Chapter Five starts the perspective analysis from the demand-side. This chapter investigates the future cement stock dynamics while exploring mitigation potentials from the material efficiency strategies. A scenario matrix, based on the per-capita stock and service lifetime, is systematically developed with the detailed narratives and justifications to delineate the future boundary conditions for China's cement stock. Through the developed MEU framework, this scenario matrix is translated to quantitative results, leading to implications for future cement consumption and potential emission mitigation.

Chapter Six explores the supply-side transition pathways for cement sector towards net-zero emissions, considering explicit demand-side dynamics. Besides am ambitious scenarios of conventional mitigation measures, such as fuel switching and clinker substitution, this chapter focuses on the deployment pathways of carbon capture and storage (CCS) to align with climate targets. Specifically, an inter-temporal linear programming model is developed to minimize the total cost for CCS deployment over time while satisfying the emission budgets corresponding to 1.5 °C, 1.7 °C, and 2.0 °C. The resulting emissions pathways, along with implications for capacity turnover and technology diffusion, are investigated and discussed.

Chapter Seven improves decarbonization pathways within specific geographical contexts. This chapter simulates future emissions distributions of cement clinker production across China's cities, based on the three representative demand scenarios from Chapter Seven. This chapter firstly downscales national clinker demand to each city. Then, a supply-demand matching module is developed to collect demand around each city, based on the available production capacity projected from turnover model. Carbon storage potentials are also estimated and then integrated to identify those cities prioritized for CCS deployments.

Chapter Eight conducts a comprehensive and in-depth discussion on the research outcomes from Chapter 4, 5, 6, and 7. This chapter highlights the advantages of MEU framework over the previous studies. Then, it summarizes the implications obtained from the case study on China's cement sector, especially integrated decarbonization roadmaps developed by the framework. Besides, some comparisons with previous studies are also conducted to validate the case results.

Chapter Nine reviews the achievement of the research objectives and summarizes the research findings. The contribution of the study to theory, methods and practice is also presented. Finally, limitations of the study and future research directions are also discussed.

1.7 Chapter summary

This chapter begins with a brief introduction to the research background. Following this, four research questions are summarized and proposed, along with the research aim and five related objectives of this thesis. The scope of the research is delineated, and the significance and contributions are highlighted. Finally, the main contents of each chapter are briefly introduced to provide an overview of the thesis structure.

Chapter 2. Literature review

2.1 Introduction

A thorough literature review can help to identify the gaps and deficiencies and summarize the research questions. And it can also provide knowledge basis for the following work in this research. Thus, this chapter will review the topics related to the research questions of this thesis.

2.2 CO_2 emissions and drivers of cement sector

2.2.1 Portland cement production

Portland cement is the most common type of cement, of which is constituted by 90-95% clinker, 2-3% gypsum and minor additives (Habert et al., 2020). As the active part of Portland cement, clinker is produced in a carbon-intensive process, because of high temperature heating traditionally fueled by coal or oil and the direct release of carbon dioxide from limestone decomposition. Figure 2-1 shows the main processes of the state-of-the-art cement production method with pre-heaters and pre-calciners. Specially, raw materials, composed of limestone, clay and small amounts of 'corrective' materials (e.g., iron ore, bauxite, and sand), are firstly crushed, mixed, and milled into a raw meal, which will be pre-heated to ~850°C by exhaust heat from the kiln in the cyclone pre-heaters, by which calcium carbonate is dissociated into calcium oxide and carbon dioxide. Then, it will be calcined in the rotary kiln at ~1450°C, where reactions between calcium oxide and other elements produce calcium silicates and aluminates. After heating from the kiln, the melted materials should be cooled rapidly to from an assemblage of the silicates alite (C_3S) and belite (C_2S), tricalcium aluminate (C_3A) and tetra-calcium aluminoferrite (C_4AF), known as clinker (Habert et al., 2020).

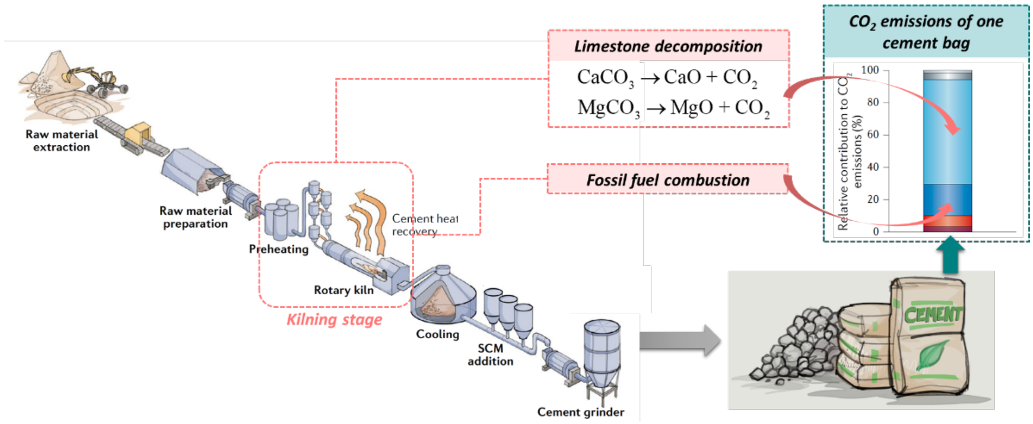

Figure 2-1 | Cement production processes (adapted from Habert et al. (2020)).

Thus, the main reactions during the Portland clinker production can be listed as below (Taylor, 1997).

$$CaCO_3 \rightarrow CaO{+}CO_2(g) \tag{2.1}$$

$$AS_4H \rightarrow \alpha\text{-}Al_2O_3{+}4SiO_2(quartz){+}H_2O(g) \tag{2.2}$$

$$AS_2H_2 \rightarrow \alpha\text{-}Al_2O_3{+}2SiO_2(quartz){+}2H_2O(g) \tag{2.3}$$

$$3CaO{+}SiO_2(quartz) \rightarrow C_3S \tag{2.4}$$

$$2CaO{+}SiO_2(quartz) \rightarrow \beta\text{-}C_2S \tag{2.5}$$

$$3CaO{+}a\text{-}Al_2O_3 \rightarrow C_3A \tag{2.6}$$

$$4CaO{+}\alpha\text{-}Al_2O_3{+}\alpha\text{-}Fe_2O_3 \rightarrow C_4AF \tag{2.7}$$

Where AS_4H and AS_2H_2 refer to pyrophyllite ($Al_2Si_4O_{10}(OH)_2$) and kaolinite ($Al_2Si_2O_5(OH)_4$), respectively. C_3S refers to Alite or tricalcium silicate (Ca_3SiO_5), which is the most important constituent of all normal Portland clinker because of it will quickly react with water and contribute significantly to early strength development. β-C_2S denotes Belite or dicalcium silicate (Ca_2SiO_4) presented as the β polymorph. C_3A represents the tricalcium aluminate ($Ca_3Al_2O_6$). C_4AF denotes the tetracalcium aluminoferrite ($Ca_4Al_2Fe_2O_{10}$). Finally, the clinker is mixed with small amount of gypsum (i.e., calcium sulfate to control the setting rate and the strength development (Taylor, 1997).

2.2.2 CO_2 emissions accounting

As for emission accounting, CO_2 emissions from cement production are categorized into process-related emissions (mainly due to the carbonate decomposition) and energy-related emissions, which can be further subdivided into emissions from fuel burning and indirect emissions for electricity consumption (Ali et al., 2011). The accounting methods are basically similar and straightforward by multiplying the activity data with the related emission factor (IPCC, 2006), despite that there are different international guidelines governing emission accounting at the national, sector, and factory level, such as the three-tier methods in the 2006 IPCC Guidelines for National Greenhouse Gas Inventories (2006), and the CO_2 emission accounting standard of Cement Sustainability Initiative (Cement Sustainability Initiative, 2011).

Energy-related emission factors are well investigated for conventional fossil fuels, while the process emission factor should be determined based on the specific stoichiometric compositions. Apparently, the content of calcium oxide dominates the CO_2 emissions of process emissions, according to the reaction (2.1). However, there are minor CO_2 emissions from the decomposition of contained magnesium carbonate ($\mathrm{MgCO_3} \rightarrow \mathrm{MgO} + \mathrm{CO_2}$), which can be traced by the content of magnesium oxide in the clinker. Therefore, the process emission factor can be derived based on the stoichiometric compositions as below.

$$\mathrm{EF_{clinker}} = \mathrm{Content_{CaO}} \times \frac{44}{56} + \mathrm{Content_{MgO}} \times \frac{44}{40} \tag{2.8}$$

where $\mathrm{Content_{CaO}}$ and $\mathrm{Content_{MgO}}$ represent the CaO and MgO contents in the clinker which should be determined based on plant-level surveys. For specific region or country, the process emission factor should be carefully estimated, as the default one recommended by IPCC (2006) may over or under-estimate the total emissions from cement production. For China, the National Development and Reform Commission of China (NDRC), which was previously responsible for the country’s climate change affairs, estimated the process-related emission factors for clinker production based on specific data collected from 128 plants in 2005, when compiled the national inventories (Department of Climate Change of

National Development and Reform Commission of China, 2012). Shen et al. (2014) surveyed the raw material, raw meal, clinker, cement and fuel of 289 production lines across the 18 provinces of China by 2012, and estimated the process emission factors by kiln types, which is lower than the default values found in the IPCC Guidelines by 1.4-3.4%. Cai et al. (2016) estimated the overall process emission factor at 0.504 t CO_2/t clinker based on the detailed information of 1,574 cement enterprises in 2013, but without claiming the specific content of CaO and MgO. Besides, the emission factors from other sources are also included for comparison as below.

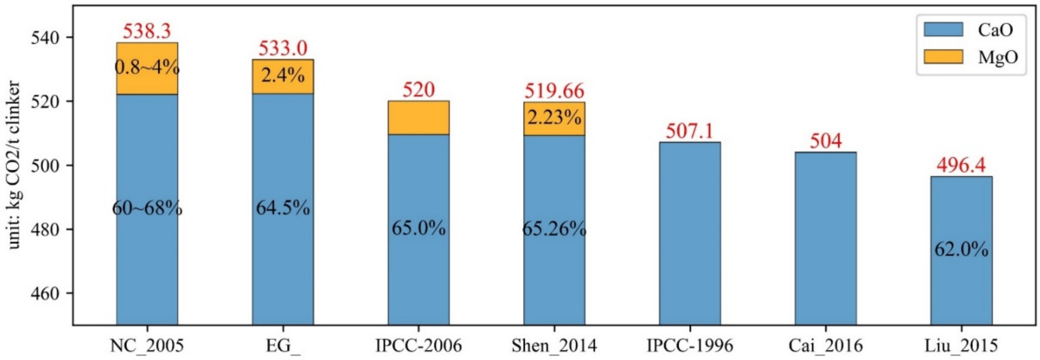

Figure 2-2 | Comparison of process emission factors of clinker production (Wu et al., 2022).

NDRC estimated the process-related emissions at 157.8 Mt CO_2 and 411.7 Mt CO_2 in 1994 and 2005 respectively in its twice communication reports submitted to UNFCCC (NDRC, 2004, 2012). Another issue is the high variations and uncertainty in energy consumption, as the amount of coal used for heating the kiln was not directly available in the official statistics but rather being estimated by different reported coal intensity (J. Liu et al., 2021).

2.2.3 Emissions drivers

Analyzing drivers of CO_2 emissions trends of countries or sectors help us find out the impact factors which contribute to emissions growth or decline. For example, such analysis on the developed economies where emissions are decreasing, can examine whether emissions reductions come from efforts to improve energy systems or just recent economic recession (K. Feng, 2019). The most common driver analysis is the Kaya identity (1989), which expresses total CO_2 emissions as a product of four driving factors: population, GDP per capita, primary energy consumption, and the carbon intensity of energy. Raupach et al. (2007) adopted Kaya identity to analyze global and regional drivers of accelerating in the early 21st century and found that global emissions growth since 2000 was driven by a slightly rebound of both energy intensity of GDP and carbon intensity of energy, coupled with continuing increase in population and per-capita GDP. However, their analysis only reviewed proportional change of drivers, rather than explicitly quantifying their specific contribution. Thus, mathematical tools, such as index decomposition analysis (IDA), have been used to supplement the decomposition identities in the following studies. Le Quéré et al. (2019) decomposed energy-related carbon emissions of 18 developed economies, where emissions decreased over 2005-2015, into final energy use, the share in energy use, the utilization, and CO_2 intensity of fossil fuels. Using logarithmic mean Divisia index (LMDI) approach to quantify relative impacts of each factor, they found that the decarbonization of these countries can be mainly explained by the displacement of fossil fuels by renewable energy and decreasing energy use. Guan et al. (2018) also used IDA to quantify the relative impacts of eight socioeconomic factors on the decline of China’s energy-related carbon emissions during 2007-2016. They revealed that the emissions peak and decline in 2013-2016 is largely attributed to industrial structure change and a decreased share of coal used for energy.

For cement sector, one of energy- and carbon-intensive industries, emissions driver can be analyzed based on either activity data (i.e., production scale for cement sector) or emission intensity, which reflects CO_2 emissions per unit of cement production. Cement production or consumption is usually decomposed into a series of socio-economic factors, such as population, per-capita GDP, and cement consumed per GDP. For instance, Cao et al., (2016) adopted STIRPAT model to analyze the drivers of China’s cement consumption, including population, urbanization, fixed investment, income level, and consumption intensity (cement consumption per GDP). Du et al. (2020) adopted LMDI to quantify the contributions of 7 demand- and 2 supply-side drivers to emissions change of annual CO_2 emissions from China’s cement sector and revealed that demand-side drivers always dominated the emissions change during the past 25 years. Lin & Zhang (2016) decomposed the total emissions into five effects from the productivity perspective, i.e., total employees, unit industrial added value per employee, energy consumption per unit added value, energy structure, and carbon intensity of energies. But this decomposition is unreasonable as it omitted a large part of non-energy emissions (i.e., process-related emissions). Shan et al. (2019) decomposed the total emissions to the structure of the construction industry, emission intensity, input efficiency, and fixed asset investment from an economic perspective. However, the fixed asset investment may not significantly relate to cement production as cement costs only account for a small part of it. While Zheng et al. (2021) decomposed emission intensity reasonably according to the components of accounting formulas, their analysis on total emissions just added a scale effect (i.e., total production), which could not reflect the effects resulting in production change.

Besides drivers of cement production, the reduction in emission intensity is further decomposed into a series of factors that can reflect technological improvement and structural change throughout production process, as shown in Table 2-1. However, there are inconsistency among the decomposed factors in these studies, leading to the under- or over-estimated effects. For example, Y. Wang et al. (2013) divided the total emissions into energy-related and process-related emissions and decomposed the former into the energy emission factors, energy structure, energy intensity, and total production, which could not lead to specific improvement as they mixed clinker production and cement grinding together. Furthermore, outsourcing carbon-intensive clinker is seldom considered in the studies specific to China, perhaps due to the minor quantity of clinker import or export, whereas it matters in the analysis for those countries reply on imported clinker or cement, such as European states (Branger & Quirion, 2015).

Table 2-1 | The studies decomposing the emissions drivers of cement sector.

No.	Literature	Region	Time period	Process emissions	Thermal efficiency	Fuel mix	Electrical efficiency	Electricity decarbonization	Clinker factor	Kiln type	Clinker outsourcing
1	(Kim & Worrell, 2002)	Brazil China Korea US	1985-1996 1988-1996 1981-1998 1981-1998	√	√	√		√	√	√	
2	(Xu et al., 2012)	China	1990-2009	√	√				√	√	
3	(Y. Wang et al., 2013)	China	2005-2009	√		√					
4	(Branger & Quirion, 2015)	EU-27	1990-2012	√	√	√	√	√	√		√
5	(Lin & Zhang, 2016)	China	1990-2010			√					
6	(J. Liu et al., 2018)	China	2005-2012	√	√	√	√	√	√		
7	(Shan et al., 2019)	China	1996-2016	√							
8	(Du et al., 2020)	China	1990-2015	√					√	√	
9	(J. Liu et al., 2021)	China	1990-2015	√	√				√	√	
10	(Zheng et al., 2021)	China	2005-2012	√	√		√	√	√	√	

1. We will not tick in the corresponding cell if the studies implicitly decomposed the driving factors, or merged two detailed factors to one single factor, unless the specific effects of the above factors are explicitly quantified.
2. Although process emissions are considered in most studies, their impacts are negligible as they assumed that process emissions intensity would be constant over years for conventional cement production.

2.3 CO_2 uptake by carbonation and quantification

The term 'carbonation' is used to characterize a complicated physicochemical reaction between atmospheric CO_2 and hydrated cement products in the presence of pore water in the construction structures. Despite its detrimental effects on structure health, its potential to sequester substantial CO_2 has gradually gain more attention and started to be considered as a formal carbon sink in the global carbon budget (Friedlingstein et al., 2022). Therefore, this section first briefly reviews the principle of carbonation reaction. Then, existing studies examining the mitigation effects on global warming, which estimates carbonation uptake at global, regional, or smaller scale, over time, are reviewed and summarized the current drawbacks.

2.3.1 Principle of carbonation reaction

The calcium oxide in cement materials is not stable over time, and cement hydration products gradually absorb atmospheric CO_2 through a physiochemical process called carbonation reaction (Huntzinger et al., 2009; Johannesson & Utgenannt, 2001; Pade & Guimaraes, 2007; Renforth et al., 2011). The carbonation reaction starts from the surface of concrete of mortar and moves inwards over time. Specifically, CO_2 reacts with Calcium hydroxide in the solution of pore water, and in turn reacts with calcium silicate, dicalcium silicate, tricalcium silicate, tricalcium aluminate and other hydrated products. The specific reaction equations are shown as follows (Xi et al., 2016).

$$Ca(OH)_2 + CO_2 \xrightarrow{H_2O} CaCO_3 + H_2O \tag{2.9}$$

$$(3CaO \cdot 2SiO_2 \cdot 3H_2O) + 3CO_2 \xrightarrow{H_2O} (3CaCO_3 \cdot 2SiO_2 \cdot 3H_2O) \tag{2.10}$$

$$(2CaO \cdot SiO_2) + 2CO_2 + xH_2O \xrightarrow{H_2O} 2CaCO_3 + (SiO_2 \cdot xH_2O) \tag{2.11}$$

$$(3CaO \cdot SiO_2) + 3CO_2 + xH_2O \xrightarrow{H_2O} 3CaCO_3 + (SiO_2 \cdot xH_2O) \tag{2.12}$$

The carbonation reaction will destroy the high pH environment of surrounding concrete which protects the steel bars of reinforced concrete from corrosion, and thus is considered by civil engineers as the major time-limiting factor for durability of reinforced concrete structures (Papadakix et al., 1991).

2.3.2 Quantification on carbon uptake at global and regional scale

Although the carbonation reaction is detrimental to structural health, it has been gradually seen as a potential carbon sink among the global carbon fluxes. Previous studies have tried to quantify CO_2 uptake by carbonation reaction at global, regional, and country levels over time (Andersson et al., 2013; M. Ma et al., 2024; Pade & Guimaraes, 2007; Xi et al., 2016). The quantification method is somehow methodologically similar with the emission accounting method above: just multiplying *uptake factor* with the quantity of the objects that could reabsorb CO_2. However, unlike the emission process, which is almost instantaneous process, carbonation uptake happens gradually over time, and thus its uptake factor depends on the rate of carbonation over time.

Integrating theoretical work, laboratory studies, and field surveys, Pade & Guimaraes (2007) explicitly determined the carbonation rate and projected CO_2 uptake by concrete (produced in 2003) structures over 100-year period in the future in four Nordic countries. Andersson et al. (2013) estimated carbon uptake by existing concrete structures in Sweden of 2011, over their use stage and after service life. However, these retrospective studies were limited to concrete structures in specific regions and did not consider other types of cement-based materials. Thus, Xi et al. (2016) comprehensively considered four different types of cement-based materials: concrete, mortar, cement kiln dust, and construction waste, over the three life cycle stages, i.e., service life, demolition, and secondary use, and conducted a quantification at the global scale. Their results revealed that up to 4.5 gigatons carbon (equivalent to 16.5 Gt CO_2) had been uptake by cement-based materials in 1930-2013, offsetting 43% of CO_2 emissions from limestone decomposition during cement production (Xi et al., 2016). And the dataset of global CO_2 uptake by cement has been subsequently updated to 2019 and 2021 (Guo et al., 2021; Huang et al., 2023). Recently, a study tailed for China revealed that 7.0 Gt CO_2 had been cumulatively sequestered in cement during 1930-2021, among which about 427 Mt CO_2 was absorbed in 2021, accounting for 8-45% of China's terrestrial carbon sink (Huang et al., 2023).

As for future, carbon uptake should be systematically projected based on the evolving cement stock. Cao et al. (2020) developed nine scenarios to outline future boundaries of global cement stock, which is projected to uptake 81-117 Gt atmospheric CO_2 over 2015-2100, leading to different time to reach net-zero cement cycle in the next half of the century. Watari et al. (2022) also synthesized Xi et al. (2016)'s quantification model to consider carbonation uptake as a significant mitigation level in Japan's net-zero cement and concrete cycle by 2050. Furthermore, about 7 billion tones alkaline materials produced globally each year (including 4 billion tons of cement), are projected to sequester 2.9-8.5 billion tones CO_2 per year by 2100, as the high pH solutions created by their aqueous dissolution can dissolves and store CO_2 in the form of solid carbonate minerals or dissolved bicarbonate ions (Renforth, 2019).

2.4 Cement stock dynamics

Converted from limestone and other raw materials, cement accumulates within a specific spatial range over time, forming the biophysical structures that support human society. In the field of Material Flow Analysis (MFA), this is referred to as '*in-use*' stock. Similar to how different types of nutrients sustain the metabolism of biological organisms, bulk materials such as cement can be considered '*macronutrients*' for human society, analogous to carbohydrates and proteins in biology, whereas critical materials like rare earth metals and gold function as '*micronutrients*', comparable to trace elements and vitamins in biological systems (Pauliuk & Hertwich, 2015). Previous studies on cement stock can be categorized into static MFA analysis, which provides the snapshot of cement cycle for a region or country at a certain time, and dynamic MFA analysis, which uses either *inflow-driven* approach to estimate historical stock or *stock-driven* approach to project future stock dynamics.

Static cement cycle illustrated a whole picture of cement and its precursor, and products embedded in our society. Kapur et al. (2009) mapped the cement cycle of the Unites States around 2000-2004, based on the MFA framework, from which they found that more cement will be required than that of traditional economic forecasts, because a significant portion of infrastructures was reaching the end of its service life and need to be replaced or rehabilitated. Further, static cement

MFA can be conducted assess performances of cement production, such as production efficiency (Gao et al., 2016) and eco-efficiency (W. Wang et al., 2016).

Dynamic MFA can retrospectively estimate historical in-use cement stock. Kapur et al. (2008) estimated historical inventories of cement stock and flows in U.S. during the period of 1900-2004. Their estimates showed that there were ~4.4 Gt cement stock in use in U.S. (equivalent to ~15 ton per capita), among which ~87% cement came from the last century. Overall, such consistent and accurate cement stock accounting aims to provide information of in-use material stocks and future discards to relevant stakeholders engaged in the infrastructure development and maintenance, to assist in better planning future rehabilitation projects and life cycle management for infrastructure systems (Kapur et al., 2008). Using a top-down approach, Cao et al. (2017) mapped global distribution of in-use cement stock among 184 economies of ten regions from 1931 to 2014, and investigated their growth patterns according to time series analysis, especially paying attention on the first and second order differences of in-use stocks.

As for future, dynamic MFA usually adopt stock-driven approach to project material consumption over the long term. Stock dynamics can serve as a more robust basis for forecasts, because stocks are less affected by short-term market fluctuations, such as market prices or product substitution, compared with inflow data (Müller et al., 2014). Also, extrapolation on inflow data is not capable of considering the effects of market saturation and resource scarcity. A pioneer work by (B. Müller, 2006) developed a generic dynamic MFA model to project future material flows based on stock dynamics. By a case of concrete of Dutch dwelling stock, 27 scenarios with three parameters (i.e., total useful floor area, service lifetime, and concrete intensity) varying between three levels (i.e., low, medium, high) were developed to explore the future possible concrete consumption towards the end of this century. These diffusion scenarios on future concrete consumption can provide early recognition of environmental problems, better investment planning in mining, and waste management. Following study by Liu et al. (2013) further related material stock dynamics to carbon emissions and mitigations concretely. Their scenario matrix formed by three levels of per-capita stock and stock saturation times (2050, 2075, and 2100) delineated aluminum in-use stock patterns and set the boundary conditions for future emissions pathways of global aluminum sector. One of significant implications is production emissions will increase dramatically, if developing countries follow the stock patterns of industrialized countries. Focusing on cement stock again, Cao et al. (2020) projected future in-use stock based on a similar scenario matrix and in turn the emissions pathways during 2015-2100, while integrating mitigation options and CO_2 uptake by carbonation reaction in cement stock. The results indicated that the stringent climate goals (such as 1.5°C) is very likely to be imperiled if cement stock continues to grow. A few other MFA studies are partly pertinent to cement stock, as they focused on building or infrastructure stocks (Fishman et al., 2016; D. B. Muller et al., 2013; Shi et al., 2012; Song et al., 2023).

2.5 Decarbonization pathways for cement sector

Decarbonization pathway is a transformational process that delivers long-term emissions reduction and sustainable development in collaboration with local communities, businesses, and other key actors (Climate Group, 2024). Generally, it starts with specific GHG reduction goals and then works backwards to identify the technologies, infrastructures, and investments that will be required to achieve it.

2.5.1 Supply-side pathways

Supply-side decarbonization pathways mainly rely on production technologies, but the focus and mitigation levers will evolve with the socio-political and technological context. Take China as an example, early attention was paid on improving energy efficiency of cement kilns in the 1990s, while improving product quality and reducing pollution (F. Liu et al., 1995). Later, Chinese officially began to promote large-scale deployment of cement kilns with preheater and pre-calciners (also known as '*NSP*' in China) to replace outdated shaft kilns. As NSP saturated in the market and marginal benefits decreased, the focus shifted from merely efficiency improvement to reinventing the future cement sector, such as moderate CO_2 emission reduction (Xu et al., 2016), green transition roadmaps (X. Liu et al., 2017; C.-Y. Zhang et al., 2021), and even recent carbon neutral pathways (Dinga & Wen, 2022). Based on the status quo of cement sector and current technological maturity, major mitigation options can be summarized as follows, while methods to systematically develop pathway are also reviewed.

2.5.1.1 Mitigation options

At present, there are four main types of emissions mitigation options for cement sector: (1) improving energy efficiency (including thermal efficiency and electrical efficiency), (2) switching fossil fuels to low-carbon fuels, (3) clinker substitution to reduce clinker-to-cement ratio, and (4) carbon capture and storage (CCS). These measures will not significantly change current product systems, such as ordinary Portland cement (OPC), whereas low-carbon alternative cement clinker gradually drew attention but are still in early development stage and may require modifications on current materials standards (Gartner & Sui, 2018; Miller & Myers, 2020).

With the new dry process kilns with pre-heater and pre-calciner to extensively replace outdate shaft and wet kilns, thermal energy demand has decreased to around 3.46 GJ/t clinker (Figure 2-3). At present, the advanced dry process kilns with six stages of cyclones pre-heaters can reduce thermal demand to ~2.8 GJ/t clinker (J. Ma et al., 2017), approaching the theoretical minimum of 1.85-2.8 GJ/t clinker, which is set by chemical and mineralogical reactions as well as necessary drying for raw materials (ECRA & CSI, 2017). Apparently, change on production process, e.g., from wet to dry process, from long kiln to preheater/pre-calciner kiln can significantly cut thermal energy demand. Other relative minor modifications on specific processes, such as additional preheater cyclone stages, improved waste heat recovery, efficient clinker cooler, and multi-channel burner, can moderately reduce thermal demand by 25-300 MJ/t clinker (ECRA & CSI, 2017).

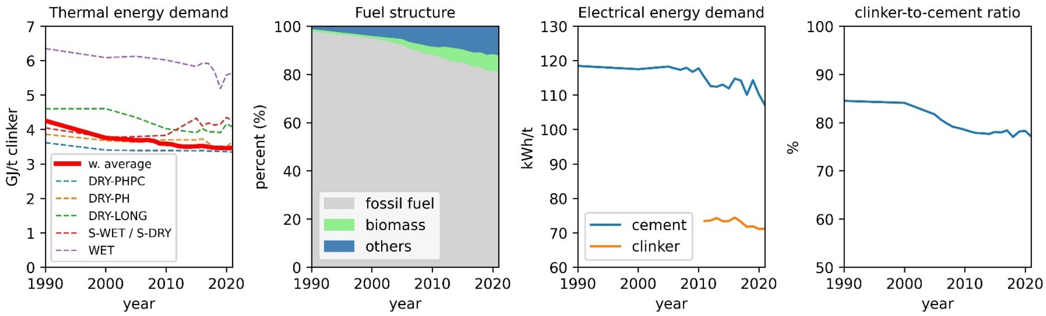

Figure 2-3 | Energy efficiency, fuel structure, and clinker-to-cement ratio of global cement sector. (Data source: "*Getting the Numbers Right (GNR)*" database 2.0 (GCCA, 2024).) (Notes: w. average represents the weighted global average. DRY-PHPC refers to dry process cement kilns with pre-heaters and pre-calciner. DRY-PH refers to dry process cement kilns with pre-heaters. DRY-LONG refers to long dry kiln without preheaters. S-WET and S-DRY denote semi-wet and semi-dry process, respectively. WET represents wet or shaft kilns.)

Fuel switching usually refers to the switch from coal to oil or gas, but increasingly biomass is coming to be the focus for a net-zero future (ECRA & CSI, 2017). Specifically, CO_2 emission factors of fuel oil and natural gas can be ~19% and ~ 41% lower than that of bituminous coal, due to their higher energy content and lower carbon content. As for biomass fuels, their carbon emissions can be regarded as zero emissions when accounting, and even can be seen as negative emissions if combined with CCS. Currently, biomass fuels used in cement industry are mainly biomass waste, such as waste wood, rice husk, sawdust, sewage sludge and animal meal (ECRA & CSI, 2017). However, the global proportion of biomass fuels was only about 7% in 2021, whereas fossil fuels still accounted for over 80% (Figure 2-3).

Clinker substitution aims to replace part of the clinker in cement using supplementary cementitious materials (SCMs), such as coal fly ash and granulated blast furnace slag. Currently, the global weighted average clinker-to-cement ratio (CCR) has declined to 0.77 by 2021 and seems to stagnate in recent years. Theoretically, there has a significant mitigation potential in CCR. For instance, a combination of calcined clay with limestone allows the substitution levels of clinker contents up to 50%, that implies CCR can be reduced to 50%, with similar mechanical performance and somehow improved durability (Scrivener et al., 2018). Shah et al. (2022) systematically assessed the historical global potential supply of secondary cementitious materials during 2002 and 2018 and found that up to 1.3 Gt CO_2-eq. emissions could be avoided in 2018, with a maximal substitution of clinker by 3.5 Gt potential supply of secondary cementitious materials.

At present, a few types of cement CCS have been proposed, simulated, and tested in small-scale pilot projects, e.g., amine scrubbing, oxyfuel (Voldsund et al., 2019), calcium looping (Rodriguez et al., 2012), and direct separation (Driver et al., 2022). Voldsund et al. (2019) compared technological performance of five cement CCS technologies, based on process simulations. While targeting 90% capture rate for flue gas, specific primary energy consumption for CO_2 avoided varies from 1.63 MJ/kg CO_2-avoided for the oxyfuel-based capture process to 7.08 MJ/kg CO_2-avoided for the amine scrubbing. Besides, cost-effectiveness is especially important for cement CCS retrofit and new installation. Liang & Li (2012) assessed the economic value of retrofitting a real modern dry process cement plant with CCS. The estimated cost was \$70 per ton CO_2 avoided at a 14% discount rate with 25 years remaining lifetime. Gardarsdottir et al. (2019) revealed an increase of 49-92% in cost of clinker production equipped with five CCS technologies, compared to the cost of clinker without carbon capture. Specifically, the lowest cost is 42 €/t CO_2 avoided of the oxyfuel-based capture process, while the highest cost is 84 €/t CO_2 avoided of the membrane-based assisted liquefaction capture process.

2.5.1.2 Developing future pathways

Scenario analysis is the basin approach to develop future decarbonization pathways for cement sector. The prerequisite is the determined future production on a year-by-year basis equivalent to the projected cement demand, without the consideration of market stock change. Then, development rates of measures are projected based on state-of-the-are knowledge (e.g., technology maturity and resource availability) to explore future emissions mitigation potentials. For instance, Cao et al. (2020) developed a scenario of five major supply-side mitigation measures for global cement sector. Among these measures, CCS can cumulatively reduce 56.7-94.2 Gt CO_2 emissions during 2015-2100, under the various cement stock and future demand. Cheng et al. (2023)'s projections and scenarios showed that carbon emissions of future cement production in developing countries except China will grow from 0.7 Gt in 2018 to 1.4-3.8 Gt in 2050, which can be cut by ~65% through developing a combination of low-carbon measures. Cavalett et al. (2024) synthesized future deployment rate of a series of mitigation measures from literature and institution reports to develop a 'representative' decarbonization pathway for European cement sector towards mid-century. Notably, they found that only about 50% annual emissions (~64 Mt CO_2 per year) can be mitigated relative to today's emissions, especially with a penetration of only 25% for CCS by 2050.

When specific goals or emissions budgets are determined firstly, annual emissions mitigation and the required deployment rates of mitigation measures can be determined accordingly and optimally under certain objectives, such as lowest overall cost. A few global Integrated Assessment Models, e.g., *IMAGE* and *DNE 21+*, modeled cement sector separately to optimize the deployment rates of four major measures discussed in the last sub-section (Kermeli et al., 2019). Also, Kermeli et al. (2019) improved the capability of IMAGE model to model cement sector, by considering plant retrofitting as a measure and availability constraints of SCMs. Furthermore, some cement sector-specific studies, sub-divided these major measures into a detailed technology list and optimized their deployment rates in a 'bottom-up' manner, while minimizing total cost (Dinga & Wen, 2022; Doh Dinga & Wen, 2021; Xu et al., 2014, 2016; C.-Y. Zhang et al., 2021). For instance, Dinga & Wen (2022) developed a bottom-up technology transition model for China's cement industry to assess the feasibility of achieving carbon neutrality by 2060, while considering co-benefits of CO_2 mitigation and uncertainty. After deducting monetized co-benefits, a net cumulative cost of 279-345 billion Chinese yuan (CNY) is still required to make a net-zero cement sector possible by 2060. However, from a technological perspective, it is not proper to simply sum the potential mitigation of individual technologies to derive the total potential reduction. This is due not only to the interacting impacts of various measures but also because some measures may double-count energy savings, potentially resulting in an estimated energy demand that is lower than the theoretical minimum (ECRA & CSI, 2017).

Furthermore, a more spatial-explicit analysis, such as plant-level analysis, may provide a more concrete data basis to improve feasibility of decarbonization pathways. Based on a detailed power plant inventory, Cui et al. (2021) developed priorities for early retirement of part of coal power plants in China, to be consistent with national emission pathways for 1.5 °C or well-below 2 °C climate goals. As for cement sector, Hills et al. (2016) developed a bottom-up model for the UK's cement plants, to explore the feasibility of synchronizing CCS installation with shutdowns for major refurbishments at plant level. Besides, regional disparity should be carefully considered in pathway development. For instance, uneven distribution of carbon storage potentials across China may significantly increase construction cost of transportation cost and limit CCS deployments in the area far away from suitable storage sites. Tang et al. (2021) developed an optimal layout for CCS deployment and pipeline construction for China's power sector, to realize carbon neutrality by the mid of century. Accessible storage sites or CO_2 transport pipeline network also matter for CCS deployment in cement sector (Hills, Florin, et al., 2016). Thus, Wang et al. (2024) developed an optimal matching between those cement plants prioritized for CCS deployment and suitable CO_2 storage sites in China, while minimizing total cost for deployment and pipeline construction. However, their spatial layout of cement CCS was only based on current emission inventory, without considering future change in cement demand and production layout across China.

2.5.2 Demand-side potentials

Demand-side solutions for mitigating climate change aim to modify the demand for goods and services by targeting choices and the adoption of technology, consumption patterns, behaviors, lifestyles, coupled production–consumption infrastructures and systems, service provision, and associated socio-technical transitions (Creutzig et al., 2018). These solutions can potentially reduce GHG emissions by 40-80% in specific end-use sectors (Creutzig et al., 2021).

2.5.2.1 Cement consumption projection

Previous decarbonization pathways usually projected future cement consumption as the basis and distribute them to specific low-carbon production routes (i.e., the paradigm of supply-side pathways). Notably, their projection implicitly implied a balance between supply and demand on a year-by-year basis, without a consideration of market stock change over time. And annual consumption is always denoted as a product of population scale and per-capita demand, which is somehow correlated with socio-economic factors, such as gross domestic product (GDP) per capita. This is attributed to that cement is one of the fundamental materials to build up essential infrastructures for people's daily lives and to support economic activities. However, per-capita cement consumption may not keep growing over the economic growth, rather, it will slow down, saturate around a certain point, then may gradually decrease, showing a non-linear trend over time (Bleischwitz et al., 2018). For instance, Van Ruijven et al. (2016) developed non-linear regression models to project future per-capita cement and steel consumption, with per-capita GDP as a predictor. Then they calibrated the model with historical data and forecasted future trend towards 2050. Also, the correlation between per-capita GDP and cement consumption shows the diverse trends across regions and states (Bleischwitz et al., 2018; Van Ruijven et al., 2016). Other predictors, such as urbanization rate (Tan et al., 2022) and fixed asset investment, which is closely related to construction cost, were also selected as a predictor in short-term prediction, e.g., 2010-2030 (Ke et al., 2012; Xu et al., 2014).

Although cement demand projected by the regression method can serve as an intuitive and simplified forecasting method, mitigation potential from specific material efficiency measures cannot be explicitly quantified in such way. In contrast, material flow analysis (MFA) can project long-term materials demand in a stock-based perspective, and assess demand reductions by more efficient use of current materials stock (B. Müller, 2006; Cao et al., 2020; Watari et al., 2022). For instance, Cao et al. (2020) explored the range of future global cement consumption during 2015-2100, through a stock-driven MFA approach and scenario analysis. In contrast, Watari et al. (2023) recommended a 'forecasting supply and back-casting demand' approach against the traditional 'forecasting demand and back-casting supply' dynamics. They figured out possible maximal production volume under the constraint of carbon budgets consistent with 1.5°C and 2°C and found that feasible supply may meet only 22-56% of the expected baseline demand in 2050.

2.5.2.2 Material efficiency

Material efficiency (ME) entails *the pursuit of the technical strategies, business models, consumer preferences and policy instruments that would lead to a substantial reduction in the production of high-volume energy-intensive materials required to deliver human well-being* (Allwood et al., 2013). ME can serve as an indicator to measure the amount of physical service provided per unit of material, and as a strategy to mitigate climate change (Hertwich et al., 2019). Six strategies of ME are identified and summarized by Hertwich et al. (2019), i.e., more intensive use, lifetime extension, light-weight design, reusing components, recycling, and improving production yield (as shown in Table 2-2 below).

Table 2-2 | Material efficiency strategies (Hertwich et al., 2019).

Strategy	Definition	Example	Targeted stage
More intensive use	Providing the same service with less product.	A higher utilization rate of products through sharing.	Use
Lifetime extension	Extending service life of existing products to provide more service.	Regular maintenance and repair on buildings for using it for more time.	Use
Light-weight design and material choice	Less material and/or lower GHG emissions in the production.	Performance-based rather prescription-based structure design to reduce material requirements (Olsson et al., 2023). Promotion of timber structure to replace concrete structures (Churkina et al., 2020).	Production
Improving production yield	Reducing waste generated during production and fabrication stage.	Reducing onsite construction waste by offsite or modular construction (Y. Zhang et al., 2024).	Production
Reuse of components	Reusing end-of-life components of products. through (such as) remanufacturing.	Reusing roof from scrapped vehicles (Sato et al., 2019).	End-of-life
Recycling	Collecting and processing wastes and then turning them into new use.	Recycled construction aggregates from building demolition waste.	End-of-life

Furthermore, these strategies are somehow qualitatively prioritized In the context of cement materials. Miller et al. (2021) reviewed the mitigation measure at various stages along its value chain and developed a cementitious materials use hierarchy to prioritize decarbonization means based on their efficiency (Figure 2-4), in which reducing cement demand is the most efficient mitigation measure.

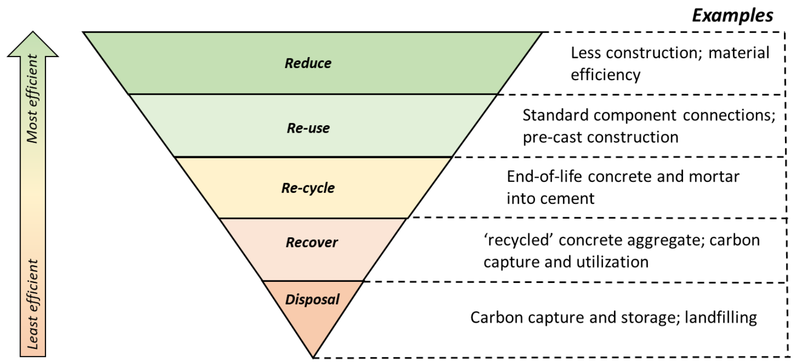

Figure 2-4 | Cementitious material use hierarchy (adapted from Miller et al. (2021)).

A few studies have assessed potential emissions mitigation realized by ME strategies at global or regional scale. Pauliuk et al. (2021) showed that implementing ME strategies can cumulatively reduce global GHG emissions until 2050 by 20-52 Gt CO_2-eq and 13-26 Gt CO_2-eq from residential building construction and passenger vehicles production, respectively. Zhong et al. (2021) developed a high efficiency scenario in which seven ME strategies are simultaneously applied to realize a 78 Gt CO_2-eq reduction (equivalent to 49%) in cumulative building material related GHG emissions during 2020-2060. Furthermore, their ME scenario can avoid ~50% of cumulative building sand consumption in the same period, trying to avoid rapidly unfolding sand supply crisis (Zhong et al., 2022). Olsson et al. (2023) found that optimizing concrete strength and steel reinforcement for building application would lead to 18.5 reduction in GHG emissions between 2015-2100 and increasing concrete system longevity by up to 4-fold from current regional average service lives will lead to a 47% reduction in cement demand and related 176 Gt CO_2-eq emissions. Watari et al. (2022) demonstrated that while 80% of production emissions in the cement and concrete cycle in Japan can be reduced through supply-side efforts from baseline levels, the remaining 20% emissions gap towards achieving net-zero can also be bridged by efficient use of cement and concrete in the built environment. Shanks et al. (2019) pointed out that material efficiency measures really matter for the cement sector's decarbonization, based on the evidence that up to 56% of cement can be saved by improving material use efficiency in the UK, leading to a 44% reduction in CO_2 emissions from production.

2.6 Research gaps

Although previous studies have made contributions to the related research topics, several research gaps remain to be addressed, which are identified and summarized as follows.

(1) *Previous decarbonization roadmaps lack a comprehensive understanding of the material-emissions-uptake nexus for the cement sector.* While significant efforts have been made to develop decarbonization strategies, the intricate relationship between material usage, emissions released during cement manufacturing, and the potential for carbon uptake through carbonation reactions has not been thoroughly explored. Understanding this nexus is crucial for accurately assessing the sector's net carbon footprint and identifying effective mitigation strategies that encompass both emissions reduction and carbon uptake.

(2) *The integration of supply- and demand-side dynamics in developing decarbonization pathways is limited.* Prior studies often focus on either supply-side mitigation measures, such as improving energy efficiency and switching to low-carbon fuels, or demand-side approaches, like reducing cement consumption through enhancing material efficiency. However, these strategies are typically considered in isolation, overlooking the synergistic benefits that can be achieved by integrating both perspectives. A holistic approach that combines supply- and demand-side dynamics is necessary to develop robust decarbonization pathways that are resilient to various future scenarios.

(3) *There is a need for spatially explicit planning on CCS deployment in the cement sector.* Most current roadmaps for CCS do not account for regional disparities in emissions sources and storage capabilities. Effective CCS implementation requires detailed spatial planning to match CO_2 sources with suitable storage sites, considering factors such as proximity, capacity, and infrastructure availability. Without this spatially explicit planning, the scaling up of CCS technologies may face significant logistical and economic challenges, particularly in regions with uneven distribution of emissions and storage resources. Identifying optimal locations for CCS deployment can

reduce transportation costs, enhance efficiency, and ensure that storage capacities are not exceeded.

2.7 Chapter summary

This chapter conducts a through literature review on the related research topics, such as emissions accounting and emissions drivers of the cement sector, cement stock dynamics and carbonation uptake, and decarbonization pathways. And three several research gaps are identified and summarized accordingly.

Chapter 3. Research methodology

3.1 Introduction

It is crucial to develop a reasonable, practical, and logical roadmap to achieve the research aim and specific objectives stated in Chapter 1. Thus, this chapter start with designing a robust research roadmap of this thesis. Literature review, scientific modeling, and scenario analysis are adopted to conduct research work throughout this thesis, and they will be briefly introduced in this chapter. Furthermore, several specific modeling techniques involved are also introduced and justified in this chapter.

3.2 Research design

Figure 3-1 displays a revised research roadmap designed for this thesis to achieve the research aim and four specific objectives stated in Section 1.3. China's cement sector is selected as a case for both retrospective and perspective analysis throughout this thesis. The research is structured into four main parts, aligning with the specific objectives. First, an integrated framework is developed to understand the material-emissions-uptake (MEU) nexus by synthesizing knowledge from dynamic material flow analysis, carbon emissions accounting, and emissions uptake quantification, demonstrated through a historical case study of China's cement sector (*Chapter 4* against *Objective 1*). Second, future cement demand is projected through demand-side scenario analysis, with the MEU framework quantifying impacts on emissions pathways, stock dynamics, and carbon uptake (*Chapter 5* against *Objective 2*). Third, integrates supply-side scenario analysis with the projected demand to develop climate-consistent decarbonization pathways, involving plant turnover simulation and inter-temporal optimization to determine CCS deployments (*Chapter 6* against *Objective 3*). Lastly, this research improves CCS deployment strategies by incorporating geographical contexts, conducting supply-demand matching, assessing local carbon storage potentials, and identifying prioritized cities for large-scale CCS deployments (*Chapter 7* against *Objective 4*). This comprehensive research design ensures that the study addresses both retrospective and prospective aspects of decarbonizing China's cement sector, integrating detailed analyses from both demand- and supply-side perspectives, and considering geographical contexts to provide robust and actionable decarbonization roadmaps.

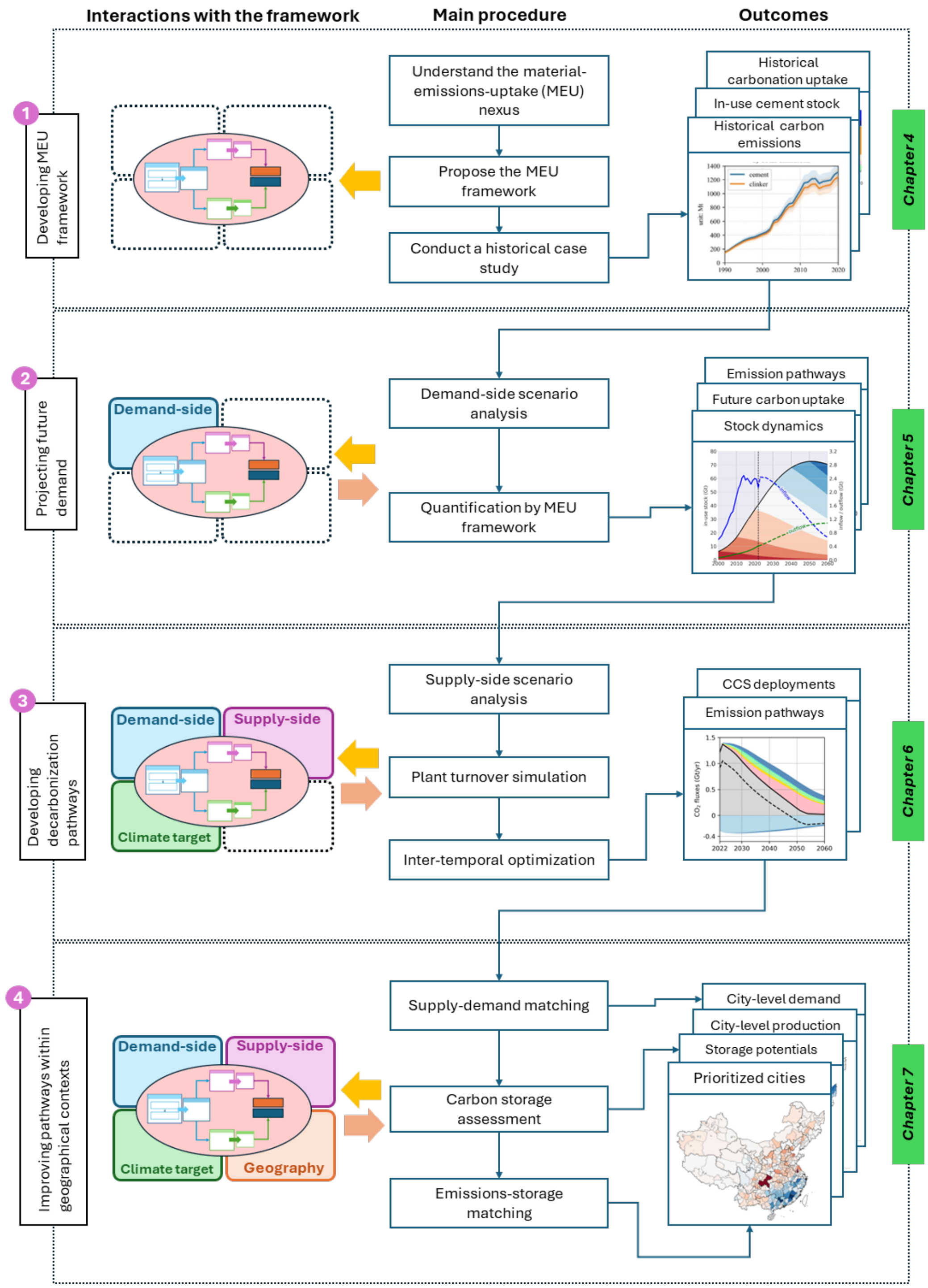

Figure 3-1 | Research roadmap of this thesis.

3.3 Research methods

3.3.1 Literature review

Literature review has been conducted throughout the whole study, to obtain a comprehensive understanding of the existing emissions accounting methods, emission drivers, emissions mitigation pathways for cement sector, systematical characterization of the cement stock in our society, future cement demand projection, and emissions uptake by carbonation. Research gaps and limitations are identified and summarized to develop the primary research aim and a series of specific research objectives. Also, official policy documents (including regulations and guidelines) issued by national and local departments, and industrial reports (both from global non-government organizations and think tanks) are carefully reviewed to identify and summarize the existing achievements and limitations in the current low-carbon transition pathways for the cement sector.

3.3.2 Scientific modeling

Generally, scientific models are built by scientists to *replicate systems in the real world through simplification*, to *perform an experiment that cannot be done in the real world*, or to *assemble several known ideas into a coherent whole to build and test hypothesis* (Mezik, 2017). Scientific models can be categorized into three types: physical, conceptual, and mathematical (Jordaan & Lategan, 2010; Mezik, 2017). Physical modeling mainly refers to scale modeling of real-life objects or phenomena re-constructed by laboratory apparatus or other facilities. Conceptual models involve assembling all the known components of a system into an abstract coherent whole, such as the very early 'billiard ball' model for the atom. And mathematical modeling is the process of describing the behavior of an element of a physical system, or a comprehensive system or phenomenon, by means of a mathematical expression, or a series of mathematical expressions (Jordaan & Lategan, 2010). Regardless of the type of model, the first step is to define the system to be modeled and the goals for the model, which typically involves delineating the boundaries literally or figuratively around what you want to model, and then determining the key variables and the relationships between those variables (Mezik, 2017). In this study, several mathematical models are used, including emission accounting, index decomposition on emissions drivers, and material flow analysis model, to characterize the historical and future dynamics of CO_2 emissions from cement production and in-use cement stocks in our society.

3.3.3 Scenario approach

Sustainable development of the cement sector necessitates long-term planning due to the system inertia inherent in current decisions, which will affect the energy and climate system for decades. For instance, technology *lock-in* effects can be exacerbated by the high costs and long lifetimes (30-40 years) of cement kilns. Additionally, the substantial greenhouse gas emissions currently produced will continue to influence the global climate system over the next century, given the slow nature of climate change processes. Therefore, this study adopts a model-based scenario approach to assess and delineate the future emissions pathways and transition roadmaps for the cement sector. Specifically, the term scenarios, is defined as a plausible description of how the future might develop, as based on a coherent and internally consistent set of assumptions ("scenario logic") about the key relationships and driving forces (Nakićenović & Swart, 2000). And the rationale of the scenario approach is that instead of estimating the most likely future, the situation moves into an assessment of possible pathways of events ("what if?") (Van Vuuren, 2007). Whilst uncertainty arises from system complexity, scenario approach can serve as projections or explorations, addressing the considerable uncertainty about the future trajectories of a system (Figure 3-2). In cases of relatively low system uncertainty, scenarios allow for projecting future implications, often involving reference scenarios with alternative projections (Zurek & Henrichs, 2007). Conversely, when there are significant questions about how driving forces may play out, especially in the long-term future, scenarios help explore the implications of various potential futures, typically results in sets of contrasting scenarios that outline a range of plausible futures (Zurek & Henrichs, 2007).

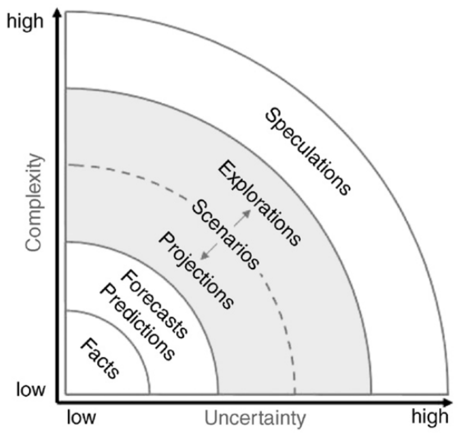

Figure 3-2 | Different approaches to assess the future in relation to uncertainty and system complexity (Zurek & Henrichs, 2007).

Finally, it should be kept in mind that long-term scenario analysis is not intended to predict the future and will almost certainly be proven at least partly wrong over time (Van Vuuren, 2007). Rather, such analysis can integrate the best available information to provide meaningful insights. By maintaining an understandable relationship between actions and the actual chain of events, scenario analysis can convey significant implications of decisions to intended users, such as policymakers and industrial stakeholders.

3.4 Modeling techniques

3.4.1 IPCC emissions estimation method

According to IPCC's guideline (2006), to estimate the total anthropogenic emissions[2] of one or more specific greenhouse gas emissions, originating from all or part of the sources categories in a certain geographical area and within a specified time span (usually a calendar year), the most common simple methodological approach is to combine information on the extent to which a human activity takes place (termed as *activity data*, AD), with coefficients which quantify the emissions or removals per unit activity (termed as *emission factors*, EF). Here, this approach can be shown in a basic equation as below.

$$Emissions = AD \times EF \tag{3.1}$$

[2] Anthropogenic emissions and removals, which means that greenhouse gas emissions and removal included in national inventories are a result of human activities (IPCC, 2006).

Thus, for instance, total emissions from an energy sector can be estimated by multiplying its fuel consumption as activity data with mass of carbon dioxide emitted per unit of fuel consumed as an emission factor. In this study, detailed activity data and emission factors of cement sector, including clinker production by kilns type, specific emission factors for calcination process (limestone decomposition and fuel combustion), are collected and compiled to estimate and analyze carbon emissions from cement sector. As for removal, carbon dioxide uptake by carbonation reactions in the cement stocks embodied in our society, which serves as a type of anthropogenic carbon removal from atmosphere, is systematically estimated in the similar approach, but with the detailed activity data (i.e., the material stock or flow that can absorb carbon gradually) and uptake factors (compared to EF, the carbon removal per unit of material stock or flow).

3.4.2 Index decomposition analysis

Decomposition analysis aims to identify and assess the drivers of observed changes over time of energy and environmental impact indicators of a nation or sector (De Boer & Rodrigues, 2020). There are two techniques for decomposing indicator changes at the sector level, i.e., structural decomposition analysis (SDA) and index decomposition analysis (IDA) (Hoekstra & van den Bergh, 2003). SDA uses input-output tables (IOT) and models as a basis to explore the link between the environmental impacts and consumption activities. For IDA, it begins by defining a governing function relating an aggregate indicator to a few pre-defined factors of interest (serving as 'indices') in a reasonable way. One of the famous IDA equations is 'Kaya identity', which precisely and meaningfully depresses the level of greenhouse gas emissions as the product of four socio-economic factors: human population, GDP per capita, energy intensity (per unit of GDP), and carbon intensity (emissions per unit of energy consumed). Then, with the defined function, various quantitative methods can be formulated to gauge the impacts of changes in these factors on the aggregate indicator (Dinda, 2004). According to their definitions, SDA requires much more data as it relies on IOTs, while IDA only requires the sector level data (Hoekstra & van den Bergh, 2003). Notably, IDA and SDA have different emphasis, as De Boer & Rodrigues (2020) pointed out that, SDA aims to explore the links between the environmental impacts and production level while IDA emphasizes on the relationship between the impacts and consumption activities. Furthermore, SDA may not support long-term continuous monitoring on structural change in the cement sector, as IOTs are released almost every five years in China. Therefore, given the research emphasis and data availability, this study adopts IDA to analyze the structural change over years (e.g., change in product mix change, decrease in sectoral energy intensity, etc.) in the cement sector.

3.4.3 Material flows analysis

As one of the central methodologies of industrial ecology, *material flow analysis (MFA)* aims to map and trace the flows of resources into and from a particular entity within human society, based on the mass balance principle (Graedel, 2019). Material flows and stocks are the most basic concepts in MFA (C. Zhang et al., 2017), and they can provide quantitative information concerning such as rates of material use, material loss to the environment, and recycling rates of scrap. When analyzing a specific region or system over time, a *dynamic MFA* can determine the *in-use* and "hibernating" stock of materials in our society, which is the emphasize of this study. Specifically, by accumulating for the difference between the likely imbalanced inflows and outflows within a time interval, in-use stock can be derived. This is usually referred to as a *top-down* approach. In contrast, a *bottom-up* approach adds up the quantity of materials of interest embodied in all kinds of products within a pre-defined system boundary to derive the stock at a certain time or over time. Also, from the temporal scale, a dynamic MFA can be either *retrospective* or *perspective*, or a combination of both (E. Muller et al., 2014). Retrospective MFA analyzes past stocks and flows based on historical data, while perspective MFA projects the future through various approaches such as data extrapolation and scenario development. Constrained by unavailable detailed long-term spatial data, this study adopts top-down retrospective MFA to estimate historical cement stock, to ensure model's internal consistency and improve the robustness of analysis. As for future towards the year of 2050 and 2060, which is target time for the achievement of global or regional climate ambitions, this study develops top-down perspective MFA to systematically project and delineate boundary conditions of future cement stock.

3.4.4 Optimization model

Generally, an optimization model consists of an objective function that needs to be minimized or maximized, decision variables that can be controlled or adjusted, and constraints that must be met. In the context of decarbonization, the objective function could be minimizing total cost of deploying mitigation technologies over time. Decision variables mainly include the levels of various technologies implemented to cut emissions, whereas constraints could include production capacity, technological feasibility, regulatory requirements, and emissions limits (Biegler & Grossmann, 2004). Furthermore, inter-temporal optimization models extend this framework over multiple time periods, allowing for the analysis of decisions and their impacts over a long-term horizon. This feature is particularly important for the cement sector, where investments in technology and infrastructure have long-lasting implications. Decisions made in one period affect options and constraints in subsequent periods, which means early investments in CCS infrastructure, for example, can reduce emissions more effectively in later periods (Yeh & Rubin, 2012).

In this research, optimization models mainly help determine the optimal combination of low-carbon technologies for cement sector to control emissions within the carbon budgets, while balancing economic and operational considerations. Here a typical inter-temporal optimization model might be formulated to minimize the total cost of decarbonization, which can be expressed mathematically as below.

$$\text{Minimize } \sum_{t=1}^{T} \left(CAPEX_t + OPEX_t + PNAL_t \right) \tag{3.2}$$

Where $CAPEX_t$, $OPEX_t$, and $PNAL_t$ signify capital expenditures cost, operational expenditures costs, and penalties for emissions (e.g., carbon tax) in period t, whereas T is the total number of periods. These three cost variables depend on the decision variables, $x_{i,t}$, which represents the production rates of a specific technology i (e.g., CCS) in each period. Constraints mainly include production capacity, emissions limits, and technological feasibility. For instance, cumulative emissions should be within a specific carbon budget:

$$\sum_{i=1}^{n} e_{i,t} \cdot x_{i,t} \leq \text{ carbon budget} \tag{3.3}$$

Where $e_{i,t}$ denotes the emissions coefficient (or emissions factor) of technology i in period t. By employing such models, it is possible to provide a comprehensive view of the decarbonization pathway over time, understand the trade-offs between different mitigation strategies, and facilitate informed decision-making by policymakers and industry stakeholders.

3.5 Chapter summary

This chapter starts with developing and illustrating a research roadmap for this thesis. Then, three main research methods involved throughout this research are briefly introduced, such as literature review and scientific modeling. Furthermore, this chapter elaborates on and justifies several modeling techniques adopted to achieve the research objectives, such as IDA and MFA. Overall, this chapter establishes the methodological foundation for the analysis and results presented in subsequent chapters.

Chapter 4. Developing an integrated modeling framework to decipher material-emissions-uptake (MEU) nexus of cement sector[3]

4.1 Introduction

Massive cement production has led to significant CO_2 emissions, accounting for approximately 8% of anthropogenic emissions. However, addressing cement production's carbon footprint requires more than just decarbonizing production, material demand also plays a critical role. Cement materials, once produced, consumed, and accumulated in various infrastructures, can persist in society for decades to over a century, forming the biophysical foundation of modern life. Thus, a systematic investigation of cement stock dynamics and their integration into future decarbonization roadmaps is essential. Additionally, cement stock can globally reabsorb substantial atmospheric CO_2 through carbonation reactions over time, as recent analyses indicate that up to 21 Gt of CO_2 were absorbed by cement carbonation between 1930 and 2019, offsetting approximately 55% of the process emissions from production (Guo et al., 2021). However, CO_2 uptake is seldom systematically incorporated into existing decarbonization pathways, particularly for China's cement sector.

Against this background, this chapter develops an integrated modeling framework to characterize the material-emissions-uptake (MEU) nexus of the cement sector. This framework synthesizes knowledge from material flow analysis, carbon emissions accounting, and carbon uptake quantification to enable: (1) systematical analysis historical stock dynamics of cement materials, including in-use stock, inflow, and outflow; (2) investigation on the interplay between CO_2 fluxes and cement stock dynamics, especially carbon uptake by carbonation reactions; and (3) quantification of net changes in CO_2 fluxes associated with the cement cycle. Given its status as the world's largest producer and consumer of cement, China's cement sector serves as a case study to demonstrate the framework's applicability.

[3] This chapter is partly based on joint research work with Prof. Zhi Cao in Nankai University.

4.2 An integrated modeling framework for material-emissions-uptake nexus of cement sector

This study proposes an integrated modeling framework to systematically characterize the material-emissions-uptake (MEU) nexus of the cement sector, as illustrated in Figure 4-1. This framework integrates dynamic material flow analysis (DMFA), CO_2 emissions accounting, and CO_2 uptake quantification to provide a holistic understanding of the cement sector's carbon impact. The development of this framework is driven by the need for a comprehensive analysis that considers the entire lifecycle of cement materials, the interplay between emissions and carbonation uptake, the integration of demand-supply dynamics, and the incorporation of spatial and temporal contexts. Traditional approaches often focus solely on emissions from production without considering the broader lifecycle of cement materials. By integrating material flow analysis with emissions and uptake accounting, this framework offers a more complete view of the climate impacts of cement sector. Additionally, understanding both demand-side (e.g., material stock and usage) and supply-side (e.g., production and emissions) dynamics allows for more robust scenario analysis and strategy development, which is essential for identifying mitigation potentials and aligning with climate targets.

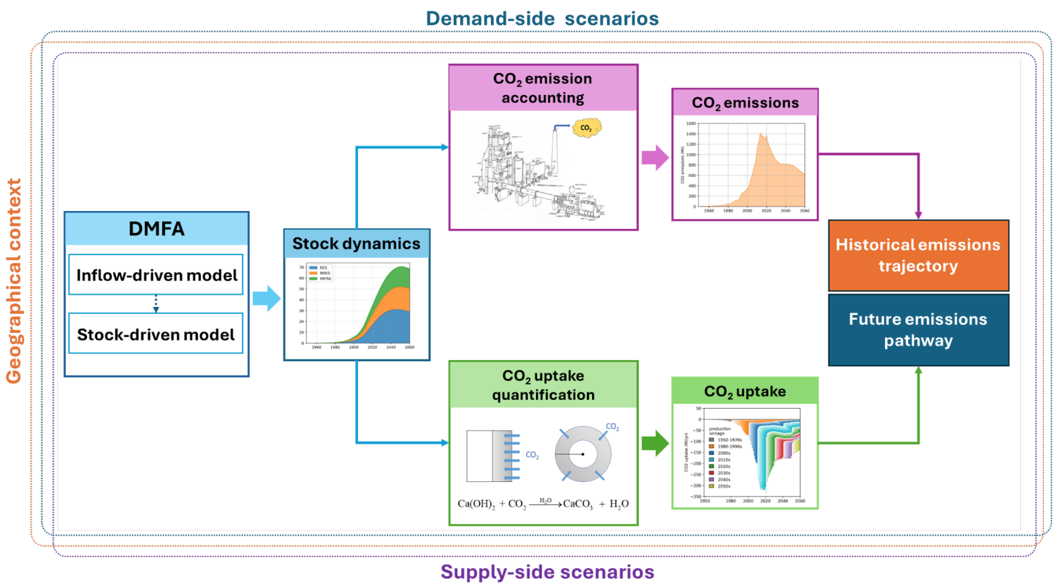

Figure 4-1 | Integrated modeling framework of the material-emission-uptake (MEU) nexus of cement sector.

The core components of the framework, referred to as modules, are as follows: Module 1, Dynamic Material Flow Analysis (DMFA), consists of inflow-driven and stock-driven models to track annual cement inflows and estimate in-use stock and outflows, providing insights into the lifecycle of cement within the built environment. Module 2, CO_2 Emissions Accounting, quantifies CO_2 emissions from cement production, including fuel combustion and limestone decomposition, offering historical emissions trajectories and future pathways under various scenarios. This is crucial for identifying major emission sources and assessing mitigation strategies. Module 3, CO_2 Uptake Quantification, measures CO_2 uptake through carbonation reactions at different stages of the cement lifecycle, providing annual and cumulative uptake estimates that significantly offset production emissions. By synthesizing these modules, the framework analyzes historical and projects future emissions pathways, considering both emissions and uptake. The framework can also incorporate geographical context and specific emissions budgets to ensure alignment with regional characteristics and global climate targets, informing spatially explicit decarbonization strategies and identifying priority areas for carbon capture and storage (CCS) deployment. The subsequent sections will introduce each module of the framework in detail, starting with DMFA in Section 4.3, followed by CO_2 emissions accounting in Section 4.4, and CO_2 uptake quantification in Section 4.5, culminating in a demonstration of the framework's application to China's cement sector in Section 4.6.

4.3 Module 1: Dynamic material flow analysis

Dynamic material flow analysis (DMFA) provides a framework to characterize materials entering and leaving a system over a period of time in a mass-balanced manner (Kapur et al., 2008; G. Liu & Muller, 2013; E. Muller et al., 2014). From a top-down perspective, Figure 4-2a illustrates the system boundary defined for cement stock accounting within DMFA theoretical context. And Figure 4-2b illustrates the calculation process enabled by a stock matrix. Here, it is assumed that the *use* phase is the only process that stores materials, while the other phases transform them without accumulating stocks. This implies that potential stocks outside the use phase are negligible and stationary over the smallest time interval considered, usually, and here the period of one year (E. Muller et al., 2014). This assumption may be challenged by interim stocks of very valuable materials created for speculation (E. Muller et al., 2014), but it is reasonable for the long-lived and stable cement and concrete materials. And spatial-temporal coverage is usually determined to be a region or country over several years to decades, with the time interval often to be period of one year.

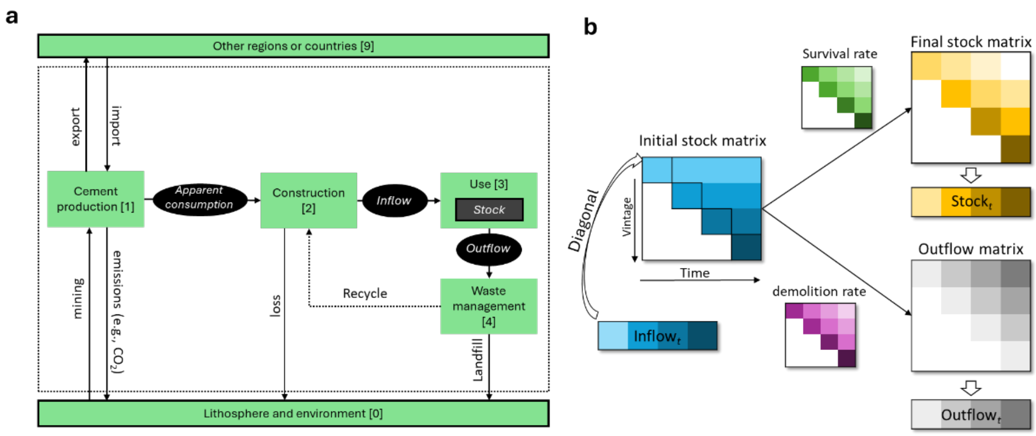

Figure 4-2 | System boundary definition (a) and the calculation process based on stock matrix in this study (b).

Depending on the goal of either retrospective or perspective analysis, two types of models can be categorized in DMFA: inflow-driven and stock-driven model (B. Müller, 2006; Bergsdal et al., 2007). In Module 1, an inflow-driven model is employed to estimate historical in-use cement stock and its per-capita evolution trajectory, while a stock-driven model will be adopted mainly to project future cement demand towards the mid-century.

4.3.1 Inflow-driven model

Inflow-driven DMFA models aims to estimate the historical in-use cement stock, based on the annual cement consumption and vintage-based service-life (Cao, Shen, Liu, et al., 2017; Cao, Shen, Løvik, et al., 2017). Specifically, annual cement consumption (i.e., inflow) will accumulate within the geographical boundary, while a fraction of them will flow out from the stock when reaching the end of their service life, thus stock, inflow, or outflow can be deduced when the other two are known variables, according to the law of mass conservation (Kapur et al., 2008). Therefore, three key variables, i.e., inflow, outflow, and in-use stock, are defined as follows. *Inflow* is the consumed cement flowing into the use phase, which equals to domestic production minus export and plus import, with some minor loss, just like dissipation of metal flows. The inflows stay in the use phase within their expected service lifetime, accumulated to form *in-use stock*. When the 'old' inflows (or the 'old' part of in-use stock) reach the end of their service-life, they will flow out from use phase, as *outflow*, which will be demolished and disposed. In this chapter, the stock and outflow are estimated by a matrix, of which the diagonal is the annual inflow, multiplied with survival rate and demolition rate, respectively. The underlying equations are described as below.

$$I_t = \mathrm{Production}_t - \mathrm{export}_t + \mathrm{import}_t - \mathrm{loss}_t \tag{4.1}$$

$$S_t = \sum_{i=1949}^{t} \left(I_i - O_i\right) \tag{4.2}$$

$$O_t = \sum_{i=1949}^{t} I_i \cdot Dr(i - 1949) \tag{4.3}$$

$$Sr(T) = 1 - \int_0^T f(x)dx \tag{4.4}$$

$$Dr(T) = \int_{T-1}^{T} f(x)dx \tag{4.5}$$

where S_t denotes the material stock within the system boundary in the year t as well as I_t and O_t represent material inputs and outputs, respectively. $Sr(T)$ denotes the survival rate for in-use stock after T years. $Dr(T)$ represents the demolition rate for the in-use stock after T years it entered use. It could be calculated from the cumulative distribution function of the lifetime distribution $f(x)$, which describes the probability that a unit will be discarded after the time x it enters use (B. Müller, 2006). Given that right-skewed distribution is consistent with the fact that buildings that survive after the demolition peak tend to stay longer than others in their cohort (Miatto et al., 2017), this chapter chooses a two-parameter lognormal distribution to characterize the lifetime distribution of in-use cement stock.

$$f(x) = \frac{1}{x\sigma\sqrt{2\pi}} \exp\left(-\frac{\left(\ln(x) - \mu\right)^2}{2\sigma^2}\right) \tag{4.6}$$

where μ and σ represent the location and scale parameters respectively.

4.3.2 Stock-driven model

As for future, a stock-driven model is employed here to project the in-use cement stock, outflow, and in turn annual consumption towards the target time, based on detailed settings of future scenarios (B. Müller, 2006; Cao et al., 2020; G. Liu et al., 2013). A stock-driven model starts with determining the future in-use cement stock by multiplying projected population scale with a contemplated trend of per-capita stock, which can be projected more reasonably within a socio-economic context than the total stock. Then annual outflow will be calculated based on the assumed service-life in the scenarios, and the annual inflow (i.e., cement demand) could be derived according to the mass balance principle. Notably, an important assumption for this module is that, due to its abundant resource availability, good workability, long-lasting durability, and versatility, cement is expected to continue to be a dominating construction material moving forward.

The specific projection process is introduced as follows. First, a modified Gompertz function (G. Liu et al., 2013) was used to simulate the development of per-capita cement stocks, assuming that no abrupt changes will take place moving forward (Eq. (4.7)). Second, total in-use stock can be derived from per-capita stock multiplying future population scale (Eq. (4.8)). Third, annual cement inflows are determined year by year, by adding up stock change and outflow during the same period (Eq. (4.9)). The per-capita in-use stock and stock lifetime will serve as the primary variables subject to alteration in the following scenario analysis. However, it's noteworthy that population, which exhibits various projections for future changes in other studies, will not be factored into the analysis of this study.

$$s_t = \frac{s_{sat}}{1 + (\frac{s_{sat}}{s_{2022}} - 1) \cdot \exp(a \cdot (1 - \exp(b \cdot (t - 2022))))} \quad (4.7)$$

$$S_t = P_t \cdot s_t \quad (4.8)$$

$$I_t = S_t - S_{t\text{-}1} + O_t \quad (4.9)$$

where P_t denotes population, s_t represents cement stock per capita in the year t, a and b denote parameters that determine the growth curve and when s_t reaches 98% of the saturation level s_{sat} at a given time. For population projections, this chapter adopts the medium growth scenario from United Nations Population Prospects 2022, and the high- and low-variants to characterize the upper and lower bounds.

4.3.3 Data source for case study

As China's cement sector is selected for a demonstrative case in this chapter, data on cement production, imports, and exports were taken from the relevant sources. For historical cement stock accounting, statistics on cement production, imports, and exports, as well as population in China are collected from the *National Data* platform of the National Bureau of Statistics. Historical service-life of China's cement stock is retrieved from an empirical study by Cao et al. (2019).

4.4 Module 2: CO_2 emissions accounting

4.4.1 Total emissions accounting

In this module, the emission factor method recommended by the IPCC Guidelines is adopted to estimate the CO_2 emissions from the cement sector in China, through multiplying the production activity data by the aggregate emission intensity to obtain the total emissions. Here the aggregate emission intensity is the amount of CO_2 emissions released by the production of a given unit of specific output (cement or clinker) at the sectoral level. Both *direct* emissions released from the cement plants, i.e., process-related and fossil fuel-related emissions, and the *indirect* emissions from purchased electricity are considered and re-divided into emissions from clinker and cement production respectively. Here, the total carbon emissions can be calculated as below:

$$C = \text{Production} \times EI \tag{4.10}$$

Where C and EI denote total emissions and emission intensity, respectively. Then, the system boundary is defined for estimating the emission intensities of cement production based on the accounting methods in previous studies and the IPCC Guidelines (Figure 4-3).

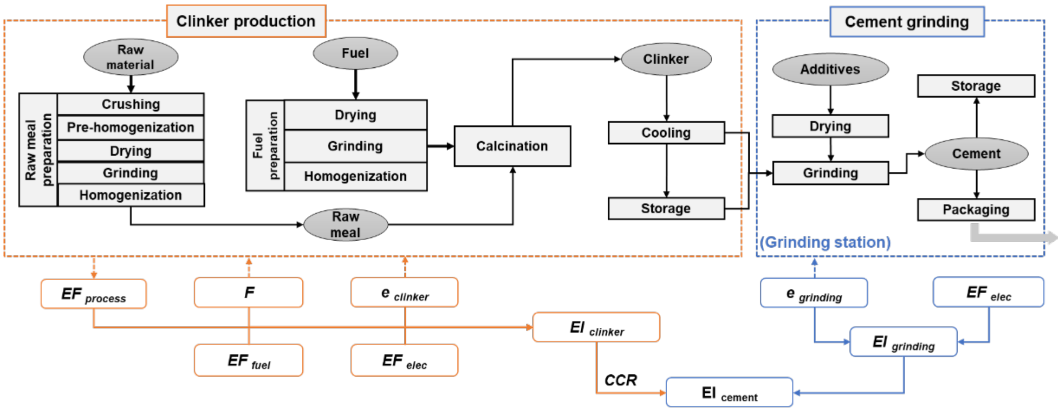

Figure 4-3 | System boundary of CO_2 emission accounting (Wu, Ng, Chen, et al., 2023).

(Notes: *EI* represents the emission intensity of a unit process of production. *EF* denotes the emission factors for fuel combustion or electricity generation. *F* and *e* represent thermal and electrical duty for unit process respectively. *CCR* denotes the clinker-to-cement ratio.)

Thus, the emission intensity, that is the total CO_2 emission released from the production of the unit product, of cement (EI_{cement}) and clinker (EI_{clinker}) could be calculated in Eq. (4.11) and Eq. (4.12), respectively.

$$EI_{\text{cement}} = EI_{\text{clinker}} \cdot f_{\text{clinker}} + EI_{\text{grinding}}^{\text{elec}} \tag{4.11}$$

$$EI_{\text{clinker}} = EF_{\text{process}} + EI_{\text{fuel}} + EI_{\text{clinker}}^{\text{elec}} \tag{4.12}$$

$$EI_{\text{fuel}} = TEI_{\text{clinker}} \cdot \sum_i w_i \cdot EF_{\text{fuel}}^i \tag{4.13}$$

$$EI^{\text{elec}} = e \cdot EF_{\text{elec}} \tag{4.14}$$

Where f_{clinker} represents the clinker content in unit product cement, i.e., the clinker-to-cement ratio (CCR); EF_{process} denotes the emission factor of limestone decomposition during kiln calcination; EI_{fuel} denotes the emission intensity for fuel combustion during calcination; TEI_{clinker} denotes the specific thermal energy intensity of clinker production, including raw materials drying and clinker calcination; EF_{fuel}^i represents emission factor of the fuel type i; w_i are weight factors to reflect fuel mix; $EI_{\text{clinker}}^{\text{elec}}$ and $EI_{\text{grinding}}^{\text{elec}}$ represents the emission intensity from electricity use by clinker production and cement grinding, respectively.

It should be noted that the above clinker emission intensity is only suitable for those cement plants without carbon capture, and storage (CCS) deployments. Currently, there are only a few pilot projects with limited scale of CCS deployment in China's cement plants. However, CCS is an indispensable lever for net-zero transition in cement plants. Therefore, an emission intensity, which can reflect the emission reduction and energy penalty by CCS, is calculated as below.

$$EI_{\text{clinker, w/CCS}} = \left(EF_{\text{process}} + TEI_{\text{clinker}} \cdot \sum_i w_i \cdot EF_{\text{fuel}}^i\right) \cdot \left(100\% - c_j\right) + TEI_{\text{CCS}}^j \cdot EF_{\text{fuel}}^i - r_{\text{bio}} \tag{4.15}$$

Where c_j denotes the capture rate on flue gas of the CCS technology j (%), TEI_{CCS}^j refers to the thermal energy penalty required for carbon capture (GJ/t CO_2 captured), and r_{bio} represents the CO_2 removal from atmosphere by biomass (kg CO_2/t clinker) when both the co-firing with biomass and CCS are applied. The fuel of 100% biomass is considered as carbon neutral and set to zero emissions in this study, whereas it is seen as negative emissions when CCS applied.

4.4.2 Decomposition on emissions drivers

After emission accounting for the cement sector, this case study decomposes both the total emissions and emission intensities of cement and clinker production, and Figure 4-4 displays the analytical process and related factors.

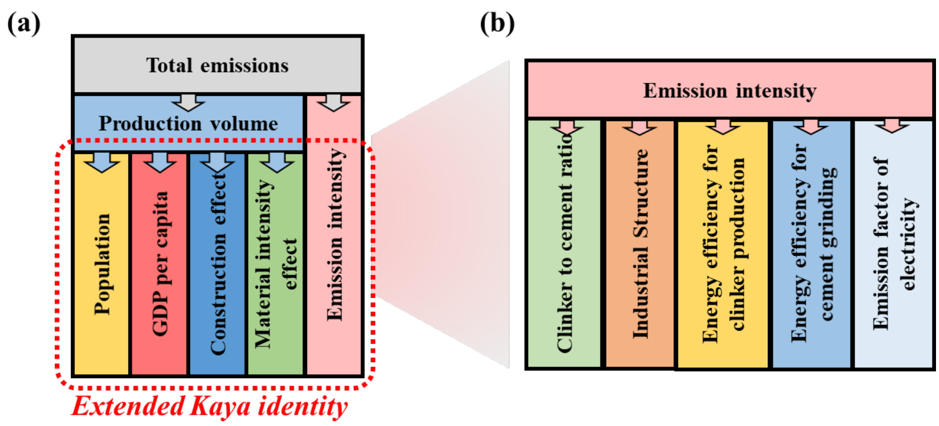

Figure 4-4 | Decomposition on total emissions and emission intensity (Wu et al., 2022).

Initially, the apparent change on total emissions originates from the production volume and the aggregate emission intensity according to the accounting equation. To investigate the impacts from the socio-economic factors, this case study adopts the Kaya identity to further decompose the emissions with two improvements, as it has the concise form and a powerful interpretation on the drivers of CO_2 emissions (Kaya, 1989). Besides analyze the socio-economic drivers of carbon emissions at country or regional level, recently Kaya identity was more applied to the analysis on drivers of carbon emissions at the sectoral level, as it can relate the sectoral emission dynamics with the socio-economic change reasonably (M. Ma et al., 2019; X. Wang et al., 2020; X. Zhang et al., 2017). However, this study makes two improvements on this identity to avoid bias and obtain further insights, when this study focuses on the cement sector. First, compared with the original Kaya identity, the energy consumption is substituted by the cement production volume, as it is improper to decompose the total emissions with energy consumption given that nearly two-thirds of CO_2 is emitted from carbonate decomposition rather than only from fuel burning. Second, this study adds the output of the construction sector into this identity. It is meaningful to consider the impact of construction sector, when this study analyzes socio-economic drivers here, as all the output of cement sector will eventually flow into the construction sector as construction materials. Thus, the extended identity can consider not only two common drivers, i.e., population and affluence level (Cao et al., 2016; M. Ma et al., 2017; Yokoi et al., 2022), but also the impacts from cement sector's downstream – the construction industry- namely construction activity level and material consumption intensity (as shown in Eq.(4.16)).

$$C = POP \times \frac{GDP}{POP} \times \frac{Con}{GDP} \times \frac{O_{cement}}{Con} \times \frac{C}{O_{cement}} = POP \times EG \times CON \times MI \times EI \quad (4.16)$$

where POP denotes the population, EG denotes the GDP per capita (at 1990 constant price), CON denotes the ratio of construction industry output (in monetary form) to GDP, and MI denotes the cement product per construction output (i.e., material intensity). Thus, the arithmetical change in total CO_2 emissions associated with cement production $\Delta C^{0 \to \mathrm{T}}$ from the base year to year T is decomposed into five factors, i.e., population growth effect (ΔC_{POP}), economic growth effect (ΔC_{EG}), construction effect (ΔC_{CON}), material intensity effect (ΔC_{MI}), and emission intensity effect (ΔC_{EI}).

$$\Delta C_{tot} = C^{\mathrm{T}} - C^{0} = \Delta C_{\mathrm{POP}} + \Delta C_{\mathrm{EG}} + \Delta C_{\mathrm{CON}} + \Delta C_{\mathrm{MI}} + \Delta C_{\mathrm{EI}} \tag{4.17}$$

According to Eq (4.11)-(4.14), the aggregate emission intensity of cement production can be calculated for each production unit. However, to reflect the sector structure of different kiln types, this chapter further introduces another weight coefficient υ_j, and the sector-level aggregate emission intensity is shown as below.

$$\begin{aligned} EI_{\mathrm{cement}} = {} & f_{\mathrm{clinker}} \cdot \sum\nolimits_j \upsilon_j \cdot \left(EF_{process,j} + TEI_{\mathrm{clinker},\, j} \cdot \sum\nolimits_i w_{i,j} \cdot EF^{i}_{\mathrm{fuel},\, j} + e_{\mathrm{clinker}} \cdot EF_{\mathrm{elec}} \right) \\ & + e_{\mathrm{grinding}} \cdot EF_{\mathrm{elec}} \end{aligned} \tag{4.18}$$

Given that this study aims to investigate the differences ($EI^{\mathrm{T}} - EI^{0}$) in emission intensities over time, this study can initially decompose the aggregate emission intensity to night factors as shown below.

$$\begin{aligned} \Delta EI_{tot} = EI^{T} - EI^{0} = {} & \Delta EI_{CCR} + \sum\nolimits_j \Delta EI_{\upsilon_j} + \sum\nolimits_j \Delta EI_{EF_{process,j}} + \sum\nolimits_j \Delta EI_{TEI_{\mathrm{clinker},\, j}} \\ & + \sum\nolimits_{i,j} w_{i,j} + \sum\nolimits_{i,j} EF^{i}_{\mathrm{fuel},\, j} + \Delta EI_{e_{\mathrm{clinker}}} + \Delta EI_{e_{\mathrm{grinding}}} + \Delta EI_{EF_{\mathrm{elec}}} \end{aligned} \tag{4.19}$$

For ease of understanding, this study merges and simplifies these effects. Given this study adopts the values of EF_{process} from field surveys by Shen et al. (2014) and assumed that it does not change over time, its impacts ($\Delta EI_{EF_{process,j}}$) can be ignored its impacts here. Then, the impacts of the shares of different kiln types (ΔEI_{υ_j}) are merged to be an aggregate effect, *Industrial Structure (IS)*. Also, thermal energy intensity and electricity intensity of clinker production are merged to be an aggregate effect *Energy Efficiency for Clinker Production* (*eff_1)*. Thus, the drivers of emission intensity can be decomposed in addictive form as below, to reflect the effects of clinker-to-cement ratio (ΔEI_{CCR}), industrial structure (ΔEI_{IS}), energy efficiency for clinker production ($\Delta EI_{\mathrm{eff\_1}}$), energy efficiency for cement grinding ($\Delta EI_{\mathrm{eff\_2}}$), and emission factor of electricity ($\Delta EI_{\mathrm{EF\_elec}}$).

$$\Delta EI_{tot} = EI^{\mathrm{T}} - EI^{0} = \Delta EI_{\mathrm{CCR}} + \Delta EI_{\mathrm{IS}} + \Delta EI_{\mathrm{eff\_1}} + \Delta EI_{\mathrm{eff\_2}} + \Delta EI_{\mathrm{EF\_elec}} \quad (4.20)$$

Given the advantages of the theoretical foundation, adaptability, ease of use and result interpretation, and perfect decomposition, Logarithmic Mean Divisia Index (LMDI) decomposition is adopted to quantify the impact from the underlying factors on the total emissions and the aggregate emission intensity (Ang, 2004). LMDI-I is adopted for the decomposition in Eq.(4.17), while LMDI-II is used for Eq.(4.20) as it contains both the additive and multiplicative forms (Ang et al., 2003). The formulas for the additive LMDI-I and LMDI-II decomposition are shown in Eqs. (4.21) and (4.22) respectively:

$$\Delta C_{x} = L(C^{T},\ \mathrm{C}^{0})\ln(\frac{x^{T}}{x^{0}}) \quad (4.21)$$

$$\Delta EI_{x} = \frac{L(\omega_{x}^{T},\ \omega_{x}^{0})}{\sum_{j} L(\omega_{j}^{T},\ \omega_{j}^{0})} L(EI^{T}, EI^{0})\ln(\frac{x^{T}}{x^{0}}) \quad (4.22)$$

where x refers to a certain effect or driver, and $\omega_{x} = EI_{x} / \sum_{i} EI_{i}$ is the weight of x in the aggregate, and the function $L\left(a,\ b\right)$ is the logarithmic average of two positive numbers given by:

$$L(a,b) = \begin{cases} \frac{a-b}{ln\,a - ln\,b}, (a \neq b) \\ a \qquad , (a = b) \end{cases} \quad (4.23)$$

To assess the role of CCS in emissions mitigation, this study adopts the Logarithmic Mean Divisia Index (LMDI) decomposition method to quantify the contribution of each mitigation effect to the total direct emissions (Ang, 2004). Six mitigation effects are identified according to the Equation (4.24), i.e., CCS, decreased demand (from population decline and material efficiency measures), clinker substitution, thermal efficiency, fuel switching, and CO_2 removal by biomass. And the calculation process is displayed as below.

$$\Delta E_{\mathrm{clinker}}^{x|^{t_1 \to t_2}} = L\left(E_{\mathrm{clinker}}^{t_2},\ E_{\mathrm{clinker}}^{t_1}\right) \cdot \ln\left(\frac{x^{t_2}}{x^{t_1}}\right) \quad (4.24)$$

$$L\left(E_{\text{clinker}}^{t_2},\ E_{\text{clinker}}^{t_1}\right) = \frac{E_{\text{clinker}}^{t_2} - E_{\text{clinker}}^{t_1}}{\ln E_{\text{clinker}}^{t_2} - \ln E_{\text{clinker}}^{t_1}} \tag{4.25}$$

Where x^{t_1} and x^{t_2} represent the values of a certain effect x in year t_1 and t_2 respectively, and L denotes the logarithmic average of the two positive numbers.

4.4.3 Uncertainty analysis

In this module, a Monte Carlo approach is adopted to assess the uncertainty distribution range of the estimated emissions. The simulation will run 10,000 times, of which each run randomly selects the values of those variables with uncertainty with equal probabilities from their uncertain range to calculate the aggregate emissions. Finally, the uncertainty range is presented as the intervals with lower and upper bounds of 95% confidence around the central calculation results (Y. Wang et al., 2020). Herein, this study assumes the values sampled from the uncertain interval of variables are normally distributed and set the different values of coefficient of variation (CV) corresponding to differentiate data quality for the Monte Carlo simulations. The CV of clinker and cement production statistics is set to 5%. The CV of energy intensities obtained by regressions on a large amount of data is also set to 5%, while that of those with poor data quality is set to 10%. As for the data with better quality, such as process emission factors from field survey, CV of them is set to 1%.

4.4.4 Data source for case study

As for emission accounting, this study conducts a survey of the CO_2 emission factors of fossil fuel and biomass from literature and other grey literature, and these EFs are displayed on the Supplementary Data of Wu et al. (2022).

4.5 Module 3: CO_2 uptake quantification

In Module 3, a physicochemical model is employed to characterize cement carbonation and estimate CO_2 update across inflows, outflows, and in-use stock of cement materials (Cao et al., 2020; Guo et al., 2021; Watari et al., 2022; Xi et al., 2016). This model succinctly parameterizes the physicochemical carbonation reactions at different life cycle stages (i.e., production, in-use, demolition, and secondary use) and is populated by region-specific data from field surveys. In this context, four categories of CO_2-absorbing entities are examined, comprising two primary cement-based materials: concrete and mortar, alongside two by-products: construction waste and cement kiln dust (CKD). Here, this chapter make the following two assumptions. First, cement-based products are characterized by simplified geometries (see Figure 4-6). Second, the diffusion front is equivalent to the carbonation front, and the area behind the front is regarded as fully carbonated (Guo et al., 2021).

<table>
<tr><th>Type</th><th>Cube</th><th>Sphere</th></tr>
<tr><td>Schematic</td><td>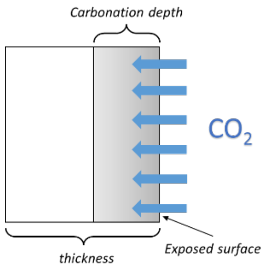
</td><td>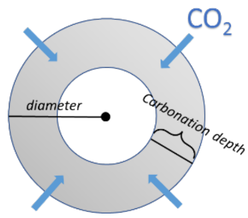
</td></tr>
<tr><td>characterized object</td><td>In-use concrete structure, such as wall, column, beam, and slab. In-use mortar rendering and plastering, etc.</td><td>Crushed concrete and mortar outflow, construction waste, and cement kiln dust.</td></tr>
</table>

Figure 4-5 | Two-dimensional schematic representation of simplified geometries (Wu, Ng, Chen, et al., 2023).

With these assumptions, the annual CO_2 uptake by cement and mortar is estimated based on the annual growth in cumulative carbonation fraction of carbonated cement-based products, cement content of the material, clinker-to-cement ratio, CaO content of clinker, the proportion of CaO converted to $CaCO_3$ within the fully carbonated clinker, and molar mass ratio of CO_2 and CaO (Eq. (4.26)). The cumulative carbonation fraction was determined by the carbonation depth and the thickness of concrete structure components, mortar layer, or diameter of demolished waste particles, based on the simplified geometry assumption (Eq. (4.27)). And determined using Fick's diffusion law (Eq. (4.28)).

$$U_t = S_t^{t_1} \cdot \Delta F_t \cdot f_{\text{cement}} \cdot f_{\text{clinker}} \cdot f_{\text{CaO}} \cdot \gamma \cdot Mr_{\text{CaO}}^{\text{CO}_2} \tag{4.26}$$

$$F_t = \frac{d_t^{t_1}}{D} \tag{4.27}$$

$$d_t^{t_1} = k \cdot \sqrt{t - t_1} \quad (4.28)$$

Where U_t is the annual uptake by concrete or mortar products; $S_t^{t_1}$ is the remained in-use stock that entered into use phase in year t_1; F_t is the cumulative carbonated fraction and ΔF_t is the annual growth in carbonated fraction; f_{cement} is the cement content in concrete or mortar; f_{clinker} is the clinker content in the cement, i.e., the clinker-to-cement ratio; f_{CaO} is the CaO content in the clinker or CKD; γ is the fraction of CaO that could be converted to $CaCO_3$; $Mr_{\text{CaO}}^{\text{CO}_2}$ is the molar mass ratio of CO_2 and CaO; k is the carbonation rate coefficient of the material, which is affected by exposure condition, CO_2 concentrations, cement additives, and coating and coverings; and $t_1 - t$ is the cumulative exposed time in years; D is the average thickness of concrete structure components or mortar layer. As for construction waste and CKD, their CO_2 uptake is estimated by an annual carbonation fraction of total mass. The reason is that they are small pieces and particles, and we assume that they will be fully carbonated within one to five years (Guo et al., 2021). The main calculation process and the components are displayed in Figure 4-6.

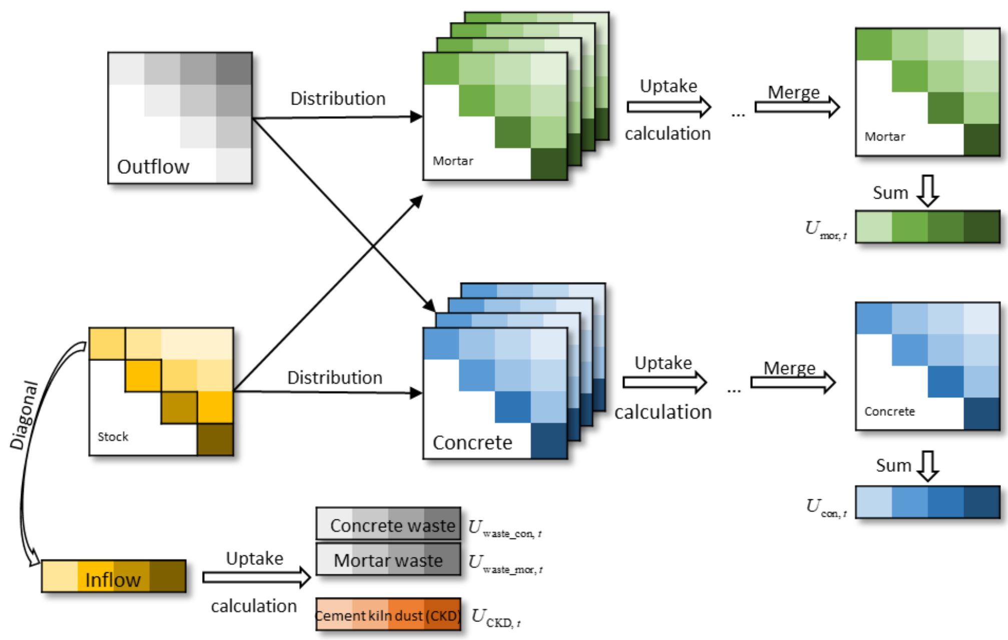

Figure 4-6 | CO_2 uptake accounting model architecture harmonized with DMFA model. Material types and service stages (a) and calculation procedure in this study (b) (Wu, Ng, Chen, et al., 2023).

4.6 A demonstrative case: China's cement sector

As the largest producer and consumer worldwide, China's cement sector plays a vital role in the net-zero transition for the global cement sector. Its cement production has risen from 65 Mt to 2,395 Mt between 1978 and 2020, representing an average growth of around 9% per annum, and this not only accounted for 56% of the global total cement production in 2018 but also dominated the global growth by 74% in the past thirty years (Andrew, 2019; NBS, 2021). There were 1,233 cement plants with 1,792 clinker production lines around the country by the end of 2020, while the overall utilization rate was always below 0.8. It is foreseen that the release of sizeable GHG emissions will continue from the existing infrastructure production, which would jeopardize the national climate target, i.e., to peak CO_2 emissions before 2030 and to achieve carbon neutrality before 2060 (Tong et al., 2019). Therefore, this chapter takes China's cement sector as a demonstrative case to test the applicability of the MEU framework.

4.6.1 China's in-use cement stock

As shown in Figure 4-7, China's annual cement consumption grew exponentially since its economic reform in 1970s, after the peak in 2014 it fluctuated over 2 gigatons and saw a sharp decrease of 10% in 2022. This consumption accumulated in the society to form all kinds of infrastructures to support our daily life and socio-economic development, here mainly refer to residential buildings, non-residential buildings, and other infrastructures. Thus, driven by the substantial consumption, in-use cement stock grew rapidly to 38.2 [36.2, 40.0] gigatons (Gt) in 2022. The outflows also climbed to 415 [276, 688] million tons (Mt) per year, as a results of relative short service-life of built environment (W. Cai et al., 2015; Cao et al., 2019). And per-capita stock has increased to around 27.2 [24.4, 30.5] tons in 2022, with 13.2 [11.7, 14.8] tons, 7.5 [6.6, 8.5] tons, and 6.6 [5.5, 7.7] tons for these three end-use sectors respectively.

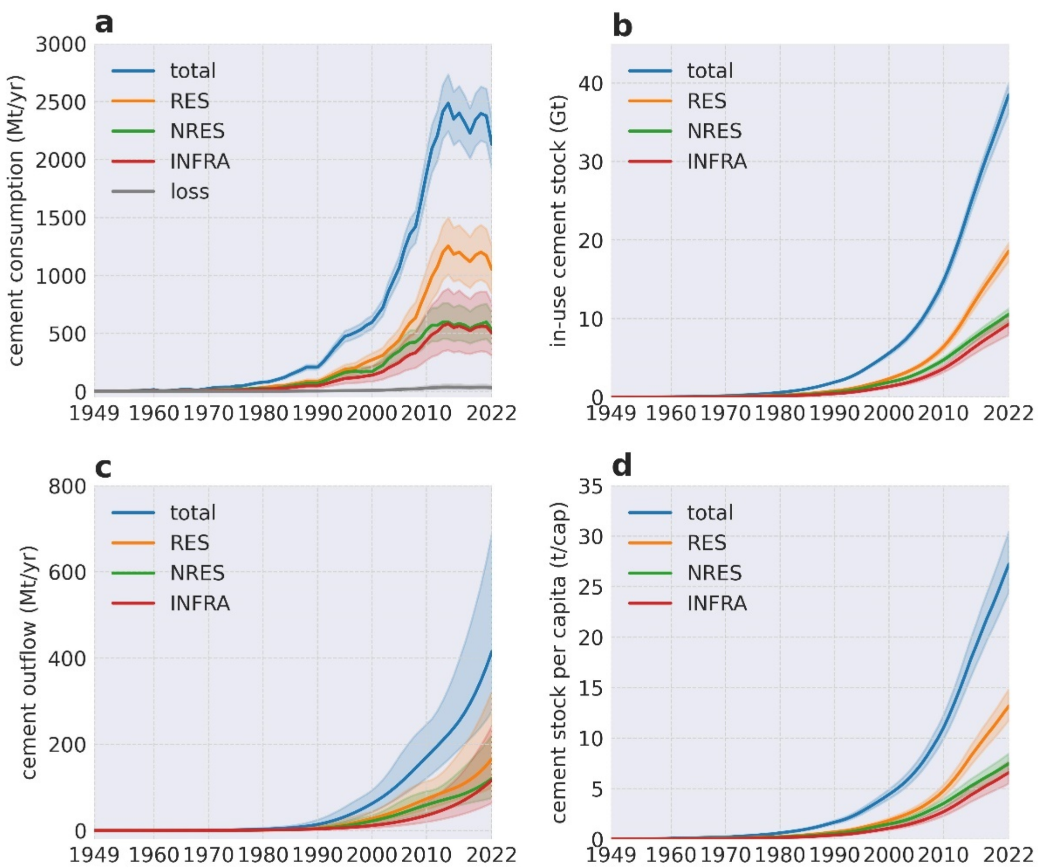

Figure 4-7 | Historical in-use cement stock in China.

4.6.2 Historical CO_2 emissions and drivers

The total CO_2 emissions from cement production in China have increased from 152.3 million metric tons (Mt) in 1990 to 1,215.9 Mt in 2014, at an average annual growth rate of 9.0%. The emissions dropped by 5.8% for the first time in 2015, due to the slump in cement demand throughout the whole country, after that the emissions climbed gradually back to above 1,200 Mt and accelerated again to a new peak of 1,313.7 Mt in 2020 (Figure 4-9a). Obviously, clinker production rather than cement production dominates the total emissions from the cement industry, as nearly 95% of total emissions is from clinker production. Meanwhile, there is a controversy on whether the emissions from the cement industry have peaked. Although a few studies with the accounting periods covered up to 2015 claimed that the carbon-dioxide emissions from the cement industry in China had peaked in 2014 (J. Liu et al., 2021; Shan et al., 2019), the total emissions grew again after 2015 and had exceeded the former peak in 2019. The proportion of process emissions from carbonates decomposition has risen from nearly 50% in

1990 to 65.9% in 2020, while that of fossil fuel burning has dropped to 26% with the energy efficiency improvement (Figure 4-9b). At the same time, there is a significant structural change in total emissions due to the rapid and large-scale penetration of NSP kilns especially in 2000-2015 (Figure 4-9c). The emissions from NSP kilns jumped from 42.1 to 1,230.7 Mt CO_2 at a high average rate of 18.4% per year between 2000 and 2020. In contrast, the emissions from shaft kilns dropped rapidly from 2003 to null in 2015 when these outdated kilns were almost eliminated (MIIT and NBE, 2011, 2012, 2013, 2015, 2016).

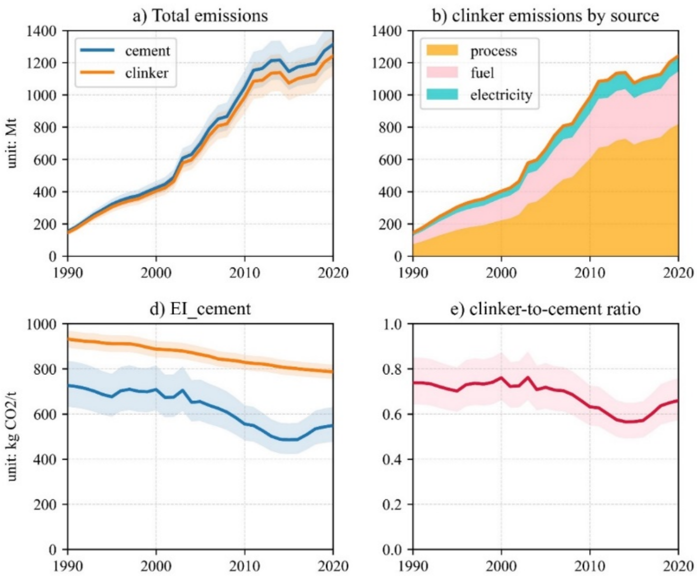

Figure 4-8 | CO_2 emissions and emission intensity of cement production in China (Wu et al., 2022). (Notes: The shaded area around the lines represents the 95% uncertainty interval of carbon emissions calculated by this study.)

While the total emissions in rising trends, the aggregate emission intensities of cement and clinker production have declined, due to the penetration of NSP kilns and continuous technology improvement. Notably, the clinker-to-cement ratio (CCR) dominates the evolution trend of emission intensity of cement production because the intensity of clinker production is monotonically decreasing (Figure 4-8d and Figure 4-8e). The emission intensity of cement production fluctuated around 700 kg CO_2/t in the 1990's. Since the accelerated promotion of pre-calciner kilns, it dropped to 485.3 kg CO_2/t cement in 2015, averaging 2.9% per year. However, it rebounded back to 548.6 kg CO_2/t cement in the recent five years, mainly due to the rising clinker-to-cement ratio. As for the emission intensities of clinker production, the emission intensity of pre-calciner kilns decreased gradually from 918.7 to 787.3 kg CO_2/t clinker between 1990 and 2020 at an average rate of 0.5% per year, while that of shaft kilns has similar reduction. In addition, the emission intensity of other rotary kilns dropped from 938.2 to 725.7 kg CO_2/t clinker during the same period, averaging nearly 1.0% per year. The drivers leading to an evolution of total emissions will be investigated based on decomposition analysis in next sub-section.

4.6.2.1 Drivers of total emissions

Initial decomposition reveals that production volume always dominates the change on total emissions, and its change is also significantly correlated to the latter (Figure 4-9). This phenomenon implies that an improvement in emission intensity could not offset the larger emission increment caused by the exponentially expansion in production. Notably, the effect of production volume and emission intensity has reversed since 2015.

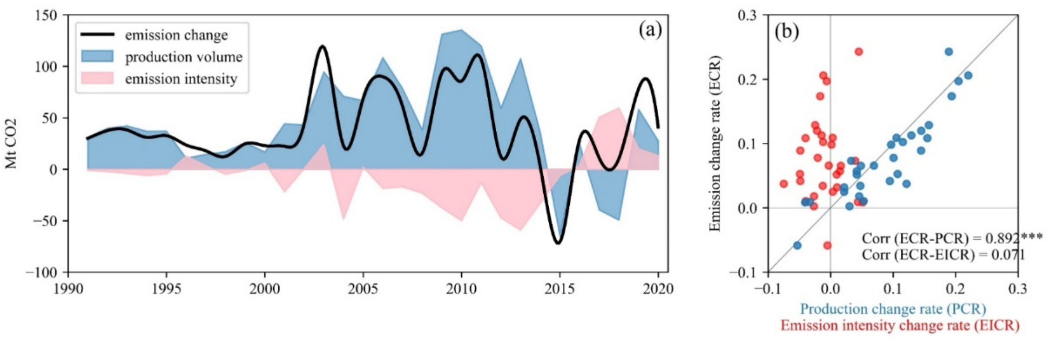

Figure 4-9 | Total emissions change caused by varying production volume and emission intensity (a), and the correlations between emissions change rate and that of production volume and emission intensity (b) (Wu et al., 2022).

(Note: Blue dots represent annual emission change rate (ECR) versus production change rate (PCR), while red dots represent ECR versus emission intensity change rate (EICR). And Pearson's correlation coefficient between ECR and PCR is significant.)

The impact of the socio-economic drivers in the past three decades can be quantified by further decomposition (Figure 4-10), and the three growth drivers are economic growth effect, construction effect and population effect in the order of magnitude. The economic growth as represented by GDP per capita is always the most significant drivers to emission growth, as it gave rise to an increase in emissions by 154.7%, 154%, and 68.5% in the past three decades, respectively. The construction effect can reflect the impact of construction activities on carbon emissions from cement production which made a significant contribution to the emission growth by 101.8% during 2000-2010. This is mainly because the construction sector gradually became a pillar of economic growth during the rapid urbanization process, with massive investment in real estate development and infrastructure construction in China during this period. The population effect diminished from 17.9% to 5.8%, as its growth has gradually slowed down in China. Compared with the relatively stable necessary housing demand caused by population growth, economic development could result in much more construction, not least newly built commercial buildings and various infrastructure facilities, and thus the driver of GDP per capita was much larger than that of population. In contrast, the material intensity effect, which reflects the material efficiency of the construction industry, significantly contributed to the emission mitigation by -78.2% and -59.4% in 2000-2010 and 2010-2020, respectively. This is always a mitigation factor as material efficiency is improving in the construction sector of China. Besides, the emission intensity effect also contributed to emission reduction, despite its contribution diminished from -39.6% to -1.4% during the same period.

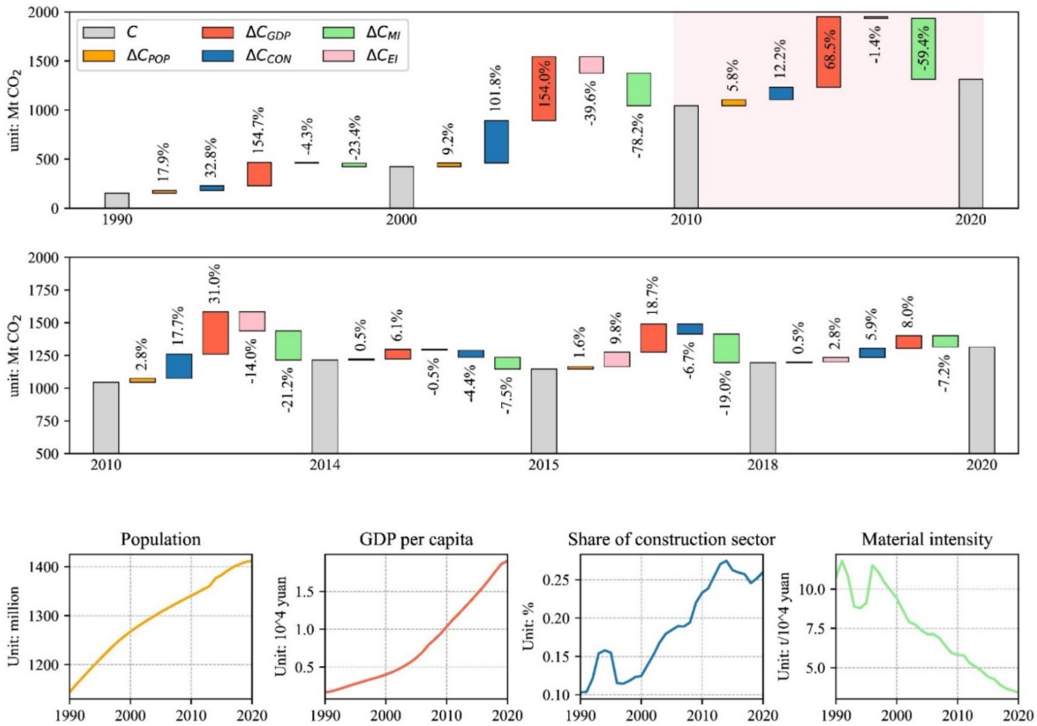

Figure 4-10 | Decomposition on total emissions (Wu et al., 2022).

A reversal of the construction effect and emission intensity effect can be seen from a further detailed decomposition analysis of the last ten years, while the relationship on size between the drivers remains basically unchanged in the decadal analysis (Figure 4-10b). Notably, since the "12^{th} Five-year Plan" (2011-2015) of the mainland China, its government decided to adjust the economic structure, implying that the economy development would not depend primarily on fixed asset investment (mostly in real estate and infrastructure development). Thus, the construction effect resulted in a decrease in emissions by 4.4% in 2015 for the first time, leading to a so-called peak in 2014. This was mainly because of the sudden decline in demand for cement product in 2015 originated from the drastic fall in real estate investment (from 10.5% to 1.0% in 2015). This mitigation effect was further expanded to -6.7% during 2015-2018 despite it rebounded back to +5.9% in the recent two years with the adjustment having gradually completed. As for the emission intensity effect, it was consistently a significant factor to curb the total emissions before 2015, especially during the large-scale promotion for the PC kilns (i.e., 2000-2015). Nevertheless, its abatement effect fell to 0.5% between 2014 and 2015, with the saturation of the PC kilns across the country. Despite it has reversed to become a driving factor in the recent five years (contributed to the emissions growth by 9.8% and 2.8% respectively), mainly due to the rising clinker-to-cement ratio in this period (Figure 4-8 d and e).

4.6.2.2 Drivers of emission intensity

Figure 4-11 presents the decomposition analysis on the aggregate emission intensity to analyze its structural change and periodic fluctuations in the last 20 years. Once again, the results show that the clinker-to-cement ratio (i.e., CCR) dominates the fluctuations in aggregate emission intensity. This effect mitigated the emission intensity by 5.2%, 11.2%, and 9.6% every five years during 2000-2015, with the CCR gradually dropped from 0.76 to 0.56. The decline in CCR was attributed to the better clinker quality caused by the newly-built advanced NSP kilns compared to the outdated low-automated shaft kiln (Xu et al., 2012). Specifically, the cement mix requires less clinker with good quality than for that with worse quality when producing the low-grade cement product, leading to the clinker savings. However, the emission intensity has rebounded by about 15%

since 2015, mainly due to the CCR (15.3%) due to the increasing requirement for clinker content in the cement mix for producing higher-grade cement product in recent years, with the phasing out of the low-grade cement product in the modified concrete specifications in China.

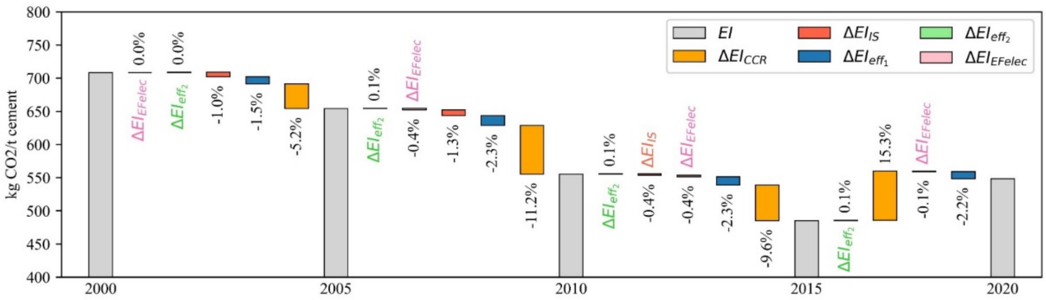

Figure 4-11 | Decomposition on the aggregate emission intensity of cement production in China (Wu et al., 2022).

Beyond the CCR, the energy efficiency for clinker production is always the second most significant mitigation factor, as it mitigated the emission intensity by 1.5-2.3% during this period. As for the industrial structure, it decreased the emission intensity by 1.0%, 1.3%, and 0.4% respectively during 2000-2015, due to the penetration of the NSP kilns and the phasing out of the shaft kilns during this period (MIIT and NBE, 2011, 2012, 2013, 2015, 2016). But the IS effect diminished with the saturation of the NSP kilns. Notwithstanding an improvement in electricity efficiency for cement grinding, its mitigation effect is insignificant. As for the emission factors for coal-fired power generation, it has gradually decreased from 1.15 to 0.85 kg CO_2/kWh in the past three decades with the continuous improvement, leading to a slight decline in the aggregate emission intensity (up to -0.4%).

4.6.3 CO_2 uptake by China's cement stock

In Figure 4-12, the evolutionary trajectory of CO_2 absorption by cement stock is depicted over an annual timeframe. Driven by a substantial increase in cement stock, the annual uptake has exhibited exponential growth, escalating from 10 million metric tons (Mt) per year in 1980 to 315 Mt per year in 2022. It is noteworthy that mortar for rendering and plastering has accounted for the highest CO_2 absorption, attributed to its surface area exposure and relatively rapid carbonation rate compared to concrete. Despite the comparatively smaller quantity of cement kiln dust (CKD) in comparison to concrete and mortar stock, its uptake scale parallels that of masonry mortar, mortar for repair and maintenance, and demolished concrete debris. Collectively, carbonation reactions have absorbed a total of 5.6 gigatons (Gt) of CO_2, with contributions of 3.7 Gt, 1.2 Gt, 0.6 Gt, and 0.1 Gt originating from mortar, concrete, CKD, and waste, respectively (Figure 4-12b).

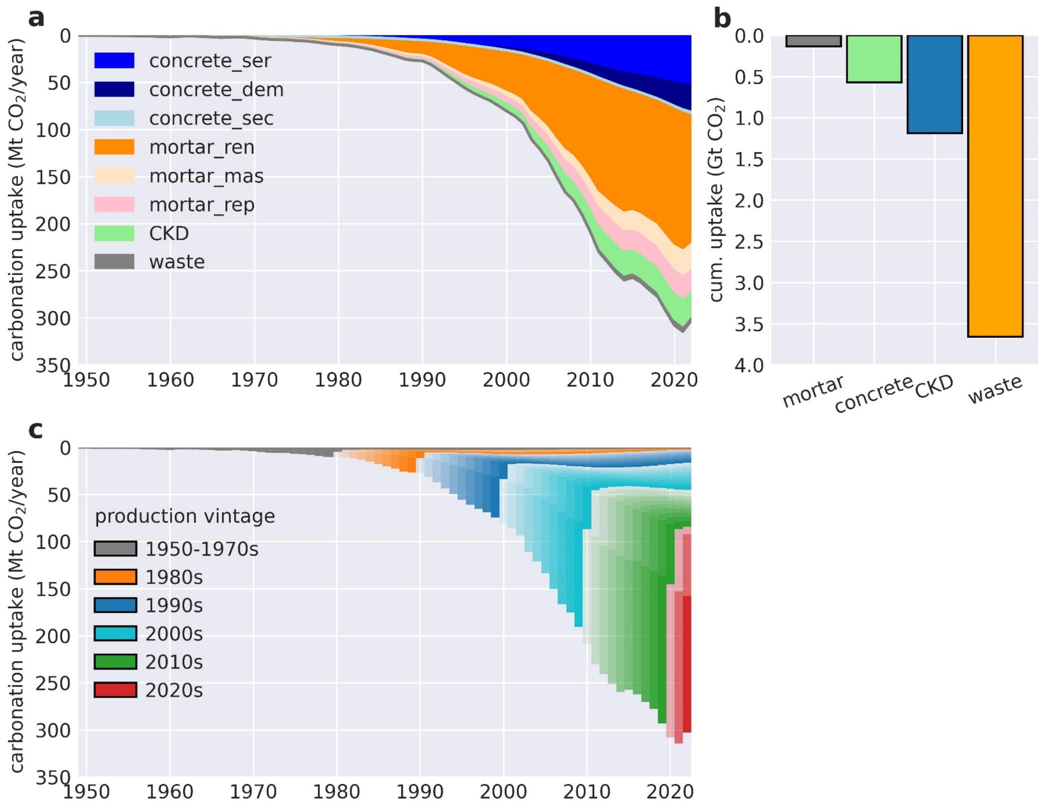

Figure 4-12 | CO_2 uptake by cement carbonation in China (1949-2022).

(Notes: For concrete, the suffixes 'ser', 'dem', and 'sec', refer to service, demolition, and secondary use stage, respectively. For mortar, the suffixes 'ren', 'mas', and 'rep', denotes the type of 'rendering and plastering', 'masonry', and 'repairing and maintenance', respectively.)

In Figure 4-12c, the enduring effects ('legacy' effects) of carbonation uptake are illustrated by vintage. For instance, it is observed that cement stock of the 2000s re-absorbed the most CO_2 uptake throughout its lifecycle within the first two years, followed by a sharp decline, indicative of a prolonged tail along the time scale. This phenomenon can be further illustrated by the unit uptake of four types of cement-based materials (Figure 4-13). A unit of cement, which was produced and entered use phase in 1949, is taken as an example. It flows into four types of cement-based materials according to the proportion specified in the accounting model. Cumulatively, a unit of cement can reabsorb 244 kg CO_2 during 1949-2022, with the contribution of 116 kg, 109 kg, 4 kg, and 15 kg from concrete, mortar, waste, and CKD, respectively (Figure 4-13a). While concrete contributes most to the cumulative reabsorption, mortar accounts the most carbon uptake in the first two years over the entire life cycle. This is mainly ascribed to the fast carbonation reaction in the surface mortar layer (i.e., rendering mortar) within the first two years (Figure 4-13b). As the carbonation depth expands at a faster rate than that of concrete, upon traversing through the entire thickness of the surface layer and completion of the carbonation reaction within the rendering mortar, the total reabsorption of mortar experiences a sharp decline. This decline reflects a transition of the overall carbonation process from the surface layer, characterized by a large, exposed surface area, to the concealed layers within built structures (i.e., masonry mortar layer), which have limited contact with atmospheric carbon dioxide.

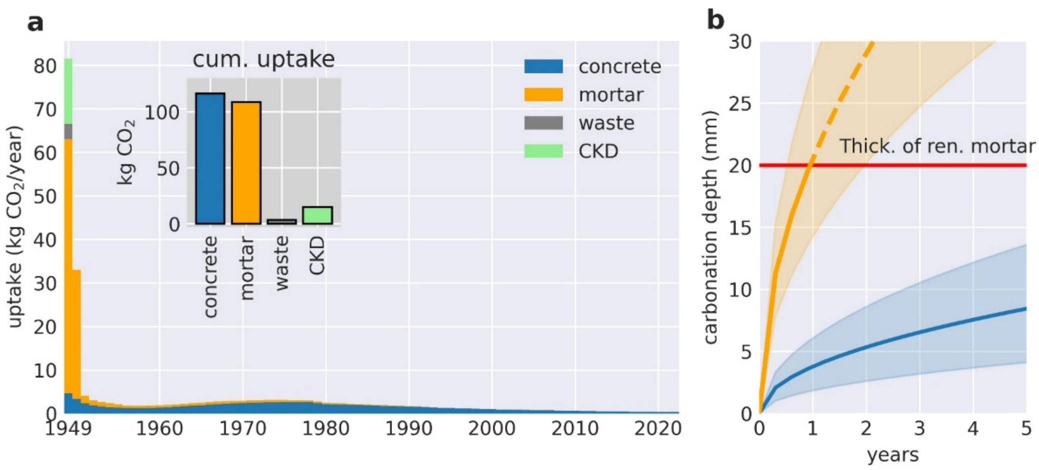

Figure 4-13 | Unit uptake of cement carbonation (a) and carbonation depth of concrete and mortar over time (b).

(Notes: 'Thick. of ren. mortar' represents the thickness of mortar layer for rendering and plastering.)

4.6.4 Net carbon emissions pathways

Integrating estimated CO_2 emissions and carbon uptake in this chapter, the CO_2 balance can be calculated for the period between 1990 and 2022, as depicted in Figure 4-14 below. On an annual basis, carbonation uptake has been able to offset approximately 17-26% of production emissions during this period. In 2020, the emissions balance was recorded at 1.0 Gt, reflecting a decrease from 1.3 Gt. Cumulatively, carbonation uptake has offset approximately 5.3 Gt, constituting approximately 21% of the total CO_2 emissions from cement production (25.2 Gt) over this period. This underscores the substantial carbon sink represented by in-use cement stock.

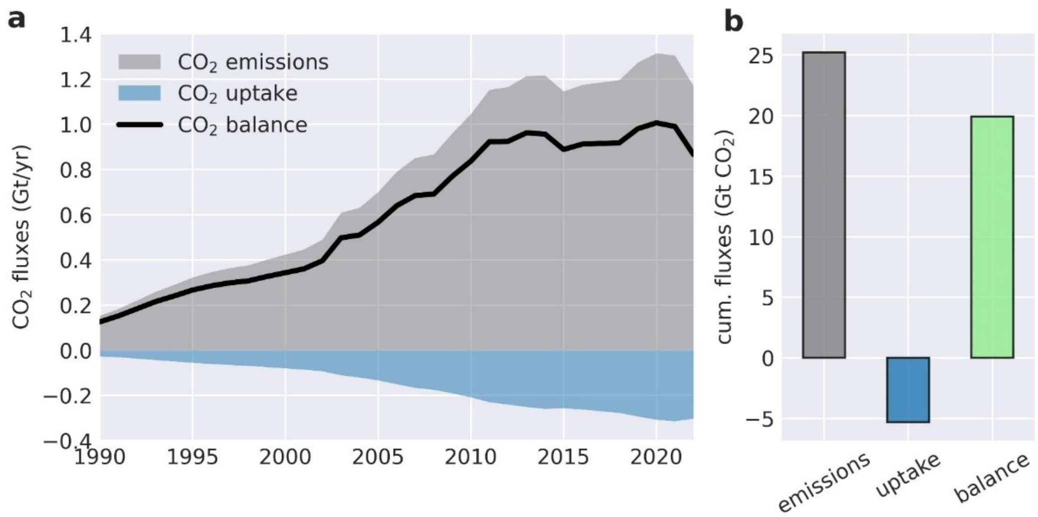

Figure 4-14 | CO_2 balance of China's cement cycle in 1990-2022.

4.7 Chapter summary

This chapter introduced an integrated modeling framework to analyze the material-emissions-uptake (MEU) nexus of the cement sector. The framework combines dynamic material flow analysis (DMFA), CO_2 emissions accounting, and CO_2 uptake quantification to provide a holistic understanding of the sector's carbon impact. By tracking cement inflows, in-use stock, and outflows, quantifying emissions from production, and measuring CO_2 uptake through carbonation reactions, this framework addresses the limitations of traditional approaches. It offers a comprehensive view of emissions and uptake, considering demand-supply dynamics and spatial-temporal contexts. The applicability of this framework is demonstrated using a case study of China's cement sector in 1949-2022, highlighting its potential for a systematic integration of both supply- and demand-side to develop decarbonization roadmaps.

Chapter 5. Future cement demand, mitigation potentials and implications for carbon emissions and uptake

5.1 Introduction

As shown in the case of Chapter 4, nearly 40 Gt cement cumulated in China's society to support infrastructures development. And the massive production, mainly driven by soaring needs for housing and infrastructure development, has positioned the cement sector as a significant source of CO_2 emissions, despite a lower emission intensity compared with metals (P. S. Fennell et al., 2021). Yet, decoupling CO_2 emissions from cement production is a challenging task, because two-thirds of its CO_2 emissions come from carbonate decomposition during calcination. In addition, large-scale deployment of alternative cement is unlikely to occur due to feedstock constraints and high manufacturing costs (Habert et al., 2020; Monteiro et al., 2017). Consequently, beyond conventional supply-side efforts, demand-side measures based on the philosophy 'using less cement', i.e., material efficiency strategies, could potentially open up the option space for decarbonizing the cement sector in China (P. Fennell et al., 2022; Miller et al., 2021).

To delineate boundary conditions of future cement stock and explore the mitigation potentials from demand-side and their implications for CO_2 emissions and uptake, this chapter systematically develops a scenario matrix to characterize the future boundary of cement stock by alternating saturated value of per-capita stock level and service lifetime, based on qualitative analysis. This chapter continues to use the case of China, based on its stock dynamics revealed in Chapter 4. As shown in Figure 5-1, these scenarios of stock dynamics serve as a layer of demand-side scenarios for MEU framework, through which quantitative analysis on future carbon emissions and uptake can be conducted to further convey explicit emissions pathways. Besides, these stock dynamics can provide a concrete data basis for making trade-off between CO_2 uptake and demand mitigation.

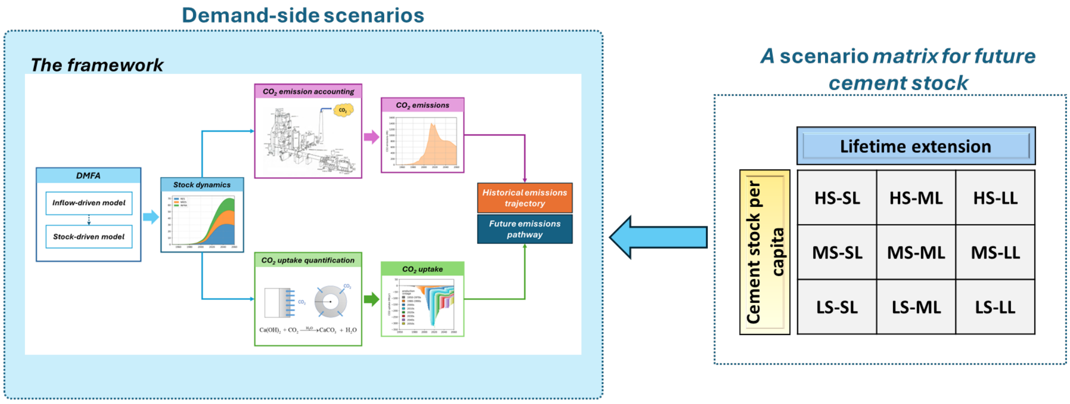

Figure 5-1 | The layer of demand-side scenarios for MEU framework.

5.2 Developing scenarios for future cement stock

In this section, scenarios for future per-capita stock and service lifetime will be developed based on detailed analysis. For the former, a Kaya-like decomposition identity (D. B. Muller et al., 2013) is developed to determine the future target levels for cement stock, of building and infrastructures respectively. Specifically, per-capita cement stock is decomposed into the per-capita service level and the cement intensity per service provided. Then, per-capita service levels, and the aggregated cement intensity, which is composed by multi-types of applications, are altered based on different rationale, and in turn to obtain a target stock level in the future. It should be noted that the mitigation potential mainly come from the more efficient use of in-use stock, rather than dematerialization on specific products. To this end, this chapter delineates three scenarios for stock levels—***Low Stock***, ***Medium Stock***, and ***High Stock***—alongside three scenarios for service lifetime—***Short Lifetime***, ***Moderate Lifetime Extension***, and ***Substantial Lifetime Extension***, respectively. The ensuing sub-sections will elaborate on the development of these scenarios.

5.2.1 Scenarios for future per-capita stock

5.2.1.1 Buildings

For cement stocks embodied in buildings, i.e., residential, and non-residential buildings, this study decomposes the stock per capita (t/cap) into service levels provided per capita (m^2/cap) and material intensity (here cement intensity) per service level provided (t/m^2).

$$s_t = \frac{S_t}{P_t} = \frac{\text{total service}_t}{P_t} \times \frac{S_t}{\text{total service}_t} = se_t \times m_t \tag{5.1}$$

Where se represents the service level provided per capita, and m_t denotes the aggregate cement intensity of per service level provided. This aggregate intensity also could be calculated from the weighted average of sub-types of building stock and their cement intensity. And it can be further decomposed as below, based on the building material types, i.e., steel, and reinforced concrete structures, hybrid structures, brick and wooden structures, bamboo, grass, and adobe structures, as well as other structures.

$$m_t = \frac{S_t}{\text{total service}_t} = \sum_{i=1}^{4} \frac{\text{total service}_{i,t}}{\text{total service}_t} \times \frac{S_{i,t}}{\text{total service}_{i,t}} = \sum_{i=1}^{4} w_{i,t} \times m_{i,t} \tag{5.2}$$

Where i represent the material types, w denotes the weight of each material type in the aggregate material intensity. The values of the weights could be calculated from the data from the 7th census. For the cement intensities here, this study adopts the proportions of cement intensities of building materials types from Yang et al. (2020) to calculate them.

Table 5-1 | Calculated cement intensities (Unit: kg/m^2).

Structure type	This study	Yang et al. (2020)
Steel and reinforced concrete	410	217
Hybrid / brick-concrete[1]	285	151
Brick-wood	51	27
Bamboo, grass, and adobe as well as others	40	21
Weighted average (The aggregate intensity)	315	-

Notes: 1. The corresponding structure type for 'Hybrid' structure in Yang et al. (2020).
2. The gap between the cement intensities of this study and Yang et al. (2020) is attributed to the denominator in their definition. In this study, the denominator is the service level provided, while that of Yang et al. (2020) is the total building floor area.

Apparently, the aggregate cement intensity here is lower than the values in the literature (Huang et al., 2013; Shi et al., 2012; Yang et al., 2020), when the service level for residential buildings is set to ~42 m^2/cap (reported in the 7th census). However, it could be attributed to the following two reasons. **First, the aggregate cement intensity here is cement use per service level provided, not per building floor area, whilst service level here are also quantified in floor area.** Residential area per capita reported in census only included the building floor area of a residence, excluding the area of auxiliary facilities, underground garage, surrounding gardens and other facilities in the modern style residential districts, which are also constructed by cement-based materials. Thus, the calculated building stock from the reported residential area per capita multiplied with total population will be lower than the real value. Given there are no documents to comprehensively reveal the area of these mentioned facilities in residential district, this chapter still adopts the residential area per capita from census to reflect service level of residential building stocks in China. **Second, part of cement flowed into brick stocks, which should be also included in the in-use cement stock.** In China, most of non-load-bearing walls or partition walls are constructed by concrete bricks in the reinforced concrete structures, rather than the clay bricks, which had been abandoned in China, due to the concerns on damaged farmland and other environmental impacts. The related policies regulated that all the cities should not use clay bricks by the end of 2010 (The State Council of PRC, 2005), and later all the counties in 2012 (National Development and Reform Commission of PRC, 2012). However, clay bricks may still be used in a few of rural areas.

Here, in the *Medium Stock* scenario, this study assumes that per-capital floor area of residential and non-residential buildings will experience a moderate increase to 50 m^2 and 15 m^2, respectively, aligning with middle-of-the-road scenarios (Fishman et al., 2021). In the *High Stock* scenario, both residential and non-residential per-capita floor areas are projected to undergo substantial increases to reach levels comparable to those observed in the United States (64 m^2 and 26 m^2), as documented in the studies by Berrill et al., (2022) and Camarasa et al., (2022). In the *Low Stock* scenario, both residential and non-residential per-capita floor areas will remain at their current levels. This implies a significant improvement in stock efficiency to provide the necessary services, albeit with a constrained stock level. Regarding the aggregate cement intensity, the approach taken involves altering the composition of the building stock, rather than reducing the intensity of specific materials. These compositions are determined to align with the narratives of the three stock scenarios.

Table 5-2 | Aggregate cement intensity and related stock composition of three stock scenarios.

Stock composition	Status quo	Low Stock	Medium Stock	High Stock
Reinforced concrete and steel structures	52.7%	80.0%	80.0%	95.0%
Brick and masonry structures	32.1%	15.0%	15.0%	4.0%
Brick-wood structures	13.6%	4.0%	4.0%	0.5%
Bio-based and other structures	1.6%	1.0%	1.0%	0.5%
Aggregate cement intensity (kg/m^2)	315	373	373	401
Growth	-	+18.4%	+18.4%	+27.3%

5.2.1.2 Other infrastructures

For infrastructure stocks, which is often characterized by linear infrastructure, this study decomposes per-capita stock into population density, infrastructure density, which also could measure the service levels provided by material stocks, and cement intensity (Eq. (5.3)). Most of mobility infrastructure, e.g., roads and railway, is measured by length. However, China has a relatively low per-capita level. For instance, China only has ~0.004 km/cap highway and ~0.0001 km/cap railway. Also, another recent analysis revealed that China only has a mobility infrastructure stock per capita of ~28 t/cap, considering asphalt, concrete, sand and gravel, timber, and steel, which is much lower than that of those highly developed countries, i.e., ~92-207 t/cap (Virág et al., 2022). Nevertheless, China also could provide adequate transportation services for rapid economic development. And China and USA seem have comparable road densities, i.e., 54.15 and ~64 km/100 km^2, respectively Therefore, it is more reasonable to project the per-capita infrastructure stock based on the service levels measured by density indicators, and the aggregate cement intensity resulted from the structural change of sub-types of end-use, rather than that simply set a single value that approaching the per-capita levels of industrialized countries, which may cause as much as multi-fold growth from the present-day levels.

$$s_t = \frac{S_t}{P_t} = \frac{A}{P_t} \times \frac{L_t}{A} \times \frac{S_t}{L_t} = \frac{1}{d_{P,t}} \times d_{L,t} \times m_t \qquad (5.3)$$

Where A represents total inhabited area of China (km^2), and L denotes the total length of the road network (km). Thus, d_P denotes the population density (cap/km^2), and d_L denotes the road network density (km/km^2), and again m represents the cement intensity of road network, which measured by cement use per unit length (t/km). For the aggregate cement intensity, the road infrastructure is taken as the representative to derive the future cement intensity by structural changes in end-use products. The calculation method for current and future material intensity is the same as that for cement stock embodied in buildings.

$$m_L = \sum_{j=1}^{5} \frac{L_j}{L} \times \frac{M_j}{L_j} = \sum_{j=1}^{5} w_j \times m_L^j \tag{5.4}$$

Here, service levels are assumed to maintain at current level, grow by 20%, and by 50%, in *Low Stock*, *Medium Stock*, and *High Stock* scenarios, respectively. The latter growth in road density by 2060 will approach the current levels of U.S. It is noteworthy that both 20% and 50% higher levels have already been achieved in some developed provinces in China (Figure 5-2). Similarly, as for other linear infrastructures such as railways, the service levels characterized by density have already reached the +20% and +50% levels in some developed provinces.

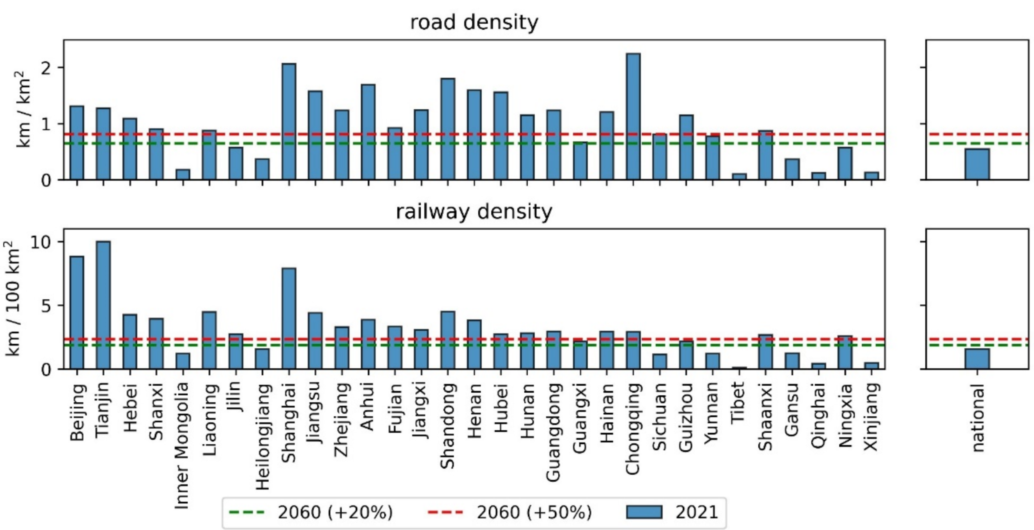

Figure 5-2 | Current and future scenarios for service levels of road and railway infrastructure in China.

In Figure 5-3, the current status and future composition of road infrastructure stocks are depicted. In the *Low Stock* scenario, while the service level remains at the current level, a portion of the existing low-class stock (e.g., sub-class roads) will be replaced by higher-class stocks (i.e., cement-intensive expressways and

Class I-II roads). Specifically, the proportions of cement-intensive products, such as expressways and Class I roads, are increased to 10% and 20% in the *Low* and *Medium Stock* scenarios, and 30% in the *High Stock* scenario, respectively, while the proportion of low-class roads will decrease significantly. Consequently, the resulting aggregate cement intensity is set to be 528 kg/m (+17%) for both the *Low Stock* and *Medium Stock* scenarios, and 633 kg/m (+40%) for the *High Stock* scenario. For other types of infrastructure, such as railways, bridges, tunnels, dams, and drainage pipelines, whose sub-types and material intensities cannot be captured in detail, this study also adopts the growth in aggregate cement intensity of road infrastructures to project the future saturated values.

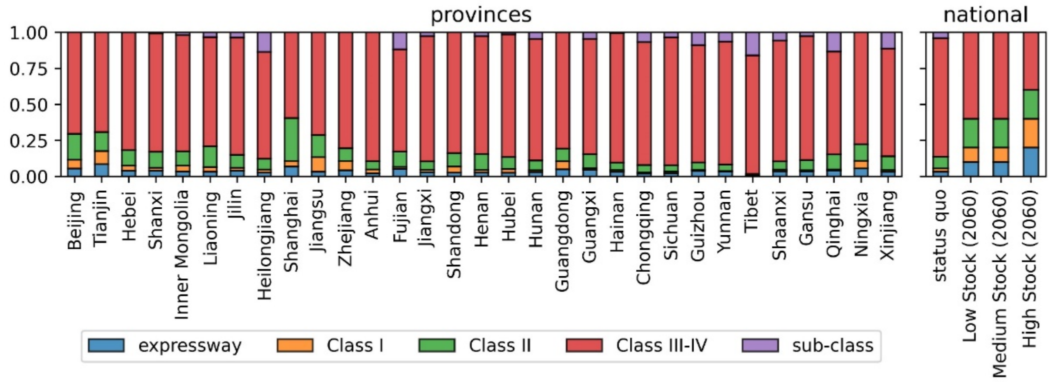

Figure 5-3 | Current and future scenarios for road type propositions in China.

5.2.1.3 Composite per-capita stock

As illustrated in Table 5-3 below, the future cement stock per capita can be derived from the detailed specific service levels and aggregate cement intensity. The composite per-capita stocks are projected to be 33.5 t, 41.3 t, and 57.6 t in the *Low Stock*, *Medium Stock*, and *High Stock* scenarios, respectively. Essentially, this study alters the growth in service levels and aggregate cement intensity to develop the above scenarios.

Table 5-3 | Assumptions on future stock level and related service levels.

Stock type	Sub-components of stock per capita	Status quo	Low Stock	Medium Stock	High Stock
Residential (RES)	Floor area per capita (m^2/cap)	41.76[1]	**41.76** (-)	**50.0**[2] (+19.7%)	**61.0**[4] (+46.1%)
	Aggregate cement intensity (t/m^2)	0.315	**0.373** (+18.4%)	**0.373** (+18.4%)	**0.401** (+27.3%)
	Stock level (t/cap)	13.15 (-)	**15.57** (+18.4%)	**18.65** (+41.8%)	**24.46** (+86.0%)
Non-residential (NRES)	Floor area per capita (m^2/cap)	12.60[3]	(-)	**15.0** (+34.2%)	**26.0**[5] (+106.3%)
	Aggregate cement intensity (t/m^2)	0.592	+18.4%	+18.4%	+27.3%
	Stock level (t/cap)	7.46	8.83 (+18.4%)	11.85 (+58.9%)	19.60 (+62.7%)
Infrastructure	Population density ($-/km^2$)[6]	-	+19.0%	+19.0%	+19.0%
	Infrastructure density ($-/km^2$)	-	-	+20.0%	+50.0%
	Aggregate cement intensity (t/~)	-	+17.0%	+17.0%	+40.4%
	Stock level (t/cap)	6.57	9.15 (+39.2%)	10.98 (+67.1%)	16.47 (+150.6%)
Composite per-capita cement stock (t/cap)[7]		27.2	33.5	41.3	57.6

1. From 7th census in China.
2. Floor area per capita of residential buildings of China in 2050-2060 for Shared Socioeconomic Pathways 2 (SSP2) (Fishman et al., 2021).
3. Floor area per capita of commercial buildings in China in 2020 (Camarasa et al., 2022).
4. Floor area per capita of residential buildings in USA in 2020 (Berrill and Hertwich, 2021).
5. Floor area per capita of commercial buildings in USA in 2020 (Camarasa et al., 2022).
6. Change in population density is calculated from the UN's population prospects.
7. Population weighted average from three sub-types of stock.

To establish a cohesive link between the detailed analyses presented earlier and the overarching descriptions of cement stock, this chapter rephrases the narratives within the context of material efficiency measures across the three stock scenarios. For ***Low Stock*** scenario, it is assumed that the more intensive use will maintain the current service levels of cement stock by 2060, but the service quality will improve, which means the aggregate cement intensity will increase by about 18% and 17% in building and infrastructure stocks, as cement-based products will more pervasively replace those non-cement products. For ***Medium Stock*** scenario, it is assumed that the current stock will expand with moderate increase in service levels by 2060, also with a same service quality improvement embodied in an increased cement intensity as Low Stock scenario. For ***High Stock*** scenario, both service levels and the aggregate cement intensity are assumed to grow significantly by 2060, approaching the levels in industrialized countries, such as United States.

5.2.2 Robustness of stock saturation assumption

Although the 'stock saturation' phenomenon has been empirically observed in a few industrialized economies (Cao et al., 2020; Krausmann et al., 2020; G. Liu et al., 2013). According to this hypothesis, a convergence of per-capita material stocks is anticipated in the future, following an S-shaped system transition between socio-metabolic regimes (Wiedenhofer et al., 2021). Although empirical evidence of this saturation pattern exists in a few industrialized countries (Cao, Shen, Løvik, et al., 2017), this chapter further conducted a forecast using an Autoregressive Integrated Moving Average (ARIMA) model (Fishman et al., 2016) to examine the robustness of the 'stock saturation' assumption in this study. The historical acceleration extrapolated constant positive values, suggesting an increasing net addition to stock (NAS) and consequently, a continued growth of the in-use stock (Figure 5-4). Additionally, Figure 5-4d reveals that points with zero NAS lie on the edge of the 95% confidence interval of the forecast, which could be interpreted as an indication of 'stock saturation' (Wiedenhofer et al., 2021). Presently, the signal of stock saturation is weak as these saturation points appear less likely to occur, but it is expected to strengthen if cement consumption continues to decline in the coming years. Despite the current weak signal, we have chosen to adopt the saturation hypothesis due to its alignment with the developmental trajectories observed in many industrialized countries, as well as China's emphasis on high-quality development today (Xinhua News Agency, 2023). The concept of material stocks saturation implies that China will achieve a 'decoupling' of economic development from resource use and transition towards a more service and consumption-based economy in the future, following a phase of rapid growth that has focused on essential infrastructure and capital stock formation (Bleischwitz et al., 2018).

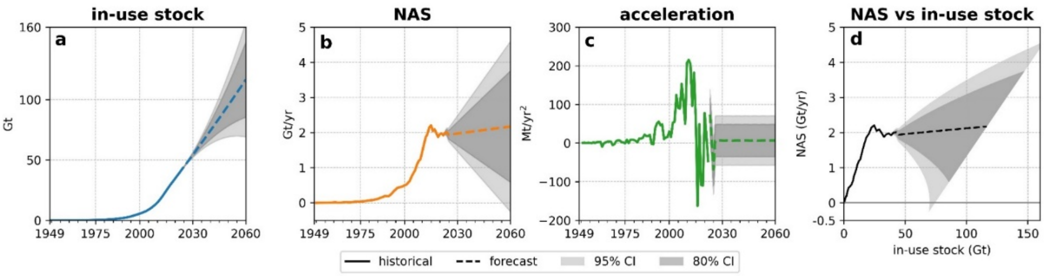

Figure 5-4 | ARIMA forecast on the (a) level, (b) NAS, and (c) acceleration based on the historical trend of China's cement stock in 1949-2060, as well as (d) the trajectory of stock to NAS ratio (Wu, Ng, Chen, et al., 2023).

(Notes: 95% CI and 80% CI refers to 95% and 80% confidence intervals of forecast respectively. NAS is the annual Net Addition to Stock, which is equivalent to inflows minus outflows in a certain year, whereas acceleration is the change in NAS between two consecutive years, or is the second order of difference of in-use stock (Fishman et al., 2016).)

5.2.3 Lifetime extension

As for service-life, this study designs three lifetime-related scenarios (i.e., ***Short Lifetime***, ***Moderate Lifetime Extension***, and ***Substantial Lifetime Extension***) to reflect the implementation of lifetime extension. In modeling the effects of lifetime extension, we assumed that the lifetime will gradually increase over time, aiming to avoid abrupt changes in projected cement inflows. The lifetime of cement-based products is determined by physical, social, and economic factors (Huuhka & Lahdensivu, 2014; G. Liu et al., 2014; O'Connor, 2004; Thomsen & van der Flier, 2011). For the ***Short Lifetime*** scenario, we assumed that the lifetime remains unchanged during 2020-2060. For the ***Moderate Lifetime Extension*** scenario, we assumed that the lifetime is extended to 50 years during 2020-2060. For the ***Substantial Lifetime Extension*** scenario, we assumed that the lifetime is extended to 70 years during 2020-2060, as land use rights in China are usually granted for 70 years (1990). The transition of service-life is depicted as below, in a matrix format delineated by two axes: time-step (years) and vintage.

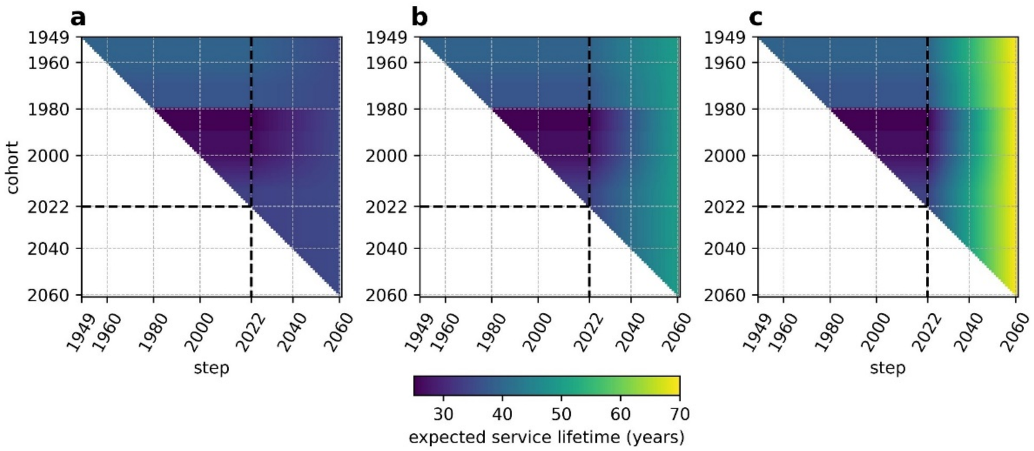

Figure 5-5 | Service-life matrix for Short Lifetime (a), Moderate Lifetime Extension (b), and Substantial Lifetime Extension (c) scenarios in this study (Wu, Ng, Chen, et al., 2023).

5.2.4 The scenario matrix

Finally, a 3×3 scenario matrix is constructed, with each of the three scenarios plotted alongside the axes representing per-capita stock level and lifetime (Figure 5-6). This matrix aims to illustrate the future boundary conditions for cement stock and delineate mitigation potentials for future consumption, especially for more-intensive use and lifetime extension.

Scenarios and key assumptions

Dimension	Scenario	Assumption
Lifetime 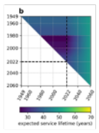	Short Lifetime (**SL**)	Lifetime remains **unchanged** during 2022-2060.
	Moderate Lifetime Extension (**ML**)	Lifetime will be extended to **50 years**[1] by 2060.
	Substantial Lifetime Extension (**LL**)	Lifetime will be extended to **70 years**[2] by 2060.
Per-capita stock 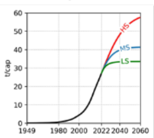	High Stock (**HS**)	Per-capita stock will grow on historical rates and saturate at **57.6 t/cap** by 2060.
	Medium Stock (**MS**)	Per-capita stock will saturate at **41.3 t/cap** by 2060.
	Low Stock (**LS**)	Per-capita stock will saturate at **33.5 t/cap** by 2060.

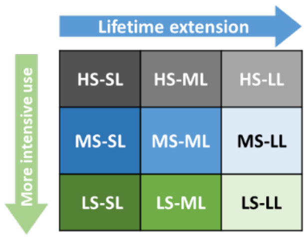

Figure 5-6 | Scenario matrix and each scenario dimension with key assumptions.

5.3 Results

5.3.1 Future cement stocks, outflows, and inflows

As shown in Figure 5-7, China's in-use cement stock has increased from 6.2 Gt to 40.5 Gt during 2000-2022. Under *Medium Stock* scenarios (Figure 5-7d, e, and f), the in-use stock will peak at 56.3 Gt by 2040 and then decrease to 51.1 Gt by 2060, if in-use stock per capita will continue to rise based on the historical rate. As economic development and urbanization often lead to lower fertility rates, population declines are expected to arrive in the 2030s (Ye, 2022), leading to a slight decline in in-use stock after the peak. If China's service level will catch up with the levels in industrialized countries, the in-use stock will grow substantially and finally peak at 72.5 Gt by 2050, after that gradually decline to 70.4 Gt in 2060 (*High Stock* scenarios, Figure 5-7a, b, and c). In contrast, the in-use stock will only increase by 17 % and peak at 47.5 Gt as early as 2030, with the implementation of material efficiency measures (*Low Stock* scenarios, Figure 5-7g, h, and i). Across all scenarios, lifetime extension will significantly change the vintage proportion of the in-use stock. Without lifetime extension, in-use cement stock built before 2020 will gradually decrease to 22.7 Gt in 2040 and finally slide to 8.6 Gt in 2060, whereas in-use stock built after 2020 will amount to as high as 45.2 Gt in 2040 and 61.8 Gt in 2060 (*High Stock* and *Short Lifetime*, Figure 5-7a). If the lifetime is extended to 70 years, in-use stock built before 2020 will survive longer and gradually slide to 28.3 Gt in 2040 and 20.6 Gt in 2060 at a slower rate, and in-use stock built after 2020 could be reduced to as low as 19.2 Gt in 2040 and 21.3 Gt in 2060 (*Low Stock* and *Substantial Lifetime Extension*, Figure 5-7i).

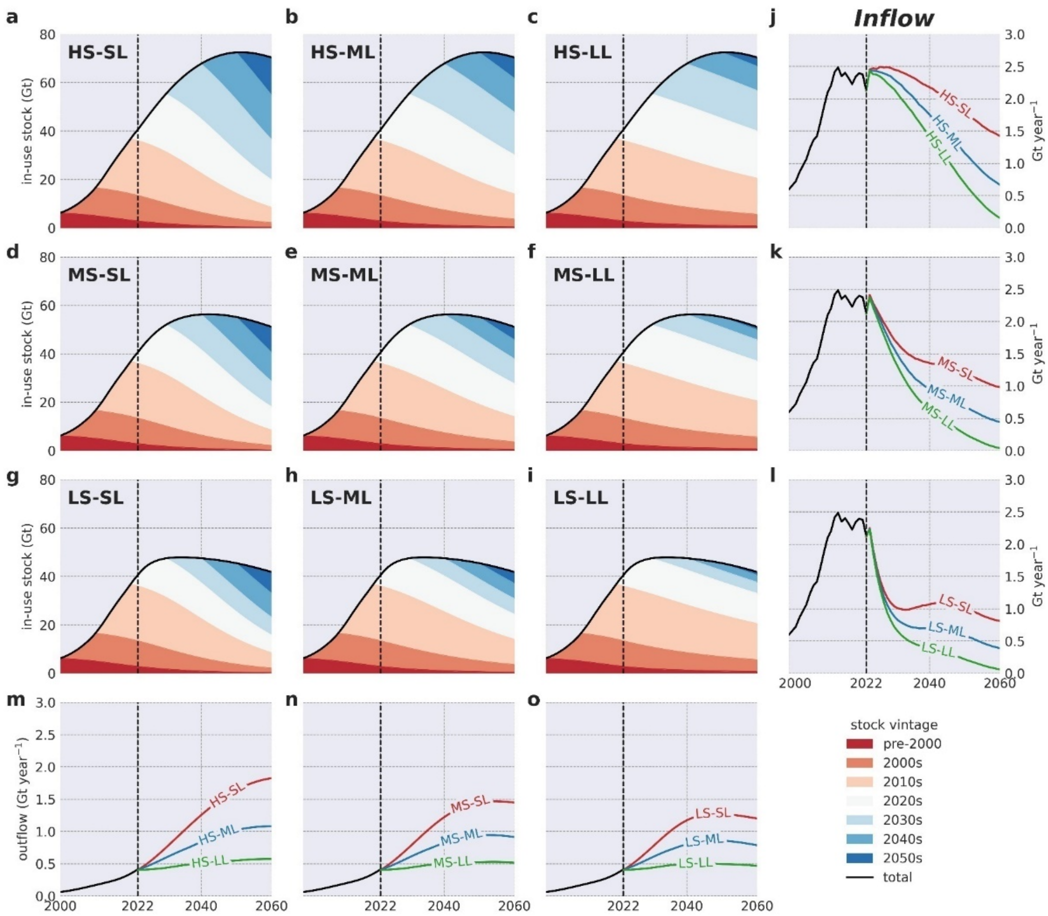

Figure 5-7 | Future dynamics of China's in-use cement stock, inflow, and outflow of all scenarios during 2000-2060 (adapted from Wu et al. (2023)).

(Notes: HS, MS, and LW denote *High Stock*, *Medium Stock*, and *Low Stock* scenarios, respectively. And SL, ML and LL represent *Short Lifetime*, *Moderate Lifetime Extension*, and *Substantial Lifetime extension* scenarios respectively.)

Therefore, the gradual saturation of cement stocks leads to declines in cement consumption during 2023-2060. Across all scenarios, China's cement consumption is projected to decrease over the next decades due to the combined effect of a declining population and saturated per-capita cement stocks. This effect could gradually decrease annual cement consumption from 2.1 Gt/year in 2022 to 1.7 Gt/year in 2030 if per-capita stock grows at the historical rate (*Medium Stock* and *Short lifetime*, Figure 5-7k). In *High Stock* scenarios, annual consumption will rebound to around 2.2 Gt/year in the 2030s after a slight decline in the near term, when much more cement is needed to build up and renovate buildings and infrastructure during 2023-2060 (Figure 5-7j). Conversely, a quick peaked per-capita stock by material efficiency improvement will constrain the annual consumption, leading to a quick and sharp decline to 1.0 Gt/year by 2030, after which annual consumption will fluctuate and eventually slide to 0.8 Gt/year in 2060 (*Low Stock* scenarios, Figure 5-7l). Lifetime extension can bend the curve of annual cement consumption across all stock-related scenarios. If the lifetime is extended to 50 and 70 years, China's annual cement consumption will substantially decrease to 387-667 Mt/year and 38-153 Mt/year by 2060, respectively. During 2023-2060, these savings could cumulatively amount to 21.3 Gt in the *Low Stock* scenarios, 24.6 Gt in the *Medium Stock* scenarios, and 28.3 Gt in the *High Stock* scenarios (Figure 5-8a). If combined, a lower per-capita stock and an extended lifetime can bring substantial cement savings, totaling 58 Gt in this period.

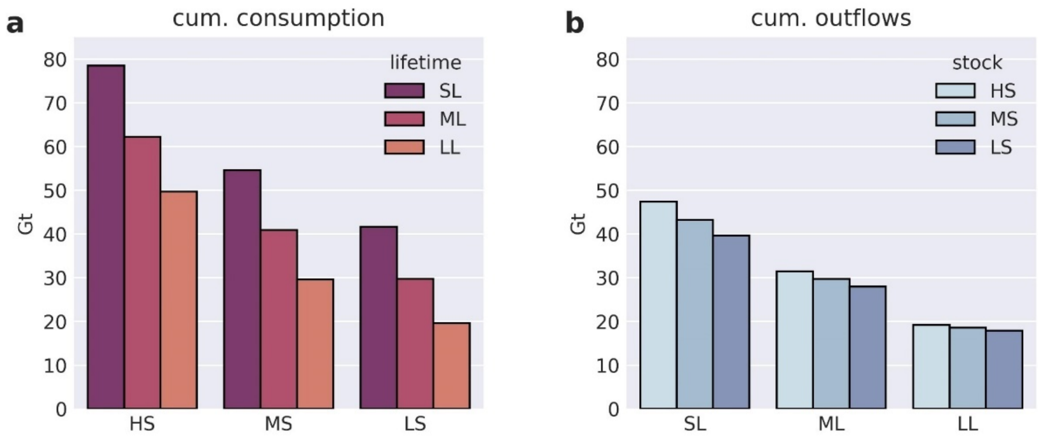

Figure 5-8 | Cumulative cement consumption and outflows in China during 2023-2060.

Regarding cement outflow, it is projected to increase across all scenarios, irrespective of stock levels and service lifetimes (Figure 5-7m-o). Notably, service lifetime is the key variable to determine annual outflows, as its impact is much more significant than that of per-capita stock level, especially in a cumulative basis (Figure 5-8b). Specially, annual outflows are expected to decrease significantly from 1.8 Gt/year to 0.6 Gt/year in 2060, with a substantial extension in service lifetime in *High Stock* scenarios. However, this reduction diminishes as stock levels decrease. When service lifetime is extended to 70 years, annual cement outflows can be reduced to approximately 0.5 Gt per year in the forthcoming decades across all three stock scenarios. Cumulatively, China is projected to generate up to 47.4 Gt of cement outflows during the period spanning 2023 to 2060. This figure could be moderately reduced to 39.6 Gt by controlling stock levels, such as through more intensive use. However, a substantial decrease to approximately 18.0 Gt could be achieved by fully extending the service lifetime of in-use cement stock in China (Figure 5-8b).

5.3.2 CO_2 uptake

Future CO_2 uptake through the carbonation of cement-related materials can be decomposed as illustrated in Figure 5-9 below. Annual carbon uptake is anticipated to decline in most scenarios, with the exception of the HS-SL scenario, where it is expected to increase from 0.3 Gt per year in 2022 to 0.4 Gt per year around 2040, before declining again to around 0.3 Gt per year by 2060. Conversely, annual uptake is projected to decrease substantially to as low as 0.1 Gt by 2060 in the LS-LL scenario. It is noteworthy that reduced in-use cement stock will diminish the uptake effects of carbonation. Maintaining stock levels unchanged, extending the lifetime to 50 and 70 years is expected to reduce total CO_2 uptake by concrete structures by 1.3 Gt and 2.3 Gt, and uptake by mortar by 1.3 Gt and 2.3 Gt, respectively. Additionally, decreased construction activities and reduced cement demand will shrink CO_2 uptake by construction waste and cement kiln dust (CKD), albeit to a comparatively lower extent.

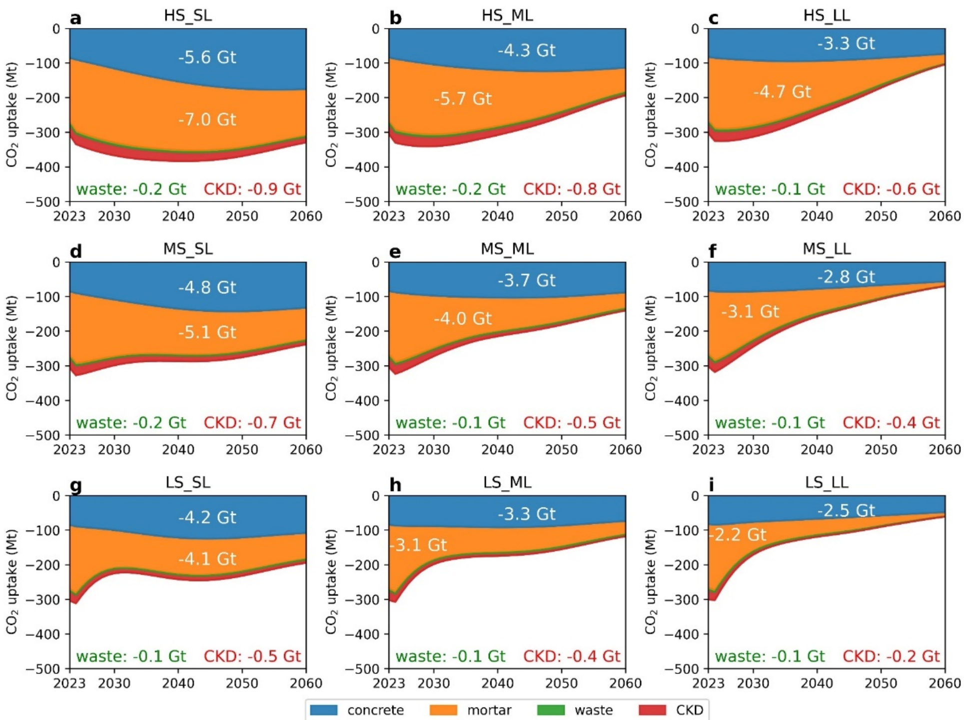

Figure 5-9 | CO_2 uptake by carbonation of cement-related materials during 2023-2060 (Wu, Ng, Chen, et al., 2023).

Notwithstanding that stock reduction and lifetime extension could unequivocally deliver emissions cut by decreasing cement production, both will inevitably shrink passive CO_2 sequestration by cement carbonation because of reduced in-use stock, inflows, and demolished outflows. Specifically, CO_2 uptake by in-use concrete structures will be almost halved during 2023-2060 in the Low Stock-Substantial Lifetime Extension scenario (1.3 Gt) compared with that in the High Stock-Short Lifetime scenario (2.3 Gt). Those materials embodied in new construction activities and cement production will decrease significantly in line with the downward trend of cement inflows, especially for rendering mortar, which will be fully carbonated and reabsorb substantial CO_2 within the first few years after entering use. Besides, avoided outflow by lifetime extension will significantly shrink CO_2 uptake by demolished concrete structures, as crushed concrete debris could dramatically increase the surface area exposed to air, leading to a further uptake within the short demolition stage. Only CO_2 uptake by masonry mortar will slightly increase (by ~0.6 Gt) by lifetime extension because it ensures enough time for CO_2 to penetrate through the thick surface rendering layer to reach the masonry mortar layer and induce its carbonation.

Additionally, a sensitivity analysis was conducted to investigate the impacts of parameters' ranges on the future CO_2 uptake. As shown in Figure 5-10 below, total CO_2 uptake during 2023-2060 will rise with an increase in the CaO contents in clinker and cement kiln dust (CKD) as well as the carbonation rates of concrete mixture. And when the proportion of CaO that could be converted to $CaCO_3$ within the fully carbonated cement and mortar (γ_1 and γ_2) decrease to their lower bounds, total uptake will significantly shrink by 17% and 22%. Further, decreases in corrector coefficients that reflect the impacts of surrounding CO_2 concentrations, coating and covers, and cement additives (β_1, β_2, and β_3) will reduce the total uptake approximately by -5%.

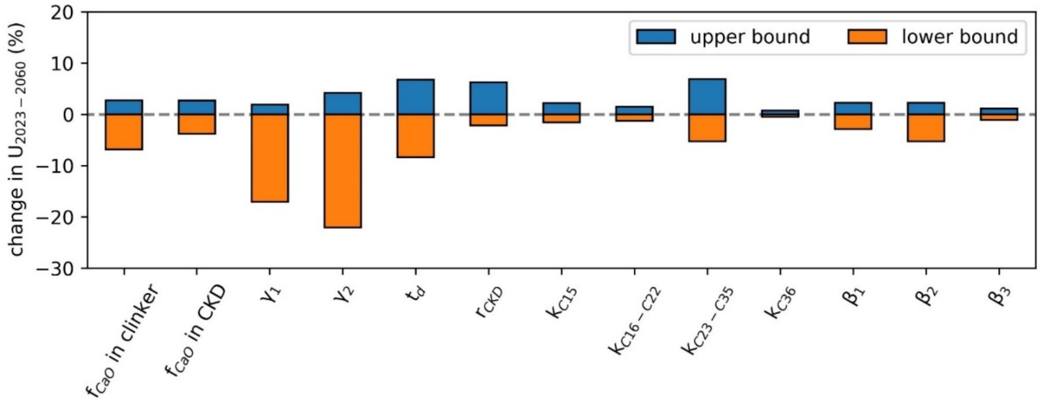

Figure 5-10 | Impacts of parameter changes on total CO_2 uptake by cement carbonation during 2023-2060 (Wu, Ng, Chen, et al., 2023).

5.3.3 Net CO_2 emissions

Future cement consumption sets important boundary conditions for decarbonizing the cement cycle. As shown in Figure 5-11, trends of annual CO_2 emissions are largely consistent with annual cement consumption across all scenarios. When no supply-side measures are taken, annual CO_2 emissions will gradually decline to 0.8 Gt/year, 0.6 Gt/year, and 0.5 Gt/year in 2060, across three stock scenarios (Figure 5-11a, d, and g). When CO_2 uptake is considered but no supply-side measures are taken, the CO_2 balance is projected to decline to 0.3-0.5 Gt/year by 2060. If the lifetime is extended to 50 years, no-action CO_2 emissions will decline to 0.4 Gt/year (High Stock and Moderate Lifetime Extension, Figure 5-11b), 0.3 Gt/year (Medium Stock and Moderate Lifetime Extension, Figure 5-11e), and 0.2 Gt/year (Low Stock and Moderate Lifetime Extension, Figure 5-11h) by 2060. While lifetime extension can deliver emission cuts, China will see considerable reductions in CO_2 uptake, as less CO_2 uptake will occur due to reduced cement consumption. When CO_2 uptake is considered, the CO_2 balance is projected to decline to 0.1-0.2 Gt/year by 2060. If the lifetime is further extended to 70 years, a substantial decrease in future consumption will result in annual CO_2 emissions dropping below 0.1 Gt/year by 2060. Indeed, the CO_2 balance is projected to be slightly negative across all three stock levels, indicating that theoretically, these demand-side strategies have the potential to facilitate a net-zero cement cycle by 2060 in China.

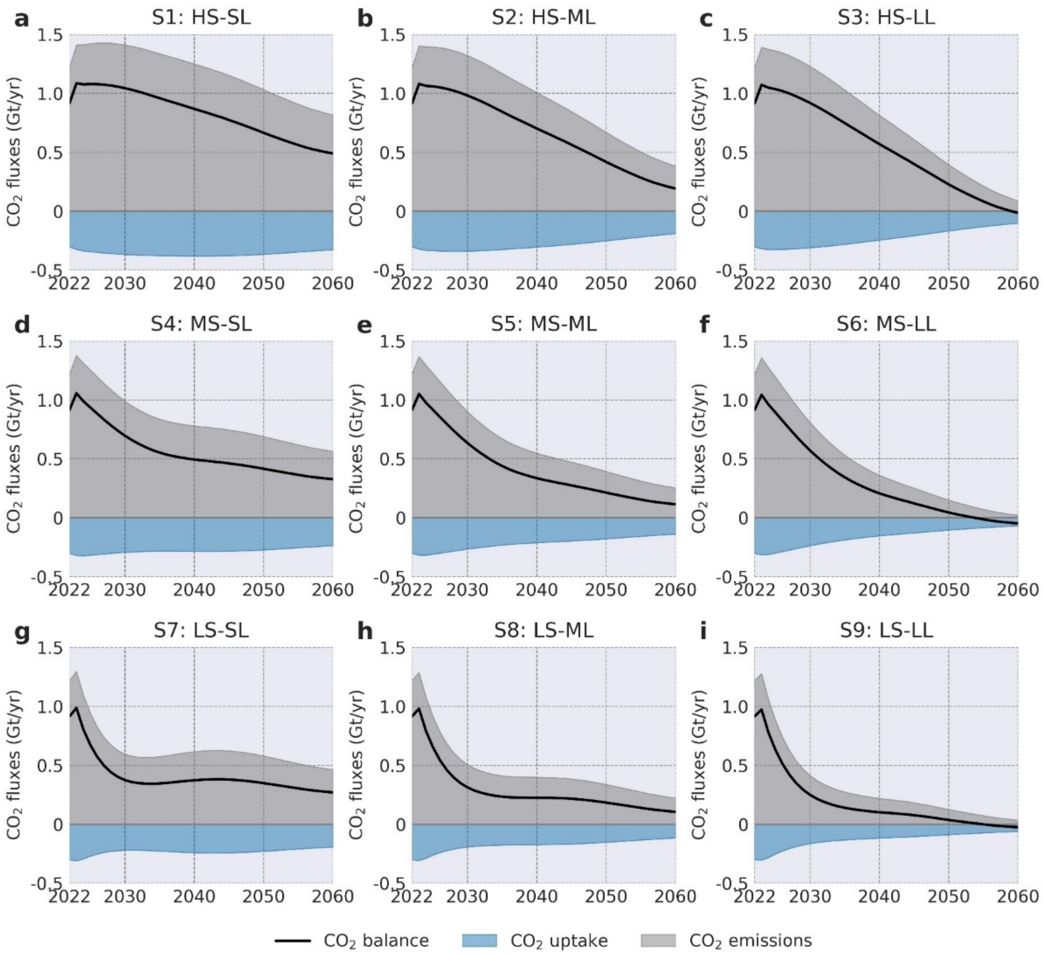

Figure 5-11 | Carbon balances of China's cement cycle in 2022-2060.

As shown in Figure 5-12, lower per-capita stocks could cumulatively reduce total CO_2 emissions by 13.7 Gt and 21.1 Gt in 2023-2060. Moderate and substantial lifetime extension will cut total emissions by 6.8-9.3 Gt and 12.6-16.5 Gt, respectively, whereas these reductions shrink with stock levels. And combining these two demand-side strategies together could totally decrease the cumulative emissions by up to 33.8 Gt CO_2 (Figure 5-12i). Also, the contribution of CO_2 uptake varies by scenario. Take two extreme scenarios as examples: in the *High Stock* and *Short Lifetime* scenario, CO_2 uptake can offset 31% of the no-action CO_2 emissions, while in the *Low Stock* and *Substantial Lifetime Extension* scenario, CO_2 uptake can offset 44% of the CO_2 emissions without supply-side actions. The varying contributions of CO_2 uptake in decarbonizing the cement cycle further indicate that CO_2 balance hinges on two boundary conditions: cement stock and lifetime. Cement stock reduction and lifetime extension can slow down the turnover of cement stocks and reduce the total societal throughout of cement, which in turn deliver emission cuts. However, due to the legacy effects of historically consumed and accumulated cement, CO_2 uptake is comparatively less affected by cement stock reduction and lifetime extension. This study therefore highlights that designing decarbonization roadmaps for the cement cycle must consider these two critical boundary conditions.

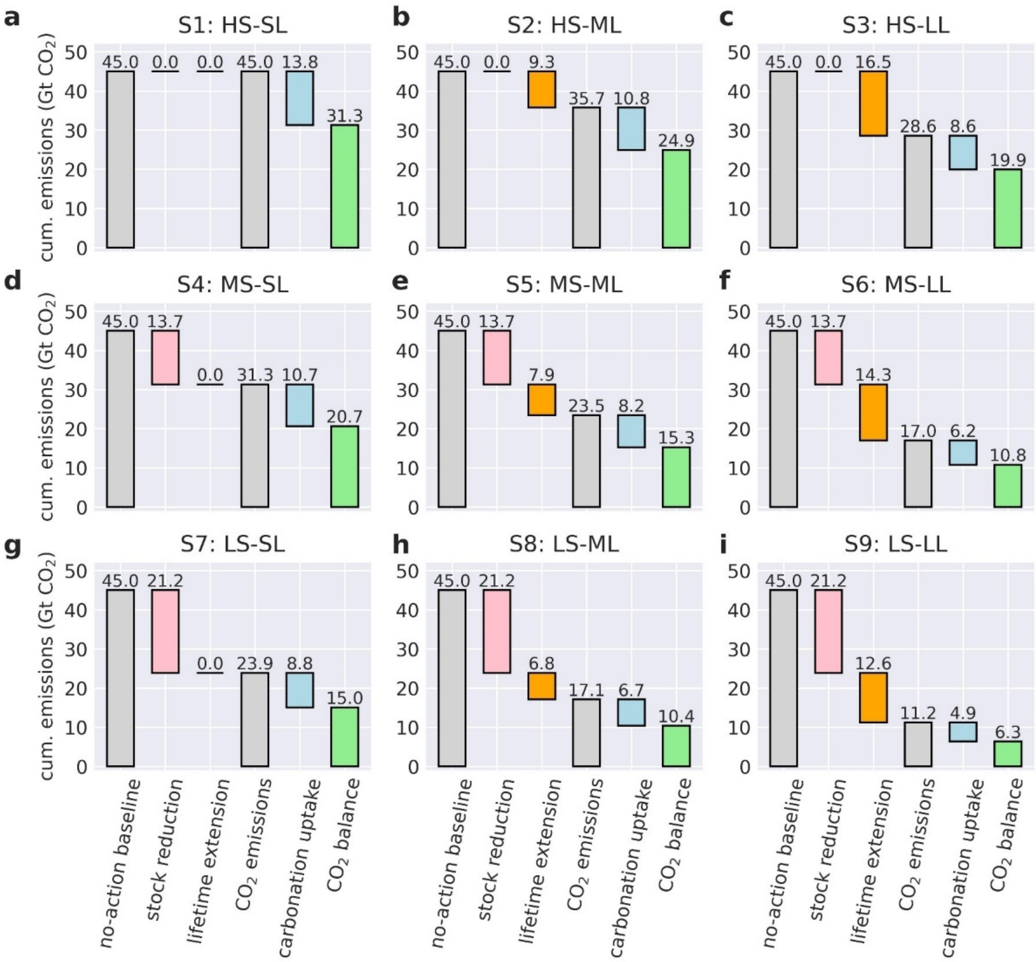

Figure 5-12 | Cumulative CO_2 emissions and uptake associated with China's cement cycle during 2023-2060. (a)-(i) cumulative CO_2 emissions reductions, uptake, and CO_2 balance of scenarios S1-S9.

5.4 Chapter summary

This chapter conducts a comprehensive scenario analysis along two dimensions: per-capita stock and service lifetime, resulting in the formation of a 3×3 scenario matrix. This matrix serves to elucidate the boundary conditions for China's future in-use cement stock, cement consumption, and outflows. By leveraging material efficiency measures on the demand side, the mitigation potentials of these strategies are uncovered through computations performed within the integrated framework. Remarkably, a substantial reduction of up to 33.8 Gt of CO_2, corresponding to 58 Gt of cement consumption, can be achieved by combining a significantly lower per-capita stock and extending the service lifetime to 70 years. Furthermore, achieving net-zero emissions across China's cement cycle by 2060 is feasible on an annual basis. However, it is imperative to carefully consider the implications, opportunities, and challenges associated with lower per-capita stocks and longer service life of cement stocks, as these changes hold profound implications for social development and quality of life in the future. Moreover, this chapter delves into the social implications, opportunities, and challenges arising from lower per-capita stocks and longer service life, particularly concerning the realization of emission reductions. Additionally, it is crucial to acknowledge the trade-offs between CO_2 fluxes in cement decarbonization road mapping, as demand-side strategies have the potential to lower CO_2 uptake by cement carbonation.

Chapter 6. Developing decarbonization roadmaps for cement sector within the MEU nexus

6.1 Introduction

Chapter 5 has explored the future boundary conditions for in-use cement stock and consumption, emphasizing their implications for carbon emissions and uptake. It quantitatively assessed the mitigation potentials from the demand-side and examined future carbon uptake through carbonation reactions. While these insights are crucial, an integration of both supply- and demand-side dynamics is necessary to develop robust decarbonization pathways for the cement sector. This integration allows for a balance between efforts on both sides, especially when planning for capital-intensive and complex technologies, i.e., CCS. Previous technology roadmaps have investigated the mitigation potentials of energy savings, emissions reductions, and green transitions (Dinga & Wen, 2022; Ke et al., 2012; C.-Y. Zhang et al., 2021), whereas the extent to which CCS should contribute to climate targets, while balancing supply- and demand-side efforts, is still not fully understood. Furthermore, the impact of plant turnover on the diffusion of low-carbon technologies has often been overlooked. Plant-level studies have explored the emission dynamics of various pollutants (X. Cai et al., 2020; C. Chen et al., 2022; L. Chen et al., 2020; Y. Chen et al., 2022; J. Liu et al., 2021; L. Tang et al., 2022), providing a bottom-up basis for technology transitions in the cement sector (Hills, Florin, et al., 2016). Yet, previous roadmaps rarely consider the turnover process of cement plants (Dinga & Wen, 2022; Ren et al., 2023; Tan et al., 2022; Xu et al., 2016; C.-Y. Zhang et al., 2021). Additionally, while prospective analyses have shown that significant committed emissions will be locked in existing fossil-fuel infrastructures based on their expected lifetimes and capacity factors (Tong et al., 2019), the impact of changing future demand has yet to be explicitly analyzed to determine how much CCS deployment is needed to address these committed emissions.

Against this background, this chapter integrates both the supply- and demand-side dynamics to systematically develop decarbonization pathways for cement sector, especially the role of CCS.

6.2 Methods

In addition to the demand-side scenario matrix developed in the preceding chapter, this chapter systematically investigates the potential role of carbon capture and storage (CCS) technologies in shaping emissions pathways toward three specific climate targets: limiting global warming to below 1.5°C, 1.7°C, and 2.0°C, respectively. Leveraging the CO_2 emissions and carbonation uptake accounting models utilized previously, this chapter delineates the future trajectory of emission intensity and total emissions in detail. An ambitious portfolio of supply-side mitigation strategies, termed the *AMB* scenario, is developed as a precursor to CCS deployment. These strategies are concurrently integrated into the turnover process of cement kilns, facilitating the derivation of sector-wide thermal energy intensity, fuel emission factors, and, consequently, aggregate emission intensity. Subsequently, these variables are input into an optimization model to determine annual CCS deployments and the associated emission pathways, while adhering to specific emission budgets. Ultimately, the chapter analyzes and discusses the requisite CCS installations and growth rates in the near-term and mid-term, offering insights into potential challenges such as imminent technology maturity, scalable business models, and stranded assets resulting from declining demand and underutilize d capacity.

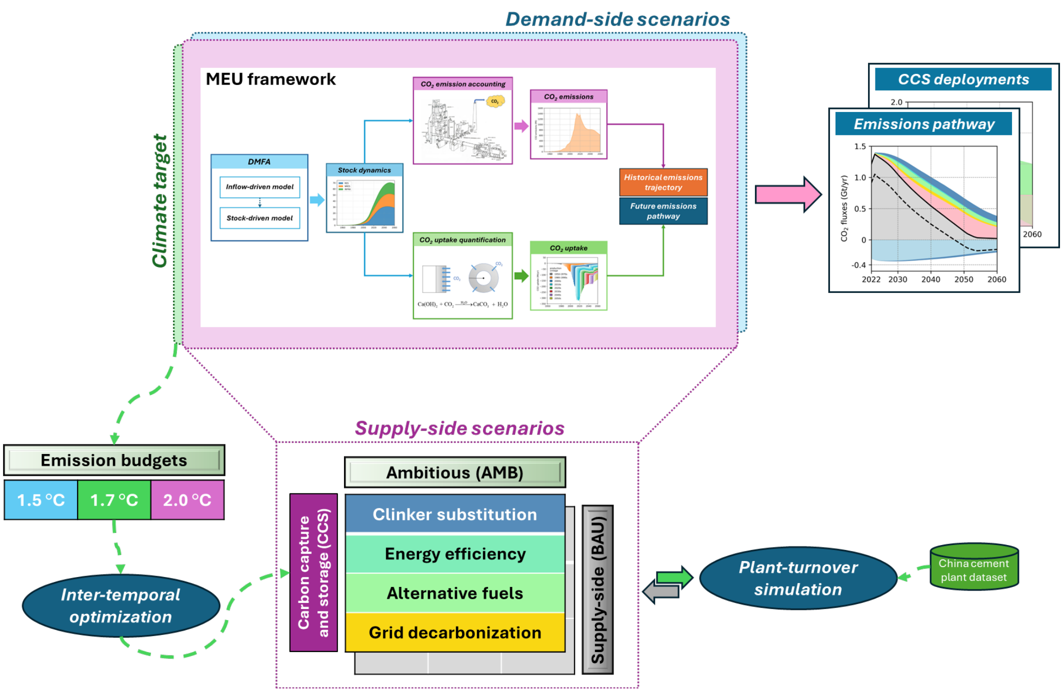

Figure 6-1 | Research flowchart and interactions with the MEU framework.

6.2.1 Supply-side scenarios

This chapter develops two scenarios to maximize the mitigation potentials from supply-side, before large-scale CCS deployments. First, a business-as-usual (BAU) scenario is developed to serve as a benchmark before a series of mitigation strategies are adopted. Then, an ambitious portfolio of four supply-side mitigation strategies (AMB), i.e., (1) energy efficiency improvement, including thermal energy efficiency and electricity efficiency, (2) switching to alternative fuels, including natural gas and biomass, (3) clinker substitution, and (4) grid decarbonization, which have considerable emissions reduction but cannot realize net-zero emissions, are implemented to fully tap conventional mitigation potentials. Whilst specific technologies can reduce thermal energy intensity (TEI) to some extent, it should be noted that by simply adding up the specific reduction potentials of single technology of one strategy to calculate the total mitigation is not accurate, because some of them have interacting impacts and may reduce the "one kJ" more than once, sometimes possibly leading to going beyond the minimum theoretical energy demand (ECRA & CSI, 2017). Thus, this study only considers the TEI reduction from replacement by the new plants and a significant retrofit for the existing plants. All existing plants as well as new plants are expected to operate for 40 years (C. Chen et al., 2022; Tong et al., 2019).

In the BAU scenario, the existing plants will maintain at the status quo, and the sector-wide thermal efficiency will be improved only by the efficient new plants, of which TEI must comply to the current *National standard for Energy-saving Design in Cement Plants* (i.e., GB 50443-2016 (Ministry of Housing and Urban-Rural Development of the People's Republic of China, 2016)). All the plants will continue to adopt coal for the heating energy supply. Besides, the clinker-to-cement ratio (CCR) in cement will also remain unchanged by 2060, as recent policies promote high-grade cement with higher clinker content than before (Wu et al., 2022).

In contrast, all the plants will conduct a significant retrofit at half of their expected lifetime in the AMB scenario. Thermal efficiency will be improved a lot in the AMB scenario, as existing plants will reduce their TEI to fulfill the requirements in GB 50443 after retrofit and new plants will adopt the current best practice to further reduce the TEI to 2.8 GJ/t of clinker. Furthermore, all new plants will be switched to natural gas, and co-fired with 30% of biomass (on a thermal basis) in their pre-calciner, while existing plants will also be co-fired with biomass after retrofit. Also, CCR will be reduced gradually to 50% with the pervasive use of low-clinker cement products in the market, such as LC^3 (Scrivener et al., 2018). As for grid decarbonization, it is reflected by decreases in CO_2 emissions per unit of electricity used due to increasing penetration of renewables (Tan et al., 2022). For simplification, this study assumes a linear transition from now to 2060 in the CCR and emission factors of electricity. A comparison of these two supply-side scenarios is displayed in Table 6-1 below.

Table 6-1 | Scenario narratives on supply-side mitigation strategies.

Dimension	Business-as-usual (BAU)	Ambitious (AMB)
Energy efficiency - Thermal efficiency	TEI of new plants only comply with the current National Standard, while existing plants remain unchanged.	TEI of new plants will decrease to 2.8 GJ/t of clinker, while that of existing plants will decrease to the level specified in the current National standard, after retrofit.
Energy efficiency - Electrical efficiency	No improvement in electrical efficiency of clinker production lines and grinding equipment.	Electrical efficiency for clinker production decreases to 57 and 50 kWh/t clinker by 2050 and 2060, respectively. Electrical efficiency for cement grinding decreases to 30 and 28 kWh/t cement by 2050 and 2060, respectively.
Fuel switching	No alternative fuels. Both the existing and new plants still adopt coal to fulfill all thermal energy requirement.	All new plants will be switched to natural gas and co-fired with 30 % of biomass fuel. Existing plants will be co-fired with 30% biomass fuel after retrofit.
Clinker substitution	CCR will maintain at the current level.	CCR will gradually reduce to 50% by 2060.
Grid decarbonization	Emission factor of electricity will maintain at the current level.	CO_2 emissions per unit of electricity used decrease to 0.07 and 0.03 kg CO_2/kWh by 2050 and 2060, respectively.
Retrofit	No retrofit.	Retrofit for efficiency improvement at half of the plant lifetime.

6.2.2 Plant turnover simulation

This study develops this module to simulate the turnover process of China's cement plants, based on the plant lists in the China Cement Industry Dataset (CCID) (Wu, 2023). In this module, those plants that reach the end of their expected lifetime will retire and transfer their capacity to the new plants. Thus, the year of starting operation and daily clinker production capacity are the key indicators, both of which are retrieved from the CCID. We assumed that those units with the age above the expected lifetime in 2020 will continue in operation but shall retire over the next five years to avoid abrupt changes in the cement kiln stock (Lu et al., 2022). The following Equations (6.1)-(6.3) delineates the turnover process defined above.

$$RC_t = \left\{ capacity^{t_1} \in TC_{t-1} \mid t_1 - t > \mathrm{PLT} \right\} \tag{6.1}$$

$$NC_t = \left\{ capacity_1^t,\ capacity_2^t,\ \ldots\ ,\ capacity_n^t \right\} \tag{6.2}$$

$$TC_t = \left(TC_{t-1} \setminus RC_t \right) \cup NC_t \tag{6.3}$$

Where TC_t, RC_t, and NC_t represent the set of total cement kilns in operation, retired kilns, and new kilns in year *t*, respectively. $capacity^{t_1}$ denotes the daily clinker production capacity of a kiln, and superscript t_1 represents the year when it started operation. PLT represents the expected lifetime of the cement plants, which will vary with scenario settings. The number of new kilns *n* is determined by the sum of retired capacity, capacity transfer ratio (α) and expected capacity ($capacity_e$) of the new plants.

$$n = \sum_{capacity \in RC_t} capacity \cdot \alpha \ / \ capacity_e \tag{6.4}$$

Here, the transfer ratio is set to 50% to reflect the 2-for-1 policy, which implies that the new production capacity is strictly prohibited from entering the market, and the capacity of retired kilns will be transferred in half to the new kilns (Ministry of Industry and Information Technology of the People's Republic of China, 2021). The expected capacity is set to 5,000 t of clinker per day.

Besides plant capacity, thermal energy intensity (TEI) for clinker production, fuel type, and process emission factors are also determined in this module. The process CO_2 emission factor is calculated based on the content of calcium oxide and magnesium oxide in clinker. Fuel type is determined based on the scenario narratives.

6.2.2.1 Thermal energy intensity

As for TEI, this chapter firstly fit it with the clinker production capacity by a linear regression model with a logarithmic x on our plant samples (Oda et al., 2012). Then, it is determined for the existing cement plants by this regression model, and obtain a sectoral aggregate TEI (3.297 GJ/t clinker) which is close to 3.250 GJ/t of clinker from the GNR Emission Report 2018 (International Energy Agency, 2021b), though the model only captures 52% of the variations (Figure 6-2a). Notably, TEI decreases with an increase in production capacity, as nowadays large plants always imply a system-wide improvement and an integration of efficient technologies. Currently, a few kiln systems can reduce TEI to as low as ~2.8 GJ/t of clinker in China (Ma et al., 2017), and this level will serve as the best available technology (BAT) benchmark in our supply-side scenario analysis.

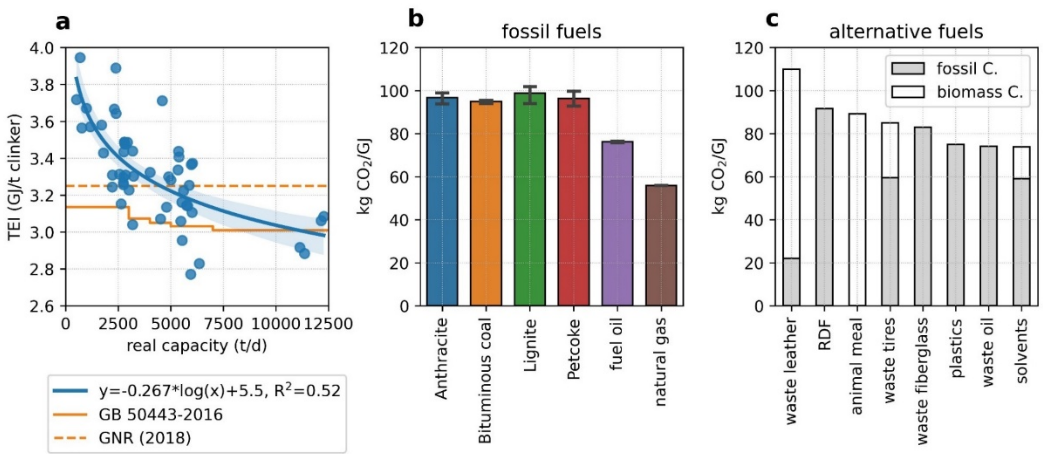

Figure 6-2 | (a) Thermal energy intensity for clinker production, CO_2 emission factors for (b) fossil fuels and (c) alternative fuels (Wu, Ng, & Chen, 2023).

(Notes: I adopt a regression model (Oda et al., 2012) to fit the relationship between the TEI and real capacity of our plant samples. Here, the real capacity refers to the daily production during the thermal testing for a cement plant. And GNR represents the Getting the Numbers Right platform. GB 50443-2016 represents the current National standard for Energy Conservation Design in Cement Plants (Ministry of Housing and Urban-Rural Development of the People's Republic of China, 2016). The source and values of emission factors of fossil and alternative fuels are displayed in the Supplementary Data.)

6.2.3 Determining CCS deployments

The annual CCS installation is determined by an optimization model as below. The objective function is to minimize the total cost required by annual CCS installment during 2023-2060.

$$\min \ \text{total\_cost} = \sum_{t=2023}^{2060} \frac{x_t \cdot uc}{\left(1+r\right)^{t-2022}} \tag{6.5}$$

Where x_t is the annual CCS installment in year t, r denotes the discount rate, and uc refers to the unit cost of CCS installment (unit: $/ton clinker production capacity of cement kiln). And the optimization should fulfill three following constraints: (1) total captured CO_2 emissions should cover the specific emissions gap, (2) the annual CCS installment should not exceed a specific ceiling rate, due to the technology maturity and available suitable capacity, and (3) the cumulative installed CCS kilns should not exceed the total clinker production capacity in operation. And these constraints are displayed as below.

$$\sum_{t=2023}^{2060} \Delta E_t \geq emissions\_gap \tag{6.6}$$

$$\sum_{i=2023}^{t} x_i \leq \text{total\_capacity}_t \tag{6.7}$$

Where ΔE_t is the annual emissions reduction by CCS deployment, i.e., the capture CO_2 emissions. As cement production scale is the same as the baseline scenario, emissions reductions mainly come from the emission intensity decreased by CCS deployments. Thus, annual emissions reductions can be calculated by the baseline emissions multiplied with the reduction rate in sector-wide emission intensity, compared with the baseline scenario (R_t).

$$\Delta E_t = E_{\text{baseline},\ t} - E_t = \text{Production}_{\text{cement},\ t} \cdot \left(EI_{\text{baseline},\ t} - EI_t\right) = R_t \cdot E_{\text{baseline},\ t} \tag{6.8}$$

$$R_t = 1 - \frac{EI_t}{EI_{\text{baseline},\ t}} \tag{6.9}$$

Here, EI represents the sector-wide aggregate emission intensity of cement production under the baseline scenarios (e.g., BAU and AMB) or the planning results. It can be derived from the penetration rate of CCS (w_t) and the *specific emission intensity* of cement production equipped with CCS facilities ($SEI_{w/CCS,t}$).

$$EI_t = w_t \cdot SEI_{w/CCS,t} + \left(1 - w_t\right) \cdot EI_{baseline,t} \tag{6.10}$$

$$w_t = \frac{\sum_{i=2023}^{t} x_i}{\text{total\_capacity}_t} \tag{6.11}$$

Again, the reduction rate in specific emission intensity equipped with CCS (ρ_t) can be certainly calculated, based on the specific technology configuration, such as a capture rate of 90%.

$$\rho_t = 1 - \frac{SEI_{w/CCS,t}}{EI_{baseline,t}} \tag{6.12}$$

Therefore, R_t can be figured out as below, by integrating Equations (6.10) and (6.12).

$$R_t = w_t \cdot \rho_t \tag{6.13}$$

6.2.4 Emissions budget

This chapter follows the practice in previous studies tailored for global steel and cement sector (Cao et al., 2020; Watari, Cabrera Serrenho, et al., 2023; Watari, Hata, et al., 2023) to estimate sectoral emission budget, in which the cement sector is assumed to contribute to global emissions mitigation in proportion to other sectors. The global capped emissions can be projected in a simplified way proposed by Raupach et al., (2014), i.e., the Equation 4 in that paper, by which the future capped emission trajectories can be estimated under the constraint of a certain carbon budget.

$$E_t^{cap} = E_{2022} \cdot \left(1 + \left(\gamma + m\right) \cdot \left(t - 2022\right)\right) \cdot e^{-m \cdot (t-2022)} \tag{6.14}$$

Where γ and m are two parameters to control future growth and mitigation rate, respectively. According to the cumulative emissions by integrate m alongside the future years (Eq. (6.15)), the parameter m can be solved as Eq. (6.16) below.

$$q(m) = \int_{2022}^{\infty} E_t^{cap} dt = \frac{E_{2022} \cdot (2m + \gamma)}{m^2} \tag{6.15}$$

$$m(q) = \frac{1 + \sqrt{1 + \gamma q / E_{2022}}}{q / E_{2022}} = \frac{1 + \sqrt{1 + \gamma T}}{T} \tag{6.16}$$

Where T is the emissions time (in years) to run out the remaining budget at current emission level. As shown in recent updated Global Caron Budget (GCB) (Friedlingstein et al., 2022), the remaining carbon budget for a 50% likelihood to limit global warming to 1.5, 1.7, and 2.0 °C has, respectively, decreased to 380 Gt CO_2, 730 Gt CO_2, and 1230 Gt CO_2, from the beginning of 2023, equivalent to T of 9, 18, and 30 years, assuming 2022 emissions levels. Here, the parameter r is set to be zero, signifying that capped emissions will decline from 2022 onward. Therefore, m can be figured out with the known T, then future capped emissions trajectories for China's cement sector are derived as below (Figure 6-3), with the assumption that its emissions mitigation rate is proportional to global emissions. Notably, the emissions trajectory aligned with the 1.5°C target is more consistent with China's ambition for carbon neutrality by 2060. In contrast, capped emissions for the 1.7°C and 2.0°C are estimated to be 0.1 Gt and 0.3 Gt, respectively. Collectively, the remaining carbon budget for the period between 2023 and 2060 is projected to be 10.3 Gt, 20.4 Gt, and 29.5 Gt for the global 1.5 °C, 1.7°C, and 2.0°C targets (with a 50% likelihood), respectively.

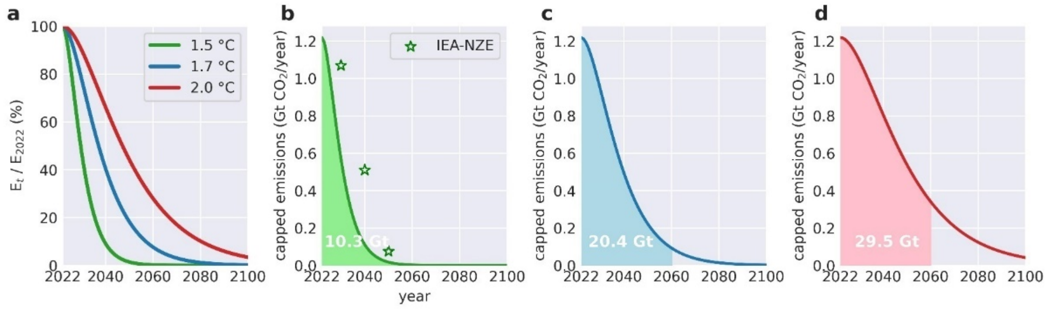

Figure 6-3 | Capped emissions trajectories consistent with remaining carbon budgets. (a) Change in the ratio of capped emissions to current emissions. (b)-(d) capped emissions trajectory and remaining carbon budget (2023-2060) for China's cement sector under 1.5, 1.7, and 2.0 °C, respectively.

This study further compares the calculated carbon budgets with those outlined in the International Energy Agency (2021a)'s net-zero emission roadmap by 2050 (IEA-NZE). In IEA-NZE, the cumulative global energy-related and industrial process CO_2 emissions during 2020-2050 will amount to just over 460 Gt, with 40 Gt from agriculture, forestry, and other land use (i.e., AFOLU). The total 500 Gt CO_2 emissions are in line with the remaining carbon budget (from the beginning of 2020) to limit global warming to 1.5 °C with a 50% likelihood (Intergovernmental Panel on Climate Change, 2023). Specifically, direct emissions (process and energy-related emissions) from the global cement sector will significantly decline from around 2.3 Gt CO_2 per year in 2020 by 18.6%, 61.2%, and 94.3% to 1.9 Gt, 0.9 Gt, and 0.1 Gt in 2030, 2040, and 2050, respectively, with the remaining emissions in 2050 will be offset by other carbon removal measures. Despite a very low sector emissions, global cement production will maintain at around 4.0 Gt per year during this period, which implies a much lower emission intensity (International Energy Agency, 2021a). However, as depicted in Figure 6-3b, the remaining carbon budget for 1.5 °C in this study is tighter than that of IEA-NZE. This discrepancy arises due to a significant portion of the budget being utilized by substantial global emissions during the years 2020-2022.

6.3 Results

6.3.1 Emission intensity of clinker and cement production

In the BAU scenario of the supply-side, the sector-wide thermal energy intensity (TEI) will maintain at around 3.30 GJ/t of clinker until 2040, after that it will gradually decrease to 3.17 GJ/t of clinker with the online of the efficient new kilns (Figure 6-4a). Reducing the expected plant lifetime to 30 years will accelerate the turnover of existing production equipment, leading to a lower TEI of 3.03 GJ/t of clinker, while retrofitting the existing cement plants to comply with the current thermal efficiency requirement (i.e., GB 50443-2016 (Ministry of Housing and Urban-Rural Development of the People's Republic of China, 2016)) can reduce the TEI to this level as early as 2035. Besides, combining these two measures, pervasive adoption of current best available practice for new plants can ultimately decrease the TEI to 2.8 GJ/t of clinker by 2060 (i.e., the AMB scenario). Furthermore, the AMB scenario will phase out coal, and adopting natural gas and co-firing with 30% biomass in pre-calciner by 2050 (Figure 6-4b). Another mitigation measure is grid decarbonization, which will contribute the similar reduction of energy efficiency improvement. Overall, these measures will totally contribute to a 23% reduction in direct emission intensity in the AMB scenario (655 kg CO_2/t clinker), compared to 865 kg CO_2/t clinker of the BAU scenario (Figure 6-4c). However, the contribution of a decreased clinker emission intensity will diminish for cement emission intensity, attributable to the discount effect resulting from the multiplication of the clinker-to-cement ratio (Figure 6-4d). Under an ambitious portfolio of supply-side mitigation strategies, the emission intensity is projected to decrease from 590 kg CO_2/t cement in the BAU scenario to 328 kg CO_2/t cement. Among these reductions, contribution from clinker substitution amounts to 138 kg CO_2/t cement, while that of energy efficiency improvement, deployment of alternative fuels, and grid decarbonization are 11, 79, and 33 kg CO_2/t, respectively.

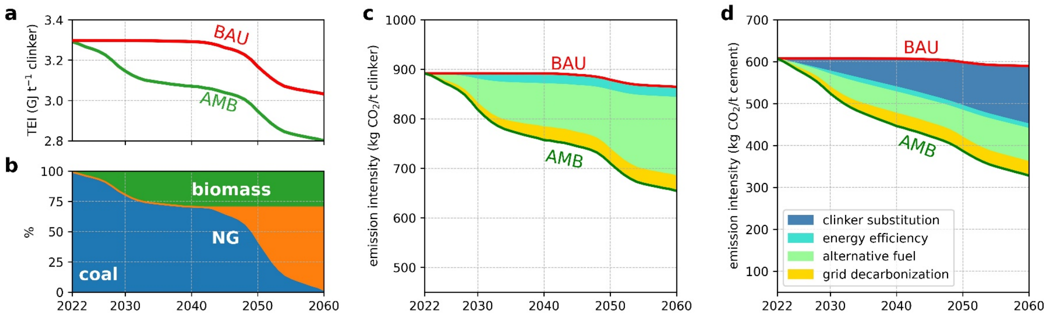

Figure 6-4 | Mitigation in emission intensity of clinker and cement production in 2022-2060 (Notes: This figure is adapted from Wu, Ng, & Chen (2023). And NG refers to natural gas.)

Combining original emissions fluxes in Figure 5-11, the mitigation effects of the above strategies can be quantified at the sector level, as depicted in Figure 6-5. Specifically, annual emissions can be reduced by 16-376 Mt CO_2/year, across the nine demand scenarios. These mitigation effects are contingent upon the future production scale of cement and clinker. For example, clinker substitution can cumulatively decrease total production emissions by ~5.0 Gt CO_2 in the HS-SL scenario, whereas in the LS-LL scenario this reduction will diminish to as low as 0.7 Gt. However, it is important to note that clinker substitution may reduce the CO_2 uptake by carbonation reactions due to the decreased presence of Calcium hydroxide embodied in future cement stocks. For instance, in the HS-SL scenario, annual uptake is projected to decrease by approximately 50 Mt CO_2 by 2060 as a result of clinker substitution. Other supply-side strategies, such as alternative fuels, grid decarbonization, and energy efficiency improvement, collectively have the potential to decrease total emissions by 0.6-3.4 Gt CO_2, 0.3-1.9 Gt CO_2, and 0.1-0.7 Gt CO_2, respectively. By combining these supply-side measures with carbonation uptake, emissions balance can be reduced to 146 Mt CO_2, 32 Mt CO_2, 89 Mt CO_2, and 75 Mt CO_2 by 2060 in the HS-SL, HS-ML, MS-SL, and LS-SL scenarios, respectively. Furthermore, emissions balance can be nearly or completely reduced to net-zero by 2060 in the HS-LL, MS-ML, and LS-ML scenarios, and potentially even achieved by 2050 in the MS-LL and LS-LL scenarios.

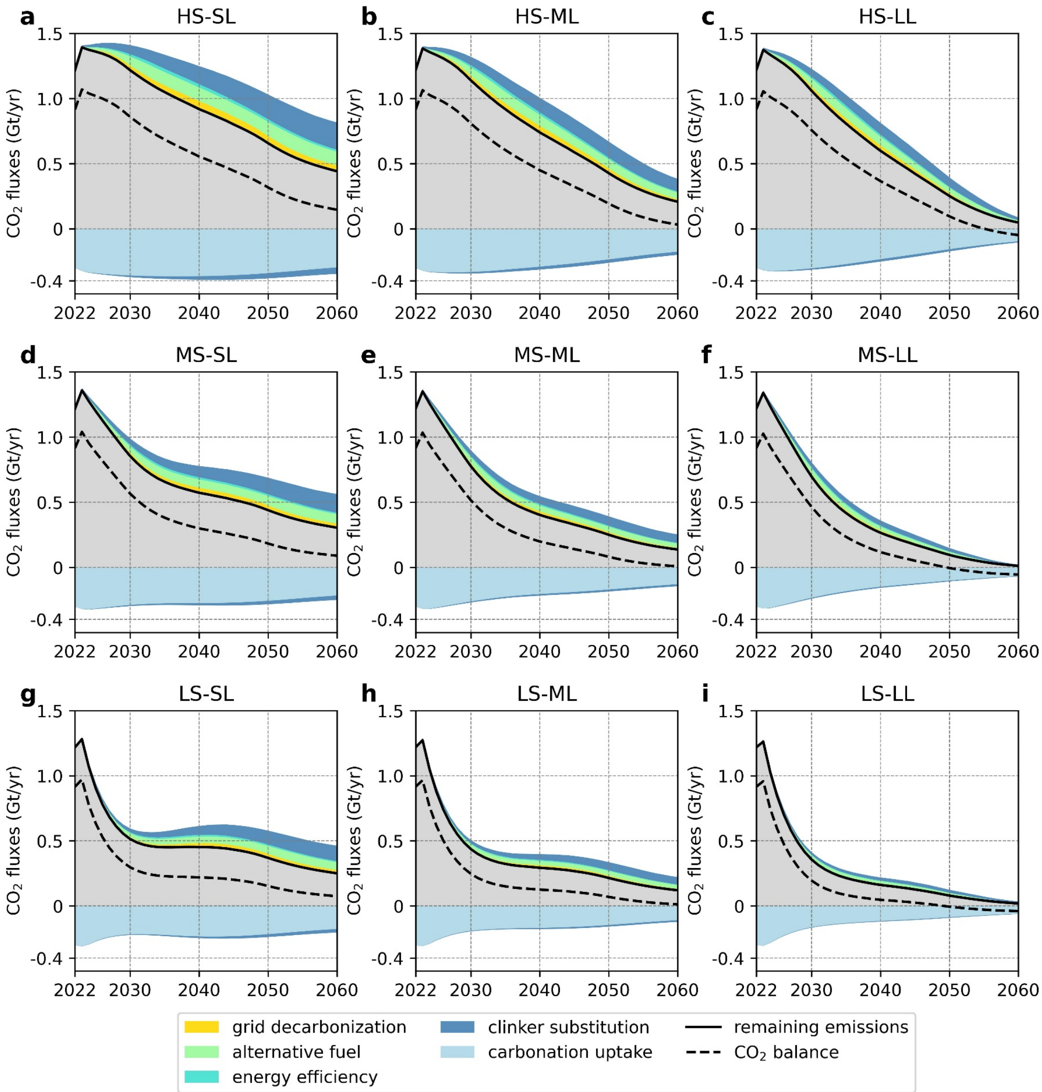

Figure 6-5 | Emission pathways of China's cement sector with the implementation of an ambitious portfolio of supply-side strategies (AMB scenario), but without CCS deployment.

6.3.2 Emission pathways consistent with climate targets

While the adoption of ambitious supply-side (AMB) strategies can substantially decrease annual emissions and potentially achieve net-zero emissions by 2060 and 2050, the cumulative CO_2 emissions in some scenarios may still surpass the stringent carbon budgets set for specific global warming targets. Figure 6-6 illustrates the emissions gaps between remaining emissions and carbon budgets across the nine demand scenarios with ambitious supply-side (AMB) strategies, considering both with and without the consideration of emissions offset by carbonation effects of cement stocks. Without the offset by carbonation uptake, most of the demand scenarios exhibit an emission gap ranging from 3.2 Gt to 23.7

Gt CO_2, assuming a very tight emission budget to limit global warming below 1.5°C with a 50% likelihood. These gaps can be significantly reduced when the carbon budget nearly doubles (1.7°C), with only the remaining four demand scenarios—three HS scenarios and MS-SL—requiring further emissions reduction through carbon capture technologies. As for the 2.0°C scenario, only the HS-SL scenario necessitates further reduction of cumulative emissions by 4.5 Gt to align with the carbon budget.

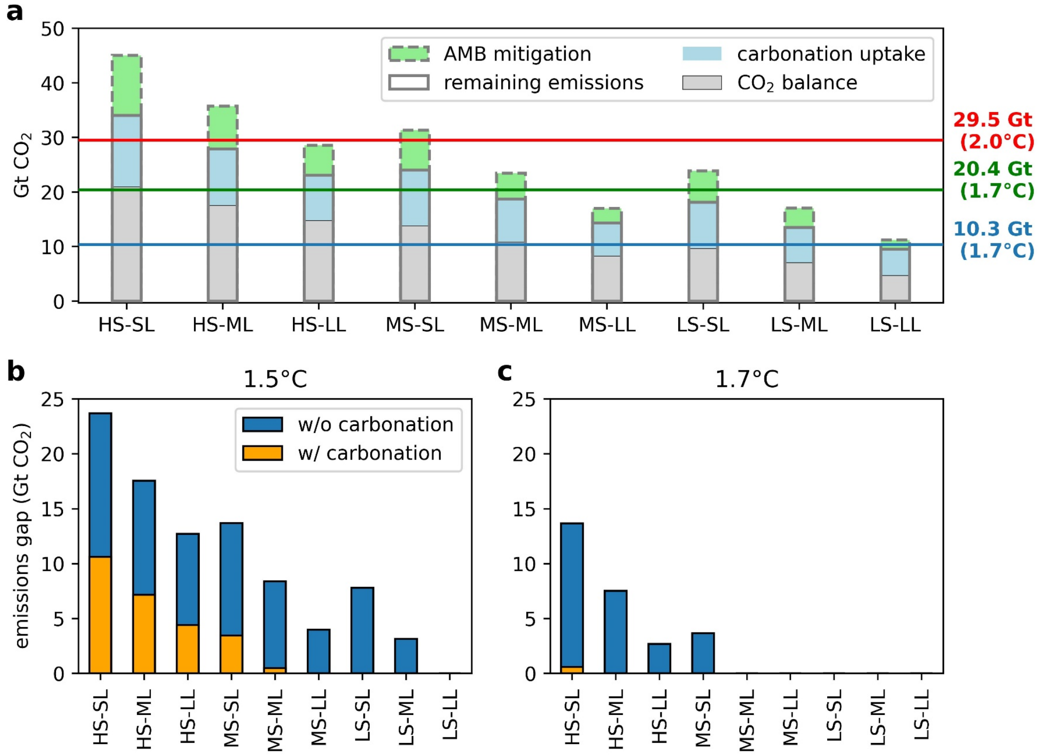

Figure 6-6 | Emissions gap between carbon budgets and remaining CO_2 emissions across scenarios (2023-2060).

However, emissions gaps can be closed when considering emissions offset by carbonation uptake (Figure 6-6b and c). Emission balances across nearly all demand scenarios are well below the emission budgets of 1.7°C and 2.0°C, whereas for the 1.5°C scenario, up to 23.7 Gt and 10.6 Gt CO_2 still need to be reduced in the HS-SL scenario, with and without the consideration of carbon uptake, respectively. These emission gaps serve as inputs to the optimization model to determine the required deployment and emissions reduction by CCS, following an ambitious portfolio of supply-side measures (AMB). As depicted in Figure 6-7, for the 1.5°C target, CCS necessitates immediate large-scale deployment in the HS-SL scenario or delayed deployment after 2030. In the HS-SL scenario, emissions mitigation by CCS will increase rapidly by approximately 70 Mt per year to 841 Mt per year until 2035, after which it will gradually decrease to about 400 Mt by 2060, due to diminished cement and clinker demand. In contrast, large-scale CCS deployment can be delayed until after 2030 in the LS-SL and LS-ML scenarios. Assuming a capture rate of 90%, significantly reduced remaining emissions will still range from 1 to 46 Mt per year by 2060 across these scenarios. Regardless of the scenario, rapid emissions decline in the near-term, even in the recent decade, is particularly urgent for the 1.5°C target. This urgency underscores the necessity for readily available and mature CCS technologies for large-scale deployments, or otherwise face a substantial decrease in future cement demand.

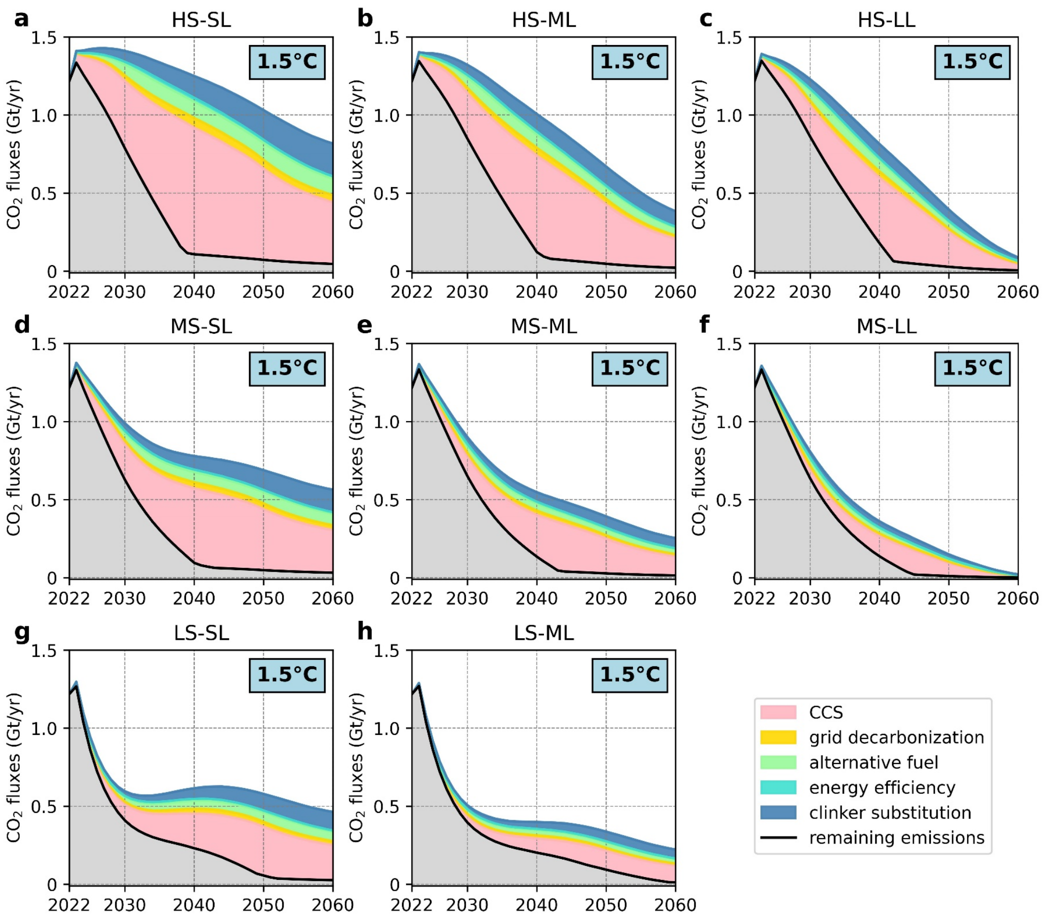

Figure 6-7 | Emissions pathways of China's cement sector consistent with 1.5 °C budget, without emission offset by carbonation uptake.

As for 1.7°C target, the emission pathways consistent with carbon budget are displayed as below (Figure 6-8a-d). Clearly, a much looser budget can delay CCS deployment until after 2030, along with a lower rate of growth in emissions reductions. Furthermore, under the 2.0°C target, CCS deployment can be postponed until 2038 in the HS-SL scenario (Figure 6-8e).

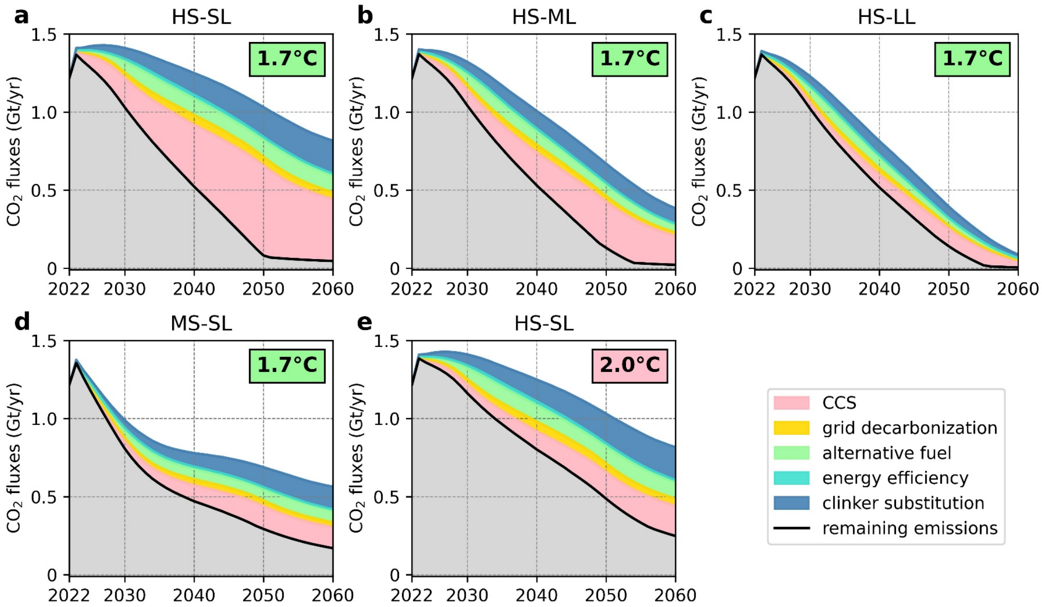

Figure 6-8 | Emissions pathways of China's cement sector consistent with 1.7°C and 2.0°C budget, without emission offset by carbonation uptake.

When considering emissions offset by carbonation uptake, CCS deployment can be delayed as much as possible and scaled down, even under the constraint of a 1.5°C target (Figure 6-9a-e). In the HS-SL scenario, CCS deployment will commence in 2034, with emission reductions increasing by approximately 66 Mt per year to reach 453 Mt by 2040. Subsequently, net emissions (i.e., emission balance) will turn negative in 2045, offsetting previous emissions excesses and ensuring total emissions remain within the available budget.

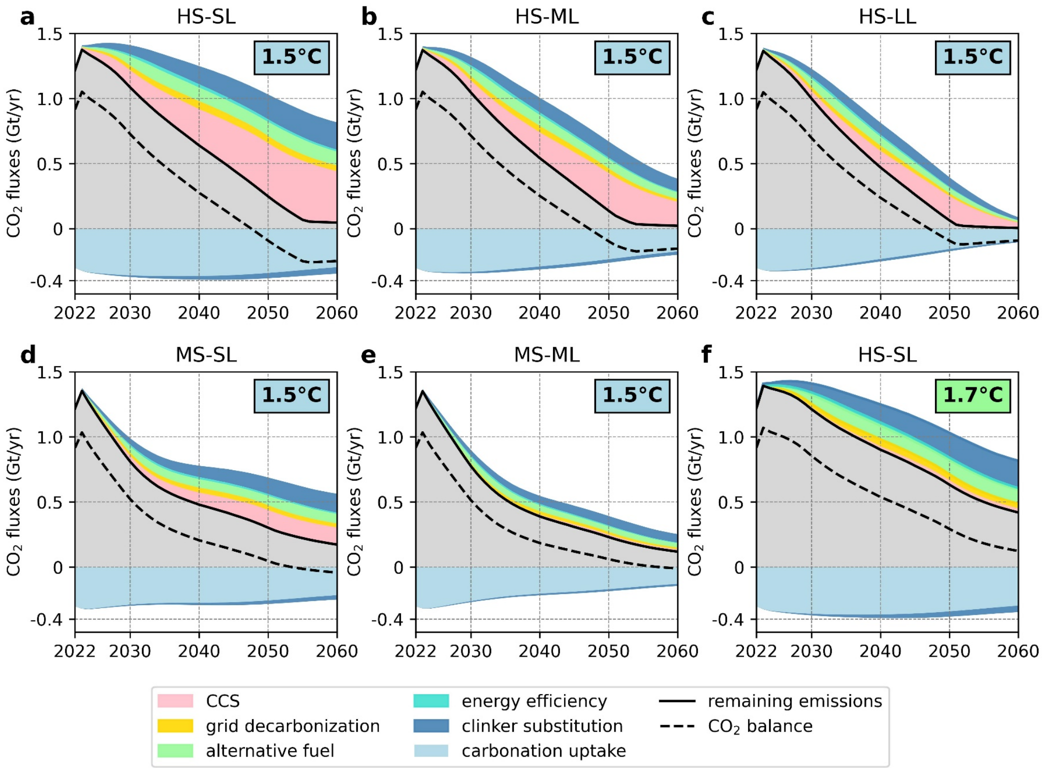

Figure 6-9 | Emissions pathways of China's cement sector consistent with 1.5°C and 1.7°C budget, with part of emissions offset by carbonation uptake.

6.3.3 Production capacity and CCS deployment

Presently, China's clinker production capacity stands at 5.7 Mt per day or 1.9 Gt per year nationwide (run for 330 days per year). The future projection of production capacity is simulated using the turnover module outlined in the Methods of this chapter. The turnover process accounts for the expected lifetime of cement plants and the capacity transfer ratio specified in the current industrial policies. When China's cement kilns are expected to operate for 40 years, the total clinker production capacity is projected to gradually decline to 1.0 Gt/year by the year 2060 (Figure 6-10a). Almost existing capacity will retire by 2060, while new capacity constructed from 2022 onwards will replace them at all. This significant decline is mainly attributed to the strict 2-for-1 capacity transfer policy currently enforced in China, due to the severe over-capacity issues in China's industry. While overcapacity can be effectively alleviated by the capacity transfer policy, it is expected to exacerbate as up to 81% of the production capacity will be underutilized when future cement demand and clinker production decrease substantially in the material efficient scenarios, such as LS-ML (Figure 6-10c) and

LS-ML (Figure 6-10c). Consequently, the large-scale existing clinker production capacity is incongruent with the reduced future demand, leading to the early retirement and stranding assets associated with the costly clinker production lines (Pfeiffer et al., 2018).

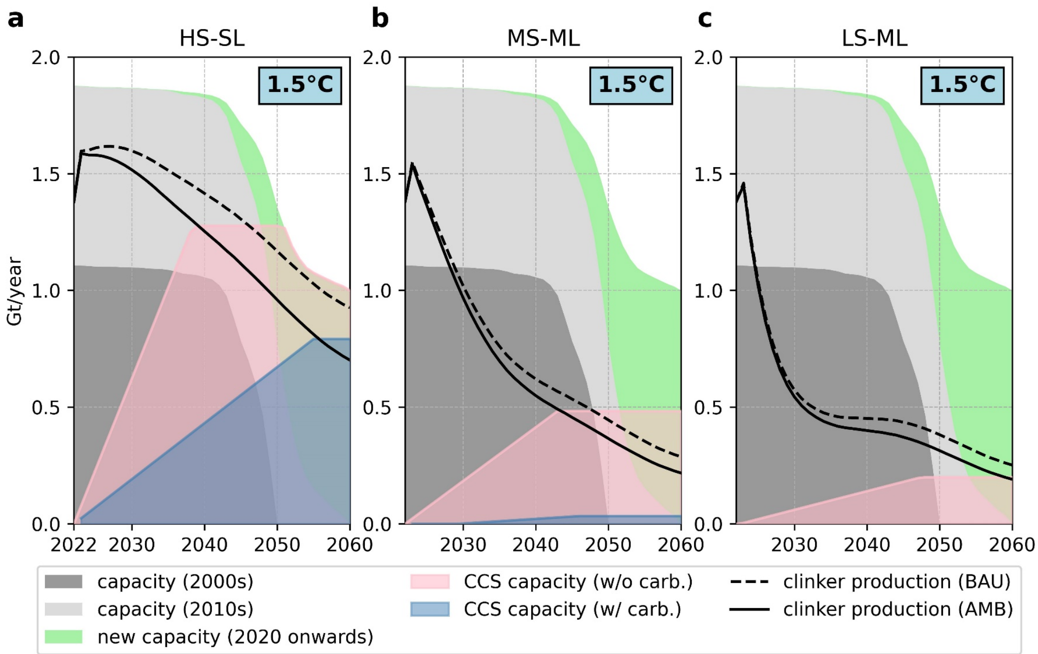

Figure 6-10 | Clinker production capacity turnover and CCS deployment in 2022-2060. (Notes: carb. represents emission offset by carbonation reactions.)

When considering the upscaling of carbon capture and storage (CCS) in China's cement sector, the requisite CCS capacity and the growth rate are contingent upon the specific demand scenario, emission budget, and whether emissions offset is taken into account. In the HS-SL scenario, targeting a 1.5°C limit, the required CCS capacity is projected to undergo rapid expansion, reaching 1.3 Gt clinker/year by 2040, with an average annual growth rate (AAGR) of 75 Mt per year during the upscaling period (Figure 6-10a). This trajectory suggests that approximately 75 cement kilns with a daily clinker production capacity of 3000 tons or 50 kilns with a capacity of 5000 tons per day would need to be deployed annually in the short term. Early deployment is expected to rely heavily on retrofitting existing cement kilns with CCS technology because of limited available new capacity under the current industrial policies, potentially resulting in a 'lock-in' situation with less efficient post-combustion capture technologies, such as monoethanolamine (MEA), rather than more efficient technologies but with a low retrofitability, such as calcium looping and oxyfuel combustion.

Moreover, a portion of this early CCS capacity may be underutilized and retired by 2060, indicating a potential risk of stranded investment in CCS infrastructure. However, if emissions offset by carbonation are considered, the required CCS capacity is notably reduced to approximately 0.8 Gt clinker/year. Material efficiency measures on the demand-side can further mitigate the reliance on CCS deployment. For example, in the MS-ML scenario, the total CCS capacity is projected to decrease to approximately 0.5 Gt clinker/year by 2060. Even in the LS-ML scenario, targeting a 1.5°C limit, only around 200 Mt of CCS capacity would be needed to capture the exceeded emissions.

Overall, the AAGR of CCS deployment exhibits a wide range, varying from 7.7 Mt per year to 75 Mt per year when targeting a 1.5°C limit, whereas it decreases to 2.0-24.0 Mt per year when emissions are offset by carbonation uptake (Figure 6-10d). For the 1.7°C and 2.0°C targets, the AAGR is further reduced to 6.8-33.8 Mt per year and 9.8 Mt per year, respectively. The implementation of carbonation offset results in a notable decrease in AAGR, from 33.8 to 1.9 Mt per year in the HS-SL scenario. Importantly, the growth rates across almost all scenarios, except for the exceptionally high demand in the HS-SL scenario without emission offset while aiming at 1.5°C, are notably lower than historical trends observed in the cement kilns with pre-heater and pre-calciner (termed as NSP in China), which diffused at an unprecedented rate to meet the substantial cement demand for socio-economic development over the last two decades (Wu et al., 2022).

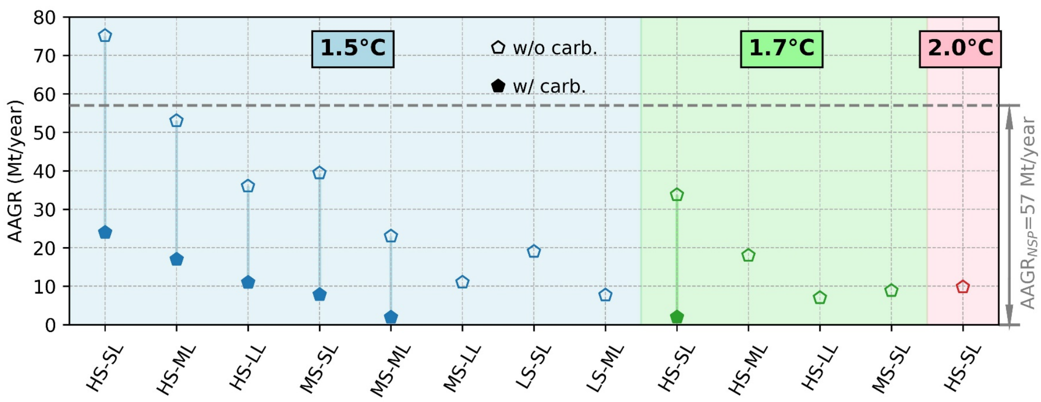

Figure 6-11 | Average annual growth rate (AAGR) of CCS deployment in China's cement sector, aiming at 1.5°C, 1.7°C, and 2.0°C. (Notes: carb. denotes for carbonation uptake.)

6.4 Chapter summary

This chapter integrates supply- and demand-side dynamics to develop decarbonization pathways for the cement sector, with a focus on CCS. It assesses the role of CCS in meeting climate targets of 1.5°C, 1.7°C, and 2.0°C by utilizing an optimization model alongside a plant turnover model to determine annual CCS deployments. Results primarily display climate-consistent emission pathways and the necessary scale of CCS deployment. The implications of deployment scale and rate are further analyzed in the subsequent discussion.

Chapter 7. Advancing decarbonization roadmaps within a geographical context: A case of future CCS deployment across China’s cities

7.1 Introduction

The last chapter has integrated supply- and demand-side dynamics to develop decarbonization pathways for the cement sector, with a specific focus on the role of Carbon Capture and Storage (CCS). However, the extent to which the emissions reduction potentials of CCS delineated in national decarbonization roadmaps can be tapped hinges on the future emissions distribution and accessible carbon storage sites (Gibbins & Chalmers, 2008; IEA, 2016). Effective CCS implementation requires detailed spatial planning to match CO_2 sources with suitable storage sites, considering factors such as proximity, capacity, and infrastructure availability (IEA, 2019). Without this spatially explicit planning, the scaling up of CCS technologies may face significant logistical and economic challenges, particularly in regions with uneven distribution of emissions and storage resources. Identifying optimal locations for CCS deployment can reduce transportation costs, enhance efficiency, and ensure that storage capacities are not exceeded (Middleton & Bielicki, 2009). Nevertheless, previous decarbonization roadmaps for cement sector lack spatially explicit guidance for practical implementation (Dinga & Wen, 2022; Ren et al., 2023; Tan et al., 2022; C.-Y. Zhang et al., 2021). Especially for CCS deployment, it is essential to consider suitable capacities for retrofitting as well as local or nearby accessible storage sites for captured emissions. Implicit spatial information or overlooking regional discrepancies may hinder the scaling up of CCS in the cement sector. Additionally, whilst some source-sink matching analyses have been conducted for CCS deployment in energy and industrial sectors (H. Tang et al., 2021; Y. Wang et al., 2024; Y.-M. Wei et al., 2021), the impacts of changing emissions layouts are seldom investigated, which may pose the risks of stranded assets of these capital-intensive facilities and infrastructures.

Therefore, this chapter addresses this gap by conducting a spatial supply-demand and emissions-storage matching analysis for CCS deployment in cement sector across China’s cities. This chapter starts with allocating future national cement clinker demand to individual cities and simulating clinker production capacity turnover. It then performs city-level supply-demand matching, estimates carbon storage potentials, and matches emissions to storage sites. Finally, strategic locations can be identified for large-scale CCS deployments, providing spatially explicit insights into the feasibility and optimization of CCS in China’s cement sector.

7.2 Method

This chapter takes China’s cities as a demonstration example to conduct spatial analysis, providing spatially explicit insights into the feasibility and suitability of CCS deployments in cement sector. Figure 7-1 illustrates the flowchart of this chapter. Specifically, three clinker demand scenarios are selected from Chapter 7 to downscale national demand to the cities. Alongside the production capacity turnover simulated at the city level, a simplified supply-demand matching model is developed to simulate future clinker production across cities. Finally, cumulative carbon emissions from clinker production will be matched with carbon storage potential estimated from explicit geographic information of oil field reserves and sedimentary basins of deep saline aquifers, to identify prioritized cities for CCS deployments in cement sector.

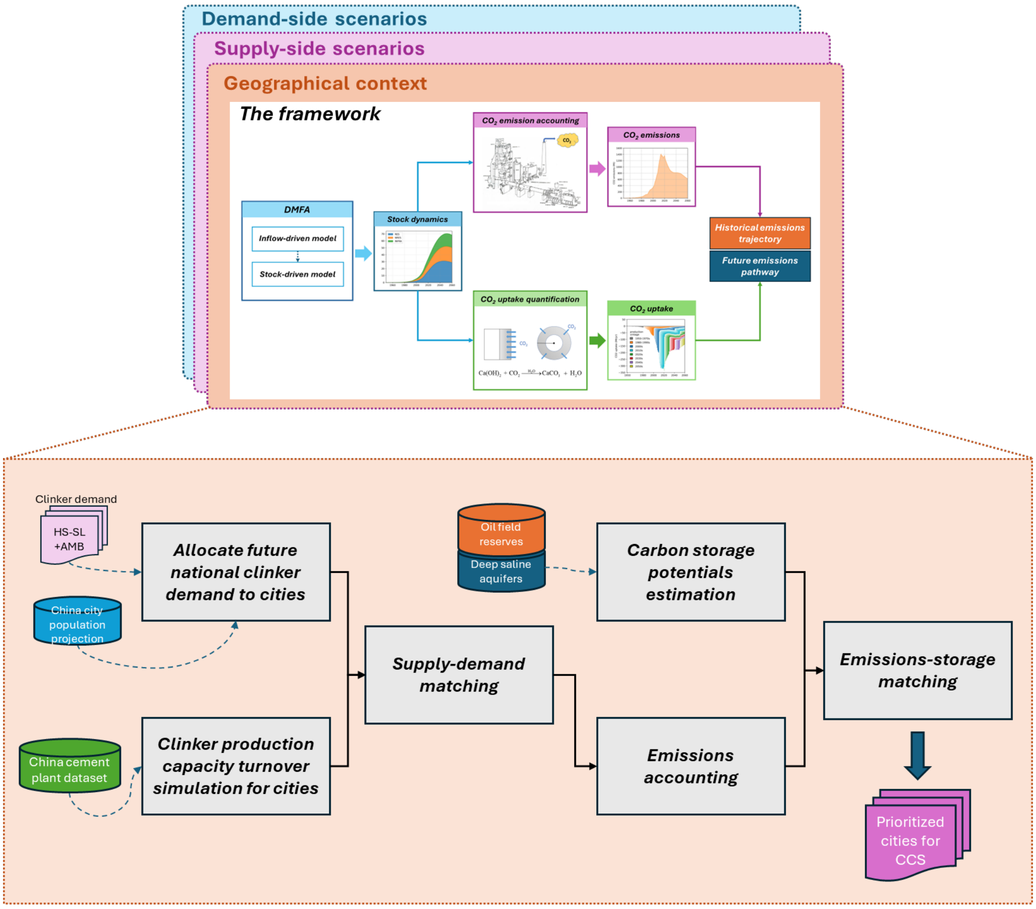

Figure 7-1 | Research flowchart of this chapter and its relationship to MEU framework.

7.2.1 Downscaling national demand to city level

Clinker demand is allocated based on the city-level population distribution, according to an assumption that all the cities have the same clinker demand per capita.

$$\text{demand}_{i,t} = \text{population}_{i,t} \cdot \text{per-capita\_demand}_{t} \tag{7.1}$$

Three clinker demand scenarios, i.e., HS-SL+AMB, MS-ML+AMB, and LS-ML+AMB, are selected from Chapter 7 to serve as the representatives of high, medium, and low clinker demand for city-level allocation. Here LS-ML is selected rather LS-LL, because LS-LL does not have an emissions gap even in the 1.5°C budget without carbonation offsets.

7.2.2 City-level supply-demand matching

This study develops a supply-demand matching module to simulate future clinker production distribution across the cities. Figure 7-2 shows the six steps of this module. In the first step, each city will self-supply their clinker demand, based on their own production capacity. In the second to sixth steps, the supply radius will enlarge gradually for iterations to allocate the remaining capacity and match supply and demand again to reduce the supply-demand gaps.

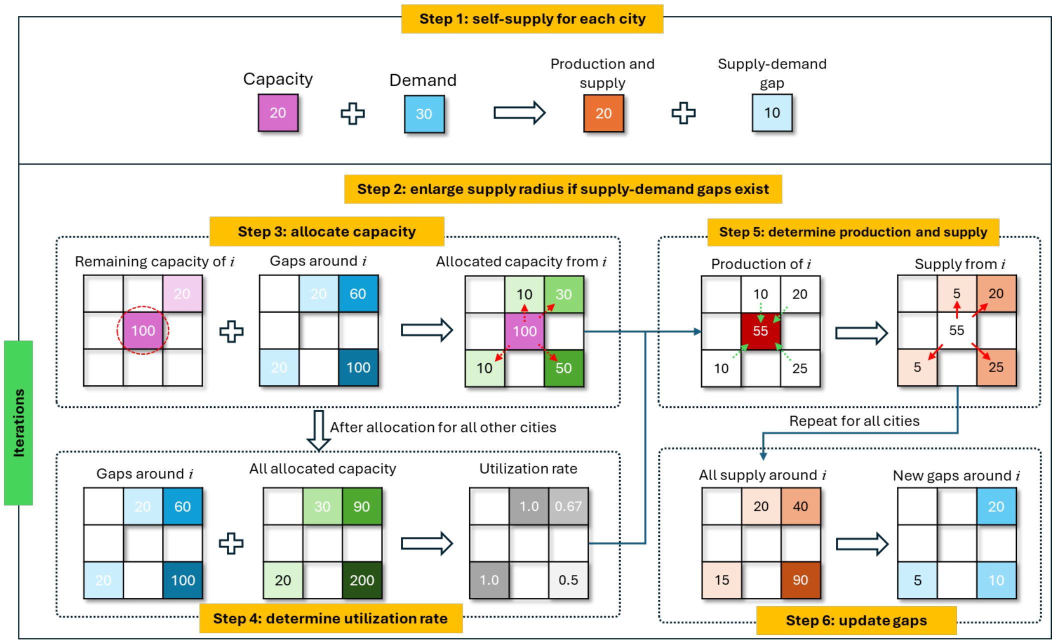

Figure 7-2 | Schematic diagram of the supply-demand matching module.

It is supposed that a city i can supply and receive supply from n surrounding cities within a specific supply radius D.

$$\text{surrounding\_cities}_i = \{\text{city}_j \mid d_{i,j} \leq D\} \tag{7.2}$$

Where $d_{i,j}$ is the highway driving distance between the city i and j, representing the transportation distances in this study. When D equals to zero, it implies that production will only supply the demand within the city (i.e., self-supply). Thus, its production (production_i^D) and supply (supply_i^0) can be determined as below.

$$\text{supply}_i^0 = \text{production}_i^0 = \begin{cases} \text{demand}_i & (\text{demand}_i \leq \text{capacity}_i) \\ \text{capacity}_i & (\text{demand}_i > \text{capacity}_i) \end{cases} \tag{7.3}$$

Some cities that do not have enough capacity to fulfill their demand will have a gap between supply and demand, whereas others that have a very large capacity may have remaining parts underused.

$$\text{supply-demand gap}_i^0 = \text{demand}_i - \text{supply}_i^0 \tag{7.4}$$

$$\text{remaining\_capacity}_i^0 = \text{capacity}_i - \text{production}_i^0 \tag{7.5}$$

When the supply radius D enlarges by a certain distance ΔD, more cities (Δn or Δm) will be included for allocation and matching. The remaining capacity will be allocated to surrounding cities according to their supply-demand gaps.

$$\text{allocated\_capacity}_{i,j}^{D+\Delta D} = \frac{\text{supply-demand gap}_j^D}{\sum_{x=1}^{n+\Delta n} \text{supply-demand gap}_x^D} \cdot \text{remaining\_capacity}_i^D \tag{7.6}$$

The utilization rate of capacity ($\text{u\_rate}_i^{D+\Delta D}$) is defined as the ratio of the gap to total received allocated capacities. This indicator can be calculated after all the allocations for all cities, and it should not exceed one.

$$\text{u\_rate}_i^{D+\Delta D} = \frac{\text{supply-demand gap}_i^D}{\sum_{x=1}^{n+\Delta n} \text{allocated\_capacity}_{x,i}^{D+\Delta D}} \tag{7.7}$$

Then, the production volume and total supply received can be determined accordingly.

$$\text{production}_i^{D+\Delta D} = \text{production}_i^D + \sum_{x=1}^{n+\Delta n} \text{allocated\_capacity}_{i,x}^{D+\Delta D} \cdot \text{u\_rate}_x^{D+\Delta D} \tag{7.8}$$

$$\text{supply}_i^{D+\Delta D} = \text{supply}_i^D + \sum_{x=1}^{n+\Delta n} \text{allocated\_capacity}_{x,i}^{D+\Delta D} \cdot \text{u\_rate}_i^{D+\Delta D} \tag{7.9}$$

Finally, after determining the production and supply for all cities, the supply-demand gaps will be updated. In this study, the above calculations from Equations (7.4)-(7.9) (i.e., Steps 2-6 in Figure 7-2) will be repeated for every increase in supply radius (ΔD), which is set to 100 km, until the overall gap declines to an acceptable level. Besides, the capacity turnover is simulated for each city by the model developed in the last chapter. Notably, new capacity will be allocated to cities where the gaps could not be bridged after all iterations of increasing supply radius, rather than unspecified locations.

7.2.3 Carbon storage potentials

Whilst CO_2 can be sequestered in oil and gas reservoirs, sedimentary basins for aquifer storage, and unmineable coal areas (Szulczewski et al., 2012), only deep saline formations and CO_2-EOR (enhanced oil recovery) in oil reserves are considered in this study, due to the concerns about the safety of geological storage (Lackey et al., 2019). And this chapter adopts the methodologies synthesized by Wei et al., (2021) to estimate carbon storage potentials of oil and gas field and saline aquifer basins.

$$EOR = \left(OOIP / \rho_{\text{oil}}\right) \cdot B_o \cdot c \cdot EXTRA \tag{7.10}$$

where $OOIP$ denotes the original oil-in-place, of which the data are retrieved from *2000 World Petroleum Assessment* (Persits et al., 2000); ρ_{oil} is the density of crude oil; B_o is the oil formation volume factor, which converts the volume of oil at standard conditions to that at reservoir pressure and temperature; and c is a "contact" factor which implies the proportion of OOIP will come in contact with the CO_2 injected into the formation, and indeed reflects the storage efficiency. $EXTRA$ represents the proportion of extra recovery to the OOIP contacted with CO_2 (unit: %), which depends on the API (i.e., American Petroleum Institute gravity) of crude oil. Subsequently, the CO_2 storage potential can be estimated by multiplying EOR with the typical ratio of required CO_2 injection to unit oil recovered (R_{CO_2}), which depends on the oil formation depth and API.

$$G_{EOR} = EOR \cdot R_{CO_2} \tag{7.11}$$

In the absence of detailed data on oil formation depth and API, the intervals bounded by lower and upper bounds are utilized to delineate the values of $EXTRA$ and R_{CO_2}, thus encapsulating the associated uncertainty.

As for deep saline aquifers (DSA), the carbon storage potential is estimated as below.

$$G_{\mathrm{DSA}} = A_{\mathrm{basin}} \times \varphi \times h \times \phi \times \rho_{CO_2-sto} \times c_{\mathrm{DSA}} \tag{7.12}$$

where A is the geographical area that defines the basin being assessed for carbon storage; φ denotes the ratio of effective area for storage; h denotes the gross thickness of saline formations within the basin; ϕ indicates the total porosity in volume defined by the thickness; ρ_{CO_2-sto} denotes the density of CO_2 at storage conditions; again c_{DSA} denotes a factor for storage efficiency, under the conditions of saline aquifer storage. The values for the above parameters are displayed in Table 7-1.

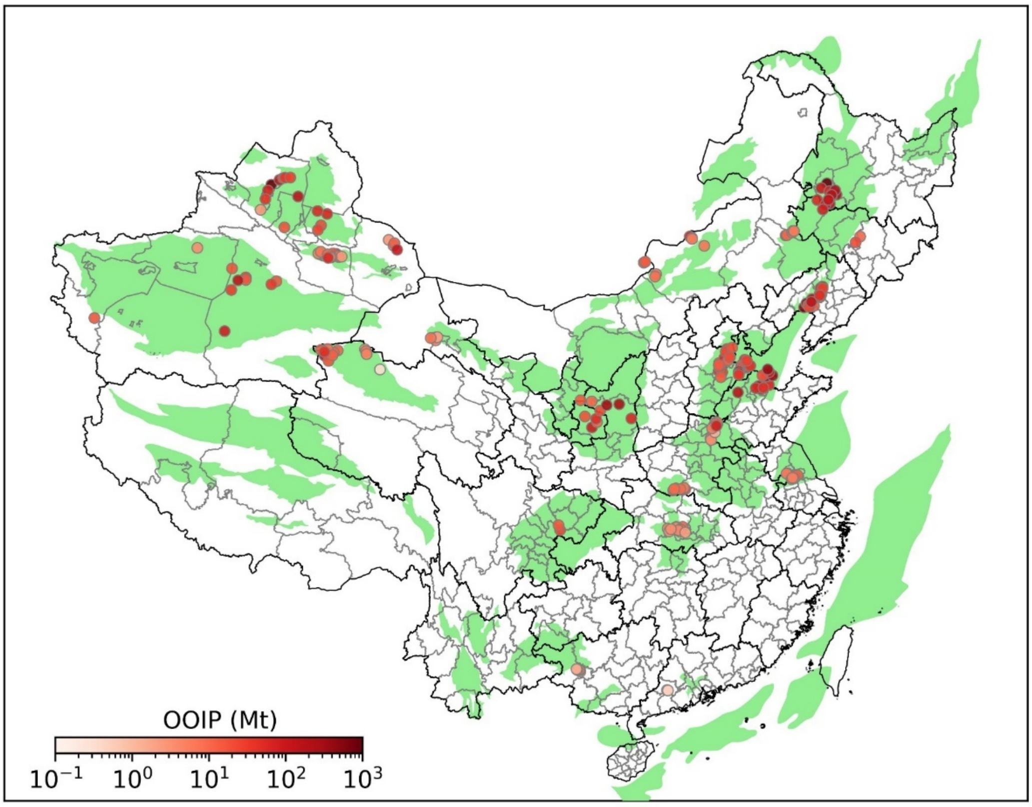

Figure 7-3 | Carbon storage potentials across China. (a) Deep saline aquifer (DSA) and (b) oil field.

Table 7-1 | Parameters and sources for estimating carbon storage potentials.

Parameter	Definition	Value	Source
ρ_{oil}	Density of crude oil (unit: t/m^3).	0.81	-
B_o	Oil formation volume factor.	[1.2, 2.0]	(Y.-M. Wei et al., 2021)
c	The proportion of OOIP that could be contacted with CO_2 flood.	75%	(IEA, 2002)
$EXTRA$	Proportion of extra recovery to OOIP. (unit: %).	[5.3, 18.3]	(Dahowski et al., 2005)
R_{CO_2}	Required CO_2 injected for unit additional oil recovered (unit: t/m^3).	[2.113, 3.522]	(Dahowski et al., 2005)
φ	Ratio of effective area for carbon storage for DSA.	[0.015, 0.025]	(Y.-M. Wei et al., 2021)
h	The gross thickness of saline formations for which CO_2 storage is assessed within the basin (unit: m).	[150, 250]	(Y.-M. Wei et al., 2021)
ϕ	Total porosity in volume.	0.2	(Y.-M. Wei et al., 2021)
ρ_{CO_2-sto}	Density of CO_2 at storage condition of deep saline aquifer (unit: t/m^3).	0.71	(van der Meer, 1993)
c_{DSA}	Carbon storage efficiency of DSA.	0.05	(Goodman et al., 2011)

7.2.4 City-level carbon emissions-storage matching

In this chapter, the supply-demand matching module (depicted in Figure 7-2) is also used to match clinker production emissions and carbon storage potentials across China's cities. Specifically, the production capacity in the module is replaced by the carbon storage capacity, whereas the demand is substituted by cumulative carbon emissions from clinker production during 2023-2060. Here, the highway pathway driving distance between the centroids of cities instead of the Euclidean distance is adopted for potential transportation pipeline construction, because it more accurately reflects terrain obstacles and provides a closer approximation to actual accessibility. Steps 2-6 of the matching process will be repeated for each incremental increase in the maximum transportation distance, up to a limit of 800 km (H. Tang et al., 2021), until the gaps between the remaining emissions and the climate target budgets can be bridged.

7.2.5 Data source

The future clinker demand data of three scenarios, i.e., HS-SL+AMB, MS-ML+AMB, and LS-ML+AMB, are retrieved from Chapter 8. For future population data used to downscale clinker demand, this chapter adopts the

“SSP2_SSPMigr3” scenario from a recently published, open-access population projection specifically tailored for China’s cities (S. Zhang et al., 2023). As for the distances between cities, this chapter computes the highway driving distances between the centroids of cities by the route planning function on Amap’s application programming interface[4], and the results are compiled to a matrix in Figure 7-4 below. Besides, the locations and area of basins and deep saline aquifers in China are retrieved from the maps of *Geologic Provinces of the Far East, 2000 (prv3al)* developed by United States Geological Survey (1999), whereas the locations and reserve of oil fields are retrieved from the *Atlas of China’s Petroliferous Basins* compiled by Li & Lv (2002).

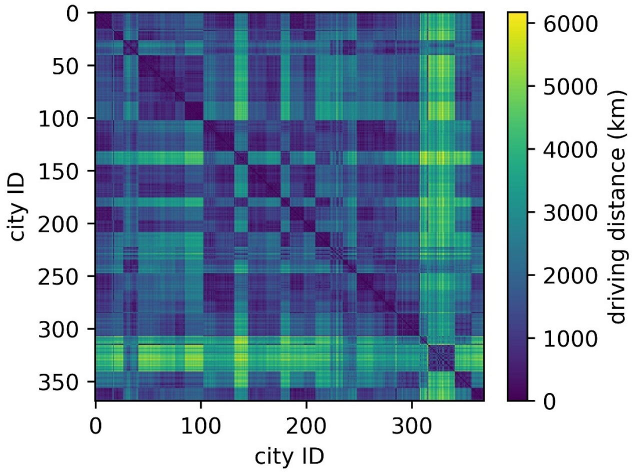

Figure 7-4 | Driving distance matrix of China’s cities in 2022.

7.3 Results and discussion

7.3.1 Cement plants in China

As shown in Figure 7-5, most of cement kilns are located in the east, south, and central of China. Among these cities, Chongqing has the highest clinker production capacity of 59 Mt per year, while city Qingyang of province Gansu has the lowest capacity of 0.27 Mt per year.

[4] Website: https://lbs.amap.com/.

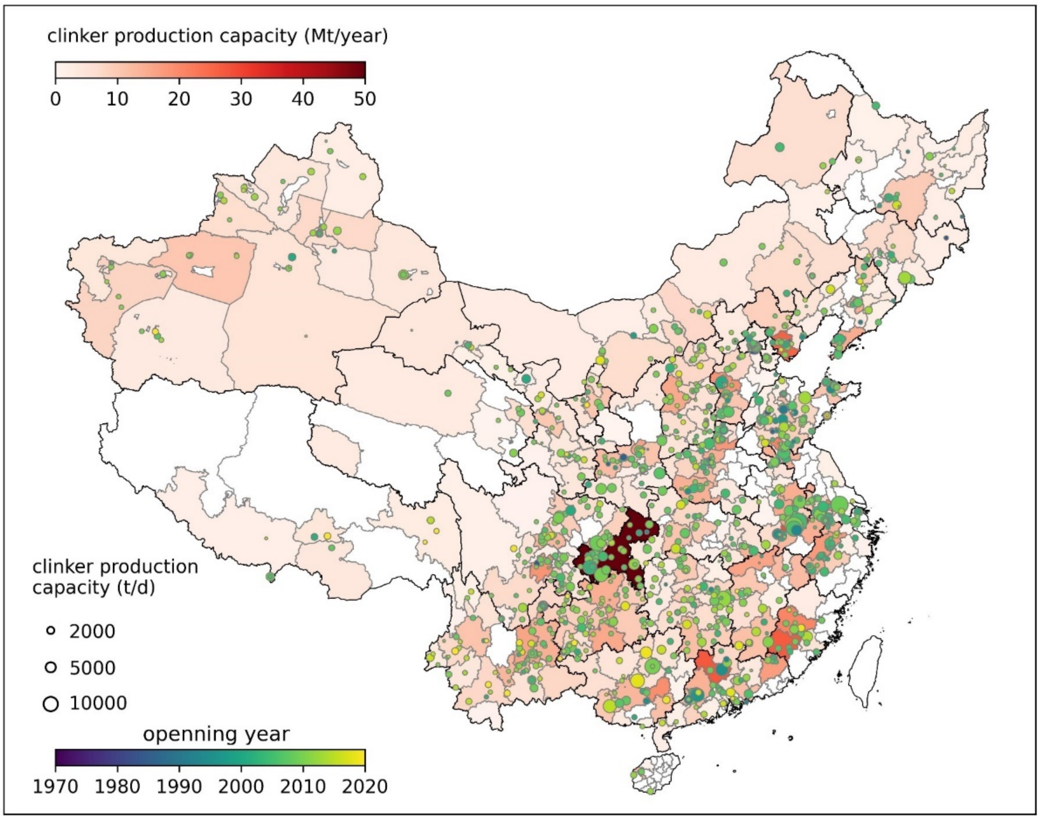

Figure 7-5 | Cement plants and clinker production capacity across the cities of China in 2020.

As for the composition of age structure, up to 98% of cement kilns were constructed during 2000-2020, while about 2% are the capacity older than 20 years (Figure 7-6a). Notably, most of new capacity (plant developed within 5 years) are located in the east, central and south China (Figure 7-6b).

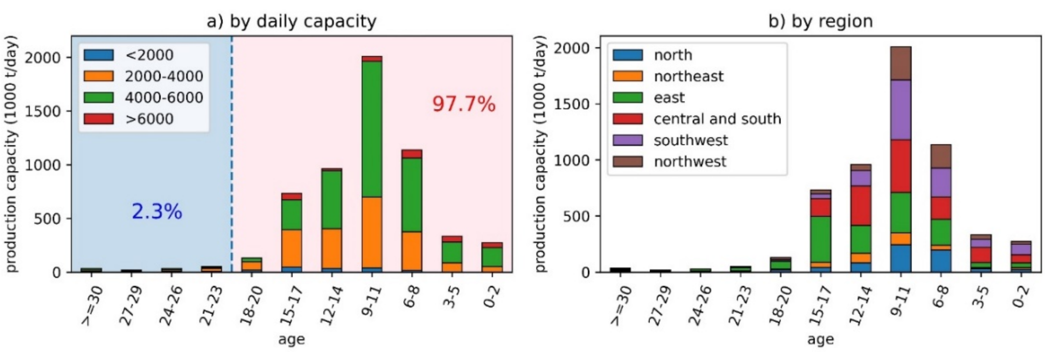

Figure 7-6 | Age structure of China's cement plants.

Here, this chapter integrates city-level clinker and cement production data from 2019 (sourced from Wang et al., 2023) with our capacity dataset to conduct an analysis on the utilization rate of production capacity and clinker flows between cities. As depicted in Figure 7-7a, the overall utilization rate of cement kilns in

China stands at approximately 81%. Among cities with clinker capacity exceeding 20 million tons (Mt) per year, Tongling, Wuhu, and Longyan exhibit utilization rates exceeding 90%, whereas Chongqing, Tangshan, and Qingyuan register rates below 80%. In terms of cement production, only four cities reported annual production exceeding 30 Mt, namely Chongqing, Yichang, Tangshan, and Longyan, while five cities produced over 20 Mt of clinker per year (Figure 7-7b).

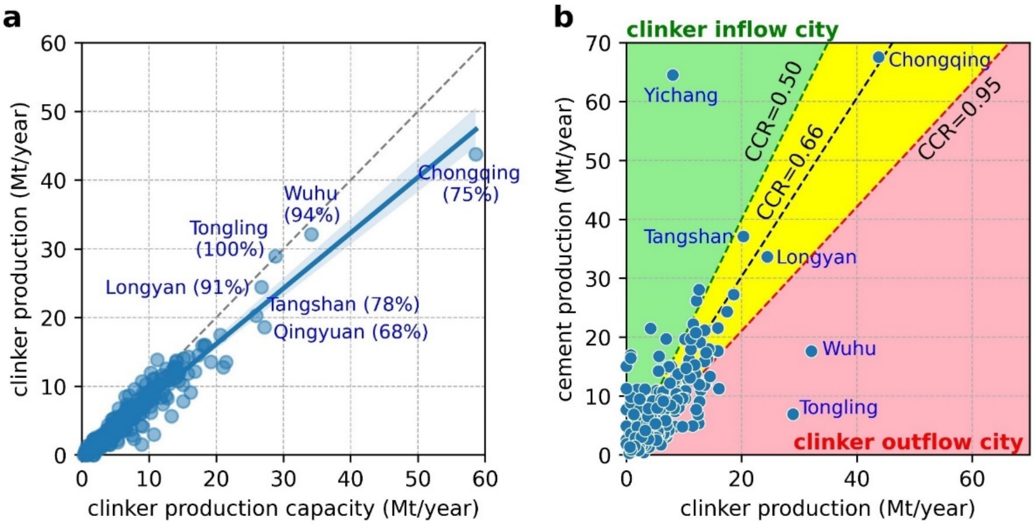

Figure 7-7 | Utilization of clinker production capacity (a) and clinker importer and exporter cities in China. (Source: City-level clinker and cement production data in 2019 are from (Y. Wang et al., 2023).)

The cities are categorized into three groups based on their nominal clinker-to-cement ratio (CCR). Cities with a CCR surpassing the theoretical maximum CCR of 0.95 are designated as absolute clinker outflow cities, boasting numerous cement kilns that produce significant quantities of clinker supplied to surrounding areas, exemplified by Wuhu and Tongling in Anhui Province. Conversely, cities with an ultra-low CCR below 0.50 (achievable through the deployment of LC3 (Scrivener et al., 2018)) are classified as absolute clinker inflow cities. These cities possess fewer cement kilns but possess numerous grinding facilities, procuring substantial amounts of clinker from other cities to produce cement. Notably, the CCRs of certain cities, including Chongqing and Longyan, closely approximate the national average of 0.66 around 2020.

7.3.2 Future clinker production and capacity at city level

Before conducting future projection, the supply-demand matching module is tested and validated based on the clinker production data in 2019. The reported national clinker production is distributed to the cities based on the population data around the same year. Then, clinker production of cities is simulated by the developed matching module. Figure 7-8 shows the supply-demand gap decreases significantly with the increase in supply radius for each iteration. The initial gap is about 600 Mt, when all the demand is self-supplied by the local capacity. When the supply radius increases to 800 km, 99% of clinker demand can be matched with the available supply around the country. To validate the accuracy of the matching module, the predicted city-level clinker production of this study is compared with the real production data in 2019 (Y. Wang et al., 2023). Overall, Figure 7-8b shows that the fitting line is close to the 1:1 diagonal line, indicating a well agreement between the predicted clinker production and the reference production. The coefficient of determination (i.e., R^2) is 0.85, and the root mean squared error (i.e., RMSE) is 2.113 Mt, reflecting a relatively high prediction accuracy for all the cities.

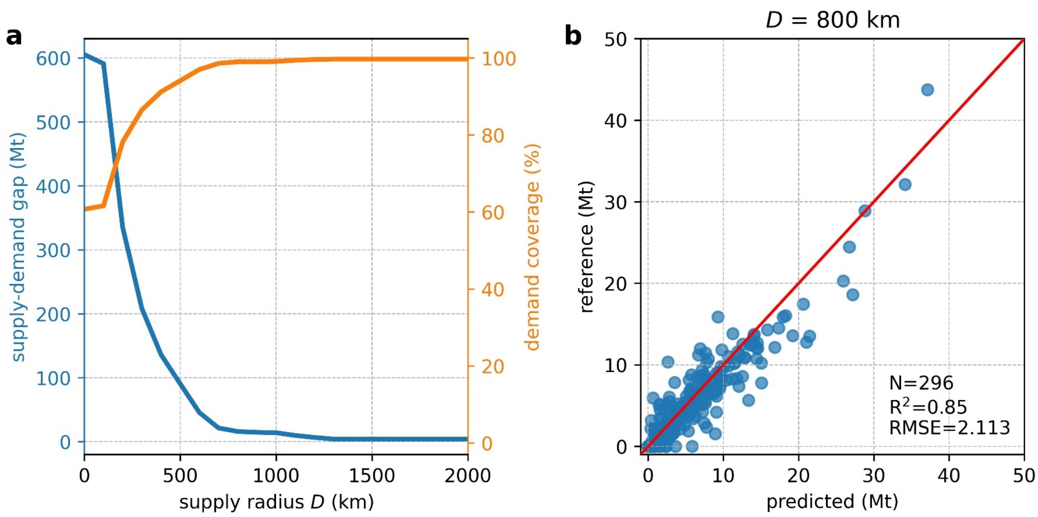

Figure 7-8 | (a) Supply-demand gap versus supply radius and (b) comparison between the predicted clinker production in this study and real production data from Wang et al. (2023).

As mentioned in the Methods, this chapter adopts three clinker demand scenarios from the last chapter for city-level simulation. Figure 7-9 displays the allocated clinker demand and the matched clinker production across China's cities in 2022, which is the start point of projection. Both clinker demand and production show a regional disparity. Specifically, Chongqing has the highest clinker demand of 33 Mt per year, whereas Shennongjia has the lowest demand of 75 kt per year. Clinker production mainly concentrates in cities with large production capacity. For instance, Wuhu, Chongqing, Qingyuan, Longyan, and Tangshan are predicted to produce 34 Mt, 33 Mt, 27 Mt, 27 Mt, and 26 Mt clinker in 2022.

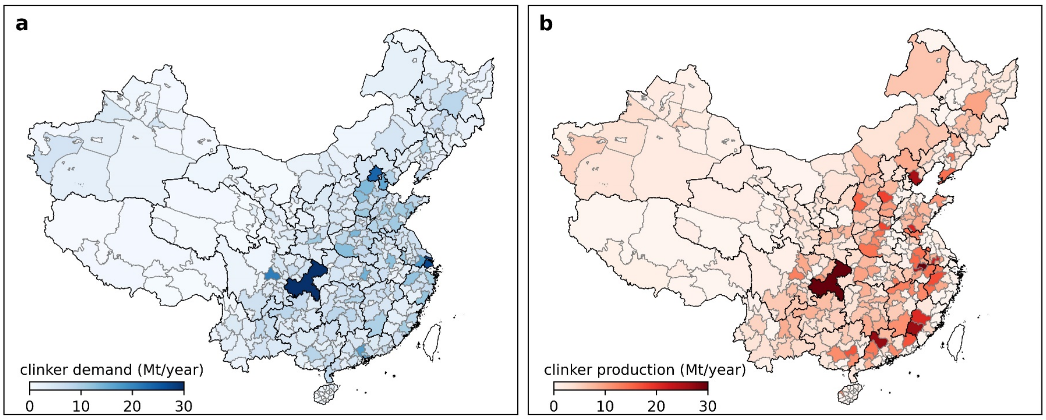

Figure 7-9 | City-level clinker demand (a) and production (b) in 2022.

Figure 7-10 illustrates the projected city-level clinker demand and production for the year 2050, across the three selected scenarios. Apparently, all the clinker demand and production decrease significantly compared to that of 2022.

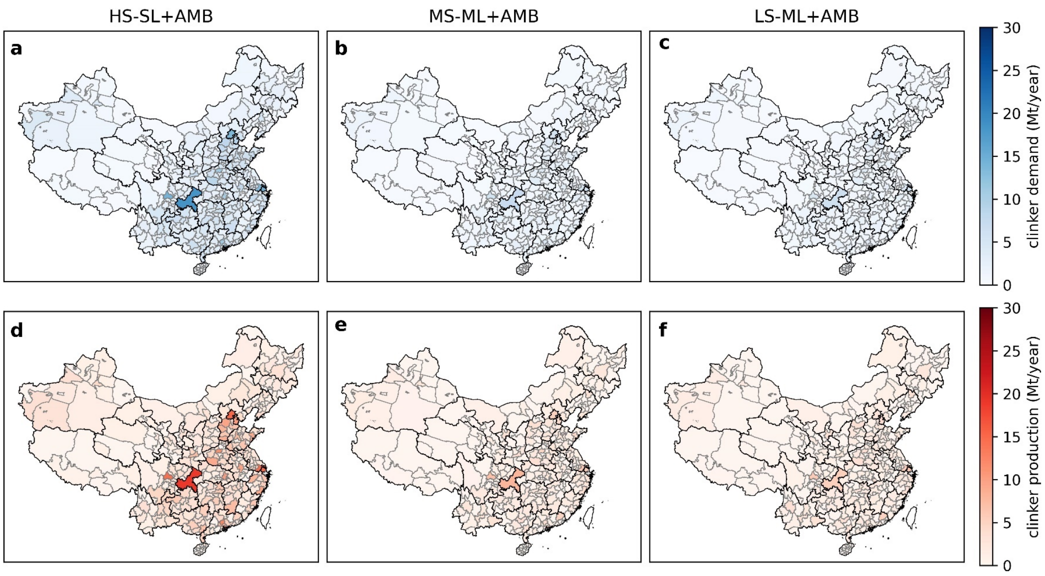

Figure 7-10 | City-level clinker demand and production in 2050 of HS-SL+AMB, MS-ML+AMB, and LS-ML+AMB scenarios.

Besides, three cities (Chongqing, Tangshan, and Qingyuan) with large clinker production capacity are selected for further demonstration (Figure 7-11). For instance, Chongqing has the largest clinker production capacity in China, whereas the current capacity will gradually retire during 2040 and 2050. Only about half of the capacity will be used for clinker production in the future two decades, and even less will be used in the other two scenarios (Figure 7-11d and g). Notably, the new capacity developed after 2040 almost depends on the local demand. In contrast, Tangshan and Qingyuan can fully utilized their clinker capacity in the HS-SL+AMB scenario, mainly due to the strong demand from their surrounding cities. Also, the re-development of new capacity will sharply decrease compared to the current, as the local demand declines to a relatively low level.

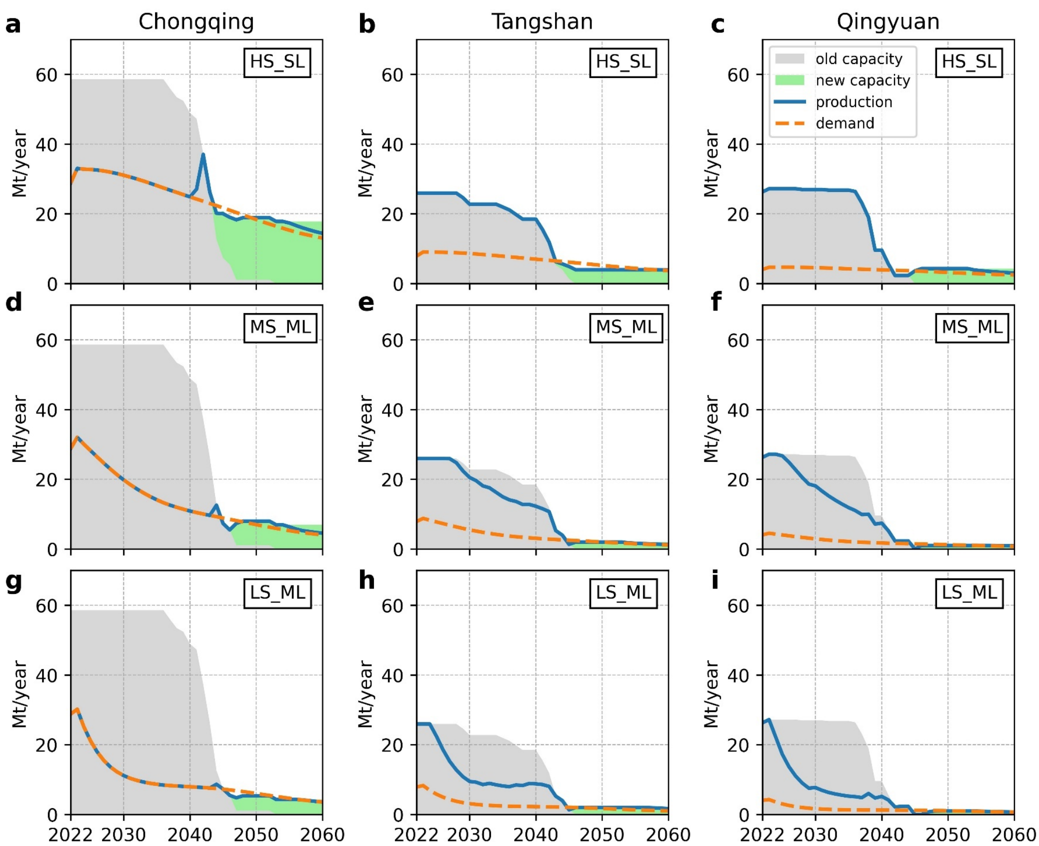

Figure 7-11 | Future clinker demand, production, and capacity of case cities in the HS-SL+AMB, MS-ML+AMB, and LS-ML+AMB scenarios.

7.3.3 Carbon storage potentials across China's cities

The carbon storage potentials of deep saline aquifers (DSA) and CO_2-enhanced oil recovery (CO_2-EOR) across China's provinces and cities are depicted in Figure 7-12 below. Cumulatively, the storage capacity of DSA and CO_2-EOR amounts to 102.0 Gt CO_2 and 9.0 Gt CO_2, respectively (Figure 7-12c). Most provinces exhibit a DSA storage capacity exceeding 1.0 Gt CO_2 (Figure 7-12d). Among these provinces, Xinjiang stands out with the potential to sequester up to 30 Gt CO_2 via DSA, owing to the presence of several large basins, such as the Tarim Basin and Junggar Basin. Geographically, the storage potentials of CO_2-EOR are primarily concentrated in the Songliao Basin in Northeast China, the Tarim Basin in Northwest China, and the Bohai Bay Basin in North China, due to the abundance of oil reserves in these regions. Consequently, provinces such as Heilongjiang, Shandong, Xinjiang, Liaoning, and Hebei boast significant storage capacities of 3.2, 1.5, 1.3, 0.9, and 0.7 Gt CO_2, respectively, accounting for the majority of the storage potentials (Figure 7-12e).

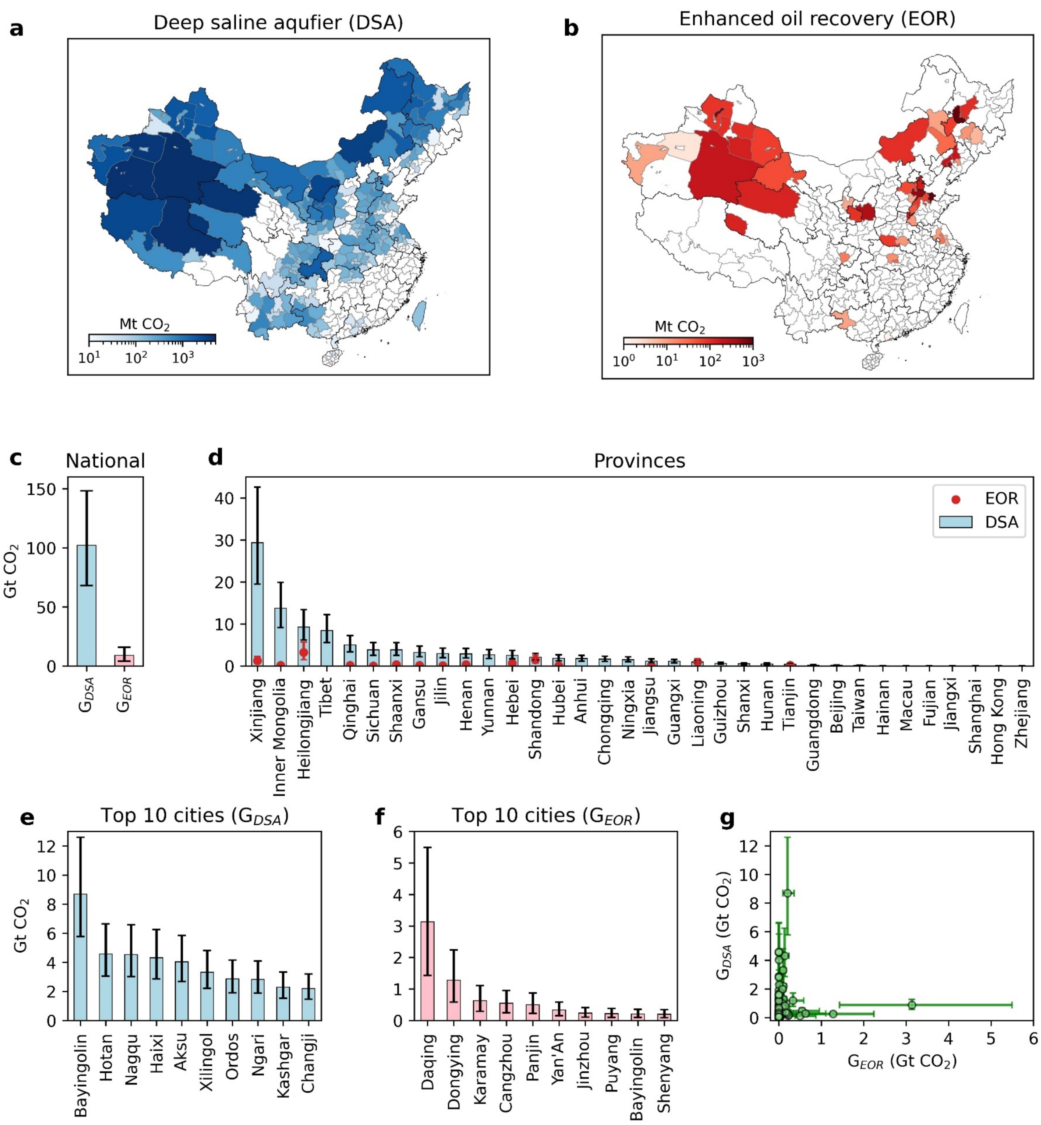

Figure 7-12 | Carbon storage potentials of deep saline aquifer (DSA) and CO_2-enhanced oil recovery (CO_2-EOR) across cities in China. (Notes: The error bar shows the 95% confidence interval of estimated storage capacity.)

From a more granular spatial perspective, focusing on city-level analysis allows for the identification of storage capacity hotspots with greater accuracy. Across China, 232 cities exhibit a storage capacity for DSA, while 47 cities possess a capacity for CO_2-EOR. Figure 7-12f and g highlight the top ten cities with significant storage capacity for DSA and EOR, respectively. Predominantly, the cities with the largest DSA capacities are situated in Xinjiang, whereas those with substantial EOR capacities are distributed across various provinces such as Heilongjiang, Shandong, and Xinjiang. Bayingolin and Daqing emerge as the cities with the most extensive storage capacities for DSA (8.7 Gt CO_2) and EOR

(3.1 Gt CO_2), respectively. Additionally, there is minimal overlap between cities with large DSA and EOR storage capacities (Figure 7-12h).

7.3.4 Prioritized cities for CCS deployment

The city-level carbon emissions-storage matching integrates the cumulative emissions derived from clinker production matched with future demand and carbon storage potentials estimated above. As shown in Figure 7-13, the initially captured and storable emissions within the cities amount to 15.7 Gt CO_2 in the HS-SL+AMB scenario. This amount exceeds the emissions gap when considering carbonation uptake but only accounts for 66% of the emissions gap when excluding carbonation uptake. The storable captured carbon emissions grow with the increase in the maximum transportation distance. When the maximum transportation increases to 400 km, total storable captured emissions approach to about 24.9 Gt CO_2, covering the scenario emissions gap. Thus, the maximum transportation distance is set to 400 km here for emissions-storage matching in the HS-SL+AMB scenario.

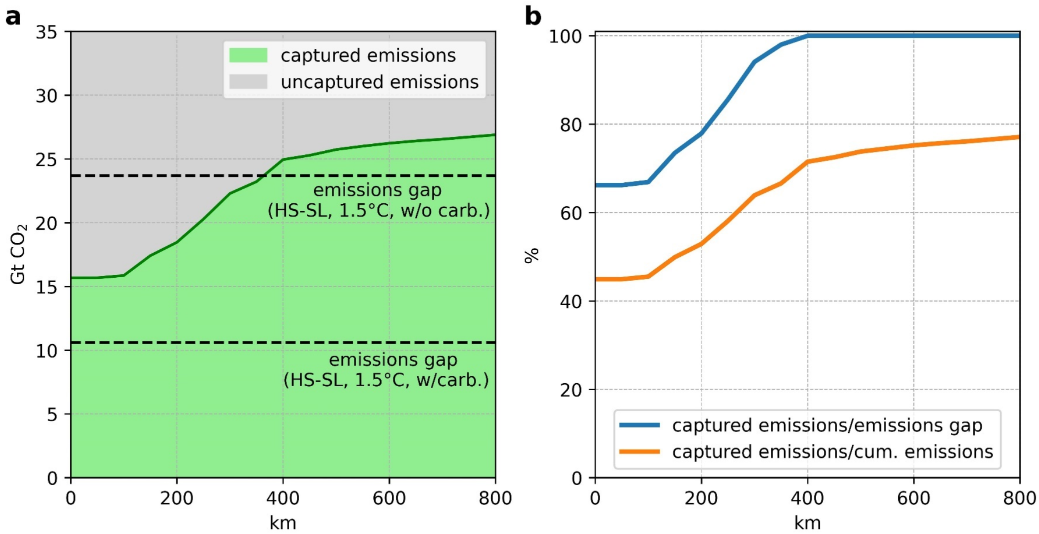

Figure 7-13 | Captured emissions and gap vary with maximum transportation distance.

The matching results of all cities across three scenarios are displayed in Figure 7-14 below. A few cities can be identified as priorities for CCS deployment, primarily due to their substantial clinker production and significant carbon storage potentials, e.g., Chongqing, Tangshan, Chengdu, and Shijiazhuang. Specifically, Chongqing can totally store 917 Mt CO_2 emissions, among which 717 Mt captured from its own clinker production and 200 Mt transported from other cities. Notably, up to 100 cities need to cumulatively capture at least 100 Mt of carbon emissions from their clinker production (Figure 7-14a) to bridge the gap between carbon emission after deploying ambitious supply-side measures and the stringent 1.5°C budget, excluding offsets by carbonation. However, some cities, such as Longyan and Qingyuan, are considered lower priorities for CCS deployment due to their distance from accessible storage sites. In contrast, self-storing captured emissions within the cities alone (without transporting and storing emissions from other cities) can reduce cumulative emissions by 9.6 Gt and 7.4 Gt CO_2 in the MS-ML+AMB and LS-ML+AMB scenarios, respectively (Figure 7-14b and c). This implies that the emissions gaps of 8.4 Gt and 3.1 Gt CO_2 are already bridged.

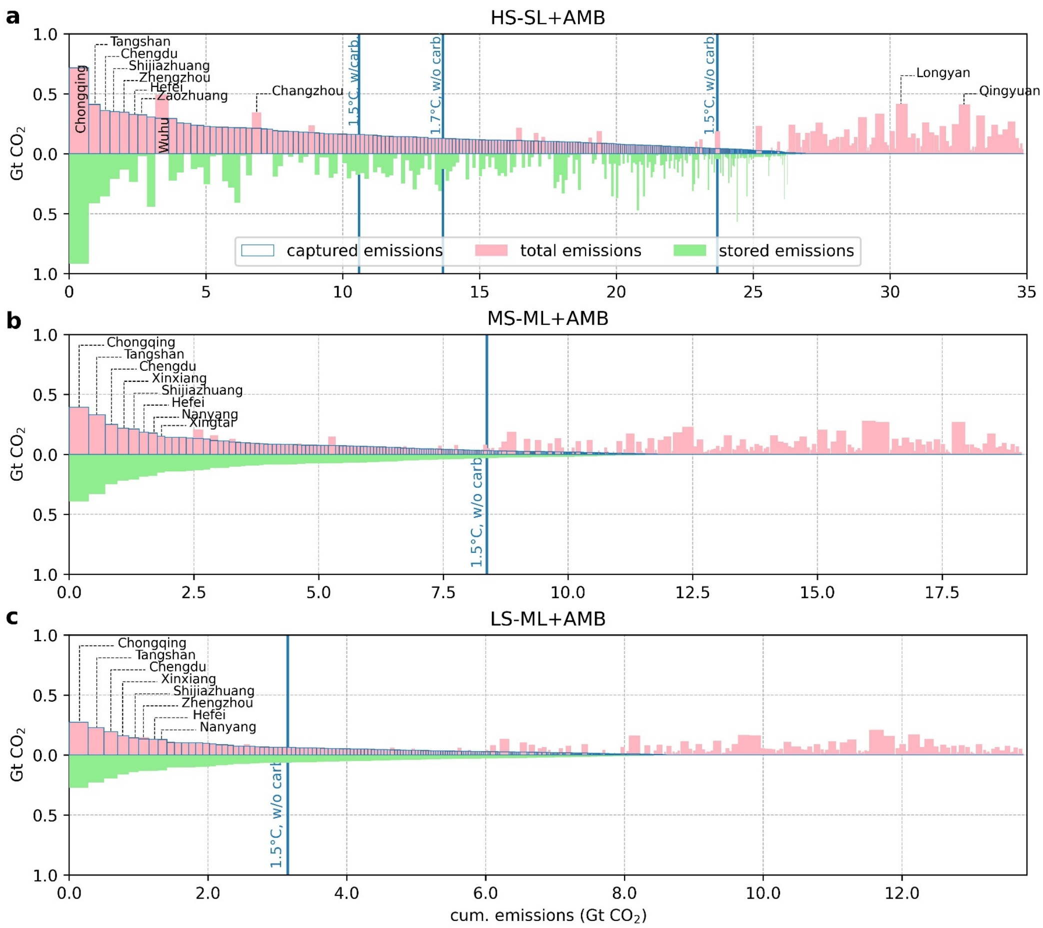

Figure 7-14 | Emissions-storage matching results for HS-SL+AMB, MS-ML+AMB, and LS-ML+AMB scenarios.

The spatial layouts of cumulative carbon emissions, captured and stored emissions, and remaining emissions further illustrate the above matching results (Figure

7-15). Notably, these layouts reveal that cities with high emissions but located far from accessible storage sites are primarily concentrated in the southeast coastal provinces, such as Fujian and Guangdong (Figure 7-15c, f, and i).

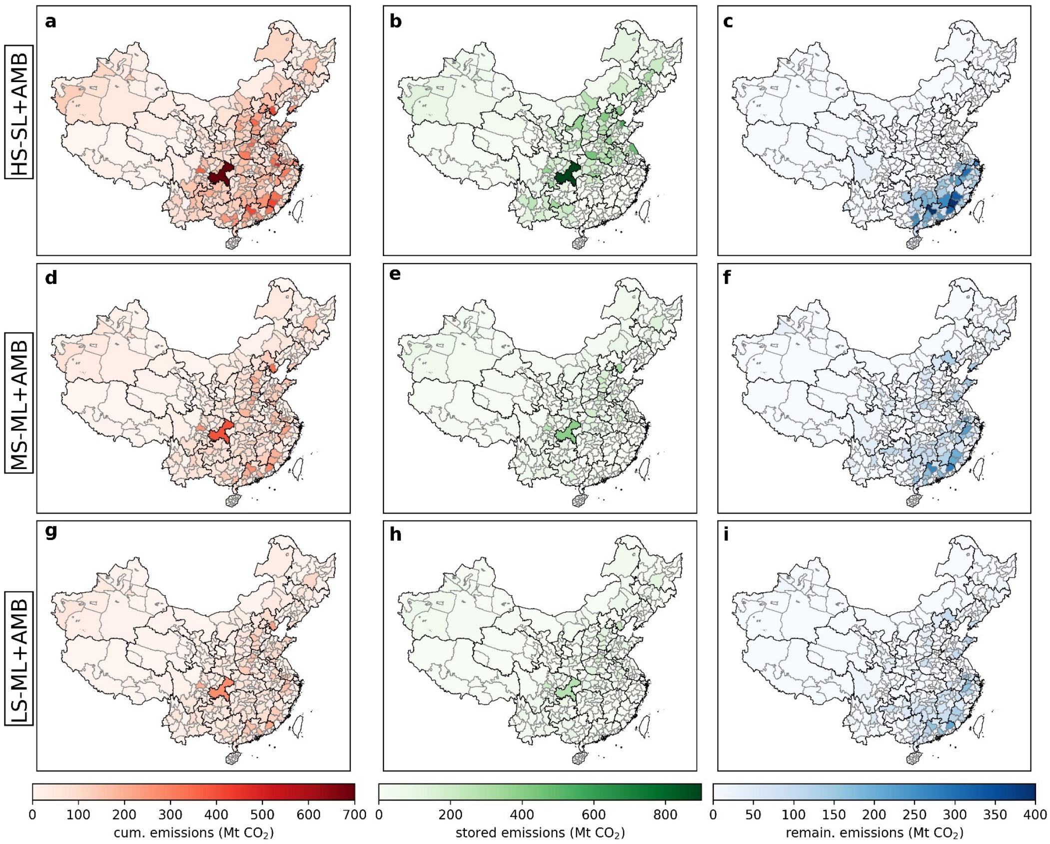

Figure 7-15 | Spatial layout of cumulative carbon emissions (a), stored emissions (b), and remaining emissions (c) for China's cities.

7.3.5 Discussion

As revealed in Chapter 4, most of carbon emissions from cement production originate from clinker production. Consequently, regions with higher clinker production should be the primary focus for emission reduction efforts, including the deployment of CCS for a net-zero transition. However, previous studies have rarely planned decarbonization roadmaps in a spatially explicit manner. This chapter addresses this gap by simulating future clinker demand and production at the city level across three representative scenarios developed in Chapter 8. Cumulative production emissions are then matched with available storage sites to identify cities with high priority for CCS deployment. The results are clear: cities with substantial clinker production and significant carbon storage capacity should be prioritized for CCS deployment in the coming decades. Conversely, cities located far from storage sites may not be suitable for large-scale deployment, mainly due to potential high transportation costs. Policy recommendations can be formulated accordingly. For instance, the central government should consider developing industrial policies aimed at the gradual retirement of production capacity in low-priority cities. This capacity could then be transferred to high-priority cities, which would better prepare for the future large-scale deployment of CCS. Additionally, such a strategy would help reduce the transportation costs associated with future carbon storage. By concentrating production capacity and CCS deployment in strategically advantageous locations, the efficiency and effectiveness of the overall decarbonization efforts can be significantly enhanced.

There are several limitations in this chapter. First, city population is used as the sole proxy to allocate national demand to cities, implying an assumption that all cities have the same per-capita demand. This assumption could be refined with the integration of more detailed city-level data, such as per-capita GDP and urbanization rates, to derive more accurate per-capita demand for cities. Second, there is a high uncertainty interval in estimating the carbon storage potentials of deep saline aquifers due to several parameters with large uncertainties. Third, the analysis considers only highway driving distance as a proxy for city distances. Although road transport currently accounts for the majority of cement and clinker transportation, the increasing share of railway and waterborne transport introduces potential bias into the results. Furthermore, instead of using Delaunay triangulation to link all emission sources and sinks as suggested by Tang et al. (2023), highway driving distance is employed as a distance proxy in emissions-storage matching. This approach not only assumes that part of emissions will be transported by road but also implicitly suggests that CO_2 transportation pipelines will be constructed along existing highways to overcome terrain obstacles.

7.4 Chapter summary

This chapter conducts a spatial supply-demand and emissions-storage matching analysis for CCS deployment across China's cities, providing spatially explicit insights into the feasibility and optimization of CCS in the cement sector. After allocating future national clinker demand to individual cities and simulating plant turnover, this chapter simulates future production emissions distributions by matching city-level clinker demand and supply. The emissions distributions are further matched with estimated local carbon storage potentials to identify strategic locations for large-scale CCS deployments. Overall, the results underscore the need for detailed spatial planning in CCS implementation to enhance efficiency, reduce transportation costs, and ensure that storage capacities are effectively utilized.

Chapter 8. Discussion

8.1 Introduction

Although the results and analysis of the material-emissions-uptake (MEU) framework have been presented separately in Chapters 4, 5, 6, and 7, a comprehensive review and discussion of the integrated framework and the insights gained from the case study are necessary. This chapter aims to provide an in-depth discussion of the framework and integrate the various empirical findings from case study in previous chapters, while trying to conduct validations on the results of case study.

8.2 Advancement of MEU framework

As reviewed in the Literature Review chapter, traditional decarbonization roadmaps often focus narrowly on decarbonization strategies within an industrial sector, particularly within the boundaries of a cement plant. While some roadmaps incorporate simplified demand scenarios, they rarely consider the future role of consumed materials. This study aims to broaden the scope to include more life cycle stages of cement materials, exploring a wider range of strategies and measures. Therefore, this study integrates and leverages the knowledge of material flows and stocks from industrial ecology to develop the material-emissions-uptake (MEU) framework. The core DMFA module in the framework provides a robust understanding of how substantial consumed cement materials accumulate in and support our society, addressing the crucial question of future cement needs. Unlike simplified projections based on per-capita material consumption, which can show significant regional discrepancies and trends (Van Ruijven et al., 2016), this approach considers the system "inertia" and acknowledges the historical consumption of bulk materials like cement and steel as the biophysical basis for our society (Pauliuk & Hertwich, 2015). Another key feature of this framework is the enhanced integration of supply- and demand-side dynamics. Supply-side mitigation efforts are determined within robust demand boundaries, relating to specific amounts of cumulative consumption (termed "in-use" stock). This in-use stock is further linked to levels of infrastructure service (e.g., Figure 4-8) and human well-being (e.g., Figure 8-2), ensuring a comprehensive and concrete foundation for future projections.

Decarbonization efforts are not limited to the supply-side. The DMFA module of the MEU framework can also reveal the mitigation potentials of material efficiency improvements on the demand-side. The underlying logic is simple: "use less, produce less, and emit less". By understanding and leveraging material efficiency strategies, substantial reductions in future demand and emissions can be achieved. For instance, this study demonstrates that extending the service life of China's in-use cement stock can cut down future cement demand by ~28 Gt. Such reductions highlight the importance of rethinking management practices in the built environment to tap into these mitigation potentials from the demand-side. This holistic approach not only optimizes material use but also aligns with broader sustainability goals, ensuring a more efficient and environmentally friendly utilization of resources.

Another critical part of MEU framework is the module of carbon uptake quantification. This module is developed and integrated under the motivation that the significant carbon sink of cement materials should not be eliminated out from decarbonization roadmaps. Besides emitting carbon dioxide, cement materials will gradually absorb atmospheric carbon dioxide through carbonation reactions throughout its life cycle. This dual role has been vividly termed as a "sponge effect" across the life cycle of cement materials, which should be carefully considered when planning for decarbonization pathways (Cao et al., 2020). It is revealed that substantial atmospheric carbon dioxide has been slowly re-absorbed around the world since 1930s (Guo et al., 2021; Huang et al., 2023, 2023; Xi et al., 2016). Whilst this potential significant carbon sink gradually gains attention (such as being compiled in Global Carbon Budget), it is still not formally accounted for in national inventories under the Paris Agreement. It this situation persists, the residual carbon emissions will need to be reduced in other ways, and in turn result in a substantial difference in the design of strategies and investments (Watari et al., 2022). Against this situation, the MEU framework designs climate-consistent decarbonization roadmaps based on comprehensive understandings of CO_2 fluxes across cement life cycle, both with and without the benefits from carbonation uptake, to be harmonized with current and future target practices.

Another critical component of the MEU framework is the module for carbon uptake quantification. This module is developed with the understanding that the significant carbon sink potential of cement materials should be included in decarbonization roadmaps. Cement materials, while emitting carbon dioxide during production, also gradually absorb atmospheric carbon dioxide through carbonation reactions throughout their life cycle. This dual role, referred to as the “sponge effect”, should be carefully considered when planning decarbonization pathways (Cao et al., 2020). Previous studies have revealed that substantial amounts of atmospheric carbon dioxide have been re-absorbed by cement materials globally since the 1930s (Guo et al., 2021; Huang et al., 2023, 2023; Xi et al., 2016). Although this significant carbon sink is gaining attention (as included in the Global Carbon Budget), it is still not formally accounted for in national inventories under the Paris Agreement. If this oversight continues, residual carbon emissions will need to be reduced through other means, leading to substantial differences in strategy design and investment (Watari et al., 2022). Against this situation, the MEU framework designs climate-consistent decarbonization roadmaps based on comprehensive understandings of CO_2 fluxes across the cement life cycle, both with and without the benefits from carbonation uptake, to be harmonized with current and future target practices.

8.3 Implications from the case of China

As shown in Figure 8-1, integrated decarbonization roadmaps are developed for China’s cement sector, by the MEU framework within the specific demand-side, supply-side, climate target, and geographical contexts. Overall, these roadmaps are enriched by four types of elements. Specifically, they incorporate a detailed understanding of future material stock dynamics (i.e., in-use cement stock, inflows, and outflows) on the demand-side, a specific emissions pathway delineated by reductions by supply-side measures and carbon uptake, CCS development within clinker production capacity, and prioritized cities for future large-scale deployments. The framework’s integration of diverse demand- and supply-side factors within the MEU nexus offers significant advantages, such as a more holistic understanding of emissions reduction potentials, identification of optimal CCS deployment strategies, and enhanced policy guidance for achieving climate targets. These roadmaps contribute to a sustainable and low-carbon future for China's cement industry, aligning with global climate goals. Furthermore, additional implications are summarized in the following sub-sections.

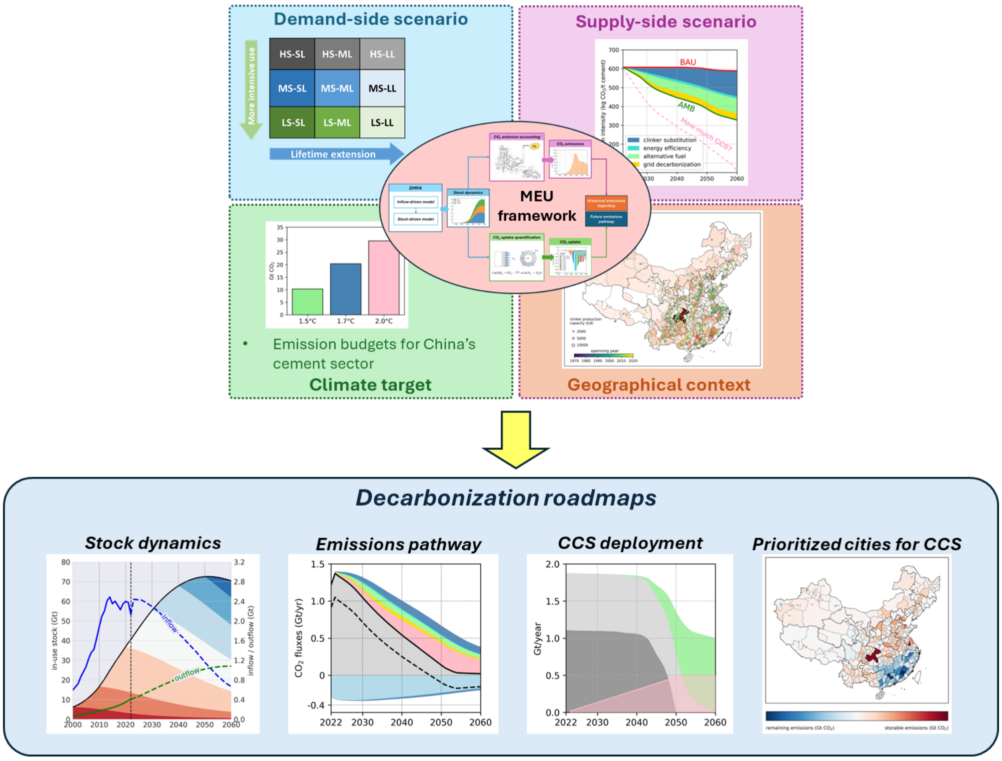

Figure 8-1 | Integrated decarbonization roadmaps for China's cement sector, developed by the MEU framework.

8.3.1 Implications of a lower per-capita cement stock

As shown in Chapter 5, a lower per capita cement stock, achieved through more intensive use, has the potential to significantly reduce future cement demand and CO_2 emissions. However, it should be noted that this reduction primarily implies a lower per capita service level rather than a decrease in cement intensity of end-use products, which cannot be easily achieved through dematerialization as seen in the past upgrades of smartphones. This raises important social implications, as essential services would need to be provided with significantly lower levels of material stocks. Several measures can be taken in the building sectors to limit per-capita floor area, including smaller dwellings, more shared spaces, increased multi-family housing (Berrill et al., 2022; Creutzig et al., 2021; Hertwich et al., 2019), while a more compact city, characterized by higher urban density, can lead to reduced infrastructure requirements per individual by more efficient transportation networks and mixed land use (D. B. Muller et al., 2013). However, it remains uncertain whether these strategies can lead to the levels outlined in Low Energy Demand (LED) scenarios (Fishman et al., 2021; Grubler et al., 2018). In the United States, there is potential to reduce per-capita residential floor space by 15% from 69.2 m^2/cap to 58.9 m^2/cap by 2060 through a combination of reducing the size of new single-family houses and increasing the proportion of multi-family houses (Berrill & Hertwich, 2021). In comparison, China appears to utilize floor space more efficiently, with its average residential area reaching a lower level of approximately 41 m^2/cap by 2020. Efficiency in the use of floor space also varies between urban and rural areas in China. Affordability issues in high-priced urban areas may limit per capita floor space, while rural areas have the potential for residents to economically build multi-story houses on their own parcels. Additionally, rural-to-urban migration leads to vacant houses for a significant portion of the year, resulting in wasted floor space.

A transition towards lower stock necessitates behavioral and lifestyle changes, along with considerations of architectural design preferences. The underlying challenge lies in achieving a reduced stock without compromising societal development and quality of life. In China, the current per capita cement stock surpasses that of many countries due to its historical reliance on cement-intensive building and infrastructure construction (Figure 8-2a). We have found a significant association between China's Human Development Index (HDI) and its per capita cement stock from 1990 to 2021 (Figure 8-2b). Extrapolating the trend reveals that while all stock scenarios would result in a higher HDI than the present, a lower per capita stock may constrain future HDI growth unless China successfully decouples its development from cement stock. Furthermore, well-being concerns should be carefully addressed, as it appears that limiting shelter services based on 'sufficiency' considerations may contribute little to overall well-being, whereas other demand-side solutions align with high levels of well-being (Creutzig et al., 2021).

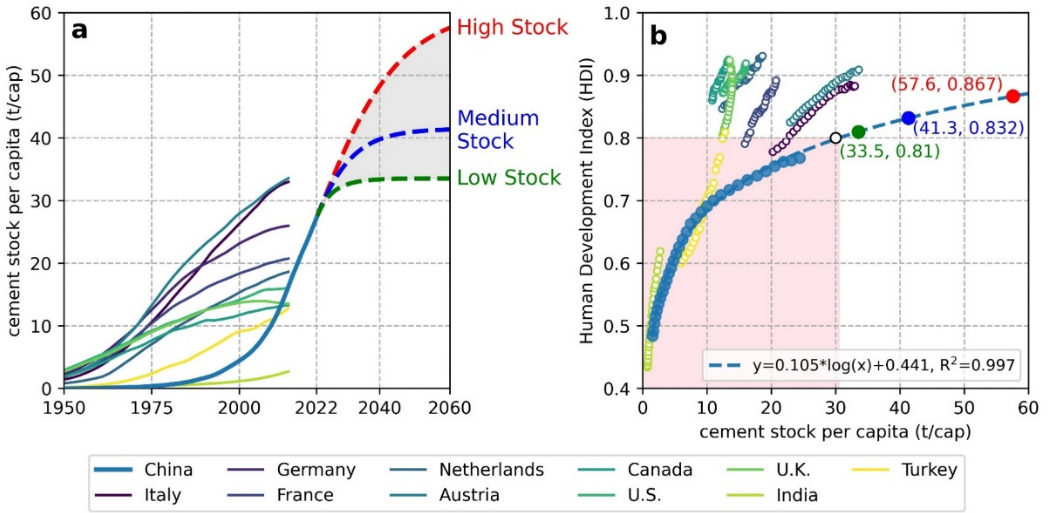

Figure 8-2 | Comparison of China's future per-capita cement stock scenarios with other countries (a), and the relationship between per-capita stock and Human Development Index (HDI) (b). Adapted from Wu et al. (2023).

(Note: The colors of the circles in (b) are the same as those of the lines in (a). The data for high-income countries are obtained from Cao et al. (2017). HDI data are collected from Home | Human Development Reports (undp.org).)

8.3.2 Opportunities and challenges of service-life extension

Both field investigations and macro-level analyses consistently confirm a significantly shorter building lifespan in China compared to the designed service-life of 50 years (W. Cai et al., 2015; Cao et al., 2019; G. Liu et al., 2014). Empirical studies have shown that premature demolitions in China are primarily attributed to external factors rather than internal degradation of building materials (G. Liu et al., 2014; O'Connor, 2004). This phenomenon of "short-lived" buildings in China ultimately reflects a premature "obsolescence" resulting from rapid urbanization over the past two decades (Thomsen & van der Flier, 2011). The discrepancy between rising expectations driven by increasing land values and the actual function and quality of buildings has led to premature demolitions. However, it is worth noting that this pattern may differ in cases where buildings are situated on valueless land, where out-of-service buildings tend to persist without undergoing demolition (Thomsen & van der Flier, 2011).

There have been some improvements observed, as the average building lifespan in China has increased by approximately 0.5 years between 2000 and 2015 (Cao et al., 2019). This extension may be indirectly validated by structural changes in China's building stocks. Over the past two decades, new buildings have become taller and more concrete-intensive than before (Figure 8-3a and Figure 8-3b), suggesting potentially longer service-life due to limitations imposed by China's property rights system. Specifically, high-rise and high-density residential districts, accommodating hundreds to thousands of households in a small piece of land, present daunting challenges for demolition and redevelopment when multiple property rights are involved. In mainland China, most building stocks are within 30 years old, with over 60% constructed during the period from 2000 to 2020. In contrast, the proportion of such buildings is relatively low in Hong Kong Special Administrative Region (Figure 8-3d). Hong Kong experienced a construction boom between the 1960s and 1980s, similar to industrialized countries in the post-war era, and buildings from that period are still in service today (Figure 8-3c). Additionally, many high-rise buildings in Hong Kong have survived for decades (Figure 8-3e), potentially supporting the argument that high-rise buildings tend to have longer service-life due to the challenges associated with redevelopment. Therefore, the average building lifespan is expected to increase overall, but the extent of this increase may depend on various practical factors.

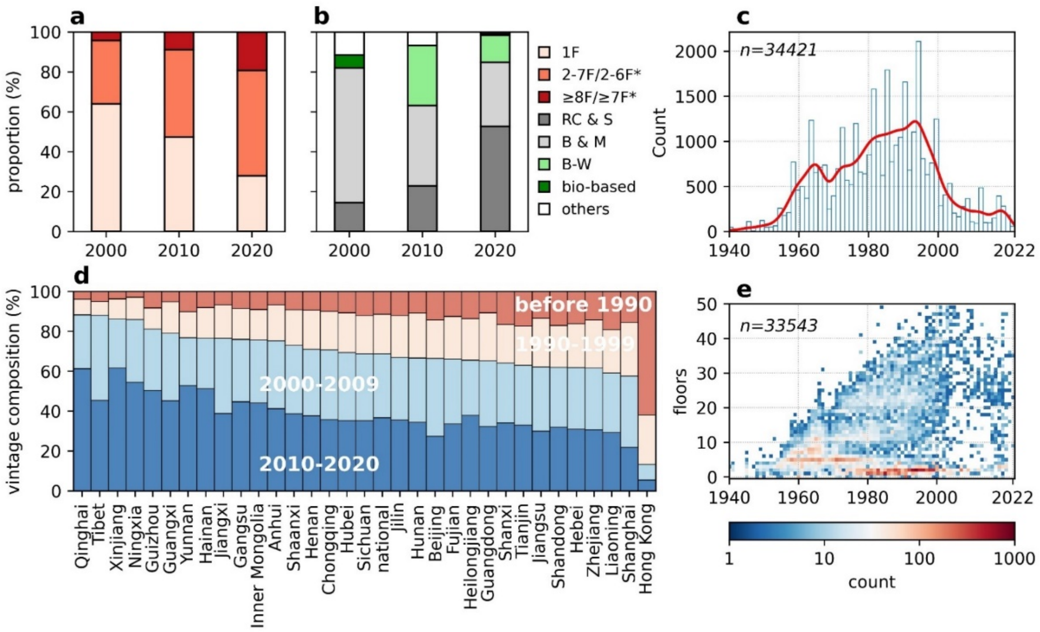

Figure 8-3 | Current composition of China's building stocks. (a) Residential building stock composition by building floor. (b) Residential building stock composition by building material. (c) Year built of private buildings in Hong Kong Special Administrative Region. (d)

Vintage composition of residential buildings by province as well as HKSAR. (e) Building floors versus year built in HKSAR (Wu, Ng, Chen, et al., 2023).

Notes: In (a), "2-6F" and "≥7F" are for 2000 and 2010, whereas "2-7F" and "≥8F" are for 2000 and 2010. RC refers to reinforced concrete structure, S refers to steel structures, B and M refers to brick and masonry structures, B-W denotes brick-wood structures, and bio-based mainly refers to structures constructed by bio-based materials. Source: Data for China's provinces are retrieved from (the 7th National Population Census in 2020), whereas the data for Hong Kong were collected from *Database on Private Buildings in Hong Kong* of the Home Affairs Department of HKSAR (2023).

While it is expected that high-rise building stocks will survive for a longer time, addressing the obsolescence of remaining aged low-rise buildings poses challenges in terms of regular maintenance, proper retrofitting, and adaptive reuse, especially when redevelopment appears to be the more economically viable choice given the ongoing urbanization in China. In Hong Kong, the presence of aged buildings also raises social concerns, particularly related to safety issues. The reconstruction of these aged and dilapidated buildings, located on valuable land, is considered a more economically viable solution compared to renovation and reuse. Consequently, there is a growing emphasis on ensuring a successful redevelopment process, which may involve implementing measures such as compulsory sales of the land on which the aged buildings are situated. Furthermore, financial considerations also play a significant role. The inflow of more vulnerable residents into the aged buildings can severely hamper maintenance investments (Thomsen & van der Flier, 2011).

From a technical perspective, the extension of service-life may give rise to side-effects that need to be carefully considered in practice. Durable advanced cement-based materials typically have higher greenhouse gas (GHG) emissions during production compared to those with lower durability (Miller, 2020). When the target service-life is significantly shorter than the physical life of durable concrete mixtures, it becomes less desirable due to higher GHG emissions, leading to a waste in durability performance. Another aspect to consider is the decline in performance as cement stocks age. This decline may result in increased heating and cooling loads due to reduced thermal insulation performance, necessitating additional energy for operation (Grussing, 2014). This technological obsolescence may require future energy retrofitting. Moreover, for road infrastructure, changes in cement-based material properties due to aging, such as surface roughness, can lead to increased fuel consumption and emissions from vehicle use (Reger et al., 2014). These considerations also apply to young high-rise buildings currently in existence, as they will undergo aging and face obsolescence in the future.

8.3.3 Speeding up CCS deployments like historical NSP kilns

In Chapter 4, emissions drivers decomposition show that the most significant intra-sectoral transition was the penetration and saturation of the NSP kilns during 2000-2015, which has a proficient energy efficiency compared with the outdated shaft kilns (Figure 8-4). During the same period, a large number of outdated cement plants with shaft kilns were eliminated under the guidance of the government's relevant policies (MIIT, 2011; State Council, 2013). The step-improved national efficiency regulations of China also urged for an improvement on energy efficiency of cement kilns. However, the mitigation effect from emission intensity never dominated the emission abatement, as it just decreased the total emissions by 4.3%, 39.6%, and 1.4% during the past three decades. In contrast, material efficiency of the construction sector contributed much more abatement, i.e., -23.4%, -78.2%, and -59.4% during the same period. Further decoupling analysis reveals that the total CO_2 emissions from cement production have yet been decoupled with GDP, which means that economic growth would continue to drive the emissions in the short-term. If we aim at a carbon-neutral cement sector in the middle of this century, something should be reversed compared with the present situations. It means that the mitigation effect of EI should expand to offset the emission growth from the production scale, and even lead to much more mitigation.

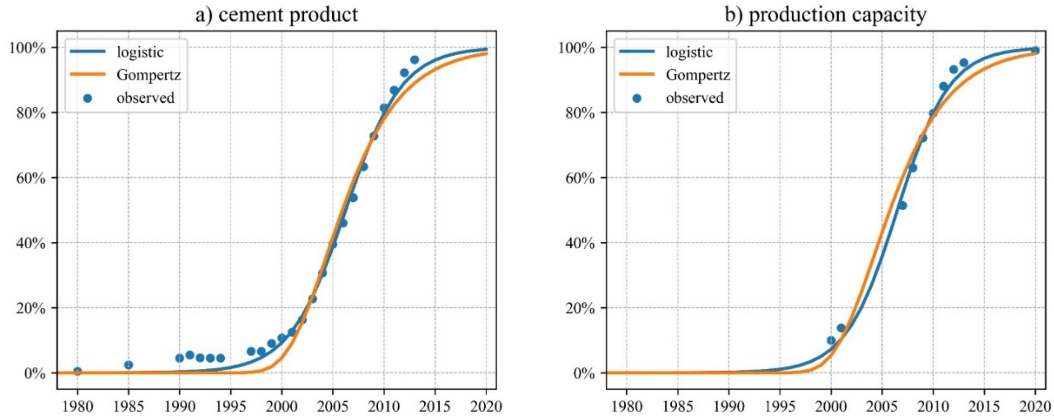

Figure 8-4 | Historical development of NSP kilns in China (Wu et al., 2022).

(Notes: The share of product produced by NSP kilns and production capacity are fitted by logistic curve and Gompertz curve, both of which are growth functions. And data were retrieved CCID.)

However, our results show that the reliance on large-scale of CCS deployment seems to be daunting when targeting with 1.5°C and without considering emissions offset, whereas it can be effectively reduced if the mitigation potentials are tapped on both sides. Another notable benefit of the low demand and AMB scenarios is an expanded time window for the preparation of CCS, which is still yet to be ready for large-scale deployment, due to the low technical readiness or vague business model, which will significantly increase the risk of project failure when the capture capacity increases (N. Wang et al., 2021). However, the window is closing, as revealed by the UNEP that current unconditional NDCs will lead to a 2.8°C and 2.6°C increase in temperature by 2100, which are far beyond the goals of the Paris Agreement (United Nations Environment Programme, 2022). The high emissions in our HS-SL scenario also echo with what the UNEP recently warns. It is urgent to cut off 45% of GHG emissions by 2030 to get on the track to limit global warming to 1.5°C. Before CCS is ready, this substantial emissions reduction for the cement sector can only be realized in our low demand scenarios, some of which are even well below the available budgets. Furthermore, the time when it is ready to capture CO_2 fully or near fully from cement plant's flus gas also matters. Historical diffusion of NSP in Chian reveals that it took over 30 years to scale up the unit production capacity from hundreds to over 10 thousand tons of clinker per day (Figure 8-5a). In contrast, the current largest capture capacity of the demonstration projects is only 50 kt of CO_2 per year (Global CCS Insitute, 2023), which is still far away from the 1 Mt CO_2 per year (for a plant which produces 5,000 t clinker per day). Whilst some end-of-pipe CCS technologies are expected to diffuse as fast as that of desulfurization (van Ewijk & McDowall, 2020), efficient calcium looping and oxyfuel combustion with low retrofitability require much more knowledge and experience accumulation, when the plant configuration will be significantly changed (Voldsund et al., 2019).

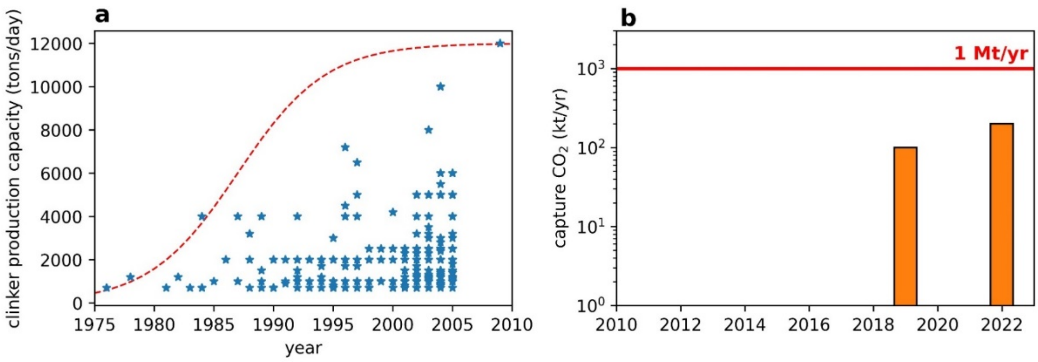

Figure 8-5 | (a) Diffusion of NSP during 1995 and 2010 and (b) current CCS demonstration projects in cement sector (Wu, Ng, & Chen, 2023).

8.3.4 Policy recommendations

Effective implementation of demand-side strategies holds significant potential for reducing future demand and greenhouse gas (GHG) emissions through the efficient utilization of material stocks. In this regard, governments play a crucial role in directing the attention towards demand-side measures. Encouraging a more compact layout of buildings, which can be specified in industry guidance or building codes, is a key approach to maximizing the efficient use of building floor area. The current shift in architectural design within the real estate market aligns with this objective, as new apartments are being designed to accommodate more rooms without a substantial increase in total floor area. This trend enables the accommodation of larger families while maintaining housing affordability. Additionally, it is pertinent to initiate a discourse on the concept of "sufficiency" in terms of per-capita building floor area (Cohen, 2020), particularly in light of climate ambitions.

Urban planners also play a vital role in extending the lifespan of buildings and mitigating premature demolitions. They should consider developing new or revising existing building zone requirements that facilitate mixed uses and repurposing of existing structures, thereby extending their longevity (Zhong et al., 2021). Where feasible, urban sprawl with a premise of minimizing adverse impacts on cropland and forest areas, could be prioritized over frequent urban sprawl, which often leads to premature demolition. It is essential to note that ensuring safety is a fundamental requirement for the prolonged utilization of buildings and infrastructure. To achieve this, mainland China should establish a robust legal and regulatory system that includes regular inspections of aged building structures and components. Valuable insights can be gained from Hong Kong's implementation of the Mandatory Inspection on Building and Mandatory Inspection on Windows regulations.

Furthermore, the cement industry faces challenges in promoting efficient material use due to its profit model, which is inherently linked to the volume of materials sold (Watari et al., 2022). Thus, incentives and subsidies may be necessary to encourage the industry to adopt more sustainable practices. Moreover, the issue of over-capacity in China's cement sector may be further exacerbated by a decline in cement demand. Underutilized capacity poses a significant risk to newly constructed and costly cement kilns, as annual cement demand is projected to remain below two billion tons based on the scenarios analysis in this study (Lu et al., 2022).

8.4 Validation on the case results

To ensure the robustness and reliability of research findings, I try to validate the estimated historical carbon emissions and projected future cement demand against results from previous studies, both of which are key outputs from the MEU framework and can significantly impact decarbonization pathways. This comparative analysis will help highlight the consistency and discrepancies between our estimates and those in the existing literature, thereby strengthening the credibility of our integrated modeling framework.

This study compared the estimated historical CO_2 emissions from China's cement sector, including process and fuel emissions, with several previous studies (Figure 8-6). As shown in Figure 8-6a, this study's estimates of total emissions are highly consistent with most previous studies, except for those by Zhang et al. (2015) and

Shan et al. (2019). The estimates of process emissions from different studies exhibit a highly consistent trend (Figure 8-6b) because they adopted similar production activity data and emission intensities. Therefore, the variations among different estimations can be mainly attributed to the estimates of fuel emissions (Figure 8-6c). These high variations result from the uncertainty in energy consumption data, as the amount of coal used for heating the cement kilns was not directly available in the official statistics but rather estimated by different reported coal intensity (J. Liu et al., 2021). This study's results also performed well compared to official estimates in National Communication Reports submitted to UNFCCC in specific years (NDRC, 2004, 2012). Total emissions differed from the corresponding estimates from NCR by 3.8% in 2005, while process emissions differed by -8.0% and -7.8% in 1994 and 2005, respectively. Overall, these comparisons demonstrate the robustness and reliability of the emission accounting module employed in the MEU framework.

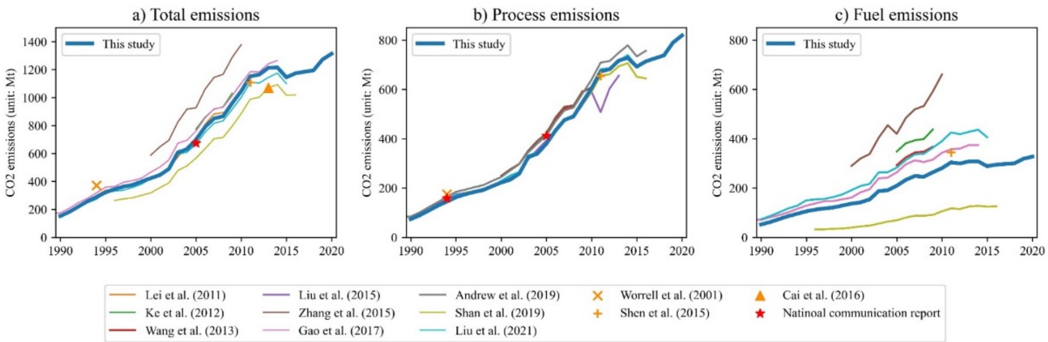

Figure 8-6 | Comparison of total CO_2 emissions (a), process emissions, and fuel emissions (c) of China's cement sector with previous studies and official reports (Wu et al., 2022).

(Note: Continuous annual emissions accounting results from Lei et al. (2011), Ke et al. (2012), Wang et al. (2013), Liu et al. (2015), Zhang et al. (2015), Gao et al. (2017), Andrew (2019), Shan et al. (2019), and Liu et al. (2021), are collected for comparison. Some results in specific years, i.e., Worrell et al. (2001), Shen et al. (2015), and Cai et al. (2016), were also retrieved for comparison. Moreover, emissions accounting from official department are included in this comparison, i.e., two national communication reports submitted to UNFCCC (NDRC, 2004, 2012).)

Furthermore, this study compares nine cement demand scenarios against various projections from previous literature published in the recent decade (Figure 8-7). Specifically, the scatter plots represent projections from previous studies, which usually rely on regression on per-capita consumption with socio-economic factors, such as urbanization rate and GDP. Both baseline scenarios (e.g., BAU scenario) and mitigation scenarios (e.g., low carbon or low demand scenarios) are extracted from literature for comparison here to justify the upper and lower bound of our results. Consequently, previous projections outlined a possible wide range of future cement demand (i.e., green shaded area in Figure 8-7). The highest scenario HS-SL in this study is still slightly lower that Tan et al., (2022)'s projection towards 2060. Conversely, the lowest scenario LS-LL will decrease sharply and keep much lower than the range outlined by literature data from 2028 onwards. Furthermore, almost all lifetime extension scenario will be lower than the literature range between 2030 and 2060. This implies that while part of scenarios lies in the literature range to justify its reasonability, part of scenarios breakthrough the range to explore a larger reduction potential. This implies that while part of the scenarios lies within the literature range, justifying their reasonability, other scenarios breaking through the range can explore opportunities for greater reduction potential.

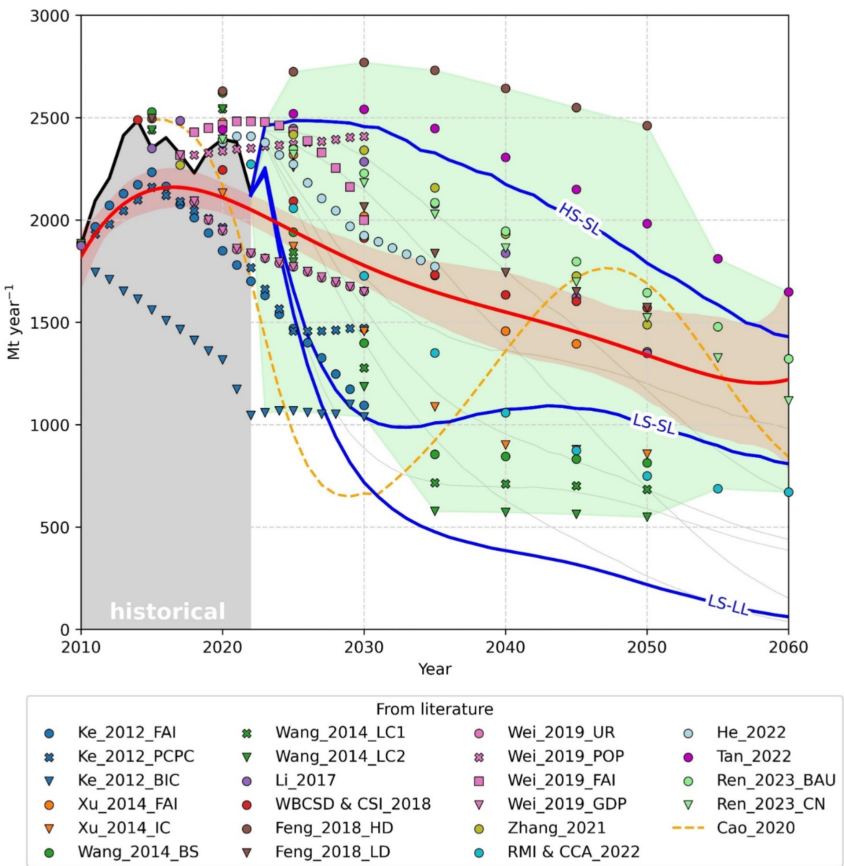

Figure 8-7 | Comparison of cement demand projection with previous studies.

Data source: (Cao et al., 2020; X.-Z. Feng et al., 2018; He et al., 2022; International Energy Agency & Cement Sustainability Initiative of the World Business Council for Sustainable Development, 2018; Ke et al., 2012; N. Li et al., 2017; Ren et al., 2023; Rockey Mountain Institute & China Cement Association, 2022; Tan et al., 2022; Y. Wang et al., 2014; J. Wei et al., 2019; Xu et al., 2014; C.-Y. Zhang et al., 2021).

Another similar work conducted by DMFA is also included for comparison and analysis (Cao et al., 2020). Notably, Cao et al. (2020)'s projection (the orange dashed line in Figure 8-7) stands out by illustrating a fluctuating trend rather than a straightforward downward or stable trajectory. This fluctuation captures the internal dynamics of in-use cement stock. For instance, a significant increase during 2040-2060 can be attributed to a massive supplement to those outflowed stock when reached the end of their service lifetime. Their trend is somewhat similar to the LS-SL scenario, which shows only minor growth during the same periods. Overall, these alignments underscore the robustness and consistency of the results in this study, while providing a more nuanced understanding of future demand to our society, compared to the extrapolations by regressions.

8.5 Chapter summary

This chapter provides a comprehensive and in-depth discussion on the research outcomes from previous chapters. First, it summarizes the advancements of the MEU framework by comparing them with previous studies. Then, it integrates the results from the case of China's cement sector to discuss the implications of its integrated decarbonization pathways developed by the MEU framework, considering both demand- and supply-side perspectives. Additionally, the chapter validates the case study results through comparisons with previous research, ensuring robustness and consistency of the findings.

Chapter 9. Conclusions

9.1 Introduction

This chapter will start with reviewing the achievement on the specific objectives of this research. Then, a series of the key findings of this research are summarized. The contributions of this research are also highlighted again from theoretical, methodological, and practical perspectives in this chapter, after all the work has been done. Finally, the limitations and the directions for future research are discussed.

9.2 Achievements of the objectives

Previous studies lack an integration of both supply- and demand-side to develop robust decarbonization roadmaps for cement sector within the material-emissions-uptake (MEU) nexus. Future cement demand and mitigation potentials are not systematically projected and investigated, and the potential emissions offset by carbonation reactions in cement materials are not fully integrated. Besides, these roadmaps also overlook regional discrepancies and fail to provide spatially explicit practical guidance for net-zero transition, especially for capital-intensive carbon capture and storage (CCS) technologies. In response, this study aims to develop an integrated framework to decarbonize the cement sector within the MEU nexus. And four specific research objectives are proposed to collectively achieve the aim as follows:

(1) To develop a framework than can characterize the material-emissions-uptake (MEU) nexus of cement sector.

(2) To project future dynamics of cement materials stock and explore the mitigation potentials of cement demand.

(3) To develop robust and efficient decarbonization pathways for the cement sector to be aligned with climate targets, within the MEU nexus.

(4) To improve practicability of decarbonization pathways by integrating geographical contexts.

To achieve Objective 1, Chapter 4 develops an integrated framework, which synthesizes dynamic material flow analysis, carbon emissions accounting, and emissions uptake quantification to characterize the MEU nexus of cement sector. This robust framework provides a detailed understanding of the interactions between material flows, carbon emissions, and carbon uptake throughout the cement lifecycle. China's cement sector is then adopted as a retrospective case study to rigorously test and demonstrate the framework's capabilities. This case study not only validates the framework but also establishes a solid foundation for the prospective analysis and development of decarbonization pathways in the subsequent objectives.

To achieve Objective 2, Chapter 5 systematically develops scenarios for future cement stock level and service lifetime, which can further investigate mitigation potentials from demand-side. These scenarios form a scenario matrix to delineate the boundary conditions of in-use cement stock and consumption. Through the integrated modeling framework in Chapter 4, Chapter 5 quantitatively revealed the implications of the varying cement consumption and its mitigation potentials on future carbon emissions and uptake.

To achieve Objective 3, Chapter 6 integrates supply- and demand-side dynamics to develop decarbonization pathways for the cement sector, with the MEU nexus. Besides explicit demand- and supply-side scenarios, it also develops a plant turnover model to simulate future production capacity to enhance the investigation on impacts from supply-side. Then, annual CCS deployments are optimized to develop climate-consistent pathways, i.e., to control the total carbon emissions below the emissions budgets of 1.5/1.7/2.0°C with a minimal cost. The implications of deployment scale and rate are further revealed based on these results.

To achieve Objective 4, Chapter 7 conducted a spatial supply-demand and emissions-storage matching analysis for CCS deployment across China's cities, providing spatially explicit insights into the feasibility and optimization of CCS in the cement sector. After allocating future national clinker demand to individual cities and simulating plant turnover, this chapter simulates future production emissions distributions by matching city-level clinker demand and supply. The emissions distributions are further matched with estimated local carbon storage potentials to identify strategic locations for large-scale CCS deployments.

Overall, the research aim of developing an integrated framework to decarbonize the cement sector within the material-emissions-uptake (MEU) nexus was achieved through the collective contributions of the four objectives. Objective 1 established the foundational framework, while Objectives 2 and 3 extended its applicability by incorporating projections of future demand and supply dynamics, ensuring that the framework could be applied to various decarbonization pathways. Objective 4 further enhanced the framework's practical relevance by integrating spatial considerations, enabling region-specific strategies for implementing mitigation technologies. Together, these objectives provided a cohesive and comprehensive approach that reinforced the framework, demonstrating its capacity to guide the cement sector's transition toward net-zero emissions.

9.3 Summary of Research Findings

The key findings of this research are summarized as below against each research objective.

Objective 1: *To develop a framework than can characterize the material-emissions-uptake (MEU) nexus of cement sector.*

Several empirical findings on the case study of China's cement sector are elucidated through the developed MEU framework. First, driven by the substantial cement consumption which is above 2 gigatons (Gt) per year recently, China's in-use cement stock has grown rapidly to 38.2 gigatons (Gt) by 2022, alongside annual outflows of around 415 Mt. Concurrently, the per-capita stock has increased to 27.2 tons. This estimation is based on the assumption that the apparent cement consumption of cement will flow into society, provide services until reaching its expected lifetime, and subsequently exist as outflows. Second, China's total carbon emissions from the cement sector have not yet peaked, having increased to 1,314 Mt in 2020, surpassing the previous peak of 1,216 Mt in 2014 after a sharp decline in 2015. The emission intensity of cement production significantly decreased from 709 to 486 kg CO_2 per ton cement produced during 2000-2015 with the penetration of the NSP kilns. However, it rebounded to 549 kg CO_2 per ton, mainly due to the increase in the clinker-to-cement ratio. Third, annual carbon dioxide sequestered by carbonation reactions in cement materials has increased to 315 million tons (Mt) by 2022, accounting for 23% of production emissions, leading to net emissions of around 1.0 Gt at the same time. Overall, carbonation reactions have cumulatively re-absorbed 5.6 Gt CO_2, with contributions of 3.7 Gt from mortar, 1.2 Gt from concrete, 0.6 Gt from cement kiln dust, and 0.1 Gt from construction waste. This macro-level uptake estimation should be used carefully and keep two assumptions in mind: (1) all the related cement stock and flows are characterized as simplified cubes and spheres and (2) the part from surface inwards identified by pH change is assumed to be as fully carbonated.

Objective 2: *To project future dynamics of cement materials stock and explore the mitigation potentials of cement demand.*

This research systematically develops a 3×3 scenario matrix along with two dimensions: per-capita stock and service lifetime, to explore future boundary conditions and mitigation potentials for in-use cement stock and cement demand during 2023-2060. The main assumption here is that the current in-use cement stock, especially per-capita stock, will stably grow and follow a logistic curve shaped transition to the saturation levels by 2060, while the changing lifetime will alter stock age-cohort composition and in turn mitigate annual outflows and inflows. Theoretically, the most efficient situation implies a substantial reduction of up to 33.8 Gt of CO_2, corresponding to a cumulative reduction of 58 Gt in cement consumption, by combining a significantly lower per-capita stock (33.5 t/cap by 2060) and extending the service lifetime to 70 years. Additionally, the net emissions offset by carbonation uptake could reach net-zero by 2060. However, the expected daunting challenges and profound social implications must be carefully understood and addressed, if aiming to fully tap these potentials.

Objective 3: *To develop robust and efficient decarbonization pathways for the cement sector to be aligned with climate targets, within the MEU nexus.*

By integrating supply- and demand-side dynamics, this research develops decarbonization pathways for China's cement sector to achieve 1.5/1.7/2.0°C targets, while emphasizing the role of CCS deployments. After deploying a portfolio of conventional supply-side measures, there remains a gap ranging from 0.5 to 23.7 Gt CO_2 between emissions and carbon budgets, to be addressed by CCS deployment. Specifically, it is assumed that the emission intensity of cement production will gradually decrease by the turnover process of cement plants, which implies that the older, less efficient plants will be replaced by newer, more efficient ones as they reach the end of their operational lifetime. This process will be complemented by CCS deployments. Results show that, in the most challenging circumstances, i.e., the highest demand against the 1.5°C target without carbonation offset, carbon emissions mitigation by CCS must increase rapidly to 841 Mt per year by 2040, implying an ultimate CCS capacity of 1.3 Gt clinker per year with an average annual growth rate of 75 Mt per year during the same period. Moreover, whilst most of the existing production capacity will be underutilized, required CCS deployments will be significantly reduced in scenarios with much lower future cement demand.

Objective 4: *To improve practicability of decarbonization pathways by integrating geographical contexts.*

This research simulates the future distribution of production emissions and matches them with estimated carbon storage potentials across China's cities to identify strategic locations for large-scale CCS deployments envisioned in national decarbonization roadmaps. Specifically, future national clinker demand of representative scenarios is distributed across the cities and matched with available supply capacity around to simulate production scale, based on the assumptions that (1) future regional demand is proportional to population scale and (2) clinker is transported by the highway and only within an economic acceptable radius (here 800 km). Then, cumulative carbon emissions from clinker production can be mapped across cities, with a focus on major producers such as Chongqing, Tangshan, and Qingyuan. Carbon storage potentials in sedimentary basins for deep saline aquifers (DSA) and carbon dioxide for enhanced oil recovery (CO_2-EOR) are primarily located in northeastern and northwestern cities. The largest storage potential of DSA is estimated at 8.7 Gt CO_2 in Bayingolin, while CO_2-EOR potential is 3.1 Gt CO_2 in Daqing. Through the ranking of 'storable captured emissions' across three representative decarbonization scenarios, several cities are prioritized for CCS in cement plants, including Chongqing, Tangshan, and Chengdu. Conversely, whereas cities at the bottom of the ranking, such as Longyan and Qingyuan, need alternative measures for deep decarbonization or should consider limiting and transferring their capacities.

9.4 Contributions of the Research

9.4.1 Theoretical contributions to the knowledge

This research develops an integrated modeling framework that characterizes the material-emissions-uptake nexus for the cement sector. This framework enables the synthesis of supply- and demand-side dynamics, offering a comprehensive view of their combined impacts on decarbonization pathways. Unlike previous studies which often treated supply and demand separately, this integrated approach allows for a more holistic analysis, enhancing the understanding of how various factors interact to influence emissions and carbon uptake. This framework also incorporates the evaluation of long-term material efficiency measures and their impact on reducing cement consumption, thereby contributing to a more sustainable development model for the cement sector. Furthermore, it provides insights into the potential trade-offs between near-term emissions reductions and long-term sustainability goals, supporting the development of balanced and effective decarbonization strategies.

9.4.2 Methodological improvements

This research introduces a simplified supply-demand matching model to simulate the future distribution of production emissions and match these emissions with suitable storage sites for CCS deployment planning. By avoiding the use of complex spatial optimization models like mixed-integer programming, this model reduces computation time while still delivering empirically accurate results. Additionally, this research advances methodologies for quantifying carbon uptake by carbonation reactions in cement materials, integrating these into broader emissions accounting frameworks. The inter-temporal optimization model for CCS deployment incorporates plant turnover processes, enhancing the realism and practicality of deployment strategies. This methodological innovation not only streamlines the analysis but also provides a more adaptable and user-friendly tool for policymakers and industry stakeholders to plan and implement effective decarbonization strategies.

9.4.3 Practical implications

This research provides spatial-temporal insights into CCS deployments in the cement sector for policymakers and industry investors. Cities with large clinker production and nearby carbon storage capacity can be prioritized for retrofitting or developing CCS capacity, reducing both pipeline construction and transportation costs. Policymakers are advised to promote capacity deployment in these regions, potentially through city-specific subsidies, while limiting new capacity development in less favorable locations. For investors, these hotspot cities offer valuable references for decision-making, helping to minimize the risk of stranded assets and optimize investments in CCS infrastructure. Furthermore, the research highlights the importance of regional planning and the need for tailored policies that consider local conditions and capacities, thus providing a more effective roadmap for achieving national and global climate targets.

Overall, this research contributes to the theoretical understanding, methodological approaches, and practical strategies for achieving a net-zero cement sector, addressing key gaps in existing studies and providing a robust foundation for future efforts in decarbonization. This comprehensive approach ensures that the findings are not only academically rigorous but also practically applicable, facilitating the transition towards a more sustainable and climate-resilient cement industry.

9.5 Limitations and future research

Despite the contributions of this research, several limitations must be acknowledged, providing directions for future research efforts.

First, in the cement stock dynamics and future projection, the study is limited by the assumption of static carbonation rates and the exclusion of potential changes in material properties over time. The impact of regional policies and technological advancements in alternative construction materials were not extensively analyzed. Besides, only three end-use sectors were considered in our cement stock accounting and projection, which may not provide a comprehensive view of all potential cement uses. Future efforts can dedicate to a more detailed categorization and, in turn, a more comprehensive projection. Due to the limited data, only two types of material efficiency measures were considered in this study. Including more types of material efficiency measures in future analyses could provide a more holistic understanding of their potential impacts.

Third, in the integration of supply- and demand-side to develop decarbonization roadmaps, the pathways are based on certain assumptions about the pace of technological adoption and policy implementation. The actual pace of these developments may vary with technology maturity, obscuring the feasibility of the proposed pathways. Moreover, the study primarily focuses on the technical and economic aspects of CCS deployment without extensively considering other potential barriers to technology adoption, such as public acceptance and concerns on carbon leakage (Habert et al., 2020). Current considerations of technology systems cannot capture future potential technological breakthroughs. For instance, a recent innovation by Dunant et al. (2024) reused cement as a component in steel recycling. They replaced part of the lime-dolomite flux for steel recycling with recovered cement paste, which can be successfully re-clinkered, with the resulting slag meeting existing standards for Portland clinker and blending effectively with calcined clay and limestone. Future research should explore adaptive strategies that can accommodate varying rates of technological and policy advancements, address non-technical barriers to CCS deployment, and consider potential technological breakthroughs.

Lastly, in the spatial analysis for future CCS planning, while providing valuable insights, the study is limited using simplified supply-demand matching models and the assumption of static storage capacities. The real-world complexities of CCS deployment, including transportation logistics and infrastructure development, may not be fully captured. Furthermore, the competition for carbon storage capacity with other sectors, such as energy and other industrial sectors, was not considered in this study. This competition may affect the availability of storage sites for the cement sector. Future research should incorporate more robust optimization techniques, and more spatial-temporal refined data, along with considering the competition for storage capacity across various sectors, to enhance the applicability and accuracy of the spatial planning for CCS deployment.

References

Ali, M. B., Saidur, R., & Hossain, M. S. (2011). A review on emission analysis in cement industries. *Renewable and Sustainable Energy Reviews*, *15*(5), 2252–2261. https://doi.org/10.1016/j.rser.2011.02.014

Allwood, J. M., Ashby, M. F., Gutowski, T. G., & Worrell, E. (2013). Material efficiency: Providing material services with less material production. *Philosophical Transactions of the Royal Society A: Mathematical, Physical and Engineering Sciences*, *371*(1986), 20120496. https://doi.org/10.1098/rsta.2012.0496

Andersson, R., Fridh, K., Stripple, H., & Häglund, M. (2013). Calculating CO2 Uptake for Existing Concrete Structures during and after Service Life. *Environmental Science & Technology*, *47*(20), 11625–11633. https://doi.org/10.1021/es401775w

Andrew, R. M. (2019). Global CO2 emissions from cement production, 1928–2018. *Earth System Science Data*, *11*(4), 1675–1710. https://doi.org/10.5194/essd-11-1675-2019

Ang, B. W. (2004). Decomposition analysis for policymaking in energy: Which is the preferred method? *Energy Policy*, *32*(9), 1131–1139. https://doi.org/10.1016/S0301-4215(03)00076-4

Ang, B. W., Liu, F. L., & Chew, E. P. (2003). Perfect decomposition techniques in energy and environmental analysis. *Energy Policy*, *31*(14), 1561–1566. https://doi.org/10.1016/S0301-4215(02)00206-9

B. Müller, D. (2006). Stock dynamics for forecasting material flows—Case study for housing in The Netherlands. *Ecological Economics*, *59*(1), 142–156. https://doi.org/10.1016/j.ecolecon.2005.09.025

Bergsdal, H., Brattebø, H., Bohne, R. A., & Müller, D. B. (2007). Dynamic material flow analysis for Norway's dwelling stock. *Building Research & Information*, *35*(5), 557–570. https://doi.org/10.1080/09613210701287588

Berrill, P., & Hertwich, E. G. (2021). Material flows and GHG emissions from housing stock evolution in US counties, 2020–60. *Buildings and Cities*, *2*(1), 599–617. https://doi.org/10.5334/bc.126

Berrill, P., Wilson, E. J. H., Reyna, J. L., Fontanini, A. D., & Hertwich, E. G. (2022). Decarbonization pathways for the residential sector in the United States. *Nature Climate Change*, *12*(8), 712–718. https://doi.org/10.1038/s41558-022-01429-y

Biegler, L. T., & Grossmann, I. E. (2004). Retrospective on optimization. *Computers & Chemical Engineering*, *28*(8), 1169–1192. https://doi.org/10.1016/j.compchemeng.2003.11.003

Bleischwitz, R., Nechifor, V., Winning, M., Huang, B., & Geng, Y. (2018). Extrapolation or saturation – Revisiting growth patterns, development stages and decoupling. *Global Environmental Change*, *48*, 86–96. https://doi.org/10.1016/j.gloenvcha.2017.11.008

Branger, F., & Quirion, P. (2015). Reaping the carbon rent: Abatement and overallocation profits in the European cement industry, insights from an LMDI decomposition analysis. *Energy Economics*, *47*, 189–205. https://doi.org/10.1016/j.eneco.2014.11.008

Cai, B., Wang, J., He, J., & Geng, Y. (2016). Evaluating CO2 emission performance in China's cement industry: An enterprise perspective. *Applied Energy*, *166*, 191–200. https://doi.org/10.1016/j.apenergy.2015.11.006

Cai, W., Wan, L., Jiang, Y., Wang, C., & Lin, L. (2015). Short-Lived Buildings in China: Impacts on Water, Energy, and Carbon Emissions. *Environmental Science & Technology*, *49*(24), 13921–13928. https://doi.org/10.1021/acs.est.5b02333

Cai, X., Cai, B., Zhang, H., Chen, L., Zheng, C., Tong, P., Lin, H., Zhang, Q., Liu, M., Tong, Y., & Wang, X. (2020). Establishment of High-Resolution Atmospheric Mercury Emission Inventories for Chinese Cement Plants Based on the Mass Balance Method. *Environ Sci Technol*, *54*(21), 13399–13408. Medline. https://doi.org/10.1021/acs.est.0c02963

Camarasa, C., Mata, É., Navarro, J. P. J., Reyna, J., Bezerra, P., Angelkorte, G. B., Feng, W., Filippidou, F., Forthuber, S., Harris, C., Sandberg, N. H., Ignatiadou, S., Kranzl, L., Langevin, J., Liu, X., Müller, A., Soria, R., Villamar, D., Dias, G. P., … Yaramenka, K. (2022). A global comparison of building decarbonization scenarios by 2050 towards 1.5–2 °C targets. *Nature Communications*, *13*(1), 3077. https://doi.org/10.1038/s41467-022-29890-5

Cao, Z., Liu, G., Duan, H., Xi, F., Liu, G., & Yang, W. (2019). Unravelling the mystery of Chinese building lifetime: A calibration and verification based on dynamic material flow analysis. *Applied Energy*, *238*, 442–452. https://doi.org/10.1016/j.apenergy.2019.01.106

Cao, Z., Myers, R. J., Lupton, R. C., Duan, H., Sacchi, R., Zhou, N., Reed Miller, T., Cullen, J. M., Ge, Q., & Liu, G. (2020). The sponge effect and carbon emission mitigation potentials of the global cement cycle. *Nature Communications*, *11*(1), 3777. https://doi.org/10.1038/s41467-020-17583-w

Cao, Z., Shen, L., Liu, L., Zhao, J., Zhong, S., Kong, H., & Sun, Y. (2017). Estimating the in-use cement stock in China: 1920–2013. *Resources, Conservation and Recycling*, *122*, 21–31. https://doi.org/10.1016/j.resconrec.2017.01.021

Cao, Z., Shen, L., Liu, L., & Zhong, S. (2016). Analysis on major drivers of cement consumption during the urbanization process in China. *Journal of Cleaner Production*, *133*, 304–313. https://doi.org/10.1016/j.jclepro.2016.05.130

Cao, Z., Shen, L., Løvik, A. N., Müller, D. B., & Liu, G. (2017). Elaborating the History of Our Cementing Societies: An in-Use Stock Perspective. *Environmental Science & Technology*, *51*(19), 11468–11475. https://doi.org/10.1021/acs.est.7b03077

Cavalett, O., Watanabe, M. D. B., Voldsund, M., Roussanaly, S., & Cherubini, F. (2024). Paving the way for sustainable decarbonization of the European cement industry. *Nature Sustainability*. https://doi.org/10.1038/s41893-024-01320-y

Cement Sustainability Initiative. (2011). *CO_2 accounting and reporting standard for the cement industry*.

Chen, C., Xu, R., Tong, D., Qin, X., Cheng, J., Liu, J., Zheng, B., Yan, L., & Zhang, Q. (2022). A striking growth of CO_2 emissions from the global cement industry driven by new facilities in emerging countries.

Environmental Research Letters, *17*(4), 044007. https://doi.org/10.1088/1748-9326/ac48b5

Chen, L., Liang, S., Zhang, H., Cai, X., Chen, Y., Liu, M., Lin, H., Li, Y., Qi, J., Tong, Y., Zhang, W., Wang, X., & Shu, J. (2020). Rapid Increase in Cement-Related Mercury Emissions and Deposition in China during 2005-2015. *Environ Sci Technol*, *54*(22), 14204–14214. Medline. https://doi.org/10.1021/acs.est.0c03512

Chen, Y., Zhang, Q., Cai, X., Zhang, H., Lin, H., Zheng, C., Guo, Z., Hu, S., Chen, L., Tao, S., Liu, M., & Wang, X. (2022). Rapid Increase in China's Industrial Ammonia Emissions: Evidence from Unit-Based Mapping. *Environ Sci Technol*, *56*(6), 3375–3385. Medline. https://doi.org/10.1021/acs.est.1c08369

Cheng, D., Reiner, D. M., Yang, F., Cui, C., Meng, J., Shan, Y., Liu, Y., Tao, S., & Guan, D. (2023). Projecting future carbon emissions from cement production in developing countries. *Nature Communications*, *14*(1), 8213. https://doi.org/10.1038/s41467-023-43660-x

Churkina, G., Organschi, A., Reyer, C. P. O., Ruff, A., Vinke, K., Liu, Z., Reck, B. K., Graedel, T. E., & Schellnhuber, H. J. (2020). Buildings as a global carbon sink. *Nature Sustainability*, *3*(4), 269–276. https://doi.org/10.1038/s41893-019-0462-4

Climate Group. (2024). *Decarbonisation pathways*. https://www.theclimategroup.org/decarbonisation-pathways

Cohen, M. J. (2020). New Conceptions of Sufficient Home Size in High-Income Countries: Are We Approaching a Sustainable Consumption Transition? *Housing, Theory and Society*, *38*(2), 173–203. https://doi.org/10.1080/14036096.2020.1722218

Creutzig, F., Niamir, L., Bai, X., Callaghan, M., Cullen, J., Díaz-José, J., Figueroa, M., Grubler, A., Lamb, W. F., Leip, A., Masanet, E., Mata, É., Mattauch, L., Minx, J. C., Mirasgedis, S., Mulugetta, Y., Nugroho, S. B., Pathak, M., Perkins, P., … Ürge-Vorsatz, D. (2021). Demand-side solutions to climate change mitigation consistent with high levels of well-being. *Nature Climate Change*, *12*(1), 36–46. https://doi.org/10.1038/s41558-021-01219-y

Creutzig, F., Roy, J., Lamb, W. F., Azevedo, I. M. L., Bruine de Bruin, W., Dalkmann, H., Edelenbosch, O. Y., Geels, F. W., Grubler, A., Hepburn, C., Hertwich, E. G., Khosla, R., Mattauch, L., Minx, J. C., Ramakrishnan, A., Rao, N. D., Steinberger, J. K., Tavoni, M., Ürge-Vorsatz, D., & Weber, E. U. (2018). Towards demand-side solutions for mitigating climate change. *Nature Climate Change*, *8*(4), 260–263. https://doi.org/10.1038/s41558-018-0121-1

Cui, R. Y., Hultman, N., Cui, D., McJeon, H., Yu, S., Edwards, M. R., Sen, A., Song, K., Bowman, C., Clarke, L., Kang, J., Lou, J., Yang, F., Yuan, J., Zhang, W., & Zhu, M. (2021). A plant-by-plant strategy for high-ambition coal power phaseout in China. *Nature Communications*, *12*(1), 1468. https://doi.org/10.1038/s41467-021-21786-0

Dahowski, R. T., Dooley, J. J., Bachu, S., & Gupta, N. (2005). *Bulding the costs curves for CO_2 storage: North America* (IEA Greenhouse Gas R&D Programme). International Energy Agency.

Davis, S. J., Lewis, N. S., Shaner, M., Aggarwal, S., Arent, D., Azevedo, I. L., Benson, S. M., Bradley, T., Brouwer, J., Chiang, Y. M., Clack, C. T. M., Cohen, A., Doig, S., Edmonds, J., Fennell, P., Field, C. B., Hannegan, B., Hodge, B. M., Hoffert, M. I., … Caldeira, K. (2018). Net-zero emissions energy systems. *Science*, *360*(6396). PubMed-not-MEDLINE. https://doi.org/10.1126/science.aas9793

De Boer, P., & Rodrigues, J. F. D. (2020). Decomposition analysis: When to use which method? *Economic Systems Research*, *32*(1), 1–28. https://doi.org/10.1080/09535314.2019.1652571

Department of Climate Change of National Development and Reform Commission of China. (2012). *National Greenhouse Gas Inventory of the People's Republic of China China*. China Environmental Press.

Department of Economic and Social Affairs of United Nations. (2022). *World Population Prospects 2022*. https://population.un.org/wpp/

Dinda, S. (2004). Environmental Kuznets Curve Hypothesis: A Survey. *Ecological Economics*, *49*(4), 431–455. https://doi.org/10.1016/j.ecolecon.2004.02.011

Dinga, C. D., & Wen, Z. (2022). China's green deal: Can China's cement industry achieve carbon neutral emissions by 2060? *Renewable and Sustainable Energy Reviews*, *155*, 111931. https://doi.org/10.1016/j.rser.2021.111931

Doh Dinga, C., & Wen, Z. (2021). Many-objective optimization of energy conservation and emission reduction in China's cement industry. *Applied Energy*, *304*, 117714. https://doi.org/10.1016/j.apenergy.2021.117714

Driver, J. G., Hills, T., Hodgson, P., Sceats, M., & Fennell, P. S. (2022). Simulation of direct separation technology for carbon capture and storage in the cement industry. *Chemical Engineering Journal*, *449*. https://doi.org/10.1016/j.cej.2022.137721

Du, T., Wang, J., Wang, H., Tian, X., Yue, Q., & Tanikawa, H. (2020). CO_2 emissions from the Chinese cement sector: Analysis from both the supply and demand sides. *Journal of Industrial Ecology*, *24*(4), 923–934. https://doi.org/10.1111/jiec.12986

Dunant, C. F., Joseph, S., Prajapati, R., & Allwood, J. M. (2024). Electric recycling of Portland cement at scale. *Nature*. https://doi.org/10.1038/s41586-024-07338-8

European Cement Research Academy & Cement Sustainability Initiative. (2017a). *Development of State of the Art Techniques in Cement Manufacturing: Trying to Look Ahead; CSI/ECRA-Technology Papers*. http://www.wbcsdcement.org/technology

European Cement Research Academy, & Cement Sustainability Initiative. (2017b). *Development of State of the Art Techniques in Cement Manufacturing: Trying to Look Ahead; CSI/ECRA-Technology Papers 2017*. http://www.wbcsdcement.org/technology

Feng, K. (2019). Drivers of peak and decline. *Nature Climate Change*, *9*(3), 188–189. https://doi.org/10.1038/s41558-019-0421-0

Feng, X.-Z., Lugovoy, O., & Qin, H. (2018). Co-controlling CO2 and NOx emission in China's cement industry: An optimal development pathway study. *Advances in Climate Change Research*, *9*(1), 34–42. https://doi.org/10.1016/j.accre.2018.02.004

Fennell, P., Driver, J., Bataille, C., & Davis, S. J. (2022). Going net zero for cement and steel. *Nature*, *603*, 574–577.

Fennell, P. S., Davis, S. J., & Mohammed, A. (2021). Decarbonizing cement production. *Joule*, *5*(6), 1305–1311. https://doi.org/10.1016/j.joule.2021.04.011

Fishman, T., Heeren, N., Pauliuk, S., Berrill, P., Tu, Q., Wolfram, P., & Hertwich, E. G. (2021). A comprehensive set of global scenarios of housing, mobility, and material efficiency for material cycles and energy systems modeling. *Journal of Industrial Ecology*, *25*(2), 305–320. https://doi.org/10.1111/jiec.13122

Fishman, T., Schandl, H., & Tanikawa, H. (2016). Stochastic Analysis and Forecasts of the Patterns of Speed, Acceleration, and Levels of Material Stock Accumulation in Society. *Environmental Science & Technology*, *50*(7), 3729–3737. https://doi.org/10.1021/acs.est.5b05790

Friedlingstein, P., O'Sullivan, M., Jones, M. W., Andrew, R. M., Bakker, D. C. E., Hauck, J., Landschützer, P., Le Quéré, C., Luijkx, I. T., Peters, G. P., Peters, W., Pongratz, J., Schwingshackl, C., Sitch, S., Canadell, J. G., Ciais, P., Jackson, R. B., Alin, S. R., Anthoni, P., … Zheng, B. (2023). Global Carbon Budget 2023. *Earth System Science Data*, *15*(12), 5301–5369. https://doi.org/10.5194/essd-15-5301-2023

Friedlingstein, P., O'Sullivan, M., Jones, M. W., Andrew, R. M., Gregor, L., Hauck, J., Le Quéré, C., Luijkx, I. T., Olsen, A., Peters, G. P., Peters, W., Pongratz, J., Schwingshackl, C., Sitch, S., Canadell, J. G., Ciais, P., Jackson, R. B., Alin, S. R., Alkama, R., … Zheng, B. (2022). Global Carbon Budget 2022. *Earth System Science Data*, *14*(11), 4811–4900. https://doi.org/10.5194/essd-14-4811-2022

Gao, T., Shen, L., Shen, M., Liu, L., & Chen, F. (2016). Analysis of material flow and consumption in cement production process. *Journal of Cleaner Production*, *112*, 553–565. https://doi.org/10.1016/j.jclepro.2015.08.054

Gao, T., Shen, L., Shen, M., Liu, L., Chen, F., & Gao, L. (2017). Evolution and projection of CO2 emissions for China's cement industry from 1980 to 2020. *Renewable and Sustainable Energy Reviews*, *74*, 522–537. https://doi.org/10.1016/j.rser.2017.02.006

Gardarsdottir, S., De Lena, E., Romano, M., Roussanaly, S., Voldsund, M., Pérez-Calvo, J.-F., Berstad, D., Fu, C., Anantharaman, R., Sutter, D., Gazzani, M., Mazzotti, M., & Cinti, G. (2019). Comparison of Technologies for CO2 Capture from Cement Production—Part 2: Cost Analysis. *Energies*, *12*(3), 542. https://doi.org/10.3390/en12030542

Gartner, E., & Sui, T. (2018). Alternative cement clinkers. *Cement and Concrete Research*, *114*, 27–39. https://doi.org/10.1016/j.cemconres.2017.02.002

Gibbins, J., & Chalmers, H. (2008). Carbon capture and storage. *Energy Policy*, *36*(12), 4317–4322. https://doi.org/10.1016/j.enpol.2008.09.058

Global Cement and Concrete Assiociation. (2024). *GNR 2.0—GCCA in Numbers*. https://gccassociation.org/sustainability-innovation/gnr-gcca-in-numbers/

Goodman, A., Hakala, A., Bromhal, G., Deel, D., Rodosta, T., Frailey, S., Small, M., Allen, D., Romanov, V., Fazio, J., Huerta, N., McIntyre, D., Kutchko, B., & Guthrie, G. (2011). U.S. DOE methodology for the development of geologic storage potential for carbon dioxide at the national and regional scale. *International Journal of Greenhouse Gas Control*, *5*(4), 952–965. https://doi.org/10.1016/j.ijggc.2011.03.010

Graedel, T. E. (2019). Material Flow Analysis from Origin to Evolution. *Environmental Science & Technology*, *53*(21), 12188–12196. https://doi.org/10.1021/acs.est.9b03413

Grubler, A., Wilson, C., Bento, N., Boza-Kiss, B., Krey, V., McCollum, D. L., Rao, N. D., Riahi, K., Rogelj, J., De Stercke, S., Cullen, J., Frank, S., Fricko, O., Guo, F., Gidden, M., Havlík, P., Huppmann, D., Kiesewetter, G., Rafaj, P., … Valin, H. (2018). A low energy demand scenario for meeting the 1.5 °C target and sustainable development goals without negative emission technologies. *Nature Energy*, *3*(6), 515–527. https://doi.org/10.1038/s41560-018-0172-6

Grussing, M. N. (2014). Life Cycle Asset Management Methodologies for Buildings. *Journal of Infrastructure Systems*, *20*(1). https://doi.org/10.1061/(asce)is.1943-555x.0000157

Guan, D., Meng, J., Reiner, D. M., Zhang, N., Shan, Y., Mi, Z., Shao, S., Liu, Z., Zhang, Q., & Davis, S. J. (2018). Structural decline in China's CO2 emissions through transitions in industry and energy systems. *Nature Geoscience*, *11*(8), 551–555. https://doi.org/10.1038/s41561-018-0161-1

Guo, R., Wang, J., Bing, L., Tong, D., Ciais, P., Davis, S. J., Andrew, R. M., Xi, F., & Liu, Z. (2021). Global CO2 uptake by cement from 1930 to 2019. *Earth System Science Data*, *13*(4), 1791–1805. https://doi.org/10.5194/essd-13-1791-2021

Habert, G., Miller, S. A., John, V. M., Provis, J. L., Favier, A., Horvath, A., & Scrivener, K. L. (2020). Environmental impacts and decarbonization strategies in the cement and concrete industries. *Nature Reviews Earth & Environment*, *1*(11), 559–573. https://doi.org/10.1038/s43017-020-0093-3

He, J., He, J., Wang, Y., Fan, Y., Shi, H., Cai, B., & Yan, G. (2022). Pathway of Carbon Emissions Peak for Cement Industry in China. *Research of Environmental Sciences (in Chinese)*, *35*(2), 347–355.

Hertwich, E. G., Ali, S., Ciacci, L., Fishman, T., Heeren, N., Masanet, E., Asghari, F. N., Olivetti, E., Pauliuk, S., Tu, Q., & Wolfram, P. (2019). Material efficiency strategies to reducing greenhouse gas emissions associated with buildings, vehicles, and electronics—A review. *Environmental Research Letters*, *14*(4). https://doi.org/10.1088/1748-9326/ab0fe3

Hills, T., Florin, N., & Fennell, P. S. (2016). Decarbonising the cement sector: A bottom-up model for optimising carbon capture application in the UK. *Journal of Cleaner Production*, *139*, 1351–1361. https://doi.org/10.1016/j.jclepro.2016.08.129

Hills, T., Leeson, D., Florin, N., & Fennell, P. (2016). Carbon Capture in the Cement Industry: Technologies, Progress, and Retrofitting. *Environmental Science & Technology*, *50*(1), 368–377. https://doi.org/10.1021/acs.est.5b03508

Hoekstra, R., & van den Bergh, J. C. J. M. (2003). Comparing structural decomposition analysis and index. *Energy Economics*, *25*(1), 39–64. https://doi.org/10.1016/S0140-9883(02)00059-2

Huang, Z., Wang, J., Bing, L., Qiu, Y., Guo, R., Yu, Y., Ma, M., Niu, L., Tong, D., Andrew, R. M., Friedlingstein, P., Canadell, J. G., Xi, F., & Liu, Z. (2023). Global carbon uptake of cement carbonation accounts 1930–2021. *Earth System Science Data*, *15*(11), 4947–4958. https://doi.org/10.5194/essd-15-4947-2023

Huntzinger, D. N., Gierke, J. S., Kawatra, S. K., Eisele, T. C., & Sutter, L. L. (2009). Carbon Dioxide Sequestration in Cement Kiln Dust through Mineral Carbonation. *Environmental Science & Technology*, *43*(6), 1986–1992. https://doi.org/10.1021/es802910z

Huuhka, S., & Lahdensivu, J. (2014). Statistical and geographical study on demolished buildings. *Building Research & Information*, *44*(1), 73–96. https://doi.org/10.1080/09613218.2014.980101

Intergovernmental Panel on Climate Change. (2006). *2006 IPCC Guidelines for National Greenhouse Gas Inventories*.

Intergovernmental Panel on Climate Change. (2023). *AR6 Synthesis Report Climate Change 2023*. https://www.ipcc.ch/report/ar6/syr/

International Energy Agency. (2002). *Opportunities for early application of CO_2 sequestration technology*. International Energy Agency.

International Energy Agency. (2016). *20 Years of Carbon Capture and Storage—Accelerating Future Deployment*.

International Energy Agency. (2019). *Transforming Industry through CCUS*.

International Energy Agency & Cement Sustainability Initiative of the World Business Council for Sustainable Development. (2018). *Technology Roadmap: Low Carbon Transition in the Cement Industry*.

Johannesson, B., & Utgenannt, P. (2001). Microstructural changes caused by carbonation of cement mortar. *Cement and Concrete Research*, *31*(6), 925–931. https://doi.org/10.1016/S0008-8846(01)00498-7

Jordaan, G. D., & Lategan, L. O. K. (2010). *Modelling as Research Methodology*. SUN MeDIA. https://doi.org/10.18820/9781920383176

Kapur, A., Keoleian, G., Kendall, A., & Kesler, S. E. (2008). Dynamic Modeling of In-Use Cement Stocks in the United States. *Journal of Industrial Ecology*, *12*(4), 539–556. https://doi.org/10.1111/j.1530-9290.2008.00055.x

Kapur, A., Van Oss, H. G., Keoleian, G., Kesler, S. E., & Kendall, A. (2009). The contemporary cement cycle of the United States. *Journal of Material Cycles and Waste Management*, *11*(2), 155–165. https://doi.org/10.1007/s10163-008-0229-x

Kaya, Y. (1989). *Impact of carbon dioxide emission control on GNP growth: Interpretation of proposed scenarios*. IPCC Energy and Industry Subgroup.

Ke, J., Zheng, N., Fridley, D., Price, L., & Zhou, N. (2012). Potential energy savings and CO2 emissions reduction of China's cement industry. *Energy Policy*, *45*, 739–751. https://doi.org/10.1016/j.enpol.2012.03.036

Kermeli, K., Edelenbosch, O. Y., Crijns-Graus, W., van Ruijven, B. J., Mima, S., van Vuuren, D. P., & Worrell, E. (2019). The scope for better industry representation in long-term energy models: Modeling the cement industry. *Applied Energy*, *240*, 964–985. https://doi.org/10.1016/j.apenergy.2019.01.252

Kim, Y., & Worrell, E. (2002). CO_2 emission trends in the cement industry: An international comparison. *Mitigation and Adaptation Strategies for Global Change*, *7*, 115–133.

Krausmann, F., Wiedenhofer, D., & Haberl, H. (2020). Growing stocks of buildings, infrastructures and machinery as key challenge for compliance with climate targets. *Global Environmental Change*, *61*. https://doi.org/10.1016/j.gloenvcha.2020.102034

Lackey, G., Vasylkivska, V. S., Huerta, N. J., King, S., & Dilmore, R. M. (2019). Managing well leakage risks at a geologic carbon storage site with many wells. *International Journal of Greenhouse Gas Control*, *88*, 182–194. https://doi.org/10.1016/j.ijggc.2019.06.011

Le Quéré, C., Ivar Korsbakken, J., Wilson, C., Tosun, J., Andrew, R., J. Andres, R., G. Canadell, J., Jordan, A., P. Peters, G., & van Vuuren, D. P. (2019). Drivers of declining CO2 emissions in 18 developed economies. *Nature Climate Change*, *9*.

Lei, Y., Zhang, Q., Nielsen, C., & He, K. (2011). An inventory of primary air pollutants and CO2 emissions from cement production in China, 1990–2020. *Atmospheric Environment*, *45*(1), 147–154. https://doi.org/10.1016/j.atmosenv.2010.09.034

Li G., & Lv M. (2002). *Atlas of China's Petroliferous Basins (2nd Edition)*. China Petroleum Industry Press.

Li, N., Ma, D., & Chen, W. (2017). Quantifying the impacts of decarbonisation in China's cement sector: A perspective from an integrated assessment approach. *Applied Energy*, *185*, 1840–1848. https://doi.org/10.1016/j.apenergy.2015.12.112

Liang, X., & Li, J. (2012). Assessing the value of retrofitting cement plants for carbon capture: A case study of a cement plant in Guangdong, China. *Energy Conversion and Management*, *64*, 454–465. https://doi.org/10.1016/j.enconman.2012.04.012

Lin, B., & Zhang, Z. (2016). Carbon emissions in China's cement industry: A sector and policy analysis. *Renewable and Sustainable Energy Reviews*, *58*, 1387–1394. https://doi.org/10.1016/j.rser.2015.12.348

Liu, F., Ross, M., & Wang, S. (1995). Energy efficiency of China's cement industry. *Energy*, *20*(7), 669–681. https://doi.org/10.1016/0360-5442(95)00002-X

Liu, G., Bangs, C. E., & Müller, D. B. (2013). Stock dynamics and emission pathways of the global aluminium cycle. *Nature Climate Change*, *3*(4), 338–342. https://doi.org/10.1038/nclimate1698

Liu, G., & Muller, D. B. (2013). Centennial evolution of aluminum in-use stocks on our aluminized planet. *Environ Sci Technol*, *47*(9), 4882–4888. Medline. https://doi.org/10.1021/es305108p

Liu, G., Xu, K., Zhang, X., & Zhang, G. (2014). Factors influencing the service lifespan of buildings: An improved hedonic model. *Habitat International*, *43*, 274–282. https://doi.org/10.1016/j.habitatint.2014.04.009

Liu, J., Tong, D., Zheng, Y., Cheng, J., Qin, X., Shi, Q., Yan, L., Lei, Y., & Zhang, Q. (2021). Carbon and air pollutant emissions from China's cement industry 1990–2015: Trends, evolution of technologies, and drivers. *Atmospheric Chemistry and Physics*, *21*(3), 1627–1647. https://doi.org/10.5194/acp-21-1627-2021

Liu, J., Zhang, S., & Wagner, F. (2018). Exploring the driving forces of energy consumption and environmental pollution in China's cement industry at the provincial level. *Journal of Cleaner Production*, *184*, 274–285. https://doi.org/10.1016/j.jclepro.2018.02.277

Liu, X., Yuan, Z., Xu, Y., & Jiang, S. (2017). Greening cement in China: A cost-effective roadmap. *Applied Energy*, *189*, 233–244. https://doi.org/10.1016/j.apenergy.2016.12.057

Liu, Z., Deng, Z., He, G., Wang, H., Zhang, X., Lin, J., Qi, Y., & Liang, X. (2021). Challenges and opportunities for carbon neutrality in China. *Nature Reviews Earth & Environment*, *3*(2), 141–155. https://doi.org/10.1038/s43017-021-00244-x

Liu, Z., Guan, D., Wei, W., Davis, S. J., Ciais, P., Bai, J., Peng, S., Zhang, Q., Hubacek, K., Marland, G., Andres, R. J., Crawford-Brown, D., Lin, J., Zhao, H., Hong, C., Boden, T. A., Feng, K., Peters, G. P., Xi, F., … He, K. (2015). Reduced carbon emission estimates from fossil fuel combustion and cement production in China. *Nature*, *524*(7565), 335–338. Medline. https://doi.org/10.1038/nature14677

Lu, Y., Cohen, F., Smith, S. M., & Pfeiffer, A. (2022). Plant conversions and abatement technologies cannot prevent stranding of power plant assets in 2 °C scenarios. *Nat Commun*, *13*(1), 806. PubMed-not-MEDLINE. https://doi.org/10.1038/s41467-022-28458-7

Ma, J., Liu, F., Guo, T., Tao, C., & Peng, X. (2017). Development and Application of 5500 t/d Pyro-system with 6-stage Preheater (in Chinese). *Cement Technology*, *4*. https://doi.org/10.19698/j.cnki.1001-6171.2017.04.002

Ma, M., Huang, Z., Wang, J., Niu, L., Zhang, W., Xu, X., Xi, F., & Liu, Z. (2024). Carbon uptake by cement in China: Estimation and contribution to carbon neutrality goals. *Science China Earth Sciences*. https://doi.org/10.1007/s11430-023-1276-6

Ma, M., Ma, X., Cai, W., & Cai, W. (2019). Carbon-dioxide mitigation in the residential building sector: A household scale-based assessment. *Energy Conversion and Management*, *198*, 111915. https://doi.org/10.1016/j.enconman.2019.111915

Ma, M., Yan, R., Du, Y., Ma, X., Cai, W., & Xu, P. (2017). A methodology to assess China's building energy savings at the national level: An IPAT–LMDI model approach. *Journal of Cleaner Production*, *143*, 784–793. https://doi.org/10.1016/j.jclepro.2016.12.046

Mezik, S. (2017). *4. Research Methods: Modeling | General Science*. https://courses.lumenlearning.com/suny-hccc-generalscience/chapter/4-research-methods-modeling/

Miatto, A., Schandl, H., & Tanikawa, H. (2017). How important are realistic building lifespan assumptions for material stock and demolition waste accounts? *Resources, Conservation and Recycling*, *122*, 143–154. https://doi.org/10.1016/j.resconrec.2017.01.015

Middleton, R. S., & Bielicki, J. M. (2009). A scalable infrastructure model for carbon capture and storage: SimCCS. *Energy Policy*, *37*(3), 1052–1060. https://doi.org/10.1016/j.enpol.2008.09.049

Miller, S. A. (2020). The role of cement service-life on the efficient use of resources. *Environmental Research Letters*, *15*(2). https://doi.org/10.1088/1748-9326/ab639d

Miller, S. A., Habert, G., Myers, R. J., & Harvey, J. T. (2021). Achieving net zero greenhouse gas emissions in the cement industry via value chain mitigation strategies. *One Earth*, *4*(10), 1398–1411. https://doi.org/10.1016/j.oneear.2021.09.011

Miller, S. A., & Myers, R. J. (2020). Environmental Impacts of Alternative Cement Binders. *Environ Sci Technol*, *54*(2), 677–686. Medline. https://doi.org/10.1021/acs.est.9b05550

Monteiro, P. J. M., Miller, S. A., & Horvath, A. (2017). Towards sustainable concrete. *Nature Materials*, *16*(7), 698–699. https://doi.org/10.1038/nmat4930

Muller, D. B., Liu, G., Lovik, A. N., Modaresi, R., Pauliuk, S., Steinhoff, F. S., & Brattebo, H. (2013). Carbon emissions of infrastructure development. *Environ Sci Technol*, *47*(20), 11739–11746. Medline. https://doi.org/10.1021/es402618m

Müller, E., Hilty, L. M., Widmer, R., Schluep, M., & Faulstich, M. (2014). Modeling Metal Stocks and Flows: A Review of Dynamic Material Flow Analysis Methods. *Environmental Science & Technology*, *48*(4), 2102–2113. https://doi.org/10.1021/es403506a

Muller, E., Hilty, L. M., Widmer, R., Schluep, M., & Faulstich, M. (2014). Modeling metal stocks and flows: A review of dynamic material flow analysis methods. *Environ Sci Technol*, *48*(4), 2102–2113. Medline. https://doi.org/10.1021/es403506a

Nakićenović, N., & Swart, R. (Eds.). (2000). *Special report on emissions scenarios: A special report of Working Group III of the Intergovernmental Panel on Climate Change*. Cambridge University Press.

National Bureau of Statistics of China. (n.d.). *National Data*. Retrieved March 4, 2024, from https://data.stats.gov.cn/english/

National Bureau of Statistics of China. (2021). *China Statistical Yearbook 2021*. https://www.stats.gov.cn/sj/ndsj/2021/indexch.htm

O'Connor, J. (2004). *Survey on actual service lives for North American buildings*. Woodframe Housing Durability and Disaster Issues, Las Vegas.

Oda, J., Akimoto, K., Tomoda, T., Nagashima, M., Wada, K., & Sano, F. (2012). International comparisons of energy efficiency in power, steel, and cement industries. *Energy Policy*, *44*, 118–129. https://doi.org/10.1016/j.enpol.2012.01.024

Olsson, J. A., Miller, S. A., & Alexander, M. G. (2023). Near-term pathways for decarbonizing global concrete production. *Nature Communications*, *14*(1), 4574. PubMed-not-MEDLINE. https://doi.org/10.1038/s41467-023-40302-0

Pade, C., & Guimaraes, M. (2007). The CO2 uptake of concrete in a 100 year perspective. *Cement and Concrete Research*, *37*(9), 1348–1356. https://doi.org/10.1016/j.cemconres.2007.06.009

Papadakix, V. G., Vayenas, C. G., & Fardis, M. N. (1991). Experimental investigation and mathematical modeling of the concrete carbonation problem. *Chemical Engineering Science*, *46*(5/6), 1333–1338.

Pauliuk, S., Heeren, N., Berrill, P., Fishman, T., Nistad, A., Tu, Q., Wolfram, P., & Hertwich, E. G. (2021). Global scenarios of resource and emission savings from material efficiency in residential buildings and cars. *Nature Communications*, *12*(1), 5097. https://doi.org/10.1038/s41467-021-25300-4

Pauliuk, S., & Hertwich, E. G. (2015). Socioeconomic metabolism as paradigm for studying the biophysical basis of human societies. *Ecological Economics*, *119*, 83–93. https://doi.org/10.1016/j.ecolecon.2015.08.012

Persits, F. M., Steinshouer, D. W., & Klett, T. R. (2000). *World Total Petroleum System Summary Result Data, 2000 World Petroleum Assessment* [Dataset]. [object Object]. https://doi.org/10.5066/P9CV5L0E

Pfeiffer, A., Hepburn, C., Vogt-Schilb, A., & Caldecott, B. (2018). Committed emissions from existing and planned power plants and asset stranding required to meet the Paris Agreement. *Environmental Research Letters*, *13*(5). https://doi.org/10.1088/1748-9326/aabc5f

Raupach, M. R., Davis, S. J., Peters, G. P., Andrew, R. M., Canadell, J. G., Ciais, P., Friedlingstein, P., Jotzo, F., Van Vuuren, D. P., & Le Quéré, C. (2014). Sharing a quota on cumulative carbon emissions. *Nature Climate Change*, *4*(10), 873–879. https://doi.org/10.1038/nclimate2384

Raupach, M. R., Marland, G., Ciais, P., Le Quéré, C., Canadell, J. G., Klepper, G., & Field, C. B. (2007). Global and regional drivers of accelerating CO_2 emissions. *Proceedings of the National Academy of Sciences*, *104*(24), 10288–10293. https://doi.org/10.1073/pnas.0700609104

Reger, D., Madanat, S., & Horvath, A. (2014). Economically and environmentally informed policy for road resurfacing tradeoffs between costs and greenhouse gas emissions. *Environmental Research Letters*, *9*, 104020.

Ren, M., Ma, T., Fang, C., Liu, X., Guo, C., Zhang, S., Zhou, Z., Zhu, Y., Dai, H., & Huang, C. (2023). Negative emission technology is key to decarbonizing China's cement industry. *Applied Energy*, *329*, 120254. https://doi.org/10.1016/j.apenergy.2022.120254

Renforth, P. (2019). The negative emission potential of alkaline materials. *Nature Communications*, *10*(1), 1401. https://doi.org/10.1038/s41467-019-09475-5

Renforth, P., Washbourne, C.-L., Taylder, J., & Manning, D. A. C. (2011). Silicate Production and Availability for Mineral Carbonation. *Environmental Science & Technology*, *45*(6), 2035–2041. https://doi.org/10.1021/es103241w

Robbie Andrew. (2023). *Global CO_2 emissions from cement production* (Version 231016) [Dataset]. Zenodo. https://doi.org/10.5281/ZENODO.831454

Rockey Mountain Institute, & China Cement Association. (2022). *Towards Net Zero: Decarbonization Roadmap for China's cement Industry*.

Rodriguez, N., Murillo, R., & Abanades, J. C. (2012). CO2 capture from cement plants using oxyfired precalcination and/or calcium looping. *Environ Sci Technol*, *46*(4), 2460–2466. Medline. https://doi.org/10.1021/es2030593

Sato, F. E. K., Furubayashi, T., & Nakata, T. (2019). Application of energy and CO2 reduction assessments for end-of-life vehicles recycling in Japan. *Applied Energy*, *237*, 779–794. https://doi.org/10.1016/j.apenergy.2019.01.002

Scrivener, K., Martirena, F., Bishnoi, S., & Maity, S. (2018). Calcined clay limestone cements (LC3). *Cement and Concrete Research*, *114*, 49–56. https://doi.org/10.1016/j.cemconres.2017.08.017

Shah, I. H., Miller, S. A., Jiang, D., & Myers, R. J. (2022). Cement substitution with secondary materials can reduce annual global CO_2 emissions by up to 1.3 gigatons. *Nature Communications*, *13*(1), 5758. PubMed-not-MEDLINE. https://doi.org/10.1038/s41467-022-33289-7

Shan, Y., Zhou, Y., Meng, J., Mi, Z., Liu, J., & Guan, D. (2019). Peak cement-related CO2 emissions and the changes in drivers in China. *Journal of Industrial Ecology*, *23*(4), 959–971. https://doi.org/10.1111/jiec.12839

Shanks, W., Dunant, C. F., Drewniok, M. P., Lupton, R. C., Serrenho, A., & Allwood, J. M. (2019). How much cement can we do without? Lessons from cement material flows in the UK. *Resources, Conservation and Recycling*, *141*, 441–454. https://doi.org/10.1016/j.resconrec.2018.11.002

Shen, L., Gao, T., Zhao, J., Wang, L., Wang, L., Liu, L., Chen, F., & Xue, J. (2014). Factory-level measurements on CO2 emission factors of cement production in China. *Renewable and Sustainable Energy Reviews*, *34*, 337–349. https://doi.org/10.1016/j.rser.2014.03.025

Shen, W., Cao, L., Li, Q., Zhang, W., Wang, G., & Li, C. (2015). Quantifying CO2 emissions from China's cement industry. *Renewable and Sustainable Energy Reviews*, *50*, 1004–1012. https://doi.org/10.1016/j.rser.2015.05.031

Shi, F., Huang, T., Tanikawa, H., Han, J., Hashimoto, S., & Moriguchi, Y. (2012). Toward a Low Carbon-Dematerialization Society: Measuring the Materials Demand and CO2 Emissions of Building and Transport Infrastructure Construction in China. *Journal of Industrial Ecology*, *16*(4), 493–505. https://doi.org/10.1111/j.1530-9290.2012.00523.x

Song, L., van Ewijk, S., Masanet, E., Watari, T., Meng, F., Cullen, J. M., Cao, Z., & Chen, W.-Q. (2023). China's bulk material loops can be closed but deep decarbonization requires demand reduction. *Nature Climate Change*, *13*(10), 1136–1143. https://doi.org/10.1038/s41558-023-01782-6

Szulczewski, M. L., MacMinn, C. W., Herzog, H. J., & Juanes, R. (2012). Lifetime of carbon capture and storage as a climate-change mitigation technology. *Proceedings of the National Academy of Sciences*, *109*(14), 5185–5189. https://doi.org/10.1073/pnas.1115347109

Tan, C., Yu, X., & Guan, Y. (2022). A technology-driven pathway to net-zero carbon emissions for China's cement industry. *Applied Energy*, *325*, 119804. https://doi.org/10.1016/j.apenergy.2022.119804

Tang, H., Chen, W., Zhang, S., & Zhang, Q. (2023). China's multi-sector-shared CCUS networks in a carbon-neutral vision. *iScience*, *26*(4), 106347. https://doi.org/10.1016/j.isci.2023.106347

Tang, H., Zhang, S., & Chen, W. (2021). Assessing Representative CCUS Layouts for China's Power Sector toward Carbon Neutrality. *Environmental Science & Technology*, *55*(16), 11225–11235. https://doi.org/10.1021/acs.est.1c03401

Tang, L., Ruan, J., Bo, X., Mi, Z., Wang, S., Dong, G., & Davis, S. J. (2022). Plant-level real-time monitoring data reveal substantial abatement potential of air pollution and CO2 in China's cement sector. *One Earth*, *5*(8), 892–906. https://doi.org/10.1016/j.oneear.2022.07.003

Taylor, H. F. W. (1997). *Cement chemistry* (2nd ed). T. Telford.

Thomsen, A., & van der Flier, K. (2011). Understanding obsolescence: A conceptual model for buildings. *Building Research & Information*, *39*(4), 352–362. https://doi.org/10.1080/09613218.2011.576328

Tong, D., Zhang, Q., Zheng, Y., Caldeira, K., Shearer, C., Hong, C., Qin, Y., & Davis, S. J. (2019). Committed emissions from existing energy infrastructure jeopardize 1.5 °C climate target. *Nature*, *572*(7769), 373–377. https://doi.org/10.1038/s41586-019-1364-3

United Nations Environment Programme. (2022). *Emissions Gap Report 2022*. http://www.unep.org/resources/emissions-gap-report-2022

United Nations Framework Convention on Climate Change. (2015). *The Paris Agreement*. https://unfccc.int/process-and-meetings/the-paris-agreement

United States Geological Survey. (1999). *Geologic Provinces of the Far East, 2000 (prv3al)* [Dataset]. https://doi.org/10.5066/P9BYRDHV van der Meer, L. G. H. (1993). The conditions limiting CO_2 storage in aquifers. *Energy Conversion and Management*, *34*(9–11), 959–966. https://doi.org/10.1016/0196-8904(93)90042-9

van Ewijk, S., & McDowall, W. (2020). Diffusion of flue gas desulfurization reveals barriers and opportunities for carbon capture and storage. *Nat Commun*, *11*(1), 4298. PubMed-not-MEDLINE. https://doi.org/10.1038/s41467-020-18107-2

Van Ruijven, B. J., Van Vuuren, D. P., Boskaljon, W., Neelis, M. L., Saygin, D., & Patel, M. K. (2016). Long-term model-based projections of energy use and CO2 emissions from the global steel and cement industries. *Resources, Conservation and Recycling*, *112*, 15–36. https://doi.org/10.1016/j.resconrec.2016.04.016

Van Vuuren, D. P. (2007). *Energy systems and climate policy: Long-term scenarios for an uncertain future*. Utrecht University.

Voldsund, M., Gardarsdottir, S., De Lena, E., Pérez-Calvo, J.-F., Jamali, A., Berstad, D., Fu, C., Romano, M., Roussanaly, S., Anantharaman, R., Hoppe, H., Sutter, D., Mazzotti, M., Gazzani, M., Cinti, G., & Jordal, K. (2019). Comparison of Technologies for CO2 Capture from Cement Production—Part 1: Technical Evaluation. *Energies*, *12*(3), 559. https://doi.org/10.3390/en12030559

Wang, N., Akimoto, K., & Nemet, G. F. (2021). What went wrong? Learning from three decades of carbon capture, utilization and sequestration (CCUS) pilot and demonstration projects. *Energy Policy*, *158*. https://doi.org/10.1016/j.enpol.2021.112546

Wang, W., Jiang, D., Chen, D., Chen, Z., Zhou, W., & Zhu, B. (2016). A Material Flow Analysis (MFA)-based potential analysis of eco-efficiency indicators of China's cement and cement-based materials industry. *Journal of Cleaner Production*, *112*, 787–796. https://doi.org/10.1016/j.jclepro.2015.06.103

Wang, X., Wei, Y., & Shao, Q. (2020). Decomposing the decoupling of CO2 emissions and economic growth in China's iron and steel industry. *Resources, Conservation and Recycling*, *152*, 104509. https://doi.org/10.1016/j.resconrec.2019.104509

Wang, Y., Höller, S., Viebahn, P., & Hao, Z. (2014). Integrated assessment of CO2 reduction technologies in China's cement industry. *International Journal of Greenhouse Gas Control*, *20*, 27–36. https://doi.org/10.1016/j.ijggc.2013.10.004

Wang, Y., Wen, Z., Xu, M., & Kosajan, V. (2024). The carbon-energy-water nexus of the carbon capture, utilization, and storage technology deployment schemes: A case study in China's cement industry. *Applied Energy*, *362*, 122991. https://doi.org/10.1016/j.apenergy.2024.122991

Wang, Y., Wu, T., Li, H., Skitmore, M., & Su, B. (2020). A statistics-based method to quantify residential energy consumption and stock at the city level in China: The case of the Guangdong-Hong Kong-Macao Greater Bay Area cities. *Journal of Cleaner Production*, *251*, 119637. https://doi.org/10.1016/j.jclepro.2019.119637

Wang, Y., Xu, M., Lv, X., Wen, Z., & Chen, C. (2023). The eco-efficiency evaluation in China's cement industry: A city-level study. *Science of The Total Environment*, *865*, 161132. https://doi.org/10.1016/j.scitotenv.2022.161132

Wang, Y., Zhu, Q., & Geng, Y. (2013). Trajectory and driving factors for GHG emissions in the Chinese cement industry. *Journal of Cleaner Production*, *53*, 252–260. https://doi.org/10.1016/j.jclepro.2013.04.001

Watari, T., Cabrera Serrenho, A., Gast, L., Cullen, J., & Allwood, J. (2023). Feasible supply of steel and cement within a carbon budget is likely to fall short of expected global demand. *Nature Communications*, *14*(1), 7895. https://doi.org/10.1038/s41467-023-43684-3

Watari, T., Cao, Z., Hata, S., & Nansai, K. (2022). Efficient use of cement and concrete to reduce reliance on supply-side technologies for net-zero emissions. *Nature Communications*, *13*(1), 4158. https://doi.org/10.1038/s41467-022-31806-2

Watari, T., Hata, S., Nakajima, K., & Nansai, K. (2023). Limited quantity and quality of steel supply in a zero-emission future. *Nature Sustainability*, *6*(3), 336–343. https://doi.org/10.1038/s41893-022-01025-0

Wei, J., & Cen, K. (2019). Empirical assessing cement CO2 emissions based on China's economic and social development during 2001–2030. *Science of The Total Environment*, *653*, 200–211. https://doi.org/10.1016/j.scitotenv.2018.10.371

Wei, J., Cen, K., & Geng, Y. (2019). China's cement demand and CO2 emissions toward 2030: From the perspective of socioeconomic, technology and population. *Environmental Science and Pollution Research*, *26*(7), 6409–6423. https://doi.org/10.1007/s11356-018-04081-2

Wei, Y.-M., Kang, J.-N., Liu, L.-C., Li, Q., Wang, P.-T., Hou, J.-J., Liang, Q.-M., Liao, H., Huang, S.-F., & Yu, B. (2021). A proposed global layout of carbon capture and storage in line with a 2 °C climate target. *Nature Climate Change*, *11*(2), 112–118. https://doi.org/10.1038/s41558-020-00960-0

Wiedenhofer, D., Fishman, T., Plank, B., Miatto, A., Lauk, C., Haas, W., Haberl, H., & Krausmann, F. (2021). Prospects for a saturation of humanity's resource use? An analysis of material stocks and flows in nine world regions from 1900 to 2035. *Global Environmental Change*, *71*. https://doi.org/10.1016/j.gloenvcha.2021.102410

Worrell, E., Price, L., Martin, N., Hendriks, C., & Meida, L. O. (2001). Carbon dioxide emissions from the global cement industry. *Annual Review of Energy and the Environment*, *26*(1), 303–329. https://doi.org/10.1146/annurev.energy.26.1.303

Wu, T. (2023). *China Cement Industry Dataset (CCID)* [Dataset]. https://doi.org/10.5281/zenodo.8083481

Wu, T., Ng, S. T., & Chen, J. (2022). Deciphering the CO<sub>2<sub> emissions and emission intensity of cement sector in China through decomposition analysis. *Journal of Cleaner Production*, *352*, 131627. https://doi.org/10.1016/j.jclepro.2022.131627

Wu, T., Ng, S. T., & Chen, J. (2023). Incorporating carbon capture and storage in decarbonizing China's cement sector for a 1.5 °C future. *Renewable and Sustainable Energy Reviews*, *Major Revision*.

Wu, T., Ng, S. T., Chen, J., & Cao, Z. (2023). More intensive use and lifetime extension can enable net-zero emissions in China's cement cycle. *Resources, Conservation and Recycling*, *198*, 107144. https://doi.org/10.1016/j.resconrec.2023.107144

Xi, F., Davis, S. J., Ciais, P., Crawford-Brown, D., Guan, D., Pade, C., Shi, T., Syddall, M., Lv, J., Ji, L., Bing, L., Wang, J., Wei, W., Yang, K.-H., Lagerblad, B., Galan, I., Andrade, C., Zhang, Y., & Liu, Z. (2016). Substantial global carbon uptake by cement carbonation. *Nature Geoscience*, *9*(12), 880–883. https://doi.org/10.1038/ngeo2840

Xu, J., Fleiter, T., Eichhammer, W., & Fan, Y. (2012). Energy consumption and CO2 emissions in China's cement industry: A perspective from LMDI decomposition analysis. *Energy Policy*, *50*, 821–832. https://doi.org/10.1016/j.enpol.2012.08.038

Xu, J., Fleiter, T., Fan, Y., & Eichhammer, W. (2014). CO2 emissions reduction potential in China's cement industry compared to IEA's Cement Technology Roadmap up to 2050. *Applied Energy*, *130*, 592–602. https://doi.org/10.1016/j.apenergy.2014.03.004

Xu, J., Yi, B.-W., & Fan, Y. (2016). A bottom-up optimization model for long-term CO2 emissions reduction pathway in the cement industry: A case study of China. *International Journal of Greenhouse Gas Control*, *44*, 199–216. https://doi.org/10.1016/j.ijggc.2015.11.028

Ye, Y. (2022). *When will China's population peak? It depends who you ask.* https://www.nature.com/articles/d41586-022-02304-8

Yeh, S., & Rubin, E. S. (2012). A review of uncertainties in technology experience curves. *Energy Economics*, *34*(3), 762–771. https://doi.org/10.1016/j.eneco.2011.11.006

Yokoi, R., Watari, T., & Motoshita, M. (2022). Future greenhouse gas emissions from metal production: Gaps and opportunities towards climate goals. *Energy & Environmental Science*, *15*(1), 146–157. https://doi.org/10.1039/D1EE02165F

Zhang, C., Chen, W.-Q., Liu, G., & Zhu, D.-J. (2017). Economic Growth and the Evolution of Material Cycles: An Analytical Framework Integrating Material Flow and Stock Indicators. *Ecological Economics*, *140*, 265–274. https://doi.org/10.1016/j.ecolecon.2017.04.021

Zhang, C.-Y., Yu, B., Chen, J.-M., & Wei, Y.-M. (2021). Green transition pathways for cement industry in China. *Resources, Conservation and Recycling*, *166*, 105355. https://doi.org/10.1016/j.resconrec.2020.105355

Zhang, S., Worrell, E., & Crijns-Graus, W. (2015). Evaluating co-benefits of energy efficiency and air pollution abatement in China's cement industry. *Applied Energy*, *147*, 192–213. https://doi.org/10.1016/j.apenergy.2015.02.081

Zhang, S., Zhao, M., Liu, Z., Yang, F., Lu, B., Zhao, Z., Gu, K., Zhang, S., Lei, M., Zhang, C., Wang, C., & Cai, W. (2023). City-level population projection for China under different pathways from 2010 to 2100. *Scientific Data*, *10*(1), 809. https://doi.org/10.1038/s41597-023-02735-6

Zhang, X., Zhao, X., Jiang, Z., & Shao, S. (2017). How to achieve the 2030 CO2 emission-reduction targets for China's industrial sector: Retrospective decomposition and prospective trajectories. *Global Environmental Change*, *44*, 83–97. https://doi.org/10.1016/j.gloenvcha.2017.03.003

Zhang, Y., Pan, W., Teng, Y., & Chen, S. (2024). Construction Waste Reduction in Buildings through Modular and Offsite Construction. *Journal of Management in Engineering*, *40*(4), 04024026. https://doi.org/10.1061/JMENEA.MEENG-5828

Zheng, C., Zhang, H., Cai, X., Chen, L., Liu, M., Lin, H., & Wang, X. (2021). Characteristics of CO2 and atmospheric pollutant emissions from China's cement industry: A life-cycle perspective. *Journal of Cleaner Production*, *282*, 124533. https://doi.org/10.1016/j.jclepro.2020.124533

Zhong, X., Deetman, S., Tukker, A., & Behrens, P. (2022). Increasing material efficiencies of buildings to address the global sand crisis. *Nature Sustainability*, *5*(5), 389–392. https://doi.org/10.1038/s41893-022-00857-0

Zhong, X., Hu, M., Deetman, S., Steubing, B., Lin, H. X., Hernandez, G. A., Harpprecht, C., Zhang, C., Tukker, A., & Behrens, P. (2021). Global greenhouse gas emissions from residential and commercial building materials and mitigation strategies to 2060. *Nature Communications*, *12*(1), 6126. https://doi.org/10.1038/s41467-021-26212-z

Zurek, M. B., & Henrichs, T. (2007). Linking scenarios across geographical scales in international environmental assessments. *Technological Forecasting and Social Change*, *74*(8), 1282–1295. https://doi.org/10.1016/j.techfore.2006.11.005